OWL Instrument Concept Study

MOMFIS

Multi-Object, Multi-Field IR Spectrograph

I. Foreword and Executive Summary

LAM.PJT.MOMF.RAP.050915_01

OWL-CSR-ESO-00000-0164

Prepared by :	Signature
Jean-Gabriel Cuby Date : 15/09/2005	

Centre National de la Recherche Scientifique - Laboratoire Astrophysique de Marseille - UMR 6110 BP 8 – 13376 Marseille Cedex 12, Tel. : 33 +4.91.05.59.00 - Fax : 33 .+4.91.05.59.47

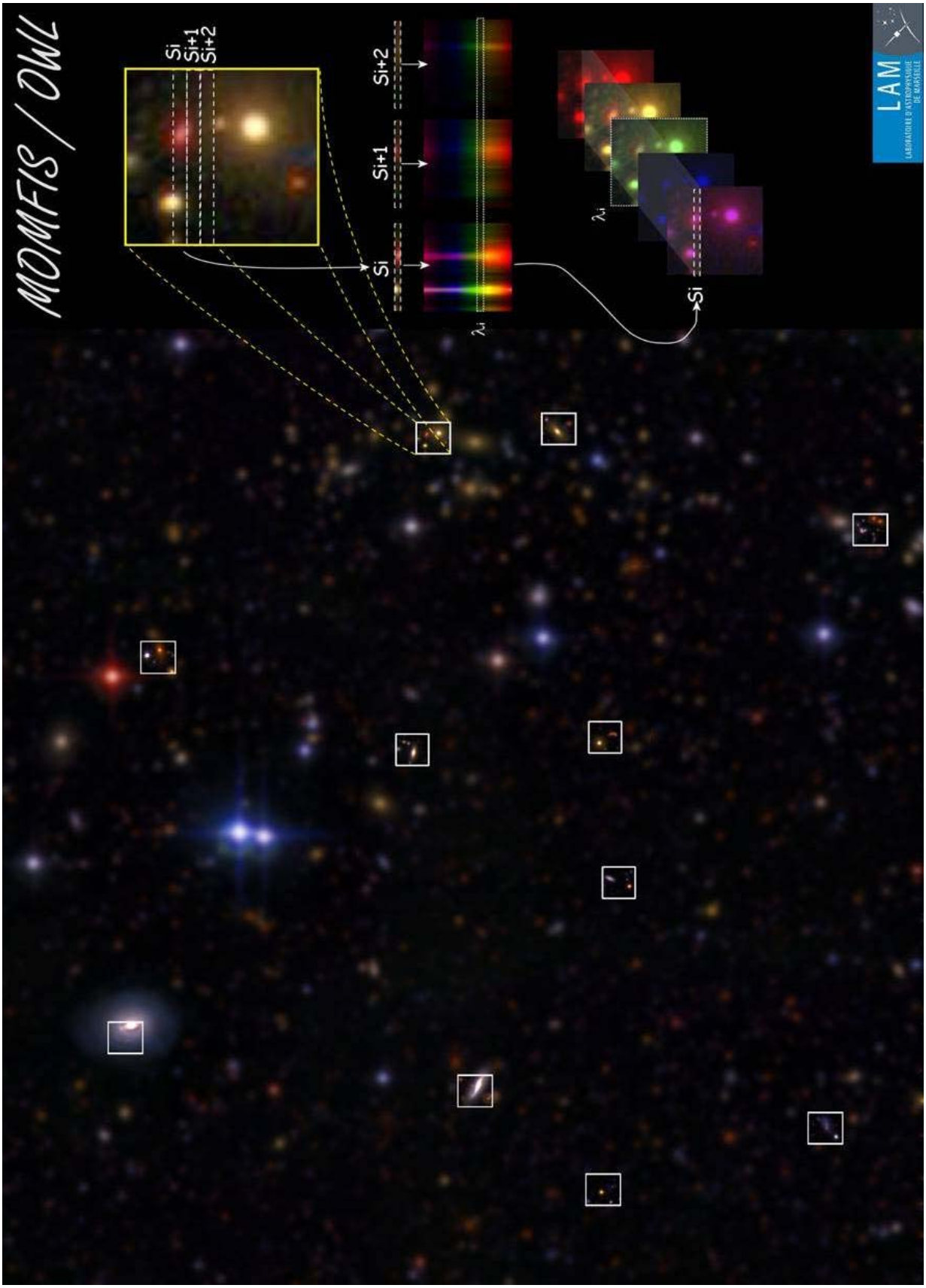
MOMFIS / OWL
Si
Si+1
Si+2
Si+2
Si+1
Si
λi
λi
Si

Change Records

Date	issue	Révision	Modification	Pages
15 Sept 2005	1	0	Final report	All

Distribution List

Institute	Name	Issue/Revision									
		1.0									
LAM	J.G. Cuby	X									
LAM	J.P. Kneib	X									
LAM	E. Prieto	X									
LAM	N. Manzone	X									
LAM	P.E. Blanc	X									
LAM	D. Burgarella	X									
LAM	O. Le Fèvre	X									
GEPI	F. Hammer	X									
GEPI	P. Jagourel	X									
GEPI	P. Vola	X									
GEPI	M. Marteaud	X									
GEPI	M. Puech	X									
LESIA	Y. Clénet	X									
LESIA	D. Rouan	X									
CRAL	R. Bacon	X									
CRAL	E. Pécontal	X									
CRAL	M. Tallon	X									
ONERA	G. Rousset	X									
ONERA	T. Fusco	X									
ESO	M. Casali	X									

Table of contents

List of Figures

List of Tables

1. INTRODUCTION

This document is the conceptual design report of MOMFIS, the OWL Multi-Object Multi-Field Infrared Spectrograph. The MOMFIS study was performed under ESO contract from December 2004 to September 2005, by a consortium of institutes:

- LAM (Marseille)
- GEPI (Paris-Meudon)
- LESIA (Paris-Meudon)
- CRAL (Lyon)
- ONERA (Chatillon)

This document is made of the following reports:

- MOMFIS executive summary. This document is conveniently organized to highlight the MOMFIS science case, instrument concept and sub-system implementation. It also presents some alternative concepts to the baseline MOMFIS design
- MOMFIS science report
- MOMFIS technical specifications
- MOMFIS technical report

The material available to the consortium before starting the study was:

- A statement of work
- A telescope interface document

More material was received during the course of the study, such as a document describing the OWL adapter-rotator concept (June 2005), a document describing the OWL sky coverage with natural stars assisted adaptive optics (may 2005), a document describing the results of adaptive optics simulations (march 2005). Several meetings with ESO took place, either in person (2 meetings) or through videoconferencing. Regular contacts took place via e-mail. Specific Adaptive Optics simulations were requested to ESO, and performed.

The scope of the study was to perform a conceptual design allowing to identify interface issues, risk development issues, key technological development areas, and to provide feedback to the OWL designers.

We essentially adopted the safest options in our design, in particular by resorting to proven technologies rather than speculative ones. In that respect, several budgets in our design are to be regarded as upper limits (e.g. mass, cost, etc.).

2. ACKNOWLEDGEMENTS

We thank ESO for calling us to carry out this study, and for positive and supportive collaboration during the whole study, and more particularly Sandro D'Odorico, Bernard Delabre, Norbert Hubin and Miska Le Louarn for their active participation. Mark Casali, in charge of the contract at ESO, was instrumental in helping us and maintaining an excellent relationship between the two teams.

We acknowledge many people from our participating institutes who have contributed to the project: Stephane Arnouts, Denis Burgarella, Pascal Dargent, Christophe Fabron, Marc Ferrari, Elizabeth Harmitt, Olivier Le Fèvre, Nataly Manzone, Bruno Milliard, Hélène Vicq, (LAM), Francois Hammer, Matthieu Puech (GEPI), Yann Clenet (LESIA), Roland Bacon (CRAL), Thierry Fusco, Gerard Rousset (ONERA) and Johan Richard (OMP).

This team will continue its activities in the framework of the Instrumentation WP of the ELT Design Study.

3. REFERENCES

3.1 Applicable Documents

[AD 01]	OWL-SOW-ESO-00000-0152	1.0	03 Dec. 2004	Statement of work for a conceptual study of an IRMOS for OWL
[AD 02]	OWL-ICD-ESO-00000-0139	1.0	5 Oct. 2004	Interface Control Document
[AD 03]	OWL-CSR-ESO-00000-0147	1.0	24 Sep. 2004	Framework of OWL instrument concept design studies

3.2 Reference Documents

[RD 01]	LAM.SCT.MOMF.SPS.050117_01	1.1	Jan. 17, 2004	MOMFIS. Scientific Specification (Science Case)
[RD 02]	Hammer et al., SPIE 5382, 2003, p. 220.		2003	FALCON: a concept to extend adaptive optics corrections to cosmological fields
[RD 03]	Memo ESO / S. D'odorico		06 June 2005	Draft Adapter Rotator concept
[RD 04]	Memo ESO / M. Le Louarn		June 2005	OWL AO Analysis report (draft)
[RD 05]	OWL-TRE-ESO-00000-xxxx	Draft	10 May 2005	Sky Coverage for OWL Adaptive Optics: GLAO and MCAO cases

4. SCIENCE CASE

A highlight science case of all the future large telescope projects is entitled: 'The End of the Dark Ages: First Light and Reionization'. After the recombination epoch, space was filled with dark matter, dark energy and neutral gas. As it continued to expand, regions of higher density stopped following the expansion, turned around and collapsed into the sites where the first objects formed. Primordial objects are thought to be primordial galaxies powered by young massive stars and early quasars accreting matter around growing black holes. As they lit up, they enriched in metals the interstellar medium, and ionized the neutral hydrogen around them. In effect, the Universe underwent another phase transition, from a neutral to an ionized state. MOMFIS is designed for this highlight science case, it aims at pushing back as early as possible into the Dark Ages to observe and characterize the sources that once re-ionized the Universe.

Figure 1 shows the expected number counts of high-z galaxies versus AB magnitude, based on extrapolation of z ~ 6 number counts.

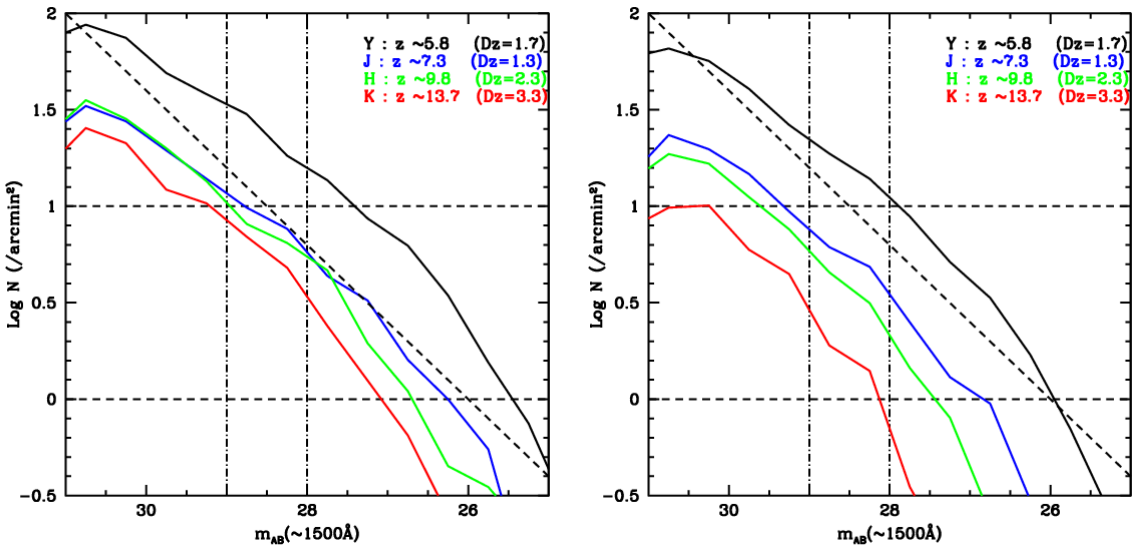

Figure 1 – High z galaxy luminosity function. Extrapolation from z ~ 6 counts

Counts prediction from extrapolation of the observed z=6 luminosity function (Bouwens et al, Stiavelli et al, Yan et al). Left: no evolution, Right: with evolution similar to the evolution observed between z=3 and z=6. The number counts refer to the 1500 A restframe UV luminosity. The redshift interval per spectral band is indicated.

From these figures one derives that 20 to 50 sources at the very least, possibly a few hundreds, can be observed in a single 5' x 5' field of view, depending on the observed band, effects of evolution, cosmic variance, etc., down to a sensitivity limit of AB=28.

In addition, Figure 2 shows the typical size of galaxies versus redshift. Simple extrapolation of this curve at higher redshifts gives the following half light radius estimates:

- 1 kpc at z = 6 corresponding to 170 mas
- 0.5 kpc at z = 8 corresponding to 100 mas

Therefore, sampling the half light diameters with ~ 10 x 10 spatial elements require a spatial sampling of about 20-30 mas, requiring in turn an exquisite image quality (AO corrected) within 50 mas or less.

Figure 3 nicely illustrates the need for an integral field spectroscopy on a real image of a strongly magnified high redshift object.

Figure 4 illustrates the performance capabilities of OWL. Reaching J_{AB}=28 on the continuum in a few hours time is feasible provided that the PSF is very sharp. 2D spectroscopy of objects extended or structured within ~ 150 mas will typically take up to 10-30 hrs of integration time with a 100 m telescope, and up to a few hundreds of hours with smaller telescopes (30 to 50 m).

Targets will ideally come from JWST. Alternatively, targets could also come from OWL imaging e.g. in the MCAO field of view. Note that there exist already several tens of high redshift candidates from space and ground observations that are too faint for spectroscopic follow-up with the 8-10 m telescopes.

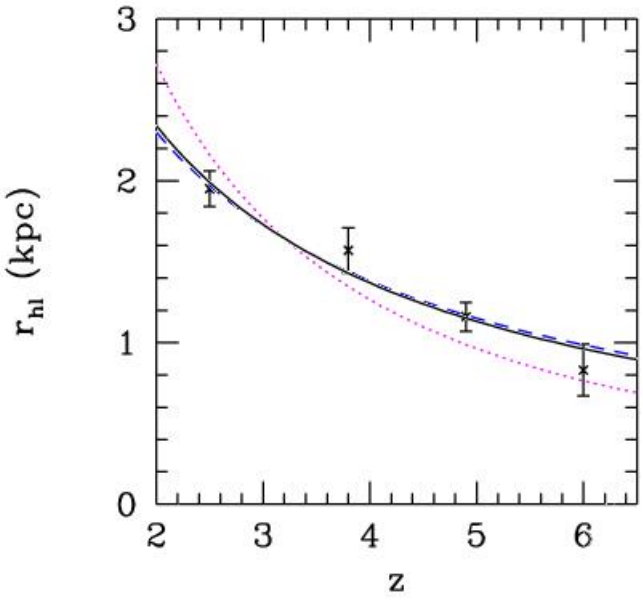

Figure 2 – Mean half light radius versus redshift

Measured from HST data on dropout samples of galaxies of fixed luminosity (0.3-1.0 $L_{*,z=3}$) (Bouwens et al., 2004, ApJ 611, L1-L4).

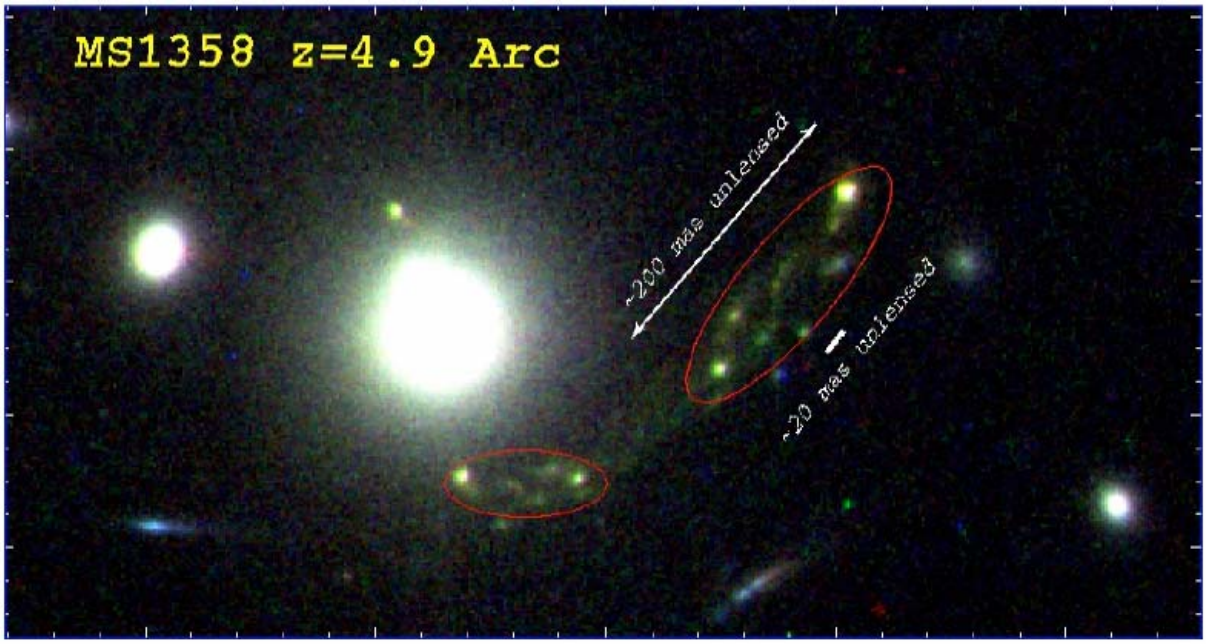

Figure 3 – HST/ACS color image (RIZ) of the MS1358+62 arc at z=4.9.

The arc is made of 2 images as indicated by the 2 red ellipses. Due to the large magnification of ~20 (for the largest ellipse) the unlensed size of the images is about 200 mas. Note that the arc displays a very complex structure of 7-8 blobs, each of them having a typical size of about 20 mas.

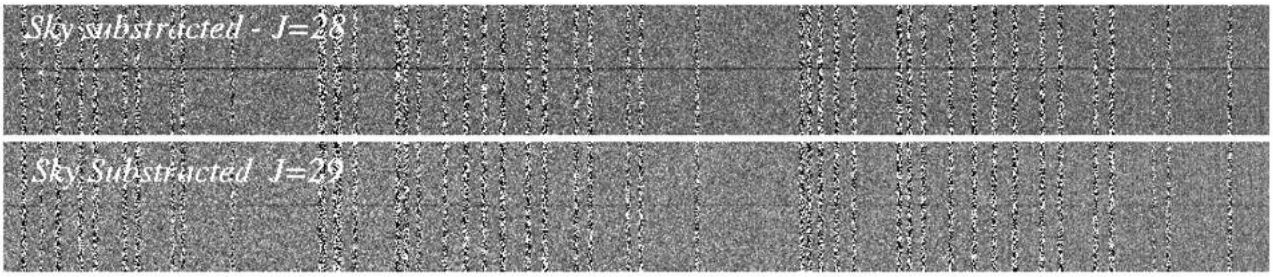

Figure 4 – Simulated spectra J=28 & J=29

Spectral resolution is 4000, integration time 10 ksec, PSF 150 mas, telescope diameter 100 m. This simulation, while illustrating that reaching J=28 is feasible, also shows the importance of reaching an exquisite image quality.

5. HIGH LEVEL SCIENCE REQUIREMENT SPECIFICATIONS

In conclusion, the top level science requirement specifications for MOMFIS on OWL are:

- Simultaneous observation of several targets over the OWL science field of view
- Spatially resolved spectroscopy of individual targets (integral field)
- Image quality: 50 milliarcseconds or better. This requires local adaptive optics correction
- A spectral resolution in the range 4000-8000 for OH suppression

The MOMFIS acronym is derived from these high level specifications: Multi-Object Multi-Field Infrared Spectrograph.

6. SUB-SYSTEMS AND SUB-SYSTEM SPECIFICATIONS

MOMFIS provides for 30 independent channels, each channel consisting of the following sub-systems:

- A target selection system consisting of pick-off and beam steering mirrors which direct the science beams from the telescope focal plane to the deformable mirrors
- Wavefront sensors sampling the full field of view on reference stars. Information from these WFS is combined to derive the local wavefront error that needs to be corrected on the targets
- A deformable mirror correcting the atmospheric perturbations in the direction of the target
- An image slicer dividing individual fields of view into 40 slices 20 milliarcsecond wide and 0.8” long
- A spectrograph providing one spectral band (Y, J, H or K) at once at a spectral resolution of ~ 4000.
- A 2k x 2k IR array. Options for 1k x 1k detectors can be considered to reduce cost.

In addition, the instrument is equipped with wavefront sensors which sample the atmosphere over the whole instrument field of view.

7. TELESCOPE INTERFACE

It is described in [AD 02] and [RD 03].

8. MULTI-OBJECT ADAPTIVE OPTICS CONCEPT

The MOMFIS science case requires images with very narrow PSF, i.e. high encircled energy within ~ 50 mas. Note that this is far from requiring diffraction limited images, however this level of image quality is beyond the expected performance of the GLAO.

In practice, image quality only needs to be improved locally where the sources targeted by the instrument are. This is achieved by having a DM on each channel which locally corrects the image quality. Wavefront sensors measure the atmospheric turbulence over the full field of view, and this information is used to correct locally each target by using the information from the neighbouring reference stars. See Figure 5 for an illustration of the MOAO concept. Variations on this principle can be considered, e.g. with the wavefront sensors operating in pseudo-closed loop when additional DMs are included in the WFS channels.

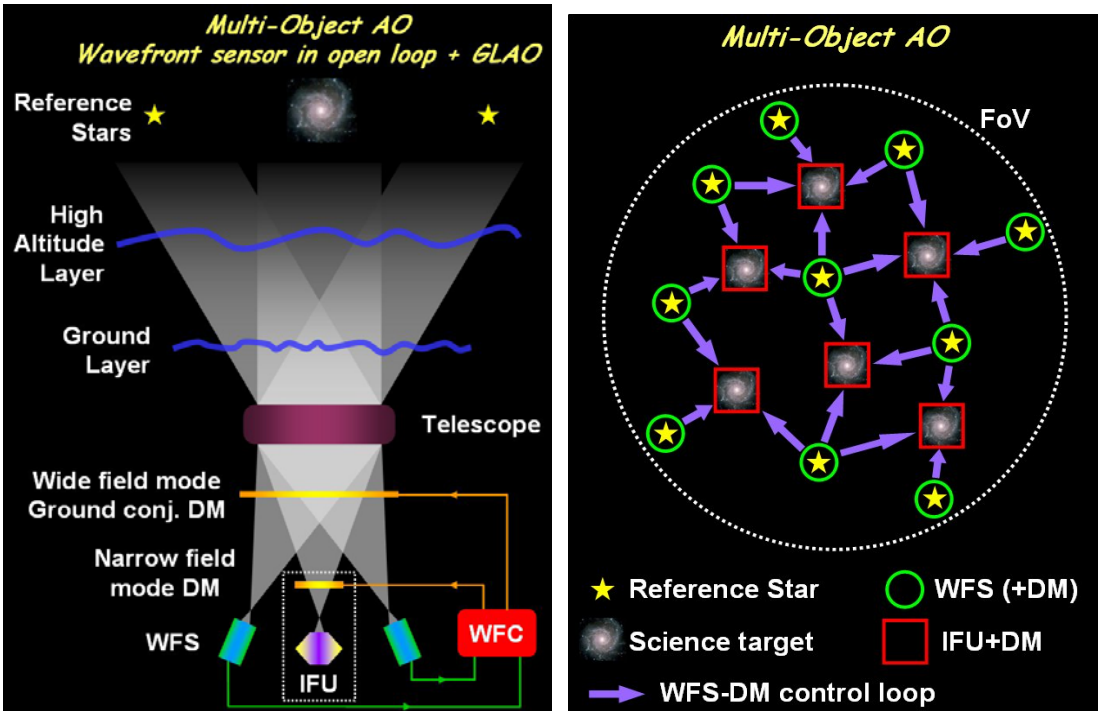

Figure 5 – Concept of Multi-object Adaptive Optics or Distributed Adaptive Optics

MOAO is combined with GLAO, and with wavefront sensors operating in open loop (courtesy ESO / AO department).

9. INSTRUMENT CONCEPT

Figure 6 illustrates the instrument concept. Pick-off mirrors are positioned and oriented in the telescope focal plane prior to the exposure. The pick-off mirrors send the light to movable steering mirrors which in turn send the light to the fixed deformable mirrors and instrument (image slicers and spectrographs). 10 wavefront sensors (number TBD) sample the atmospheric wavefront over the telescope field of view.

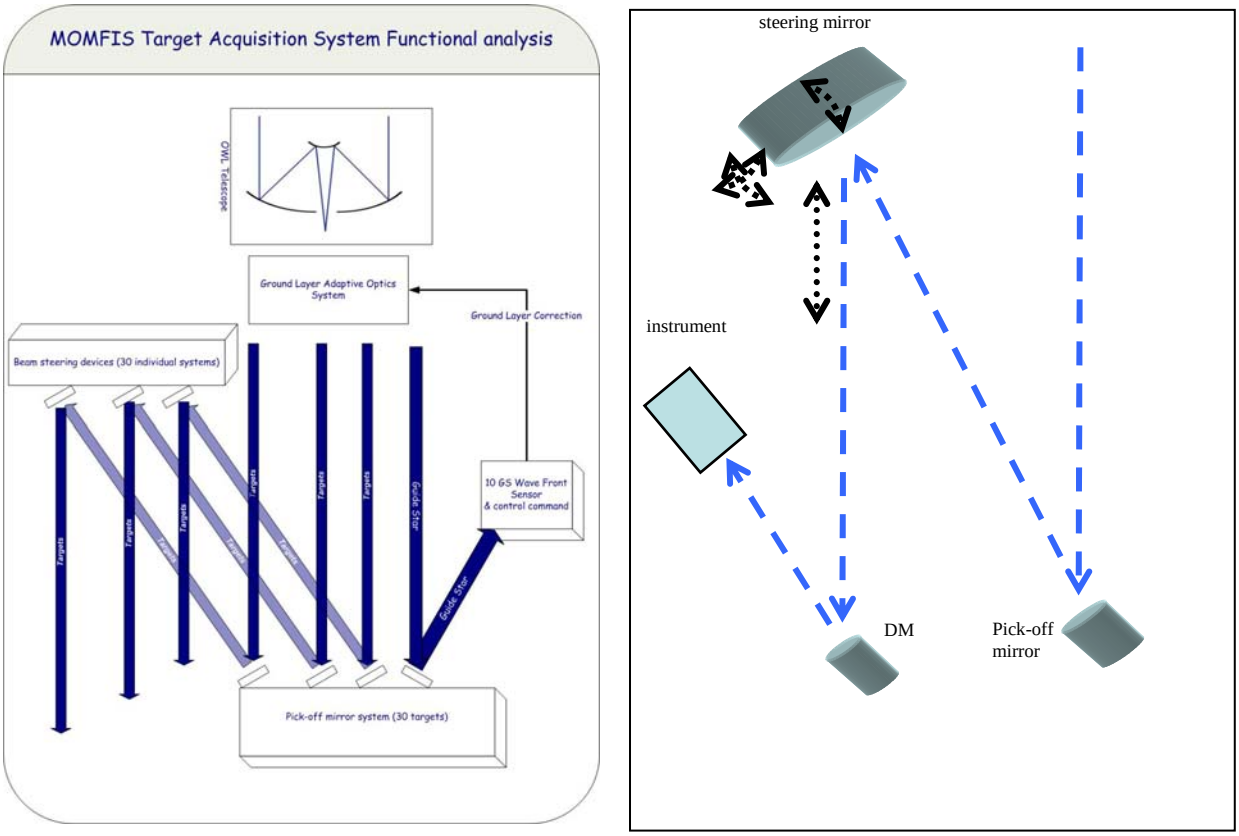

Figure 6 – MOMFIS Operational Concept

10. CONCEPTUAL DESIGN

From these notional concepts, the rest of the instrument design was performed with the following philosophy in mind: resort to proven technology and as much as possible to existing concepts or instruments, and take the safest approaches whenever necessary. There are 2 points worth mentioning in particular to illustrate the 'spirit' that guided us for the design:

- We chose to design the instrument thermally stabilized. This adds complexity to the instrument (large 2 m entrance window, thermal enclosure), and increases its weight. Depending on detailed trade-off studies to perform further down the road, this item could be dropped, however we chose to include it in the baseline.
- Our baseline option does not foresee the use of starbugs (motorized autonomous systems in the focal plane, in our case the pick-off mirrors), although such systems are actively pursued and the prospect for their successful development is bright. Instead, we resorted to classical positioner type of systems, such as 2dF or Oz-Poz.

Accordingly, the budgets resulting from our design shall somehow be regarded as upper limits. The baseline design presented below is in a sense the 'toughest' solution. Optional solutions and / or simplifications are then analyzed.

In total, the baseline instrument features 30 fully identical beams and 10 cryostats with 3 spectrographs per cryostat. The instrument is modular, highly redundant, and designed for easy preventive or corrective maintenance. Figure 7 – MOMFIS conceptual optical layout illustrates the MOMFIS optical layout.

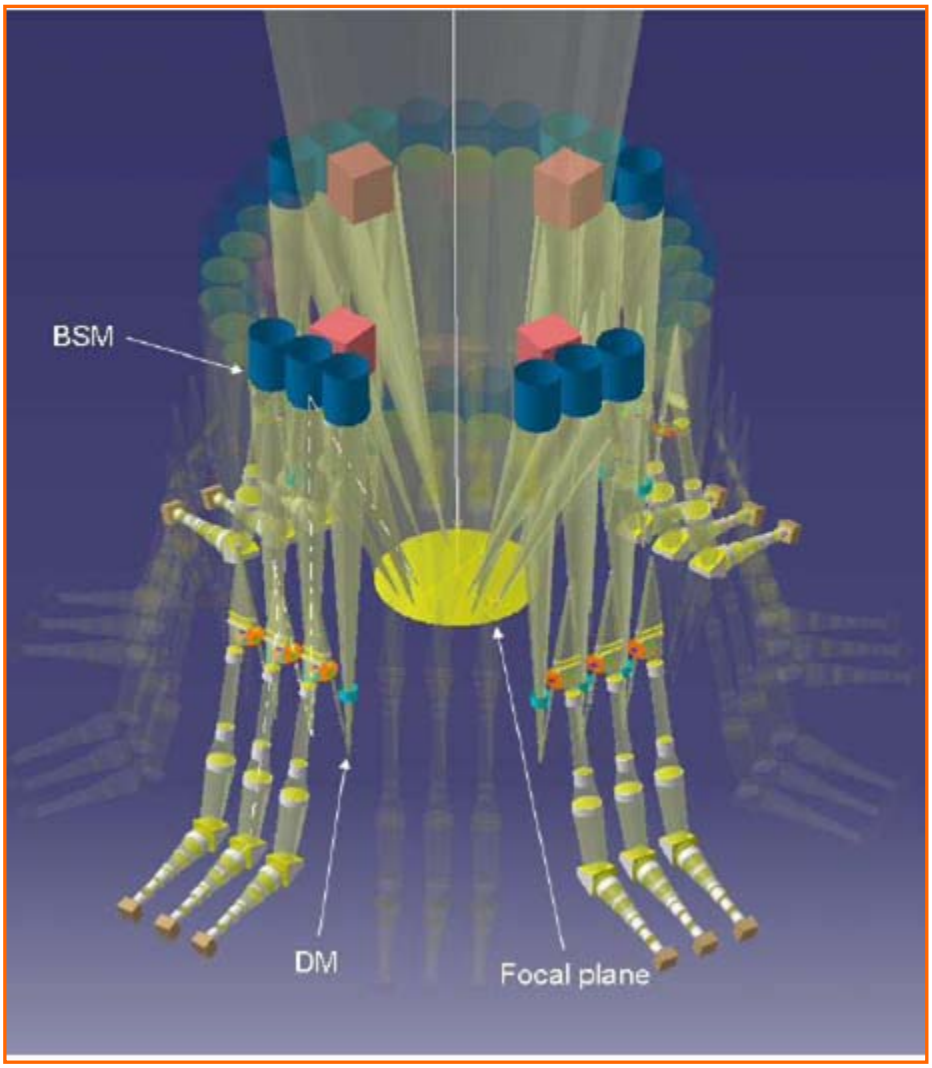

Figure 7 – MOMFIS conceptual optical layout

Conceptual optical implementation showing the focal plane (yellow), the beam steering mirrors (blue cylinders), the wavefront sensors (pink boxes), the atmospheric dispersion compensators (cyan), the filter wheels (orange), and the slicer and spectrograph optics. The overall height of the instrument as shown is 3.5 m.

10.1 Beam steering mirrors

The beam steering mirrors are key components of MOMFIS. They need to move in translation and in rotation to compensate the optical path length from the (movable) pick off mirror to which they are associated in the focal plane and the (fixed) deformable mirror

underneath the BSM. In addition, the BSM needs be deformable (2 orthogonal spherical deformations) in order to compensate the spherical aberrations introduced by the spherical pick-off mirror.

Figure 8 shows the concept of the BSM.

LAM has experience in developing beam steering mirrors and a prototype similar to the one presented below is being developed as part of the OPTICON JRA on smart focal planes. A model has been developed for designing the BSM (Figure 9).

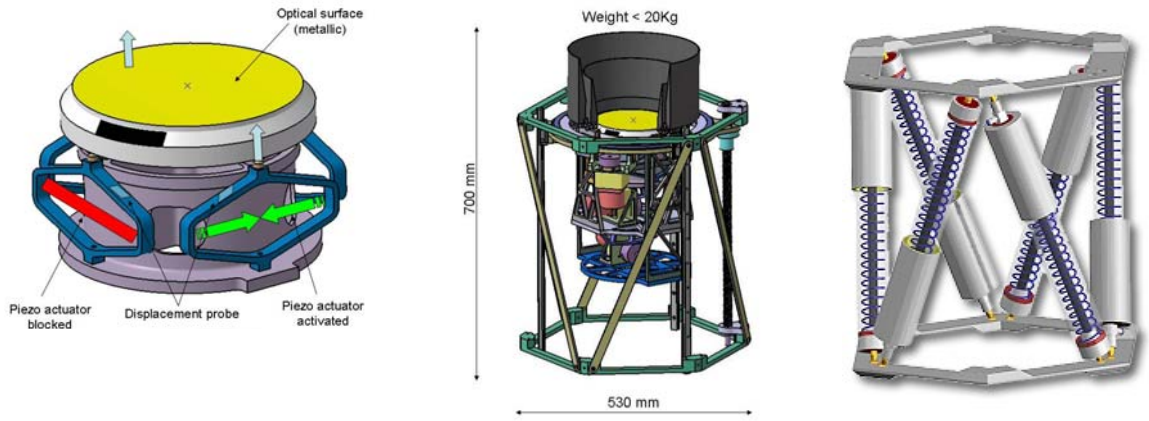

Figure 8 – Beam Steering Mirror concept

Left: the beam steering mirror design. Two pairs of piezo-electric actuators deform the mirror in a toroidal shape (different radii of curvature in two orthogonal planes perpendicular to the mirror surface). Middle: mechanical implementation of the BSM: z translation and rotation around 3 axes. Left: example of an hexapod structure under consideration to replace the mechanical structure.

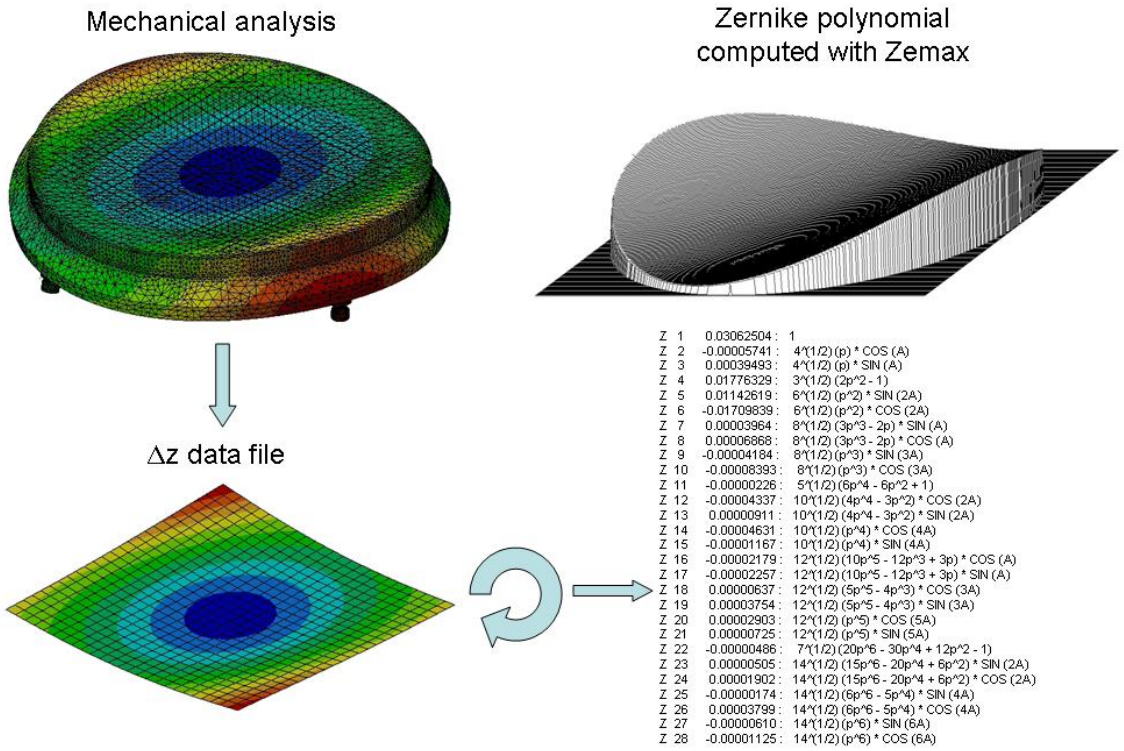

Figure 9 – Beam Steering Mirror: Opto-mechanical modelling

Finite Element Mechanical Analysis and Optical (Zernicke polynomials) analysis are performed iteratively by changing the attachment points until the right deformation is achieved. This model allows to carefully design the mechanical implementation of the mirror.

10.2 Deformable mirrors

The design and study of the DMs suitable for MOMFIS is a task that goes far beyond the scope of the present study. Active R&D programs on adaptive optics systems and components are being carried out as part of the OPTICON and ELT Design Study European programmes and led by ESO. The OWL Blue Book extensively describes the Adaptive Optics development plan, in particular MOAO, and we refer to this document. For the sake of this report, it is enough to say that the DMs shall be micro deformable mirrors with ideally up to 200 x 200 actuators to provide the adequate level of image correction. Moreover, the DMs shall work in cooled (-40^{o}C) or cryogenic environments.

The DMs are certainly one of the risky development items required for MOMFIS. However, MOMFIS could still operate with somehow degraded performance, without MOAO and therefore without DMs (or with low order DMs), see section 13.

10.3 Image slicers

Figure 10 shows the optical layout of the image slicer, together with a picture of a prototype component developed at LAM. Image slicers technology is well mastered and there aren't any development risk for these components.

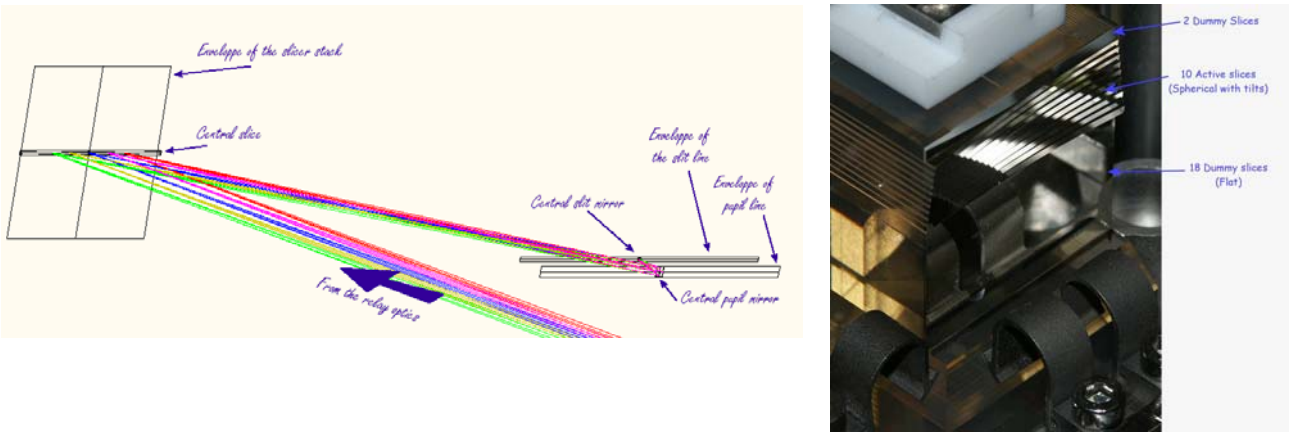

Figure 10 – Image slicer.

Left: optical layout and principle of operation. Right: example of a prototype image slicer developed as part of the JWST/NIRSpec project, with specifications similar to the MOMFIS ones.

10.4 Spectrographs

Figure 11 shows a conceptual design of the spectrograph. It uses standard glasses and provides image quality within the specifications.

There are no development risks associated to this sub-system.

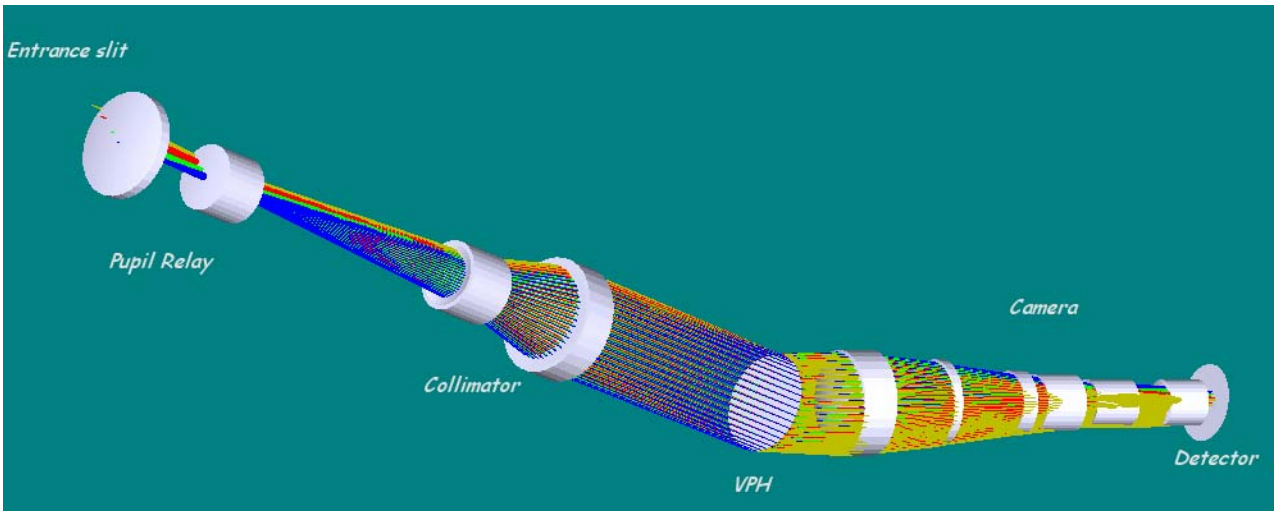

Figure 11 – Spectrograph layout. 2k x 2k detector and F/1.8 camera

10.5 Structure and thermal enclosure

Figure 12 shows the instrument main structure. It features a large rotator (4.5 m in diameter) and an entrance window and thermal enclosure isolating the instrument from the external environment. The 10 cryostats are mounted on a supporting flange inside the rotator. The positioner and focal plate exchange mechanism is on one side of the rotator and a ring supporting the BSM and the WFS is attached to the rotator via a Serrurier truss on the other side.

The study of this mechanical structure considered lightweight materials (e.g. carbon / epoxy) to reduce the overall weight, while preserving performance under gravity loads.

A FEA analysis was also performed. The differential motions under 1 g for 60^{o} inclination are exceeding the optical specifications, however within limits that could be easily controlled with internal metrology.

The baseline foresees thermal stabilization, requiring a large (2 m in diameter) entrance window and a thermal enclosure.

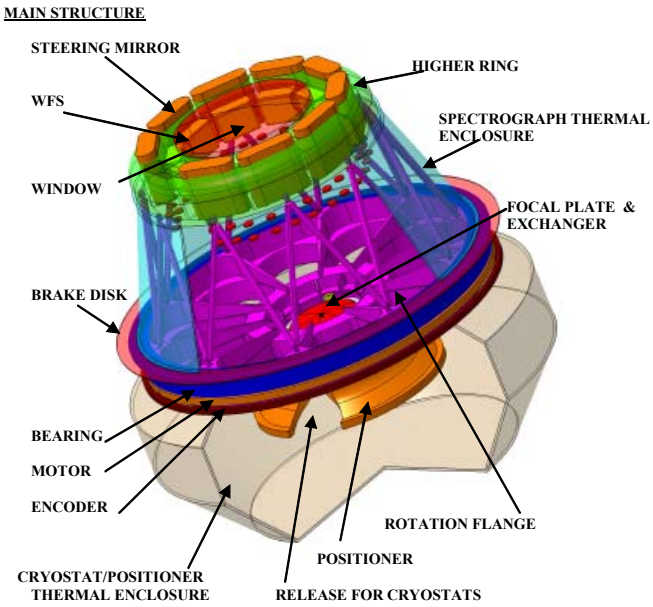

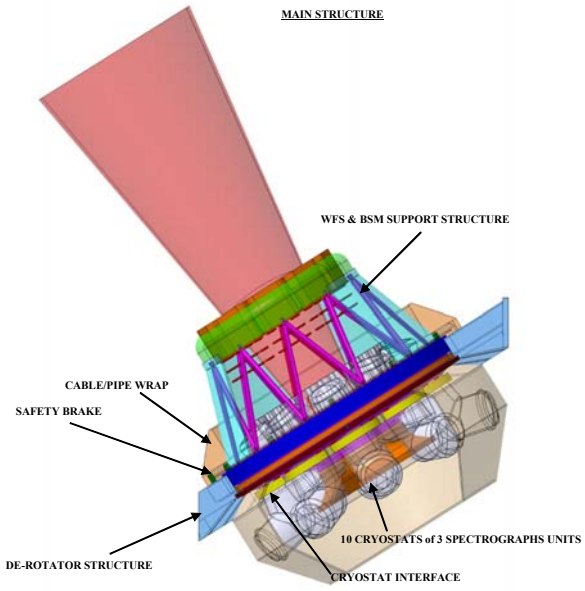

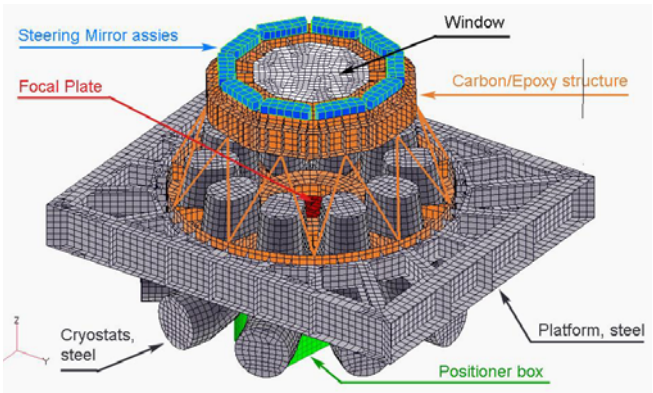

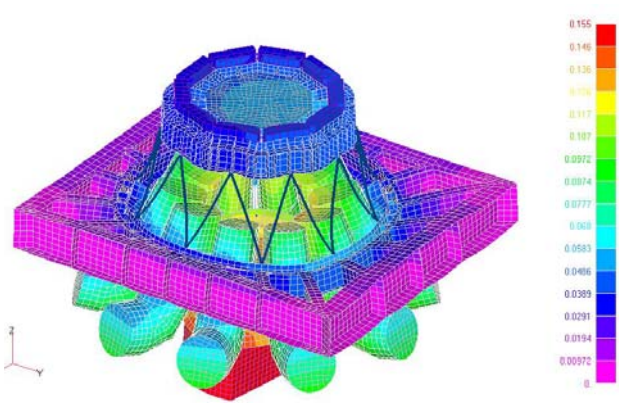

Figure 12 – Main structure

UL: Mechanical structure showing the rotator, spectrograph support structure and serrurier truss supporting the BSM and WFS ring. UR: side view with cryostats, enclosure, etc. LL: distribution of materials in main support structure. LR: FEA analysis, amplitude of the deformation.

10.6 Positioner

The positioner is inspired from the 2dF. It is attached directly onto the instrument. One plate is being configured by the robot while the other is observing. One an observation is completed the focal plates are swapped by the tumbler mechanism, and the new observation can start.

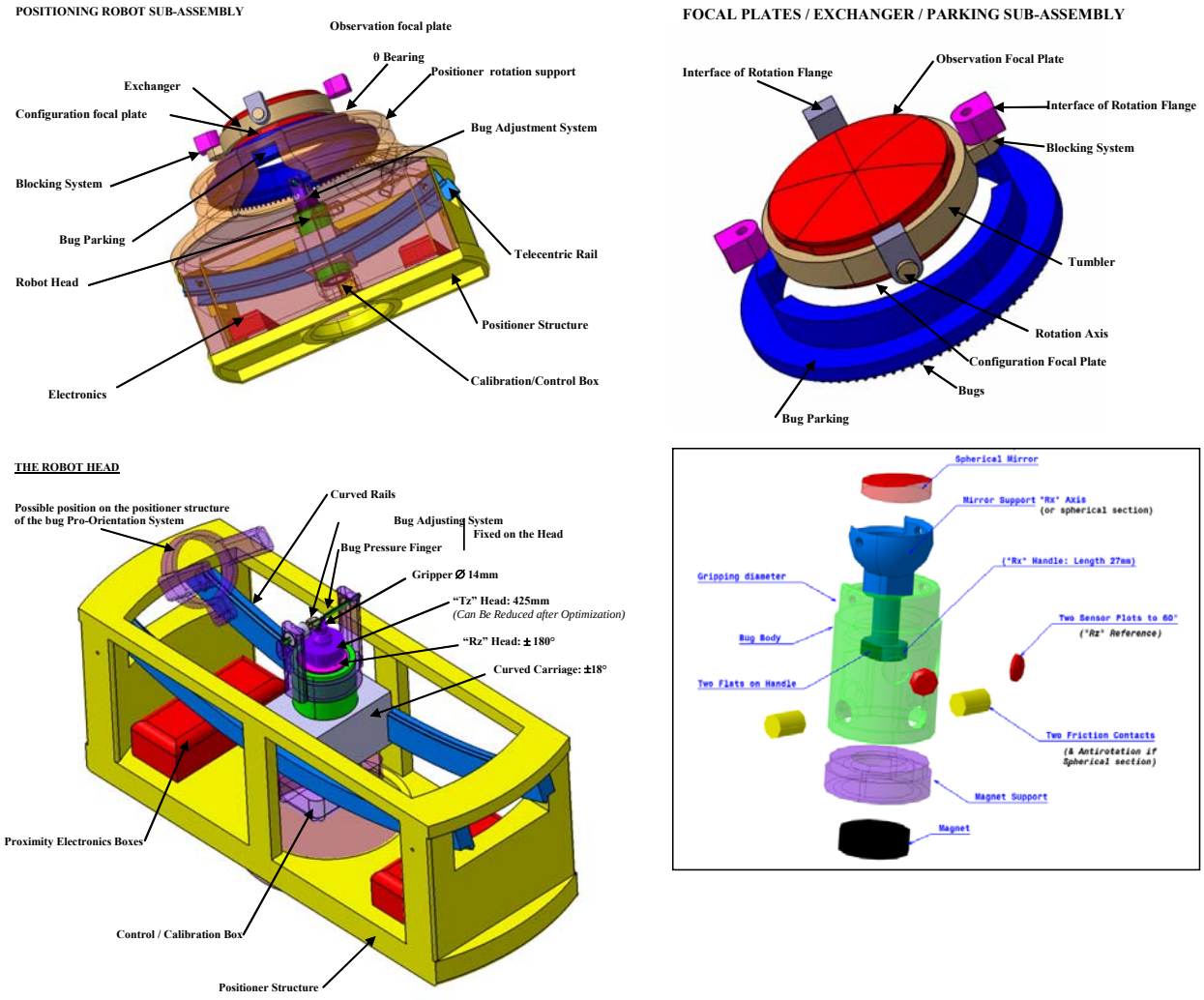

Figure 13 – Positioner and sub-systems

UL: Positioner system – UR: the tumbler exchange mechanism
LL: the robot head on its R rail. LR: detail of one pickoff mirror

10.7 Cryostats

The cryostats were designed so as to include 3 spectrographs. This represents a good compromise between a single huge cryostat with 30 channels and 30 small cryostats with one spectrograph per cryostat. This solution provides a high level of redundancy and limits the impact of instrument failures. An 11th cryostat could be developed for preventive maintenance purposes allowing to cycle maintenance operations over the 11 cryostats while having one permanently as a spare and the 10 others in operation.

Figure 14 shows the cryostat design. Cooling requirements per cryostat are 2-3 cryo-coolers or ~ 200 LN2 liters/day.

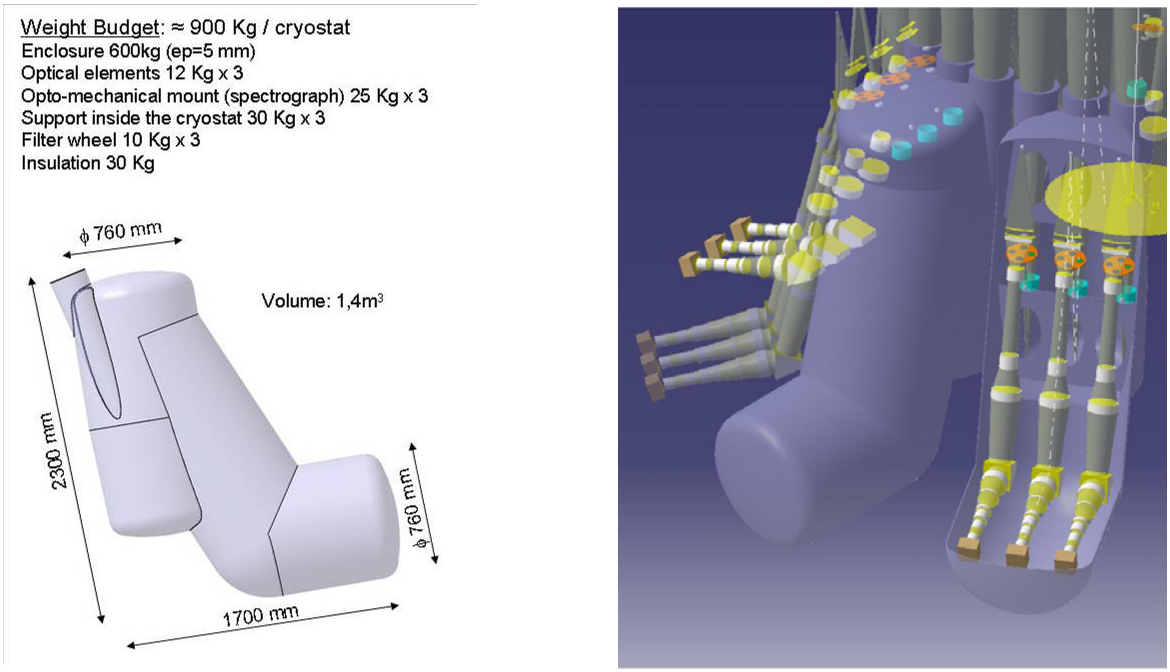

Figure 14 – Cryostat concept

Left: cryostat characteristics. Right: Opto-mechanical implementation in instrument

10.8 Calibration

Figure 15 shows the concept of the calibration unit. The beam steering mirrors look at an integrating sphere at the periphery of the focal plane, offering the adequate beam speed (F/6) and the configuration flexibility and speed of the beam steering mirrors. Calibration can be performed at any time, irrespective of the focal plane configuration.

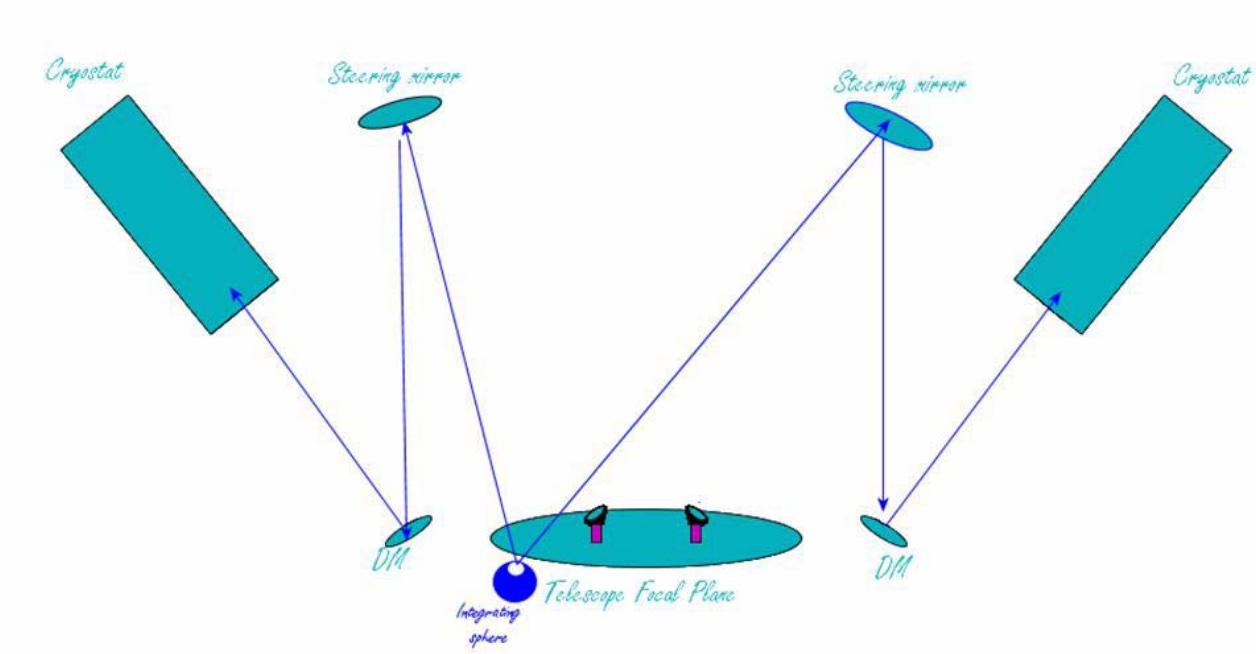

Figure 15 – Calibration concept

10.9 Metrology

Internal metrology is required for the instrument integration, alignment testing, calibration, operation and maintenance. Because of the long optical paths involved in the instrument and of the mechanical flexures mostly due to the changing gravity, it is likely that metrology will be required for closed loop control of the various parts of the instrument (in particular beam steering and deformable mirrors).

10.10 Overall implementation

Figure 16 shows the complete instrument in the focal station.

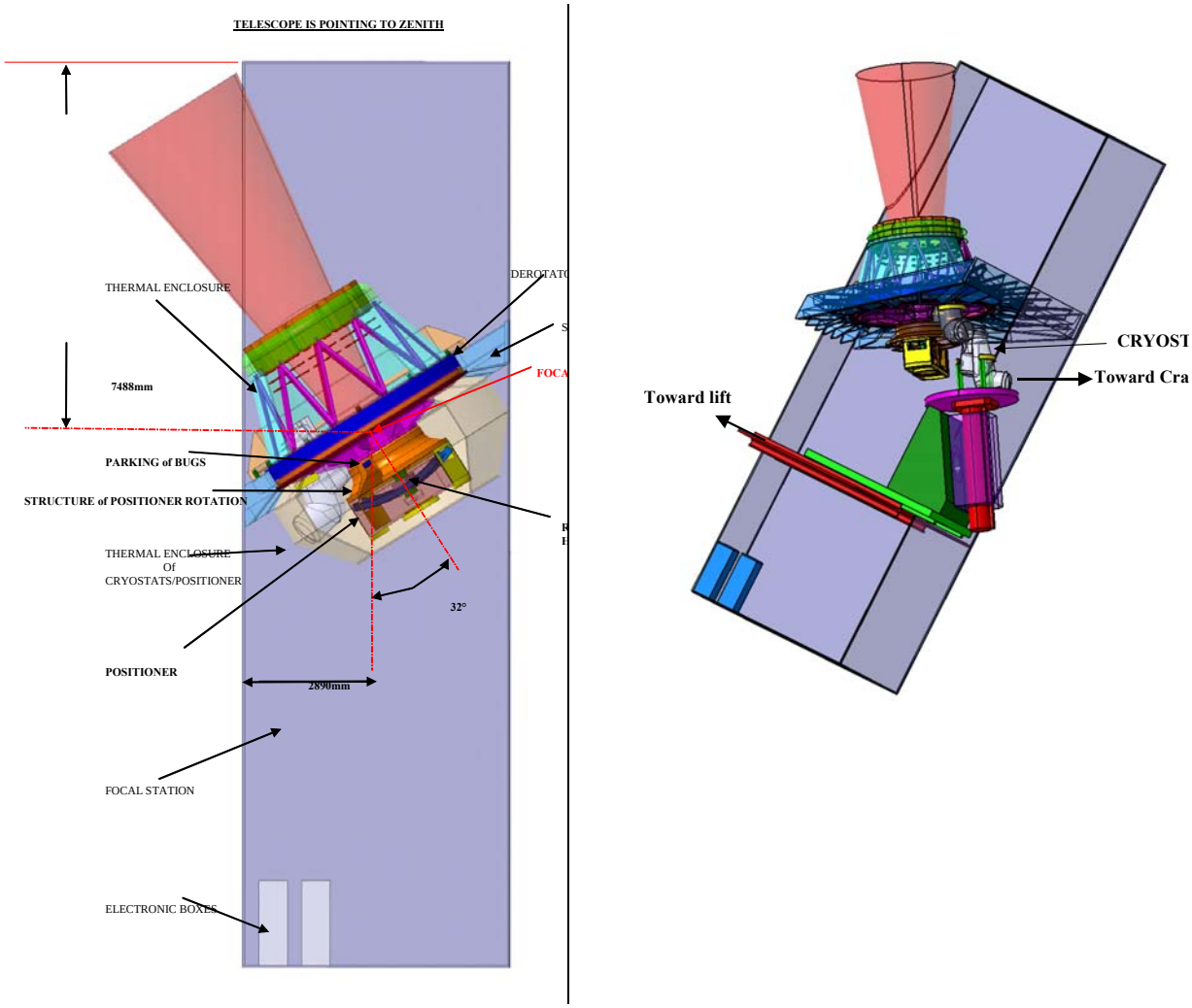

Figure 16 – Implementation in the focal station

Left: View of the instrument as installed in the focal station. Note the 2 electronic racks at the bottom. Right: illustration of the maintenance plateform and of the extraction carriage foreseen to extract either the cryostats or the positioner.

11. PERFORMANCE

MOMFIS allows to observe 30 targets in integral field mode (0.8" field of view) at once in the Ø 5' OWL scientific field of view down to IR AB magnitudes of ~ 28. This ideally meets the science high level specifications.

12. TECHNOLOGICAL DEVELOPMENTS AND ROADMAP

The entire instrument concept relies on exiting and well demonstrated technologies, but for 2 items which will require specific developments and roadmaps:

- multi-object adaptive optics (MOAO). MOAO is at the core of the MOMFIS operation, it requires several wavefront sensors sampling the atmospheric wavefront over the

telescope and one deformable mirror per channel (assuming telescope provides ground layer correction). The MOAO concept has never been implemented and needs further studies and laboratory and / or on-sky prototyping to be demonstrated and validated. Laser guide stars are a must for full sky coverage.

- Internal metrology. Internal metrology and control of the main optical elements is required in the instrument to compensate for flexures (the focal station is not gravity stable) that cannot all be absorbed by the stiffness of the structure. This internal metrology will also be used for alignment, calibration and operation purposes.

13. OPTIONS

At this stage, several options to the baseline instrument described above can be contemplated:

- **Option#1: No MOAO**. 1st phase and / or fallback solution without adaptive optics. In a first implementation phase, MOMFIS could be deployed without the deformable mirrors which can be replaced by flat mirrors, or low order deformable mirrors. Wavefront sensors would still be required for telescope control. Exquisite image quality could still be obtained in the central field of view (1 to 2 arcmin multi-conjugated adaptive optics field), gently degrading towards the outer edge of the OWL field of view (ground layer correction only). More than just a 1st light option, this option is actually also a fallback option in case MOAO developments fail or prove to be more difficult than expected to implement
- **Option#2: No K band.** A second option is to resort to partial cryogenic cooling combined with moderate cooling (-40°C or so) of the whole instrument. This option allows to simplify the cryogenics and mechanics of the instrument, albeit at the expense of the performance in the K band.
- **Option#3: 2 objects per spectrograph**. This option allows significant simplification of the instrument by reducing by a factor two the number of spectrographs at the expense of the individual field of view of each channel (0.6" x 0.6"). The number of cryostats would be ~7 for 28 channels in total.
- **Option#4: 1k x 1k arrays**. This option allows simplification of the spectrograph design and (possibly) significant cost savings by resorting to 1k x 1k arrays instead of 2k x 2k arrays. It is also at the expense of individual IFU field of view. The number of cryostats is unchanged.

14. ALTERNATIVE DESIGNS

Alternative designs to MOMFIS have been considered. They could take the form of traditional multi-slit spectrographs (MOS), or fiber-fed spectrographs still requiring the pick-off and adaptive optics stages. Designs for these alternative designs are presented. The MOS instrument could serve as an OWL first light instrument that could be used for commissioning and initial science.

14.1 Classical MOS. An OWL first light instrument ?

For the sake of completeness, we have designed multi-slit spectrographs that could meet, in part, the MOMFIS science specifications. While the field of view would be significantly smaller, and the integral field spectroscopic advantage lost, we see a number of good reasons why a MOS spectrograph could be contemplated:

- Excellent first light instrument for telescope testing & commissioning, while allowing to carry out top science in the early telescope phases
- Compact, using the standard telescope adapter rotator
- Reasonable cost

Figure 17 shows a tentative design for a MOS instrument. Two optical designs were performed with reflective and transmission slit plane to illustrate that micro-mirrors or micro-shutters could be used, depending on their future developments and performance. Movable slits could be used instead. Note the F/1 camera in both cases. The Field of view with a F/1 camera and a 2k x 2k detector is ~ 1.1'. Optionally, 4 such instruments could be associated with a total field of ~ 2' x 2'. The mass of 1 spectrograph and cryostat is estimated to be < 500 kg. 4 such instruments could fit on the OWL adapter / rotator, perfectly matching the MCAO field of view, and offering unique science capabilities. Note that no ADC is included in the design.

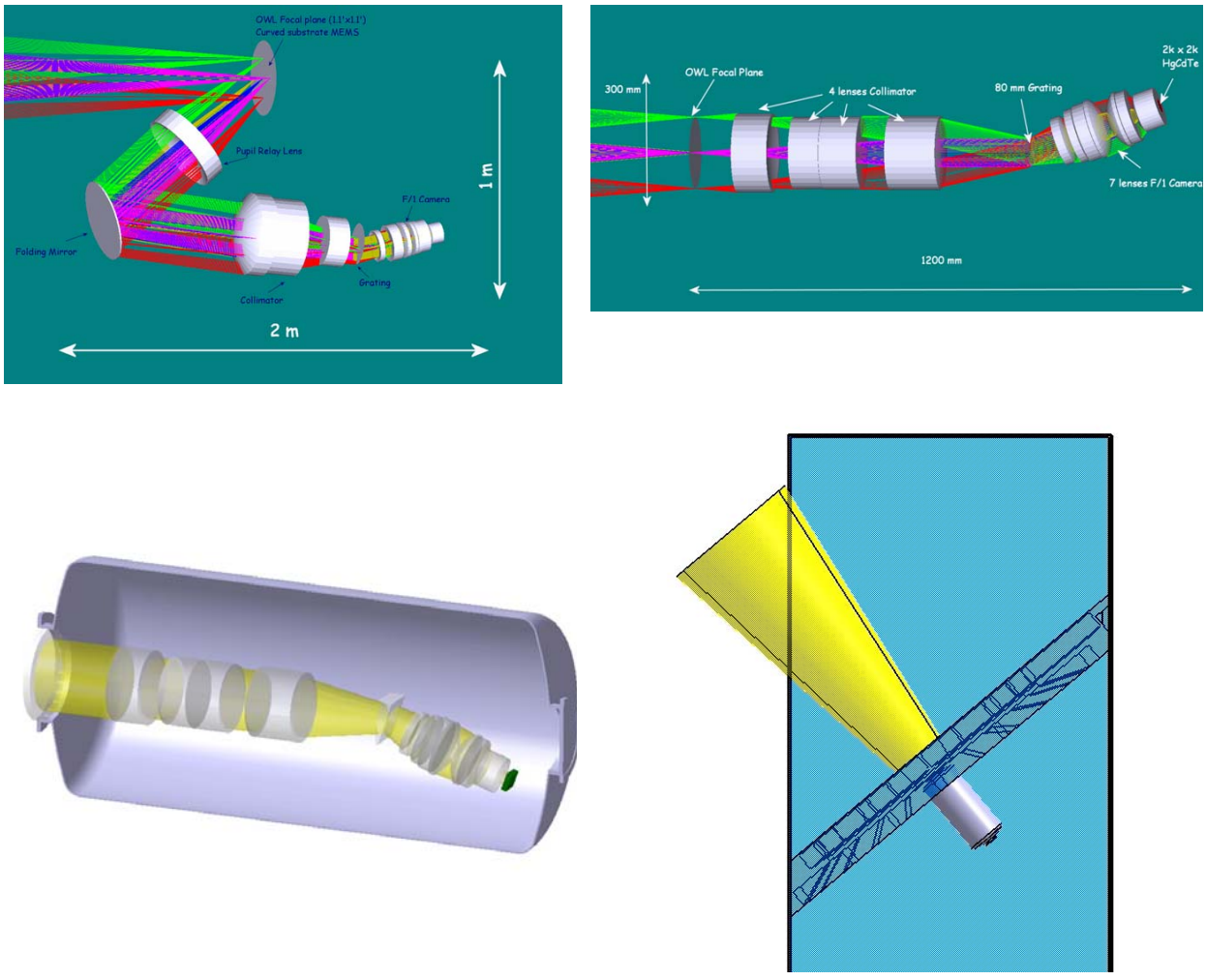

Figure 17 – MOS Alternative Design

UL: Optical design with micro-mirrors. UR:Optical design with micro-shutters. LL: cryostat concept (micro-shutter of movable slits design). LR: rough implementation in the OWL focal station.

Table 1 – Characteristics of the MOS design

Field of view	1.1' x 1.1'
Spatial sampling	30 mas
Beam speed	F/1
Number of objects	> 100
Spectral Resolution	4000
Total mass	< 500 kg

14.2 A (OH suppressed) fiber fed spectrograph

Another interesting alternative design could be to use fibres. Although we were not keen to consider fibres for the regular baseline instrument, we consider useful to mention this possibility, as it may become a very serious one if OH suppressed fibres being developed elsewhere come to reality. These fibres could have built-in OH suppression (in the form of Bragg gratings) at a resolution of 10,000 or higher, providing a perfectly clean spectrum, free of all OH lines. The spectrograph would just need to provide a spectral resolution of a few 1,000 to better resolve the lines in the target spectra.

In this case, the instrument would consist of the MOMFIS parts until the image slicer (i.e. pick-off mirrors, BSM, DMs and ADC), and the fiber link would play the role of image slicer (fibre bundles) relaying the light to the spectrographs all assembled in a cryostat located in the space reserved for heavy instruments below the telescope altitude cradles [RD03]. For the sake of completeness we checked that our baseline MOMFIS spectrographs could fit in one single technical room. This is illustrated Figure 18, all spectrographs, arranged back to back, fit in a cylinder 3 m long and 2 m in diameter.

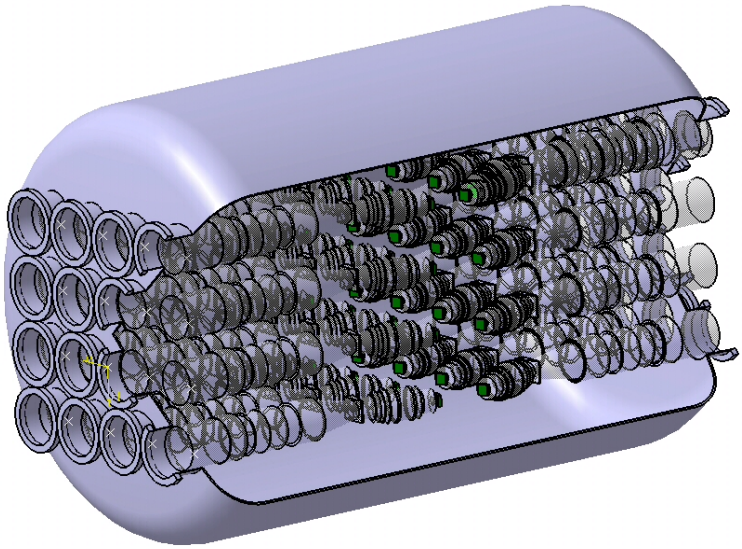

Figure 18 – Sketch of the 30 MOMFIS spectrographs assembled in a single cryostat

15. GROWING TELESCOPE

Both the MOMFIS baseline concept and the alternative multi-slit (MOS) concept could be used in the 'growing telescope' phase, under the condition that the telescope pupil is grown in an annular shape (no need for rotating pupil masks).

16. BUDGETS

- **Mass budget**: the estimated mass of the baseline instrument is ~ 25 tons, with a total range of 15-25 tons, depending on options and final characteristics.
- **Throughput budget**: the estimated throughput of the whole optical train (per channel) is ~ 30%
- **Thermal budget**: the baseline instrument foresees thermal stabilization at the site median temperature (or slightly lower). This requires less than 1 kW of heating / cooling. Option#2 foresees cooling at -40°C, which would require ~ 10 kW of cooling power.

17. COST AND SCHEDULE ESTIMATE

MOMFIS is a complex instrument. Its development and integration will require a broad range of expertise and facilities across Europe. The hardware cost is estimated to be in the range 30-40 M€, depending on the selected options, and the required manpower (at institutes) in the range 150-250 person-years. The instrument development requires 10 years, including a few years of continuing R&D activities.

18. NON COMPLIANCE ISSUES AND FEEDBACK TO OWL

The main non-compliance issues with telescope interface raised by MOMFIS as designed are:

- Adapter rotator provided by interface not adequate (2 tons limit). This adapter rotator has been removed and replaced by a larger one (4.5 m diameter).
- A consequence is that the OWL guide / adaptive optics probes cannot be used. MOMFIS provides alternative WFS probes, however different from the original ones. The telescope has to rely on these probes, hence creating a difference between instruments
- Another consequence is the reduction of the technical field available for the guide probes by a factor 2 in area
- Weight. The baseline exceeds the specified weight limit by 5 to 10 tons. Optional designs with reduced characteristics (e.g. number of channels or size of individual IFU fields of views) could comply with the mass budget
- Instrument handling. It is unclear whether and how the instrument can be integrated at all in the focal station as it is.

More generally, the OWL focal station hanging in the middle of the telescope is a serious concern for integration and maintenance purposes. This is in particular so because all the instruments share the same physical location and severe conflicts between the various instruments and telescope maintenance and integration activities can be expected.

Additional feedback comments to OWL and ESO as the organization leading the efforts towards the realization of the European ELT are:

- **Telescope diameter**. Good for science, but severe performance risks, in particular in adaptive optics
- **Number of telescope mirrors**. Possibly not better or worse than other ELT designs providing less telescope mirrors but adding mirrors for GLAO/MCAO.
- **F/6 beam**. A severe constraint for instrument design, back focal distance, etc.
- **Focal station vs gravity**. Not having a gravity stable platform is not a show stopper (e.g. Cassegrain instruments on other telescopes), however definitely an added difficulty for instrument design, development, and later for integration and maintenance.
- **Adaptive Optics**. To be studied and developed at telescope system level, whether it is part of the telescope or of the instrument
- **Sky coverage**. Poor sky coverage does not seem to be an option for an ELT as a science factory. Aggressive studies of the sky coverage and use of laser guide stars are strongly recommended.
- **Standardization**. Preliminary definition of the standards shall start as soon as possible, in particular for electronics that requires significant weight and volume reduction compared to VLT electronic standards.
- **Preparing the community**. ELT instruments will require huge resources and facilities from the community. European programs such as OPTICON and ELT Design Study are extremely successful in getting the community involved and ready, and these programs shall be continued and strengthened.
- **Extending instrument studies**. The OWL instrument studies are an excellent and more focused complement to the instrumentation activities carried out in the

OPTICON and ELT Design Study programs. They should be continued after the OWL review has taken place as the project evolves.

19. ABBREVIATED TERMS

Abbreviations used in this document are provided below.

Abbreviation	Meaning
ADC	Atmospheric Dispersion Compensator
AO	Adaptive Optics
BSM	Beam Steering Mirror
DM	Deformable Mirror
ELT	Extremely Large Telescope
ESO	European Southern Observatory
FALCON	Fibre spectrograph with Adaptive optics on Large Fields to Correct at Optical and Near-infrared
FEA	Finite Element Analysis
FOV	Field of View
FWHM	Full Width at Half Maximum
GLAO	Ground Layer Adaptive Optics
GS	Guide Star
HST	Hubble Space Telescope
ICD	Interface Control Document
IFU	Integral Field Unit
JRA	Joint Research Activity
LGS	Laser Guide Star
LN2	Liquid Nitrogen
mas	Milli-arcsec
MCAO	Multi-Conjugate Adaptive Optics
MLI	Multi Layer Insulation
MOMFIS	Multi-Object, Multi-Field IR Spectrograph
MOAO	Multi-Object Adaptive Optics
MOS	Multi-Object Spectrograph
N/A	Not Applicable
NGS	Natural Guide Star
OWL	Overwhelmingly Large Telescope
PSF	Point Spread Function
PTV	Peak To Valley
QE	Quantum Efficiency
TBC	To Be Confirmed
TBD	To Be Determined
TMT	Thirty Meter Telescope
VPH	Volume Phase Holographic
WFE	WaveFront Error
WFS	WaveFront Sensor

OWL Instrument Concept Study

MOMFIS

Multi-Object, Multi-Field IR Spectrograph

II. Scientific Specification (Science Case)

LAM.SCT.MOMF.SPS.050117_01

Prepared by :	Signature
J.-P. Kneib for the Science Team Date : 15/09/2005	
Approved by :	Signature
J.-G. Cuby Date : 15/09/2005	

Centre National de la Recherche Scientifique - Laboratoire Astrophysique de Marseille - UMR 6110 BP 8 – 13376 Marseille Cedex 12, Tel. : 33 +4.91.05.59.00 - Fax : 33 .+4.91.05.59.47

Change Records

Date	issue	Révision	Modification	Pages
17 Jan 2005	1	0	Preliminary report	All
15 Sept 2005	2	0	Final report	All

Distribution List

Institute	Name	Issue/Revision									
		1.0	2.0								
LAM	J.G. Cuby	X	X								
LAM	J.P. Kneib	X	X								
LAM	E. Prieto	X	X								
LAM	N. Manzone	X	X								
LAM	P.E. Blanc	X	X								
LAM	D. Burgarella	X	X								
LAM	O. Le Fèvre	X	X								
GEPI	F. Hammer	X	X								
GEPI	P. Jagourel	X	X								
GEPI	P. Vola	X	X								
GEPI	M. Marteaud	X	X								
GEPI	M. Puech	X	X								
LESIA	Y. Clénet	X	X								
LESIA	D. Rouan	X	X								
CRAL	R. Bacon	X	X								
CRAL	E. Pécontal	X	X								
CRAL	M. Tallon	X	X								
ONERA	G. Rousset	X	X								
ONERA	T. Fusco	X	X								
ESO	M. Casali	X	X								

Table of contents

List of figures

1. INTRODUCTION

This document presents a motivating science case for the OWL telescope using an infra-red multi object multi-field Infra-Red spectrograph (MOMFIS). This document will help define the technical specifications required for this instrument.

In particular, we want to constrain the following quantities:

- The exact wavelength coverage of the instrument: for example: 0.9 to 2.5 micron, in particular we want to justify or not the need for the K-band and possibly longer wavelength bands. A different instrument may cover the> 3-micron window though.
- The multiplex capability needed for such an instrument and how it is obtained: with multi-slit, multi-IFU, or with a unique large IFU, by discussing the merit of the different solutions.
- The size of the field of view to be covered (where slits/IFUs have to be placed) and the total size of sky covered by the multi-IFUs or the single IFU.
- The spectral resolution needed as a function of wavelength, and the number of photometric bands to be covered.
- The number of detectors, which is a function of the multiplex of the instrument and the spectroscopic mode to be chosen.
- The spatial resolution needed to be achieved and as a consequence the pixel size.

In order to quantify these values, we will need to characterize the following parameters:

- The expected target size,
- The expected target density as a function of wavelength (or photometric bands),
- The expected target flux,
- The target SED and emission/absorption line properties and strengths,
- The typical observing time needed to observe the targets,
- The observational strategy for the science programmes and their estimated duration for completion.

We will try also to put the proposed science in the perspective of the other instruments and facilities that will likely be in function before or at the time of OWL. This can have an impact in the target selection, and thus on the science that can be achieved.

Note: in this report we will use WMAP cosmology (Ω_m=0.3, Ω_λ=0.7, H_0=70 km/s/Mpc). Size will generally be expressed in mas (mili-arcsec) and all magnitude will be quoted in the AB system. We recall that 1 nJy corresponds to an AB magnitude of 31.4, and that for standard infra-red filters: $J_{AB}=J_{vega}+0.9$, $H_{AB}=H_{vega}+1.4$, $K_{AB}=K_{vega}+1.9$

2. SCOPE

This document concentrates on one science case (the first galaxies in the Universe) and derives the top level specifications required for this particular case. This corresponds to the Statement of Work of the MOMFIS study ([AD 01]). The analysis presented in this document was largely performed independently from similar work carried out e.g. by the OPTICON ELT

science case working group. It is satisfactory and encouraging that both analyses derive the same conclusions and very similar requirements.

3. REFERENCES

3.1 Applicable Documents

[AD 01]	OWL-SOW-ESO-00000-0152	1.0	03 Dec. 2004	Statement of work for a conceptual study of an IRMOS for OWL
[AD 02]	OWL-ICD-ESO-00000-0139	1.0	5 Oct. 2004	Interface Control Document
[AD 03]	OWL-CSR-ESO-00000-0147	1.0	24 Sep. 2004	Framework of OWL instrument concept design studies

4. MAIN SCIENCE CASE: THE FIRST GALAXIES IN THE UNIVERSE

4.1 Introduction

In the last five years, our understanding of the high redshift Universe has been challenged by the discovery of a number of 5<z<~7 galaxies (e.g. Franx et al 1999, Ellis et al 2001, Hu et al 2002, Cuby et al 2003, Santos et al 2004, Kneib et al 2004, Yan et al 2004, Bunker et al 2004, Bouwens et al 2004). Those galaxies have been either detected through ground-based narrow-band imaging with the current largest telescopes (at redshift z~5.7 and z~6.5 which correspond to the reddest optical windows clean of strong OH lines), or using the 'classic' Lyman-break drop-out technique mostly using deep Hubble Space Telescope (HST) images with ground-based spectroscopic confirmation using the largest telescopes available. Other search where done through direct blind spectroscopic (Santos et al 2004, Martin & Sawicki 2004). Most of the studies where done in blank fields, but a few others used the gravitational magnification of massive clusters. Lensing is particularly useful in magnifying distant objects thus allowing to unravel their morphology, or to detect the faintest objects that would otherwise be impossible to detect. Figure 1 shows the lensed arc (z=4.9) in the cluster MS1358+62 where a complex structure with 7-8 blobs of typical size of 20 mas each are revealed. This extreme example is showing a complex morphology, which may be common at very high redshifts where active star formation will appear in the densest region of the fragmented clouds.

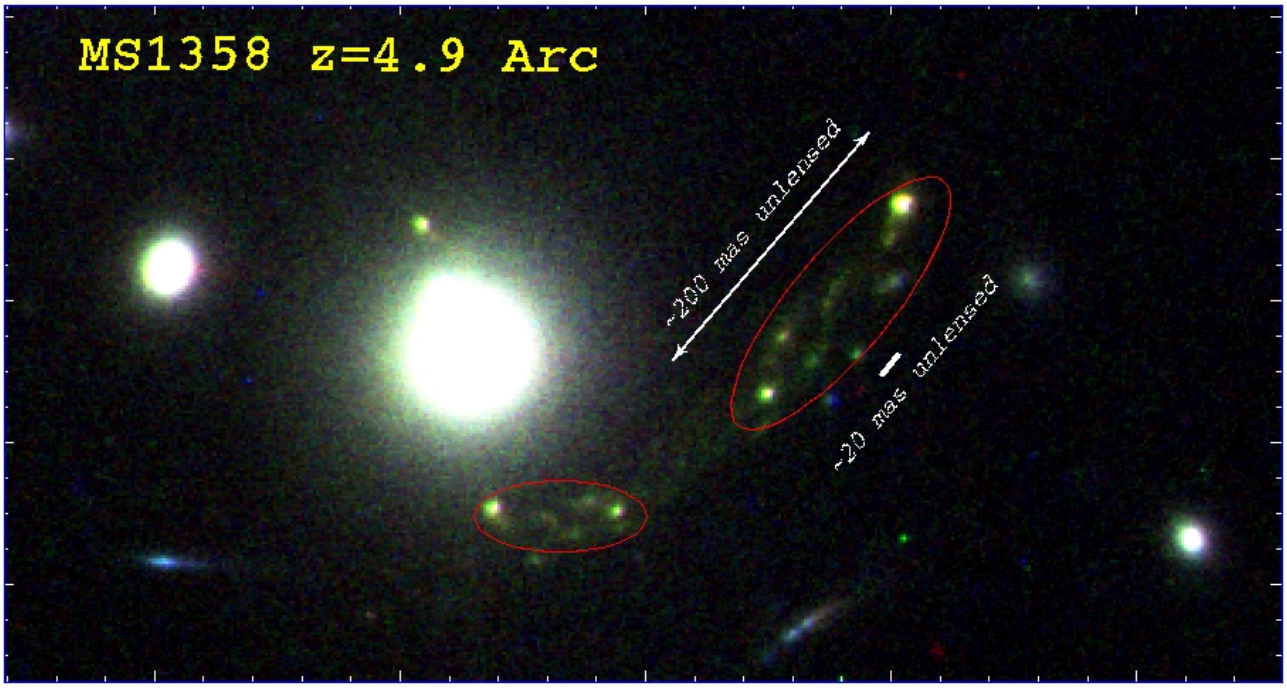

Figure 1 – HST/ACS color image (RIZ) of the MS1358+62 arc at z=4.9.

The arc consists of 2 images as indicated by the 2 red ellipses. Due to the large magnification of ~20 (for the largest ellipse) the unlensed size of the images is about 200 mas. Note that the arc, as likely other high redshift sources, displays a very complex structure of 7-8 blobs, each of them having a typical size of about 20 mas.

Some of these galaxies have been recently detected with *Spitzer* allowing a more complete detailed spectral energy distribution analysis (Egami et al 2005 and Figure 2, Eyles et al 2005) using multi-wavelength data (covering the 1 to 5 micron region). In particular they show that at z~6 a fair amount of old stars are already in place, advocating that the first epoch of star formation happened at even larger redshift (likely z>10).
More recently, pushing the current largest telescopes to their limits a number of even higher redshift candidates (z>7) have been tentatively identified (Pello et al 2004, Bouwens et al 2005, Richard et al 2005).
But going over the z=7 limit, means moving to the infra-red wavebands (redder than 1.0 micron) as the strong UV continuum of star-forming galaxies is red-shifted in the near infra-red. Although, the current attempts to break the z~7 barrier have identified some candidates, it is unlikely that a large number of such systems will be discovered and studied in detail before the next generation of instruments and telescopes come on-line. Although, the new generation of ground based multi-objects spectrographs (MOIRCS on Subaru, EMIR on GTC and KMOS on VLT) to be installed on 8-10m telescopes will likely provide useful constraints on the brightest z>7 candidates that are being discovered, such study will likely only be possible thanks to the gravitational amplification of cluster lenses and will likely be limited to a few tens of objects. Furthermore, very limited spatial and dynamical information are likely to be gained except may be in a very few number of exceptional strongly magnified cases similar to the z=4.9 source shown in Figure 1 (for example using OSIRIS with laser guide star on Keck).

The next generation of telescope such as the James Webb Space Telescope and the Extremely Large Telescopes (ELTs) will be **the facilities** that will allow a detailed study of star formation in the z>7 Universe (corresponding to the first billion years in the history of the Universe). Other facilities working at other wavelength will also probe such high redshift region but will be sensitive to different physical phenomenon: ALMA will probe the dusty part of this period showing or not the importance of dust in the early assembly of galaxies; large aperture X-ray telescope will probe the AGN activity and show when and how the first black holes where formed; sensitive Gamma-Ray telescope may probe the death of the most massive stars in the very early Universe. Each of these probes will be complementary in studying this distant part of our Universe, which will remain out of reach before these facilities come on line.

The immediate application of a 1-2.5 micron facility will be to measure accurately the number density and the spectral and dynamical properties of high redshift star forming galaxies at z>7. These measurements are particularly interesting for two main different reasons:

Reionization: After the Big-Bang the Universe cooled down and neutrons and protons combined together to form neutral hydrogen. Latter on, the first stars and galaxies formed by the collapse of hydrogen clouds within dark matter halos, thus ending the Dark Ages of the Universe. The very low metallicity composition of the Universe in the early times favours the formation of very massive stars (up to 1000 solar mass, Abel et al 2000, Bromm & Larson 2003, Schaerer et al 2003) – the so called population III stars – which because of their strong UV flux start to re-ionise the intergalactic medium (IGM). When the flux density of UV photons coming from the forming stars/galaxies was large enough that all the Universe quickly 're-ionises' itself. Although, we believe that galaxies and not quasars are responsible for the re-ionisation of the Universe (Yan & Windhorst 2004) we have only a rough idea of when that happened. The possible measurement of the nearly complete Gunn-Peterson absorption in front of the most distant quasars known to date at z=6.0-6.4 (Djorgovsky et al 2001, Beckert et al 2001), and the WMAP measurement of the optical depth of Thompson scattering by reionised electrons (Kogut et al 2003) both suggest that re-ionisation occurs between redshift 7<z<15 (corresponding to a period spanning from 250 Myr to 750 Myr after the big-bang). Witnessing this phase transition of the Universe and how exactly it happened is key to our understanding of its evolution.

Population III stars: the first stars were made of the nucleo-synthesis material and thus contains almost no metals (compared to the Solar metallicity). Because of their very low/zero metal content we expect those stars to be very massive and very hot and thus have a very short life-time, some of them, depending on their exact mass, ending as bright supernova, possibly producing a burst of gamma-rays. Pop III stars are predicted to first appear in the Universe at some point between $30 < z < 50$ (see e.g. Yoshida et al 2003, Cen 2003, Mackey et al 2003, Wise and Abel 2003), and to cease being formed when the metallicity exceeds a critical metallicity Z_{crit} that is estimated to be in the range $Z_{crit} \sim 10^{-4}$-10^{-3} $Z_{\odot}$ (see e.g. Oh et al 2001, Bromm and Larson 2003). This threshold may well be exceeded as early as $z \sim 15$ (Mackey et al 2003, Yoshida et al 2003) but some Pop III star-formation may survive alongside higher metallicity star-formation to redshifts $z \sim 5$ if the mixing of metals in the intergalactic medium is incomplete (see e.g. Scannapieco et al 2003 for detailed models). Because of their high-temperature (>90 000 Kelvin) these stars will ionise twice Helium, thus producing a strong HeII emission lines, which will however last only a few Myr. The most prominent emission line features of the first stars/galaxies will however be the

Lyman-alpha line. However, till the Universe is fully re-ionize, Lyman-alpha can be strongly absorbed making unclear the probability of visibility of this line in the 7<z<15 window. Observation of the shape of the absorbed Ly-alpha line may constrain the geometrical properties, importance of outflows and dust content and distribution of the first objects as well as the line of sight distribution of the faint undetected galaxies (Wyithe and Loeb 2005). Moreover, as shown at lower redshift (z~2.5) by Pettini et al (2002) it is reasonable to think that metallic absorption lines at 1450 and 1900 angstroms can be used to trace the metallicity of galaxies and monitor the metal enrichment of the IGM over this period.

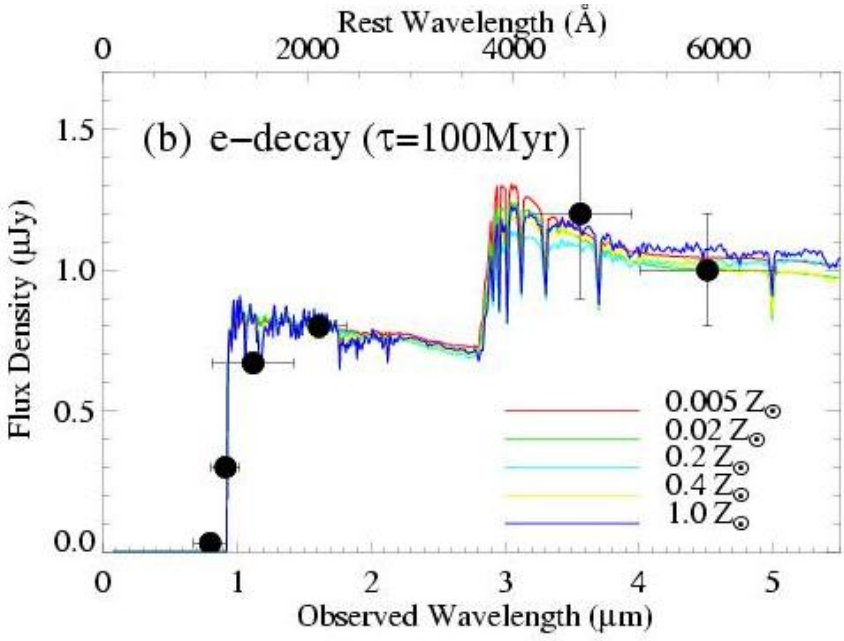

Figure 2 – The Spectral energy distribution of one of the most distant galaxy known to date at z~6.8 (Egami et al 2005)

The UV light is detected in the 1-3 micron window, as the optical light is shifted to the 3-6 micron window.

As detailed above, the infra-red domain (0.9 to 2.5 um) is particularly well suited to probe the UV continuum and Ly-alpha and HeII lines of the first star forming galaxies covering the 7<z<~15 period. The mid infrared domain (3 to 6 micron) will cover the rest-frame optical light (the older star population) of galaxies over the same redshift range. It is however likely that the higher the redshift the less likely it will be to find old stars; furthermore these wavelength are very difficult to observe through the Earth atmosphere, making a space telescope a better observatory for this domain.

The re-ionisation of the Universe and the study of the very first galaxies harbouring the population III stars is thus clearly a domain of investigation for the future decades, and in particular for a near-infra-red instrument on OWL.

4.2 Observing the 7<z<15 Universe

Particularly relevant to this science topic, is the next generation space telescope: the James Webb Space Telescope (JWST). JWST is a NASA/ESA 6.5m (if not de-scoped) near infrared optimised telescope to be placed at L2 around 2013. JWST will have 3 instruments on board: (1) NIRCAM a 0.6 to 5 micron imager, (2) NIRSPEC a multi-slit (3.5'x3.5' field of view, with up to 100 slits, and 200 mas slit width) spectrograph, having also a single IFU (~3"x3" field of view) and covering the 1.0 to 5 micron domain, and (3) MIRI a 5 to 25 micron imager.

Figure 3 gives the expected sensitivity for JWST as a function of wavelength in imaging and spectroscopy mode (R=1000). Although JWST will be very powerful in imaging mode reaching in 100 ksec nJy sources (or 31.4 AB mag) in the 1-4 micron interval, these faint objects to be discovered are likely to be unreachable in spectroscopy mode using JWST itself. Indeed for a resolution R=1000 in 100 ksec, the 10 σ JWST limit will be of the order of ~100 nJy (or 26.4 AB mag). This spectroscopy limit corresponds to the faintest objects detected in the recent Hubble Ultra Deep Field (UDF). Thus, JWST should in principle be able to measure the redshift of most of the objects detected in the UDF, a handful of them being $6<z<8$ galaxy candidates (Bouwens et al 2004) and may be a few will be at even higher redshift ($8<z<10$, Bouwens et al 2005). Although JWST is likely to image with NIRCAM $7<z<\sim20$ galaxies, it is much less certain that it will be able to measure the spectra of a large number of galaxies at $z>10$. However, this will depend strongly on the luminosity and size evolution of galaxies beyond $z\sim7$, which will likely remain unknown until JWST is launched. Note, that some understanding may be gained sooner using gravitational telescope using HST/NICMOS, or possibly WFPC3 if it could be successfully implemented on HST. Those studies will likely only guide the design of future telescope and instruments, but not give a comprehensive picture of the early Universe as required to really understand galaxy formation.

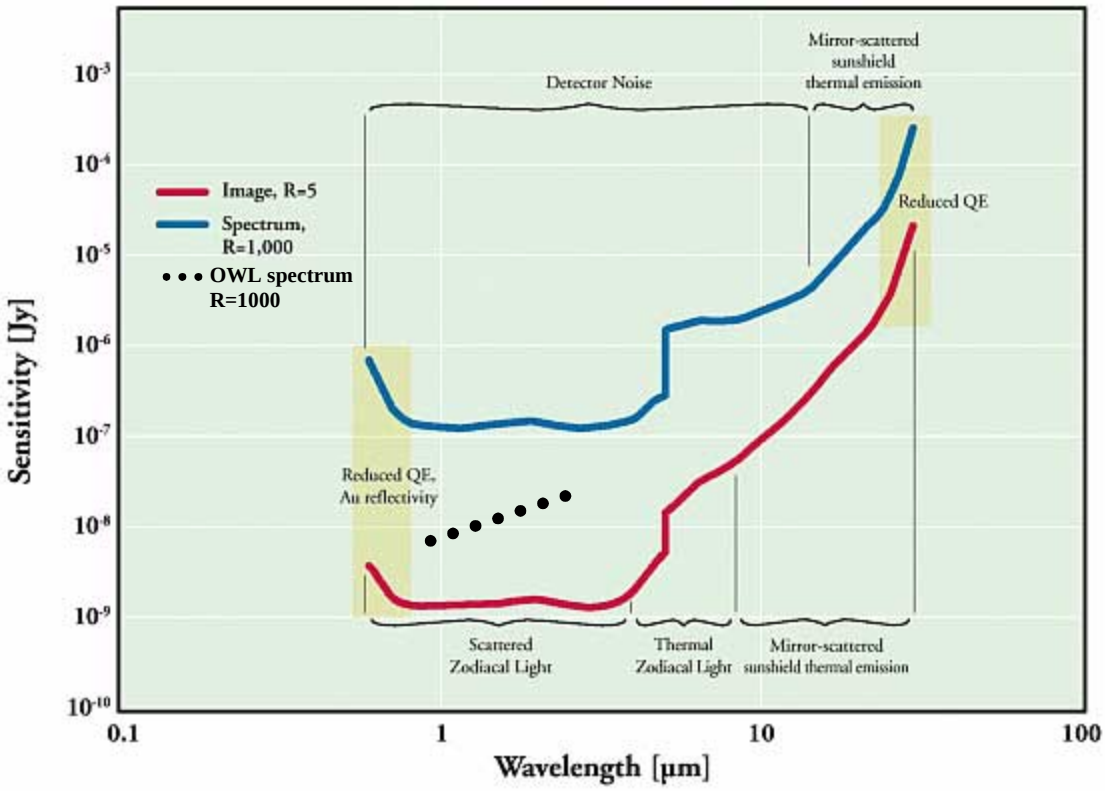

Figure 3 – Expected JWST sensitivity as a function of wavelength for imaging and spectroscopy

The two lines show the limiting, 10 sigma flux for a point source at the North Ecliptic pole over a 100 ksec exposure time, red curve is for imaging mode (R=5), blue curve is for spectroscopy with R=1000; the jump at 5 micron is caused by the switch in detector technology. The dots correspond to the expected OWL limits in spectroscopy mode (R=1000) *for a **10 ksec exposure*** as given by the ESO OWL ETC.

The spectra of the very first galaxies in the Universe is thus likely to come with the advent of the Extremely Large Telescopes (ELTs) planned to be built in the next decade. For example, with a 100m telescope (the OWL concept studied here) we will be able to image and take high signal to noise spectra of the galaxies re-ionizing the Universe, and we will also likely witness the very first stars either directly or through the detection of their SuperNovae (SN). In Figure 3 we are contrasting the likely sensitivity of OWL in spectroscopic mode to the one of JWST (note the different integration time). Compared to 30-m class telescope, OWL should be at least 10 times more sensitive (gain in collecting area, but also a possible gain due to sharper PSFs), which will effectively allow taking spectra of the very first objects. In comparison a 30-m ground based telescope will be slightly better than JWST in terms of sensitivity in the near infrared domain. At longer wavelength (>2.5 micron, the thermal emission of a ground-based telescope and the atmosphere are likely to be too important to be competitive to a space facility like JWST, restricting the ground-based interest of this domain to brighter targets.

With these above considerations in mind, we believe that a near infrared spectrograph on OWL covering **the 0.9 to 2.5 micron domain** could address the following science topics regarding the early Universe:

1. A detailed study of galaxy evolution in the high redshift Universe: 7<z<15 (when Ly-alpha is entering the IR domain, and when HeII is leaving it) by taking spectra and measuring the redshift of the order of ~5000 galaxies. Such survey will allow to study in detail:
    - The luminosity function as a function of redshift and environment (in particular the characterisation of the faint end slope, which should be compared to galaxy halo mass function prediction);
    - Measure galaxy size as a function of redshift and luminosity, thus probing the early assembly of galaxy structure;
    - Measure the clustering evolution which may constrain the early galaxy formation theories
    - Characterisation of the galaxy SED (although this will be relatively limited as we will only be sensitive to the UV rest-frame with this instrument) which will help characterising the IMF of those galaxies and the impact of dust;
    - Measuring the Ly-alpha line profile and intensity and contrasting it to the HeII line, which give clue on the importance of Pop III stars, and the importance of dust absorption, which may give a statistical picture of the structure of the first galaxies;
    - Characterisation of the IGM and the amount of metals, through the measurement of metal absorption lines that will characterised the metallicity of galaxies;
    - Probe quasar formation earlier than z=7 (we expect a few percent of the galaxies having AGN activities);
    - Constrain the star formation history at z>7, which will impact galaxy formation theories;
    - Constrain the epoch of re-ionisation and determine how quickly this phase transformation last.

2. Probing the epoch of the formation of the first stars/galaxies likely to be at z>9, that could possibly be followed up to z~18 when Ly-alpha is leaving the K-band window
    - Measure the redshift of the very first galaxies up to z~18 and measure their dynamical properties,
    - Probe the nature of stars in the most distant galaxies: pop II vs. pop III (using the HeII emission line as a tracer for pop III stars, only possible until z=15).

3. Measuring the redshift of supernovae at z>2.5 up to the z~18, and determine the properties of their host galaxies:
    - Detecting the SN of Pop III stars, possibly in combination with wide-field SNe search conducted with OWL or other near-infrared telescopes, or by gamma-ray burst experiments;
    - Constrain the physics of the supernovae of very massive stars, by a spectroscopic monitoring of high redshift SNe;
    - Test possible Cosmological implication, particularly regarding the nature of the Dark matter and energy.

4. Use cluster lenses as additional natural telescope to characterize in details the structural and dynamical properties of the faintest and most distant galaxies that will likely be the

most demanding in terms of sensitivity. Lensing, may also help in the detection and study of high redshift SNe.

In the next section, extrapolating the latest observations and theoretical prediction of the high redshift Universe, we will try to quantify the parameters expected to characterize the galaxy population at z>7 that can be studied with OWL, as well as discussing the other 3 topics above that are the key science drivers of the MOMFIS instrument.

5. EXPECTED PROPERTIES OF THE FIRST GALAXIES

5.1 Galaxy number density

One of the first parameter we ought to estimate is the galaxy number density of high redshift galaxies. The easiest way is to extrapolate the number deduced from the numerous studies of z=5-6 galaxies, for example:

- UDF counts of z~6 galaxies: Bouwens et al 2004 (UDF optical and IR).
- Lensing estimates: Kneib et al 2004, Richard et al 2005

as well as comparing them to theoretical predictions such as Stavielli et al 2004

With a simple model we can estimate that the z > 7 galaxy number density will be a few per square arcmin per Delta-z (with of course a dependence on the redshift) down to magnitude AB=28-29 (the likely OWL spectroscopic sensitivity in 10ksec for S/N=5 and compact object). Figure 1 shows predictions for the cumulative galaxy number counts at rest frame 1500 Angstrom per photometric infrared bands from z~6 to z~14. Two scenario were assumed, one with no evolution just extrapolating the number density of sources from what we know at z~5 to higher redshift, and one with mild evolution. To the AB=28-29 limit we expect a few to a few tens object per square arcmin depending on the photometric band and the redshift probe. Of course the most difficult part is the highest redshift bin (12<z<15) where galaxies are substantially deemed and where the sensitivity of OWL is worse (in terms of AB magnitude), there we expect only one or at most a few objects per sq arcmin. With such densities, and with a dedicated efficient instrument it is therefore possible to foresee measuring the spectra of a few thousands of objects, which is needed to conduct proper statistical analysis of this distant population.

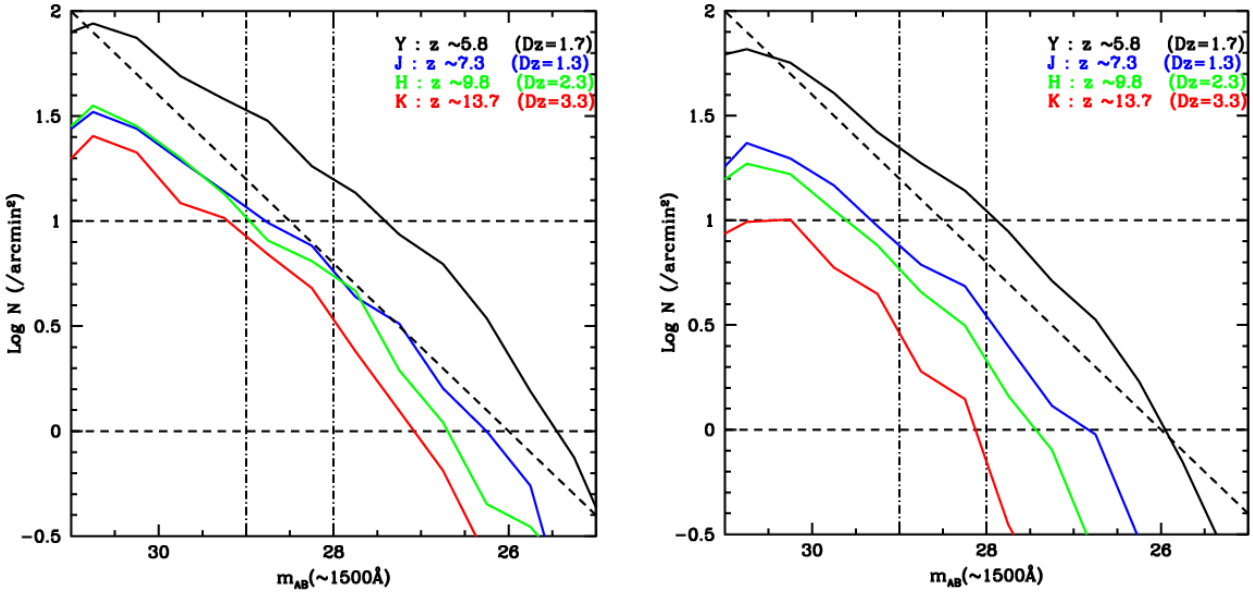

Figure 4 – Predictions of galaxy counts.

Counts prediction per photometric bands, assuming the LF of observed z~5 galaxies (Bouwens et al 2004, Stiavelli et al 2004, Yan et al 2004) and extrapolating it to higher redshift, assuming a non-evolving SED. Left figure is for a no evolution model of the luminosity function, the right figure has a mild evolution in number density. Model was stopped at m=31 which explain the incompleteness for fainter magnitude. Evolution in size of 1/(1+z) was assumed here. The vertical dashed lines are respectively the point source Y/J sensitivity (m=29) and H/K sensitivity (m=28) for a S/N of 5-10 and an exposure time of 10ksec, these numbers assumes a spectral resolution of R=1000 and a pixel size of 15 mas (following the OWL ETC).

5.2 Galaxy size and morphology

An other important parameter is the size and morphology of these distant galaxies. The current analysis, best discussed in Bouwens et al (2004) show that the typical galaxy size above z>4 (expressed in kpc) decreases with redshift, following a $1/(1+z)^m$ relation, with the exponent being in the following range: m=1.0-1.5. The favoured exponent value for this relation is m=1 as shown in Figure 5 and Figure 6.

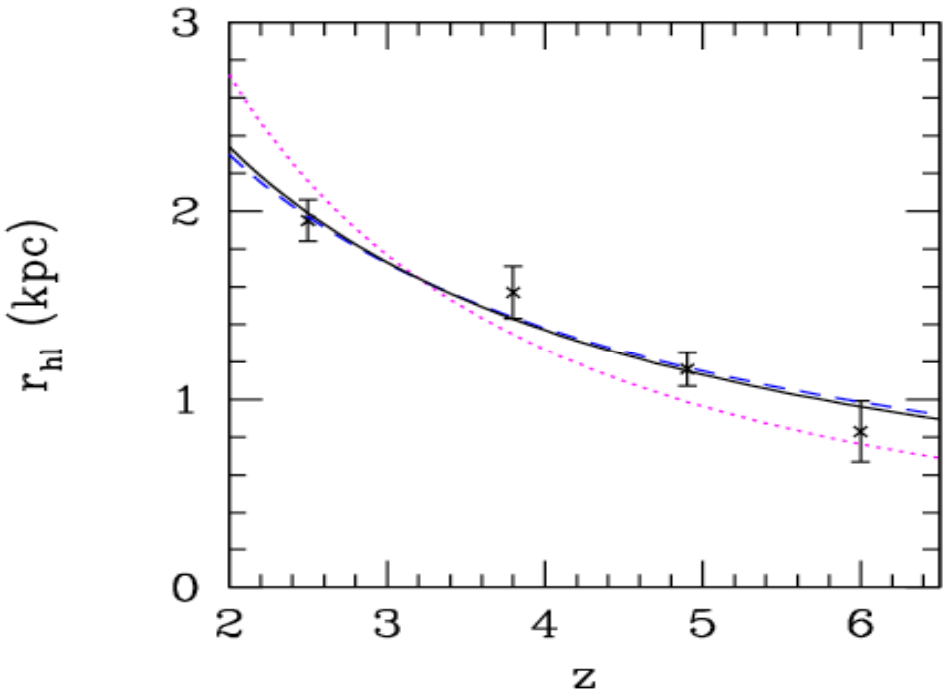

Figure 5 – Mean half light radius versus redshift for objects of fixed luminosity (0.3 − 1.0L*,z=3).

Shown are data (crosses with 1 erors on the mean) from z ~ 2.5 HDF-N + HDF-S U-dropout sample and UDF B, V , and I dropout samples plotted at their mean redshifts z ~ 3.8, z ~ 4.9, and z ~ 6.0, respectively (from Bouwens et al 2004). The dotted magenta line shows the $(1 + z)^{-1.5}$ scaling expected assuming a fixed circular velocity and the dashed blue line shows the $(1 + z)^{-1}$ scaling expected assuming a fixed mass (Mo et al. 1998). A least squares fit favors a $(1 + z)^{-1.05}$ scaling (solid black line).

Thus assuming a size of 1 kpc at z~6 (or 180 mas) [See Figure 5, but also Kneib et al 2004 for a lensing estimate], this means that:

- At z~10, the galaxy size has: 500-650 pc (120-150 mas)
- At z~15, the galaxy size has: 300-450 pc (95-110 mas)

To optimise the sensitivity, the spatial resolution of an instrument should in principle match the size of the objects to be studied. Considering the above estimate means that there is no need to achieve the diffraction limited image resolution of a 100m telescope. However, adaptative optics is required in order to achieve a 60-100 mas image resolution to match galaxy size. A pixel size of 30 mas would thus sample reasonably well the PSF.

However objects can be structured as seen in the strongly magnified arc in the MS1358+62 cluster shown in Figure 1. Thus to sample the different blobs in the galaxy, higher spatial resolution may be needed to optimise the sensitivity on the smallest components, it is therefore important to have at least one smaller pixel scale. This could be very critical for detection of SN in these very distant galaxies or the detailed study of the first quasars and AGN. Indeed the typical size of AGN taurus is believed to be less than 100 pc which would corresponds to 20 mas at z~6 or 30 mas at z~15. So a pixel scale of 10 is strongly desirable, as it will allow detailed dynamical measurement of those distant objects.

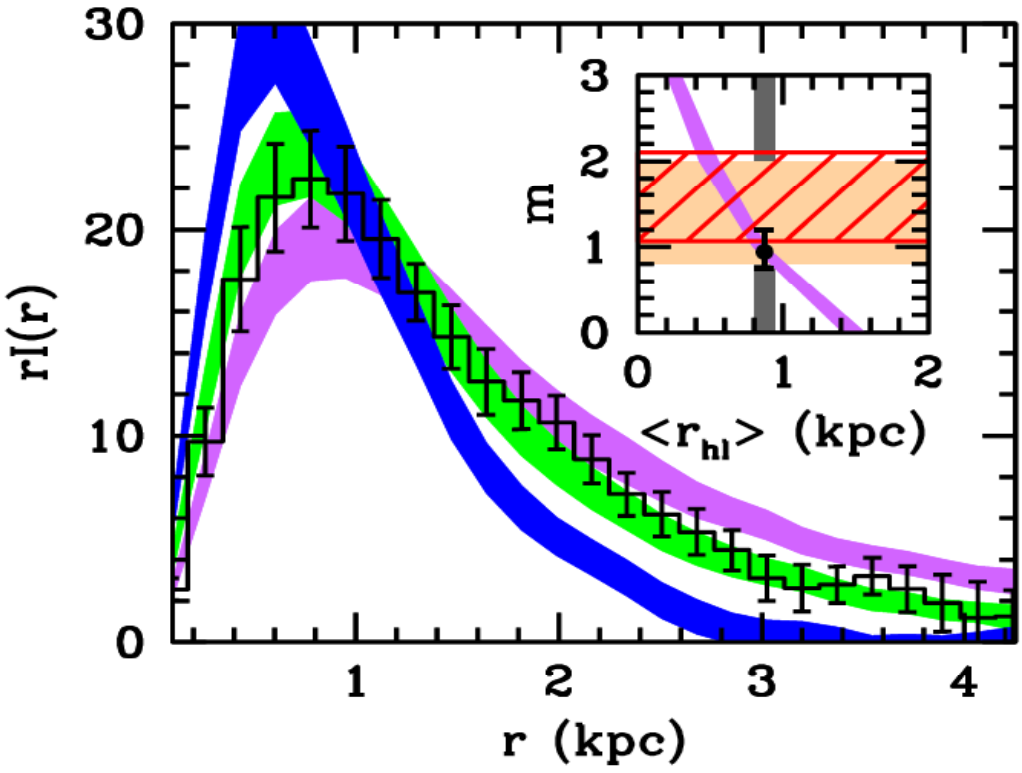

Figure 6 – Mean radial flux profile from a UDF i-dropout sample

The mean radial flux profile determined for the 15 intermediate magnitude (26.0 <z850,AB < 27.5) objects from our UDF i-dropout sample compared against that obtained from similarly-selected U-dropouts cloned to z ~ 6 with different size scalings: $(1 + z)^{0}$ (violet shading), $(1 + z)^{-1}$ (green shading), and $(1 + z)^{-2}$ (blue shading). The inset shows how the mean size of the projected U-dropouts (shaded violet region) vary as a function of the $(1+z)^{-m}$ size scaling exponent m. Since the mean half-light radius is ~0.87 kpc (shown as a gray vertical band), this suggests a value of 0.94 for the scaling exponent m (from Bouwens et al 2004). Note that the total extend of a galaxy is 5 to 6 times the half light radius.

5.3 The spectral energy distribution of the first galaxies

In the near-infra-red we will only be sensitive to the rest-frame UV spectrum of galaxies with 7<z<15. The spectrum will be dominated by the emission of the most massive stars and the spectral features that can be expected are the following:

- An almost flat continuum (expressed in f_{nu}), slightly decreasing with wavelength with a slope which will be steeper (bluer) for more massive stars or for less metallic stars. Note that the slope can be reddened by dust absorption;
- A Ly-alpha break due to the Gunn-Peterson absorption of molecular hydrogen distributed along the line of sight toward the object;

- A Ly-alpha line (1216 Angstrom rest) in emission (if the IGM is sufficiently ionised) with asymmetric absorption produced by outflows leading to an asymmetric line. However, the absorption can be complete depending on the geometry of molecular clouds around the stars and the amount of dust;
- The HeII line in emission (1640 Angstrom rest-frame) characteristic of Population III stars (Schaerer 2003, and Figure 8) and that should have a large equivalent width during the first few million years,
- Metal lines (Si and O in particular) in absorption will be useful to identify the redshift for the brighter objects when no emission line is present. They can also give interesting constraints on the metallicity of the IGM in these very distant galaxies, thus probing the metal enrichment of these systems.

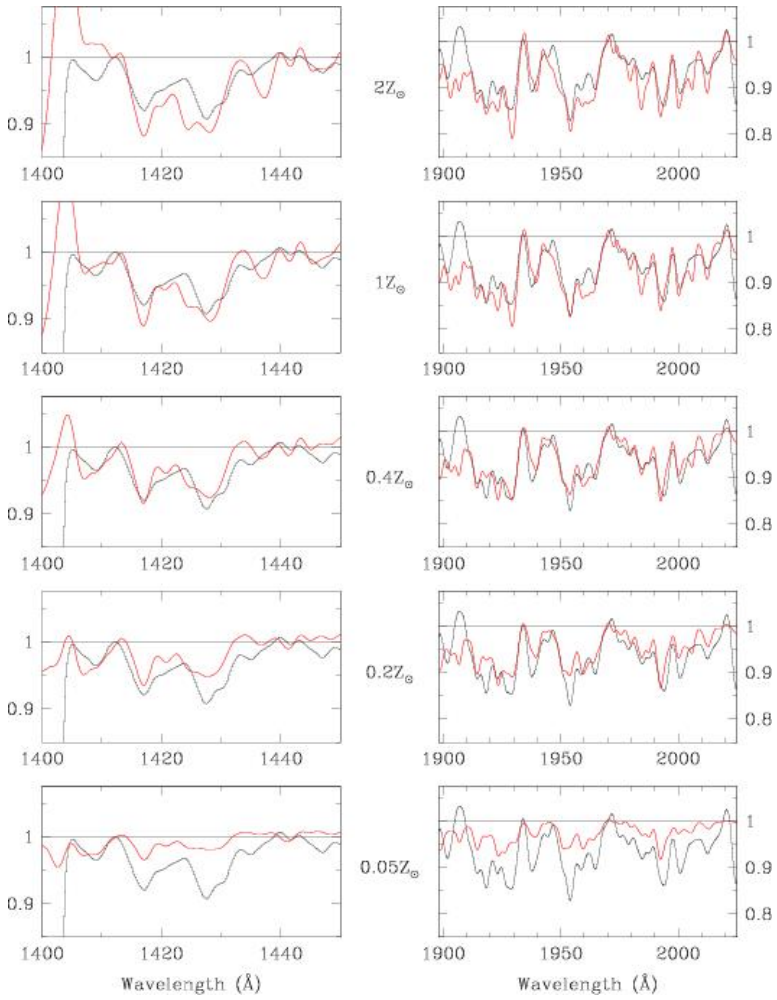

Figure 7 – The detailed UV rest-frame absorption features in the strongly lensed z~2.7 cB58 compared to star forming galaxy models with different metallicities.

These two spectral windows at 1400-1450, and 1900-2050 angstrom are probably the best ones to derive constrains on the metallicity of the IGM (Rix et al 2004).

The table below gives the redshift corresponding to Ly-alpha, HeII and 1500 angstrom continuum for the 4 standard infrared bands:

NIR Band and limits	z(Ly-alpha)	z(HeII)	z(cont at 1500A)
Y : 0.9-1.15	6.4-8.5	(4.5-6.0)#	5.0-6.7
J : 1.15-1.35	8.5-10.1	6.0-7.2	6.7-8.0
H : 1.45-1.80	10.9-13.8	7.8-10.0	8.7-11.0
K : 1.95-2.45	15.0-19.1	10.9-13.9	12.0-15.3

Note: # at these redshifts it is unlikely to observe HeII in galaxies.

The number in the table show that it is important to have wavelength coverage *on typically 2 IR bands* to be able to characterize the nature/physics of the first galaxies for a given redshift range as indicated with colour highlighting. Furthermore, it demonstrates that K-band will be useful for galaxies at z>10 in order to be able to measure the HeII line up to z=15 (then observed at 2.5 um).

5.4 Population III stars

Population III stars are thought to be the first generation of stars. Having low metallicity because they formed from primordial gas, they are expected to be very massive up tot 500-1000 solar masses. Being more massive, they will be hotter than population II stars and shorter lived. Their high temperature (>80 000K) means they will be able to ionize twice the Helium thus having a unique feature: the HeII emission line, to characterize them. Schaerer (2003) has in particular derived synthetic models shown in Figure 8 and Figure 9, characterizing the continuum and line properties of these Population III stars.

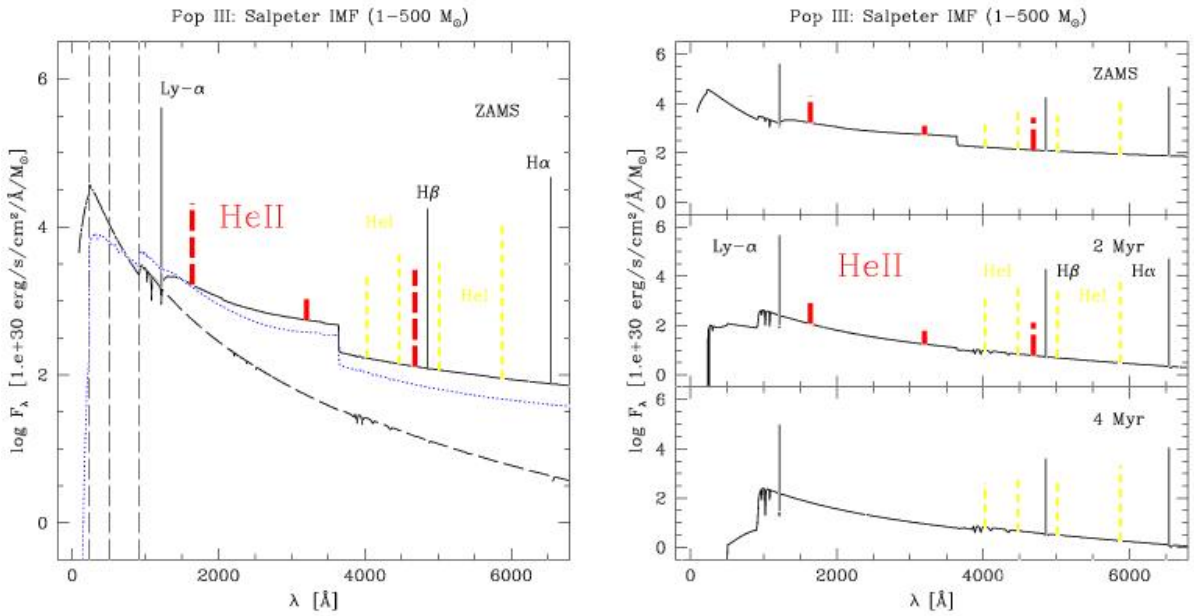

Figure 8 – The continuum and line properties of Population III galaxies (from Schaerer 2003)

The He II feature will not survive long as it equivalent width is dropping quickly after a few million years due to the enrichment of the IGM.

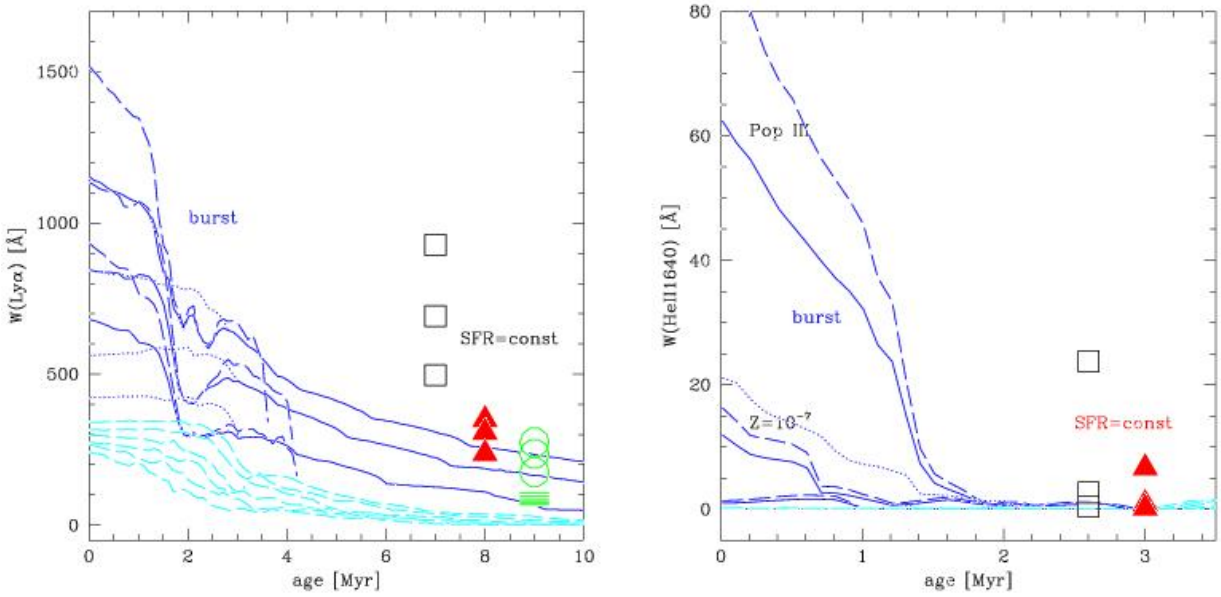

Figure 9 – Temporal evolution of the Ly equivalent width (left panel) and HeII equivalent width (right) for instantaneous bursts at all metallicities

The very metal-poor models (Z = 0, 10^{-7}, and 10^{-5}) with the IMFs C (50-500 $M_\odot$), B (1-500 $M_\odot$) and A (1-100 $M_\odot$) are shown as short-dashed, solid, and dotted lines respectively from top to bottom. The remaining metallicities (for IMF A) are shown with dashed lines. The equilibrium values for SFR= const at metallicities $Z \leq 10^{-5}$ are plotted on the right (at arbitrary ages) using open squares for the IMF C, filled triangles for IMF B, open circles for IMF A, and using short lines for higher metallicities (with IMF

A). Note the very large maximum W(Ly) predicted at young ages. W(HeII)>~5 Angstrom are only expected at the lowest metallicities ($Z<\sim10^{-7}$), except if hot WR-like stars not included in the tracks were formed e.g. through important stellar mass loss. (from Schaerer et al 2003).

5.5 Supernovae and Gamma-Ray Burst in z>7 galaxies

The detection and the study of Supernovae (SNe) is important for at least two reasons: 1. the use of local SNe (both type Ia and II) as 'calibrated' standard candles (Phillips 1993, Hamuy et al. 2001, Hamuy & Pinto 2002) provides a direct measurement of the expansion rate of the Universe H_0, and their detection at z > 0.3 allows to measure its deceleration parameter and to probe different cosmological models (Perlmutter et al. 1998, 1999; Riess et al. 1998); 2. The evolution of the cosmic SN rate provides a direct measurement of the cosmic star formation rate (SFR). Indeed the rate of core-collapse SN explosions (SN II, Ib/c) is a direct measurement of the death of stars with masses in the range 8-30 $M_\odot$ (although it is still debated if stars more massive than 30 $M_\odot$ could make "normal" type II/Ibc SNe, or rather collapse forming a Black Hole with no explosion at all, or even make a different kind of explosion like Gamma-Ray Burst; see, e.g., Heger et al. 2001).

Based on previous results obtained by Madau et al. (1998), Miralda Escude & Rees (1997), Mackey et al. (2003) and Weinmann & Lilly (2005), Della Valle et al (2005) estimate an observed rate of up to 2 SNe/yr per square arcmin (for any redshift). They also include the very powerful Pop III SNe that are expected to be produced by pair-creation in zero-metallicity massive stars, in the range $140-260M_\odot$ (Heger et al. 2001). We can estimate that SNe-Ia will be detectable up to $z\sim5$ while SNe-II (bright) up to $z\sim7-8$. The SNe of the most massive Pop III stars (>175 $M_\odot$), should in principle be easily detectable up to $z\sim20$ (Heger et al. 2001) as shown on Figure 10 and Figure 11. However, due to the Gunn-Peterson absorption Pop III SNe are unlikely observable beyond z~18. The SNe rate of Pop III stars is pretty uncertain, and different values can be found in the literature. The latest estimates by Weimann & Lilly (2005) are relatively low with a rate of 4 deg^{-2} yr^{-1} at $z \sim 15$ but obviously there is a very large uncertainty in these numbers and they will need to be confronted to observation. Hence, dedicated search will be necessary. The most massive Pop III SN should be relatively bright (in terms of a large aperture telescope) and should be found relatively easily with JWST or the next generation of ground based telescopes. The most massive SNe may also produce burst of gamma rays, which would be an alternative way of finding them. As shown in Figure 11, OWL/MOMFIS would provide an effective spectroscopic follow-up down to masses of 175 $M_\odot$.

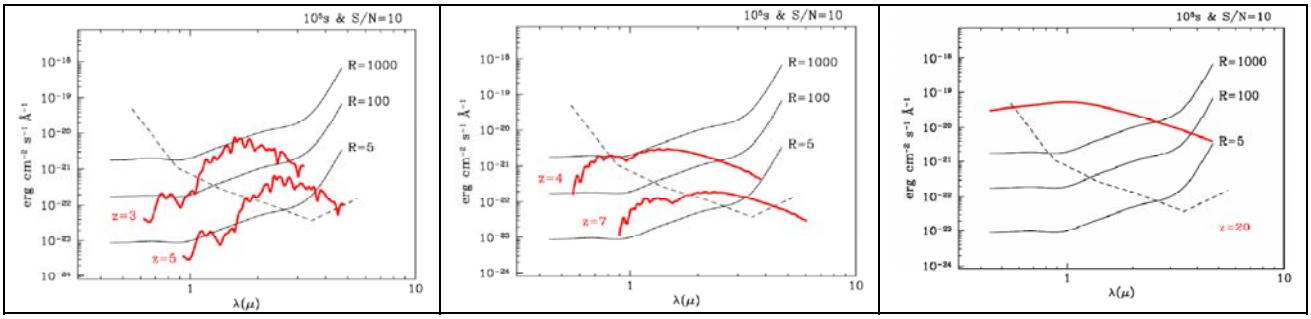

Figure 10 – The spectroscopic template for three types of SN templates as viewed in the rest-frame of the observer at different redshift.

Left: type Ia SNe; Center*:* bright SNII; Right: Population III stars) The three solid lines denote the fluxes corresponding to a S/N=10 for OWL exposures of 100 ksec at different resolutions. The dashed line is the threshold (R=5) for JWST (from Della Valle et al 2005).

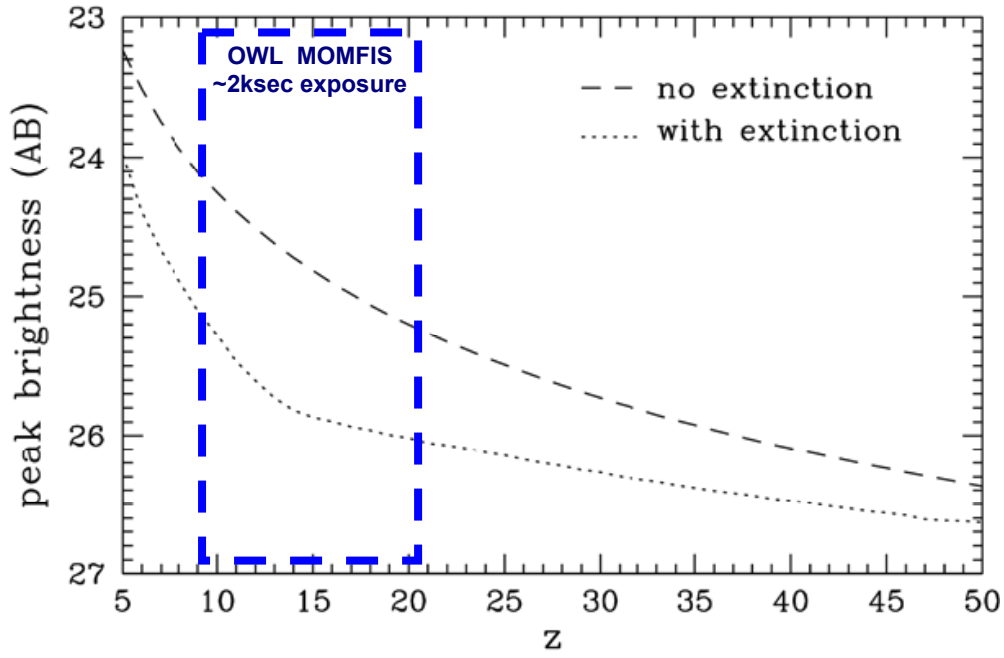

Figure 11 – Observed peak brightness of 250 $M_\odot$ Pop III SNe as a function of redshift in the spectral region around Ly-α assuming both no significant extinction and the "worst case" extinction for the Ly-α region.

At wavelengths longward of Ly-α, the peak brightness declines by only 0.5 magnitude to rest-frame 0.5μm wavelength. Note that these peak brightnesses are well within the sensitivy of OWL in spectroscopic mode at all redshifts of interest. A 200 $M_\odot$ Pop III SN is expected to be fainter by 1.7 magnitudes and a 175 $M_\odot$ one by 3.5 magnitudes, starting to be at the limit of OWL spectroscopic sensitivities. Thus only the most massive Pop III SNe can be studied with OWL/MOMFIS. (Adapted from Weimann & Lilly 2005).

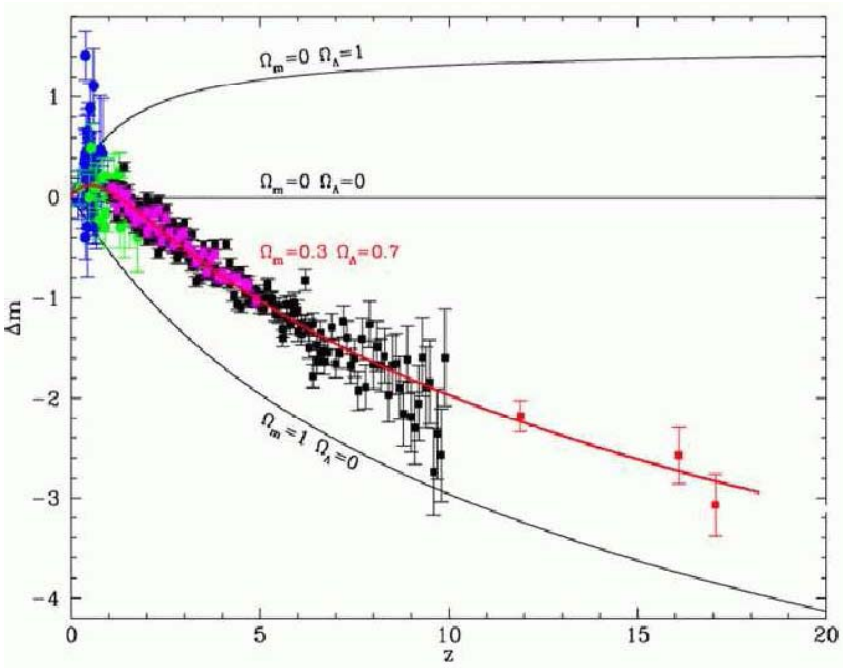

Figure 12 – Hubble diagram for the simulated ELT observations of SNe.

Pink, black and red dots represent type Ia, type II (+Ib/c) SNe and SNe from Pop III stellar population respectively. Blue and green dots are 'real' SNe observed with ground based telescopes and HST, respectively (from Della Valle et al 2005).

Figure 12 is showing the Hubble diagram for SNe that could be detected with OWL. MOMFIS would be essential in measuring the redshift of all the SNe with z>2.5. With the IFU mode, it will not only secure the redshift of the SN, it will allow a detailed measurement of the properties of the host galaxy, which would be impossible with a slit spectrograph.

5.6 Lensing magnification

Well know cluster lenses provide magnification larger than 10 on ~0.05 sq.arcmin (in the source plane). This region is then imaged around the cluster core on sizes of 1-3 sq.arcmin (in the image plane). This magnification effect is providing a substantial magnification gain in studying faint and distant objects. Cluster lenses will be important to probe the highest redshift galaxies and SNe to study their morphology, measure their spectra and study their dynamical properties. The typical size of the highest magnification region matches the OWL/MCAO field of view of a few sq.arcmin, thus the multi-object capabilities of the near-infrared spectrograph should be able to "follow" those high amplification regions to benefit from this natural magnification. This would be much easily achieved with multi-IFU units instead of multi-slits as the objects of interests can be crowded in the critical line regions.

To maximally benefit of the lensing magnification to probe the high redshift Universe, a infrared spectrograph should follow this requirements:

- *Field of view:* Critical line regions are typically 1-1.5 arcmin in diameter for the most massive clusters, defining the minimum required field of view to benefit from the lensing amplification.
- *IFU geometry:* The IFUs should have the possibility to have a compact distribution of the order of the size of the critical line region.
- *Total FOV probed*: One could use the different IFUs to conduct a serendipitous search for Ly-alpha or HeII emission line in the critical line region. To be most effective the total FOV probed by the different IFUs should be maximised (without scarifying a good sampling of the PSF).

By the time OWL will be in operation, we should know well about ~100 massive clusters acting as powerful gravitational telescope. Assuming that a 200 sq.arcsec in the source plane is magnified by a factor larger than 10, it means that for 100 clusters about a total of 5.5 sq.arcmin (in the source plane) is amplified by a magnification factor larger than 10. Thus mapping the critical line would allow discovering and taking spectra of the most distant objects in the Universe. With a density of ~10 per sq.arcmin (for galaxies at z>8 down to AB=29), this will mean of the order of ~50 strongly magnified objects at z>8 (with magnification larger than 10) will be detected allowing for these ones to have a detailed morphological and dynamical study. Note that a larger number of objects will have a smaller magnification, but they still will be useful to study as representative objects of lower luminosity or higher redshift that the one studied in blank field areas.

Gravitational lensing will be particularly interesting to image and take the spectra of strongly magnified (rare) objects, as well as studying the less strongly amplified objects. In particular we could imagine that to follow up dedicated clusters to search for the SNe in strongly lensed galaxies.

5.7 Target Selection

Due to the impressive OWL sensitivity, targets are likely to come from the James Webb Space telescope or other ground based extremely large telescope (OWL included). Targets could also come from other large aperture telescope working at other wavelength (Far infrared, (sub)millimetre, radio or X-rays) but would require OWL pre-imaging in order to check their near-infrared flux. Thus a relatively wide-field (>4x4 sq.armin) infrared imager with good image resolution (<100 mas) for OWL will be essential to conduct the key science proposed for MOMFIS.

MOMFIS could also provide the target by itself by conducting blind spectroscopic, this could be in particular useful for searching line emitting only object (such as Ly-alpha blobs) at z>7. This could be done in blank field, but also in massive cluster of galaxies to benefit from the lens magnification. In order to be effective such blind spectroscopy would benefit from a large total field of view from the different IFUs.

5.8 Other Issues

As the targets that will be fed into MOMFIS can come from other facilities, especially those coming from other large telescopes working in a different wavelength than near infrared, it is essential that OWL can access a large fraction of the sky, which means that Laser Guide Stars should be part of the AO system.

6. OTHER SCIENCE TOPICS

6.1 The Growth and Evolution of High Redshift Galaxies after the first Gyr of the Universe

Although the discovery and study of the first light in the Universe is key to the understanding of galaxy formation processes (see the main science case), the study of galaxy evolution in the expanding Universe from the 1st Gyr to nowadays is yet to be understood in details.

Today, we simply ignore most of the galaxy physical properties in the distant Universe. More fundamentally, simply studying the baryonic component of galaxies is equally inadequate since the mass of any structure in the Universe is dominated by dark matter on some scales and because of the complexity of the physical processes that control the growth of the baryonic components of galaxies (shocks, feedback from massive stars and AGN, merging, interplay between dark and baryonic matter, etc).

In the next decades, one of the major goals of astrophysics will be to map the distribution and growth of both the baryonic and dark matter components of galaxies from low redshift (z~0.5) to high redshift (z~4). Although the nearby Universe z~0.5-1 will be accessed with current facilities using the current or next generation of instruments, the higher redshift part z=1 to 4, can only be accomplished with 30-100m class telescope by *mapping* out the

spatially resolved kinematics, star-formation, and chemical abundances of galaxies as well as measuring the kinematics of their satellite objects (both their internal kinematics and their velocity relative to the most massive component).

When and how baryons come to reside in spheroids and disks? There are two competing explanations. The classical pictures are the ``monolithic collapse'' of Eggen, Lynden-Bell, & Sandage (1962) versus the (hierarchical) merging model of Searle & Zinn (1978). The hierarchical picture of galaxy formation and evolution is, for many excellent reasons, widely favoured (e.g., Ellis 1998). It predicts that small galaxies formed first and that massive galaxies grew at later times by the accretion and merging with smaller (proto) galaxies. Monolithic collapse, as the name suggests, is a simple process in that the gas collapses over a few crossing times and the star-formation proceeds rapidly. When including realistic feedback mechanisms from the intense star-formation, such collapse is stretched out to about 1 Gyr.

While we think we have a reasonable understanding of the boundary conditions of galaxy evolution, we do not understand the details. In either model, forming a galaxy is very complex and requires an understanding of the physics of massive star-formation, feedback from the stellar winds and supernova explosions, non-linear collapse of individual clouds and gas fragments on scales of sizes of individual stars to star-complexes and spiral arms (about 10 orders-of magnitude), radiative cooling and shock heating on a comparable scale, the growth of angular momentum and the impact of star-formation on this growth, and many other processes.

To map the galaxy halos evolution (both the baryonic and dark matter component) from z~4 to z~1 will require to obtain spectra of very faint and physically small galaxies. This is necessary because we wish to probe the dynamics of galaxies in the halos and also obtain redshifts of possible background sources that have been lensed by the gravitational potential of individual galaxies. Coupled with spatially resolved measurements of the dynamics of the parent (most massive) galaxy in the halo, it is possible then to construct a mass versus radius for galaxy as a function of there estimated baryonic mass and angular momentum. Of course, since any halo is likely to be populated by several tens of galaxies, many of which may be too faint to obtain the required measurements, means that one would have to attach many galaxies with similar total baryonic mass contents. Making such measurements would then yield the total dark matter mass and the fraction contributed by the baryons. In addition, the measurement of the dynamics of the objects in the halo would allow us to estimate the likely merging time scale and thus the likely rate of growth of mass and angular momentum of the parent galaxy.

The galaxies in individual halos will be moving relative to the parent galaxy at velocities of several tens of km/s. Low mass star-forming local galaxies that populate the halos at low redshift typically have emission line luminosities (H-alpha, [OIII]5007, [OII]3727 which are the strongest optical emission lines in low mass, low metallicity galaxies that are likely to be the most appropriate targets in the halos) of $10^{39\text{-}40}$ ergs/s/cm^2. At z=3, the luminosity distance is ~8×10^{28} cm. The typical flux of an emission line in the halo galaxies would then be about 10^{-19} to 10^{-20} ergs/s/cm^2. Thus, even on a 100m, the integration time is likely to be nights for each field.

This project will require a spectrograph with multiple integral field units (IFUs). Each IFUs should ideally cover up to few sq. arcsec and should be deployed over a few square arcmin to acquire the spatially resolved dynamics of several galaxies. Assuming a 50-100mas spatial resolution, it will provide exquisite details on velocity fields of large galaxies down to few hundreds parsecs (resolving the kinematics and chemical properties of all galaxies seen

in Hubble Deep Fields observations). Gathering such information on sample of a few thousands galaxies should provide a clear understanding of the growth of galaxies both in low and high-density region of the Universe.

Critical technical requirement:

- multiple IFUs with a large field of view of a few square arcsec,
- spatial resolution of 50-100mas,
- largest wavelength coverage to detect multiple emission/absorption lines for chemical diagnostics,
- A minimum resolution R=4000 to be able to probe the galaxy dynamics,
- A large number of IFUs in order to be able to measure a few thousands of galaxies to complete significant statistical work.

6.2 The centre of the Milky-Way

The improved angular resolution achievable on OWL with AO (possibly reaching the diffraction limit) will offer an extreme accuracy for astrometric and spectroscopic stellar measurements. With an astrometric precision ~20 times higher than the diffraction limit for high signal-to-noise objects, one can expect an astrometric limit of ~0.2 mas. Similarly, a spectroscopic precision of ~10 km/s in the radial velocities measurements could be reached with a spectral resolution R=6000.

Even if we take into account the confusion limit resulting from the brighter stars, the number of stars observable in the central 100 mas will gain about at least an order of magnitude compared to the 10 stars observed presently with 8-10m class telescope (cf Weinberg 2005, ApJ in press, astro-ph/0404407).

Diffraction limited AO observation, covering a region of ~4”x4” will then give about 10-100 thousands of stars. Thanks to the proper motion and radial velocity monitoring of this greater number of stars, deviations from Keplerian motions should be observable with OWL (Newtonian retrograde precession due to the differential amount of mass between the apocenter and the pericenter in case of an extended distribution of matter; relativistic prograde precession) as well as the Roemer effect, due the variable difference in time between the stellar emission and the observation during the orbital motion.

Thanks to these improved precisions and effect measurements, new constraints at an extreme accuracy should be brought to:

1) the black hole mass of our Galaxy,
2) the distance to the Galactic Centre,
3) the extended distribution of matter (parameters of the power law models),
4) the galactic dark matter halo profile through the galactic shortest to longest axis ratio,
5) the central stellar population and stellar formation history.

To reach this exciting science, the critical technical requirements are:

- Large single IFU or multiple IFUs using a mapping strategy (over tens of square arcsec),
- Diffraction limited adaptive optics over a few tens of square arcsec,
- Longest wavelength (K band) to minimize the Galactic absorption,
- A high spectral resolution R=8000,
- Regular monitoring of the Galactic centre.

7. HIGH-LEVEL INSTRUMENT SPECIFICATIONS

Focussing on the main science driver, as well to some extent considering the other possible science topic to be conducted with the MOMFIS instrument, we will now convert the science requirements in terms of high-level instrument specifications. We will address 6 high level specifications as described in the introduction:

1) **Wavelength coverage:**

As we have seen the wavelength coverage will define the redshift domain for which distant galaxies can be visible. If the infrared spectrograph stops at 1.8 micron (without the K-band) then we will be limited basically to z<11. The K-band will allow the redshift domain 11<z<15 (and may be up to z=18 for Lyman-alpha emitter) to be explored. This domain is particularly important as it strongly increase the likelihood to find and study the Population III stars that will be more numerous at the highest redshift.

Furthermore the K-band spectroscopy is still very competitive compared to JWST sensitivity, hence it would make thanks to keep it in the design of the instrument.

2) **Spectroscopic mode:**

Three different concepts can be considered for a spectrograph aiming to gather information on a number of objects: multi-slit, multi-IFU or single large IFU.

Although the multi-slit would be the simplest design, it will likely limit a lot the science output that can be achieved. This is true for both the main science driver, and the secondary science topics. As we have seen particularly in the strongly magnified arc at z=4.92, distant galaxies will likely not have a simple morphology, but will be made of blobs as the primordial clouds fragment following the collapse of the highest density region. Depending on the geometry (distribution of dust and HI clouds) the Lyman-alpha photons may escape at places where no continuum is detected, similarly as in the Lyman-alpha blobs that have been discovered at z~3. 3D information will allow a complete description of the physics and dynamics of the first galaxies.

A single large IFU would need to be very large to be efficient in selecting high-z galaxies, indeed in a given patch of the sky the number density of galaxies will be dominated by lower redshift galaxies (z<6) which means that we are loosing a lot in terms of efficiency. Furthermore, blind search mapping can also be done with multi IFU (providing that the total field of view [number of IFU times the individual field of view size] is sufficiently large, that is a few tens of square arcsec: an area sufficient to conduct serendipitous search of the first galaxies or look at different regions of the galactic centre or other nearby galaxies).

We, thus conclude that a multi-IFU instrument would be *the most versatile multi-object instrument*, as one could position IFU on selected targets and we can also work efficiently in a blind search avoiding to target unwanted galaxy population.

3) Accessible field of view:

We have seen that the typical number density of source down to the spectroscopic sensitivity limit at (R=1000) that is Y/J~29, H~28.5 and K~28 (AB mag) is of the order of ten or a few tens of objects per square arcmin (of course only a few of them will be at z>11, that is only detected in K-band). If we want to really understand the physics of the first galaxies we will need to gather a few thousands of such objects. The typical exposure time to reach the above limits will be a couple of hours of science exposure, so let us say one night to simplify accounting for overhead and different possible spectroscopic set-up. Taking one hundred nights as a reasonable amount of time for a single science project (this correspond to the largest VLT allocation for large programme), this means that we need to have a multiplexing of about 30-40 to finally gather a few thousands galaxies at z>7. This requirement compared to the number density of such sources (that is quite uncertain) and folding in an 50% efficiency factor to select objects that can be highly clustered, means that the total field of view that needs to be accessible for positioning the multi-IFUs will have to be at a minimum 3x3 square arcmin. Furthermore, in view of the special interest of lensing clusters, IFUs should have the possibility to be positioned in relatively compact region of about 1 square arcmin.

4) Spectral resolution:

The first requirement in terms of spectral resolution is to have a sufficiently high resolution in order to resolve the OH lines sufficiently well to have a large fraction of the wavelength domain without OH line contamination. Resolutions of 3000-5000 are necessary to reach about 80% of the wavelength domain free of OH lines (this depends on the wavelength as some parts are worst than others).

Such high resolution will be very useful to search for emission line only objects, and to maximise the detection one has to have a velocity resolution that matches the intrinsic velocity dispersion of the system. The conversion of the spectral resolution in term of velocity resolution can be expressed by the formula:

$$\Delta v = \frac{c}{R(1+z)}$$

where c is the speed of light, R the spectral resolution and z the redshift. Therefore, for R=4000 and z=10, the velocity resolution will be 7 km/s, for R=8000, the velocity resolution will be 3.5km/s. We see, here, that R=4000 is adequate for the main science objectives (allowing to be sensible to relatively small system in terms of their mass), and we may even resample to smaller spectral resolution to increase S/N or produce a detailed image.

If N is the number of pixel in the wavelength direction then the resolution R can be written as a function of N, the central wavelength: λ_c and the window coverage in lambda: w_λ:

$$R = \frac{N}{2.5}\frac{\lambda_c}{w_\lambda}$$

If covering the full band available for each near infrared photometric bands we can determine the resolution as a function of the CCD size:

NIR Band and limits	λ_c / w_λ	R for a 2k CCD	R for a 4k CCD
Y : 0.9-1.1	5	4000	8000
J : 1.1-1.35	4.9	3900	7800
H : 1.45-1.75	5.33	4300	8600
K : 2.0-2.4	5.5	4400	8800

We see in this table that 2k CCD would match the desired resolution of the instrument perfectly.

5) Plate scale / Image quality:

To maximise the signal to noise, the image resolution should match roughly the size of the structure we are aiming to observe, indeed this will maximise the surface-brightness within the spatial resolution and thus the S/N of spectra. This can be readily seen in the simulation shown in Figure 13 below.

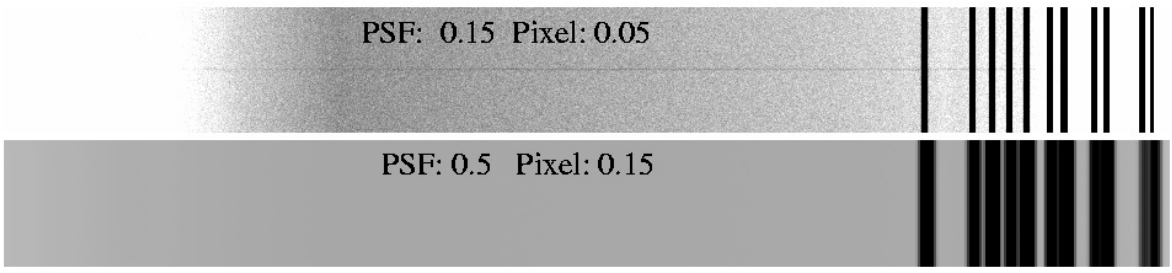

Figure 13 – Simulated 10ksec exposure, R=4000 long-slit spectrum of a Y=28 object with a size of 0.15 arcsec

A 30% efficiency for the instrument and OWL are assumed as defined in the OWL-ETC. By matching the spatial resolution to the size of the object, a high S/N spectrum can be obtained.

Hence, following the object size expected for high redshift galaxies, we require a spatial resolution of at least 50-100 mas, which corresponds to a pixel scale of 20-30 mas. In some cases, we may wish to obtain even higher spatial resolution to reach even smaller structures (AGN, SN, blobs in forming galaxies) so a resolution 3 times smaller, may be of strong interest.

6) Field of view of individual IFUs

The minimal number of element per IFUs is probably at least 16x16: to cover the full object size, allow dithering, and perform efficient sky subtraction. A 40x40 area may be more adequate thus feeding a full 2Kx2K detector. With 20 mas per pixel, this mean an IFU would cover 0.8x0.8 sq.arcsec. For 40 IFUs, we will then be able to cover a total field of view of 25.6 sq.arcsec.

8. ABBREVIATED TERMS

Abbreviations used in this document are provided below.

Abbreviation	Meaning
ELT	Extremely Large Telescope
ESO	European Southern Observatory
ETC	Exposure Time Calculator
FOV	Field of View
GLAO	Ground Layer Adaptive Optics
IFU	Integral Field Unit
JWST	James Webb Space Telescope
MOMFIS	Multi-Object, Multi-Field IR Spectrograph
MCAO	Multi-Conjugate Adaptive Optics
OWL	Overwhelmingly Large Telescope
PSF	Point Spread Function
SN	SuperNova
WMAP	Wilkinson Microwave Anisotropy Probe

OWL Instrument Concept Study

MOMFIS

Multi-Object, Multi-Field IR Spectrograph

III. Sub-system Specifications

LAM.OPT.MOMF.SPT.050128_01

Prepared by :	*Signature*
Eric Prieto *Date : 15/09/2005*	
Approved by :	*Signature*
Jean-Gabriel Cuby *Date : 15/09/2005*	

Change Record

Issue	Rev.	Paragr.	Page	Date	Observations
1	0	All	All	28/01/2005	First issue
2	0	All	All	15/09/2005	Final Report

Distribution List

Institut	Name	Issue/Révision									
		1.0	2.0								
LAM	J.G. Cuby	X	X								
LAM	J.P. Kneib	X	X								
LAM	E. Prieto	X	X								
LAM	N. Manzone	X	X								
LAM	P.E. Blanc	X	X								
LAM	D. Burgarella	X	X								
LAM	O. Le Fèvre	X	X								
GEPI	F. Hammer	X	X								
GEPI	P. Jagourel	X	X								
GEPI	P. Vola	X	X								
GEPI	M. Marteaud	X	X								
GEPI	M. Puech	X	X								
LESIA	Y. Clénet	X	X								
LESIA	D. Rouan	X	X								
CRAL	R. Bacon	X	X								
CRAL	E. Pécontal	X	X								
CRAL	M. Tallon	X	X								
ONERA	G. Rousset	X	X								
ONERA	T. Fusco	X	X								
ESO	M. Casali	X	X								

Table of contents

List of Figures

1. INTRODUCTION :

This document specifies the OWL-MOMFIS technical requirements. The specifications appear in the technical report [RD 02].

2. SCOPE

The high level science specifications are described in [RD 01]. From these top level requirements and the instrument concept ([RD01]) the sub-system requirements can be derived. This document summarizes these sub-system requirements. Since this is a conceptual study, several sub-system specifications could not be derived, and / or remain TBC/TBD.

3. REFERENCES

3.1. Applicable Document

[AD 01]	OWL-SOW-ESO-00000-0152	1.0	03 Dec. 2004	Statement of work for a conceptual study for a conceptual study of an IRMOS for OWL
[AD 02]	OWL-ICD-ESO-00000-0139	1.0	5 Oct. 2004	Interface Control Document
[AD 03]	OWL-CSR-ESO-00000-0147	1.0	24 Sep. 2004	Framework of OWL instrument concept design studies

3.2. Reference Document

RD 01	LAM.SCT.MOMF.SPS.050117_01	1.0	17 Jan 2005	MOMFIS: Science Specification
RD 02	LAM.PJT.MOMF.RAP.050708_01	2.0	15 Sep. 2005	MOMFIS: Final report

4. SUB-SYSTEM LIST

Sub-system	Parts	Comment and function
Pick-off mirrors system		
	Pick-off mirrors (POF)	Small spherical mirrors magnetically attached to the support plate
	Telescope Focal plane plate	Magnetically supporting all Pick-off mirrors
	Positioning robot	Positioning all POF on the focal plates
Channel addressing systems		
	Beam Steering Mirrors	
	Deformable mirror	
Wave Front Sensors		

	Multi-Object AO WFS	TBD
	Telescope/GLAO WFS	ESO WFS (ESO furniture)
	AO control command	Control ESO GLAO (ESO furniture) Control DAO
Atmospheric Dispersion Correction system		
	Prism 1	
	Prism 2	
	Prism rotator system	
Integral Field Units		
	Magnifying optics	
	Slicer Units	
	Pupil mirror units	
	Slit mirror units	
Spectrograph unit		
	Collimator units	
	Camera units	
	VPH/Filter units	
	Detector units	
Support Structure		
Thermal enclosure		
Cryostats		
	Cooling system	
Control electronics		
	Proximity electronics	
	Remote cabinets	
	Computers	

5. TARGET ACQUISITION SYSTEM

5.1. Function

Figure 1 shows the functional analysis of the target acquisition system.

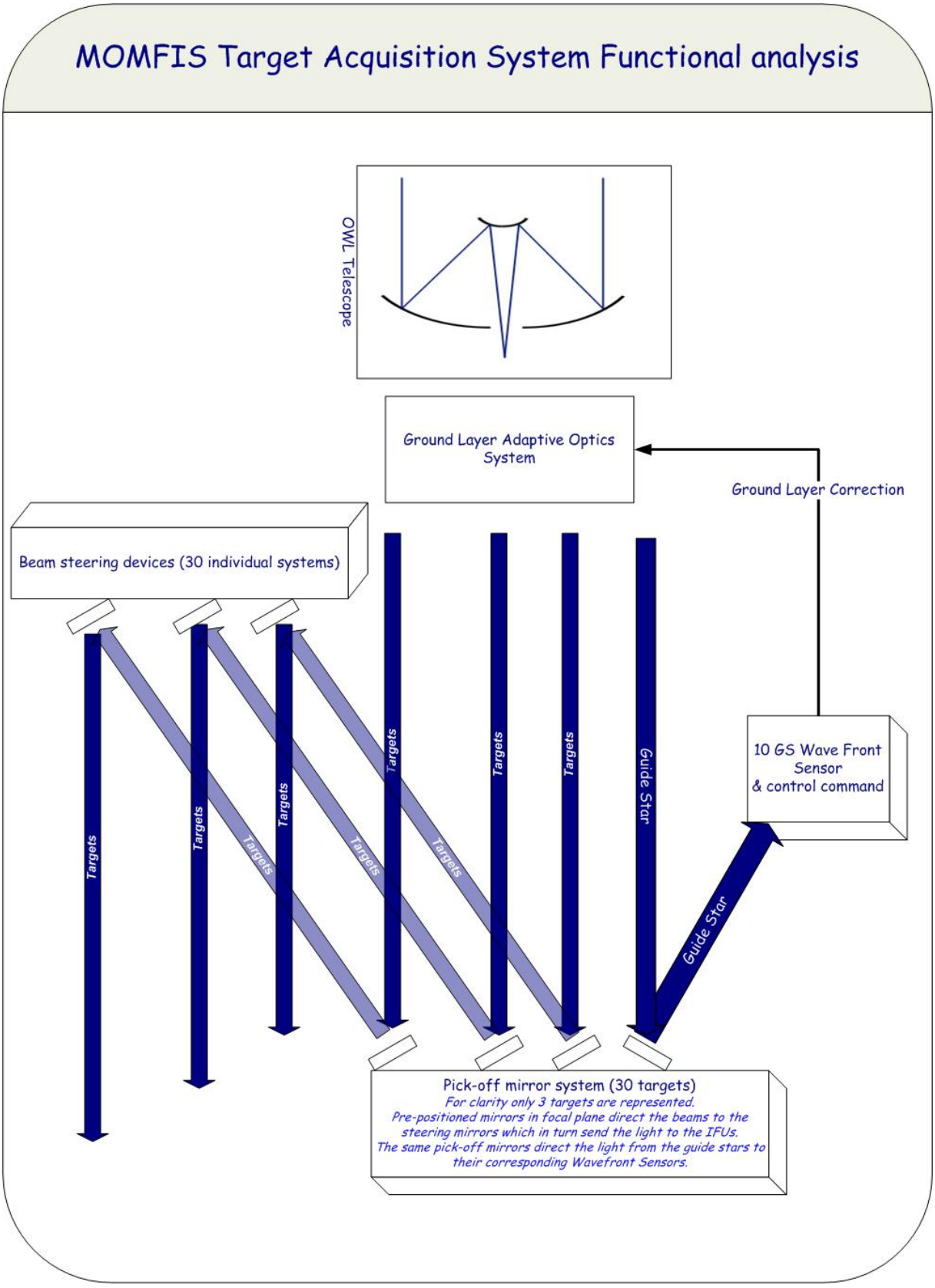

Figure 1: Functional analysis of the target analysis system (the system of distributed AO correction in not represented)

5.2. Pick-off Mirror system

This system includes:

- The pick-off mirrors: these mirrors are positioned in the telescope focal plane with a robot. They are magnetically held in place on the telescope focal plane plate.
- The Telescope Focal Plane plate: This spherical plate mimics the telescope focal plane 120mm behind it. The function of this plate is to hold the pick-off mirror in place during the observation.
- The positioning robot: This unit picks and places the pick-off mirrors in and from their parking positions and their observation positions. The robot is similar to the 2dF robot.

The three systems have to be operated at 10°C. The thermally stabilized environment has to enclose this system. This specification comes from the specification of the instrumental background (see section 8.

5.2.1. Pick-off mirrors:

This mirror has to catch the beam coming from the target and send it to the steering mirror.

Specification	Value	High level specs / Comment
Curvature radius	- 100 mm	5'x5' FOV
Diameter	< 15 mm	Close packed observation requirement. Corresponds to 5" on sky.
Height	TBD	
Optical surface tilt	0° to 10° (precision 10")	Could be an adjustable tilt or a preset tilt High-level specs: 5'x5'
Optical surface positioning error	< 10µm	TBC with a high level specification on the pointing accuracy
Optical surface stability	<1µm	Shift wrt the telescope beam; this value can be translated in tilt: 2" TBC with a high level specification on the pointing stability
Optical surface quality	25nm rms	TBC with a high level specification on WFE
Optical surface roughness	2 nm rms	TBC with the High level spec on overall throughput
Optical reflectivity	>98.5%	TBC with the High level spec on overall throughput
Operating temperature	10°C	The system has to be operational at room temperature.

5.2.2. Telescope focal plane plate:

Specification	Value	High level specs / Comment
Curvature radius	2200 mm	
Surface quality	10µm PTV	TBC with a high level specification on the pointing accuracy
Error slope	< 10”	TBC with a high level specification on the pointing accuracy
Diameter	875 mm	FOV: 5’x5’
Thickness	TBD	
Operating temperature	10°C	
Material	TBD	Low CTE and magnetic layer
Thermal dilatation	1µm over the diameter for a thermal variation of 1°C	Insure the position stability of the bug during the exposure TBC with a high level specification on the pointing stability
Thermal conductance	High	Minimize the thermal gradients TBC with a high level specification on the pointing stability
Weight	TBD	

5.2.3. Positioning Robot:

Specification	Value	High level specs / Comment
Positioning error (X,Y)	10µm	In the tangential plane to the telescope focal plane TBC with a high level specification on the pointing accuracy
Rotation along X	Range: +/- 10° Accuracy: 20’’	
Oz positioning	Range: 360° Accuracy: 20”	Oz axis perpendicular to the telescope focal plane TBC with a high level specification on the pointing accuracy
Reconfiguration time	< 60 sec	TBC with a high level specification on time
Operating temperature	10°C	The system has to be operational at room temperature
Minimal distance between Bugs	15 mm	5” on sky

6. SPECTROGRAPH AND AO CORRECTION SYSTEM

6.1. Beam Steering Device

The function of these devices is to:

- Re-image the telescope on the deformable mirror
- Ensure to have a pupil image quality compatible with the AO correction
- Maintain the magnification factor constant regardless of target position in the focal plane

Specification	Value	High level specs / Comment
Positioning error Z	10µm	TBC with a high level specification on WFE
Translation along the Z axis	+/- 200mm Accuracy: 0.05 mm	TBC; FOV: 5'x5'
Oz positioning error	1'	Oz axis perpendicular to the telescope focal plane TBC with a high level specification on the pointing accuracy
Oz rotation range	12°	FOV 5'x5'
Ox; Oy tilt positioning error	10''	TBC with a high level specification on the pointing accuracy
Ox,Oy rotation range	+/-10°	FOV: 5'x5'
Ox; Oy tilt positioning stability	0.1"	TBC with a high level specification on the pointing stability
Ox,Oy rotation axis	Coincident on the mirror vertex within XXµm (TBD)	
Reconfiguration time	< 60 sec	TBC
Operating temperature	0 - 10°C	The system has to be operational at room temperature - TBC
Optical surface curvature surface radius	-4000 mm	
Zernicke aberration correction	Astigmatism in both directions With a range of +/- 5% of the curvature radius	FOV: 5'x5'
Surface quality	30 nm rms	

6.2. Deformable mirror

Specification	Value	High level specs / Comment
Diameter	20 mm TBC	
Number of actuator	200x200	High level specs on AO

		performance
Surface quality	TBD	TBD with a high level specification on WFE
Surface roughness	<3nm rms	
Optical surface reflectivity	> 98.5%	TBC with a high level specification on overall throughput
Operating temperature	77K	Question: possibility to have DM operated @RT for tests purpose

6.3. Integral field unit

6.3.1. Magnifying optics

The function of these sub-systems is to:

- Provide a cold stop on a pupil image
- Re-image the telescope focal plane to the adapted plate scale on the slicer unit

Specification	Value	High level specs / Comment
Entrance pupil size	20mm	
Output F-ratio	F/206	
Image surface size	80x80 mm	
Image surface curvature	Plane	
Exit pupil position	Any position could be fitted in the slicer unit	
Exit pupil aberration	To be corrected with the slicer design	
Spot diagram	< 2000 m diameter within a band	
WFE	TBD	

6.3.2. Slicer units

The function of these sub-systems is:

- Sample the FOV at 20 mas in one direction in 40 slices
- Re-image the telescope pupil on the pupil mirror

Specification	Value	High level specs / Comment
Number of slices	40	
Width of slices	2 mm	For 40 slices. In the case of 30 slices, the width could go down to 0.9mm
Curvature radius	TBD	
Length of the slices	80 mm	40 x width

Optical surface quality	50 nm rms	TBC with a high level specification on WFE
Optical surface roughness	< 2nm rms	TBC with the high level specification on throughput
Optical surface reflectivity	> 98.5%	TBC with the high level specification on throughput
Ox; Oy tilt error for individual slices	10 “	Generic specification, TBC
Operating temperature	77°K to 300°K	

6.3.3. Pupil mirror units

Specification	Value	High level specs / Comment
Number of mirror	40	
Width of individual mirrors	3 mm TBC	
Curvature radius	TBD	
Height of individual mirrors	5 mm TBC	
Optical surface quality	50 nm rms	TBC with the high level specification on WFE
Optical surface roughness	< 2 nm rms	TBC with the high level specification on throughput
Optical surface reflectivity	> 98.5%	TBC with the high level specification on throughput
Ox; Oy tilt error for individual slices	10 “	Generic specification, TBC
Operating temperature	77°K to 300°K	

6.3.4. Slit mirror units

Specification	Value	High level specs / Comment
Number of mirror	40	
Width if individual mirrors	3 mm TBC	
Curvature radius	TBD	
Height of individual	5 mm TBC	
Optical surface quality	50 nm rms	TBC with the high level specification on WFE
Optical surface roughness	< 2nm rms	TBC with the high level specification on throughput
Optical surface reflectivity	> 98.5%	TBC with the high level specification on throughput
Ox; Oy tilt error for individual slices	10 “	Generic specification, TBC
Operating temperature	77°K to 300°K	

6.4. Spectrograph units

6.4.1. Collimator

Specification	Value	High level specs / Comment
Entrance FOV	140 mm	For 40 slices linear
F-Number	8	
Pixel size	75µm	
WFE	TBD	TBD with the high level specification on WFE
Pupil image size	150 mm	
Focal length	1200mm	

6.4.2. Camera

Specification	Value	High level specs / Comment
Image FOV	36 mm	Number of pixels per ifu
F-Number	1.8	20mas high level specification on spatial sampling
WFE	TBD	TBD with the high level specification on WFE
Pupil image size	150 mm	
Focal length	270 mm	

6.4.3. Grating

The grating shall have 50 000 lines across the pupil to give the R=8000, and 25000 for R=4000.

6.4.4. Detector

The pixel size shall be 18µm.

Specification	Value	High level specs / Comment
Pixel Size	18 µm	
Wavelength range	0.9µm to 2.4µm	Wave length coverage high level specification
Frame size	2048x2048	
Quantum Efficiency	>80%	Instrument overall throughput high level specification
Operating temperature	77°K TBC	
Operating temperature stability	1°K TBC	

6.5. Wave front sensor

6.5.1. Adaptive optics Wave Front Sensor

Specification	Value	High level specs / Comment
Sub-aperture number	200x200	

6.5.2. Telescope Wave Front Sensor

This item is ESO furniture.

6.6. Adaptive optics control system

The AO system shall provide ensquared energy better than 30% in 50mas.
The AO system has to provide an image with a WFE of TBD nm rms.

6.7. Atmospheric dispersion correction system

The Atmospheric dispersion correction (ADC) shall minimize the image elongation due to atmospheric dispersion from zenital angle variation from 0° to 60°. The blur shall be kept inside a pixel (20 mas) while the monochromatic WFE is below 10nm.

6.8. Thermal enclosure

The thermal enclosure shall provide a constant temperature of 10°C (or -40°C in option #2). This temperature shall be stabilized at +/-1°C. The gas shall be air to allow human intervention and dry to prevent condensation.
The external temperature will vary from 0°C to 15°C (assuming that the telescope is inside a thermalized dome during daytime).
A door plus a removable airlock shall be foreseen to allow people and small equipment to enter and exit the enclosure.

6.9. Cryostat

The internal environment shall be stabilized at a temperature compatible with the observation in K band (except for the option #2).
The detector shall be stabilized at 77°K +/- 1°K.

6.10. Support structure

Specification	Value	High level specs / Comment
Gravity vector	Any direction	This requirement is severe, even a rotating Nasmyth instrument is less constraint. A vertical instrument axis on a Nasmyth platform would relax

		this specification
Time to be considered for all flexure specification	1800 s	Maximal individual exposure time
Thermal variation to consider	1 K	
Operating Temperature	0 to 10°C	-40°C in option #2
Tilt flexure	< 10 µrad	Between sub-structures (beam steering mirrors, focal plane assembly, spectrograph entrance, etc.)
Translation flexure	100µm	Same comment as above

6.11. Control electronic system

TBD

7. OPERATIONAL SPECIFICATION

7.1. Temperature control

The time for the thermal enclosure to return to the nominal temperature from any extreme temperature (long interventions, dismounting, etc.) shall be less than 24 hrs.

This time shall be less than 3 hrs after a 1 hour intervention with the enclosure door open (daytime operations).

The cooldown time and stabilisation at operational temperature of the cryostats shall be less than 48 hrs.

7.2. Reliability

To be specified (mean time between failures, etc.)

7.3. Maintainability

Most of the maintenance procedures inside the thermal enclosure shall last l hr or less (daytime operations). Major interventions such as removal of a cryostat, interventions on the robot, etc., shall require less than 6 hrs.

A set of dedicated tools shall be available for easy maintenance and intervention in the enclosure. Specific access to all sub-systems shall be implemented.

Diagnostic tools shall be implemented to have a precise remote diagnostic and limit on-site interventions.

7.4. Integration

The instrument shall be designed in sub-assemblies allowing modular integration, alignment, testing and calibration.

Specific tools for integration and alignment shall be designed.

8. NUMBER OF WARM MIRRORS – EMISSIVITY

The instrumental background shall not deteriorate the telescope and atmospheric background by more than a certain fraction $\mathcal{F}$, equivalent to a degradation of $\mathcal{F}/2$ of the signal to noise ratio.

Typically, if one accepts a degradation of the S/N of 25% at most, one can tolerate a degradation of the instrumental background of 50% at most under background limited conditions [we ignore for simplification the impact on the S/N of the reduced overall transmission due to an increase in system emissivity].

This requirement allows in turn to specify the number of warm mirrors that can be tolerated in the instrument, and / or the operating temperature of these mirrors.

We note first that the thermal background only dominates in the K band (in spectroscopy between the OH lines, the default case for MOMFIS), whereas in the J and H bands the continuum emission between the OH lines dominates. Therefore, the analysis below only holds for the K band, practically between 2.1 and 2.4µm.

We write the background that the instrument sees as follows:

$$B = B_{tel} + B_{ins} + B_{atm}\,(1 - e^{-\tau Z}) \qquad [1]$$

Where B_{tel} is the background from the telescope, B_{ins} the instrumental background, B_{atm} the atmospheric background and τ is the atmospheric optical depth at the wavelength of interest at zenith and Z is the airmass.

Considering the best part of the K atmospheric window between 2.1 and 2.35 microns where there are very few atmospheric absorption lines, the emission from the atmosphere can be confidently neglected in comparison to the telescope emission within the range of operational airmasses. This is particularly so because of the 6-mirror design of the telescope.

Therefore, the specification can be written as:

$$B_{ins} \leq \mathcal{F} \times B_{tel} \qquad [2]$$

One can write the telescope background as:

$$B_{tel} = \varepsilon_{tel}\, B(\lambda, T_{ambient}) \qquad [3]$$

ε_{tel} is the telescope emissivity and B is a black body function of wavelength (λ) and temperature. $T_{ambient}$ is the site temperature (+10°C in average as per the ICD). ε_{tel} can be expressed as N_{tel} times (1 - $\eta_{tel}(\lambda)$) where N_{tel} is the number of telescope mirrors (6, all assumed identical) and $\eta_{tel}(\lambda)$ is the reflectance of one telescope mirror.

$$\varepsilon_{tel} = N_{tel} \times (1 - \eta_{tel}(\lambda)) \qquad [4]$$

As for the instrumental background, we assume N_{warm} mirrors at the same ambient temperature as the telescope, plus N_{cold} mirrors operating at a T_{cold} temperature (typically -30 to -40° C), and finally one entrance window of either the cryostat or the cold environment with an emissivity ε_{window} (typically 2%).

$$B_{ins} = (\varepsilon_{window} + N_{warm} \times (1-\eta_{ins}(\lambda))) \times B(\lambda, T_{ambient}) + N_{cold} \times (1-\eta_{ins}(\lambda)) \times B(\lambda, T_{cold}) \quad [5]$$

where $\eta_{ins}(\lambda)$ is the reflectance of one warm or cold instrument mirror. All instrument mirrors are assumed identical and reflectance independent of temperature.

Finally, equation [2] gives:

$$(\varepsilon_{window}+N_{warm}\times(1-\eta_{ins}(\lambda)))\times B(\lambda, T_{ambient}) + N_{cold}\times(1-\eta_{ins}(\lambda))\times B(\lambda, T_{cold}) \leq \mathcal{F} \times N_{tel}\times(1-\eta_{tel}(\lambda))\times B(\lambda, T_{ambient}) \quad [6]$$

Assuming now that telescope and instrument mirrors are all of the same type, i.e. $\eta_{tel} = \eta_{ins}$ one simply gets:

$$N_{warm} + \frac{\varepsilon_{window}}{1-\eta_{ins}(\lambda)} + N_{cold} \times B(\lambda, T_{cold}) / B(\lambda, T_{ambient}) \leq \mathcal{F} \times N_{tel} \quad [7]$$

We use the Planck law:

$$B(\lambda, T) = \frac{2hc^2}{\lambda^5} \frac{1}{e^{hc/(\lambda kT)} - 1} \quad [8]$$

$$B(\lambda, T_{cold}) / B(\lambda, T_{ambient}) = \frac{e^{hc/(\lambda k T_{ambient})} - 1}{e^{hc/(\lambda k T_{cold})} - 1} \quad [9]$$

The behaviour of $B(\lambda, T_{cold}) / B(\lambda, T_{ambient})$ over the wavelength of interest is represented figure 1. In the domain [2.1 – 2.4 µm], the ratio above varies approximately from 0.02 to 0.03. Let's adopt a mean value of 0.025, i.e. a factor of 1/40.

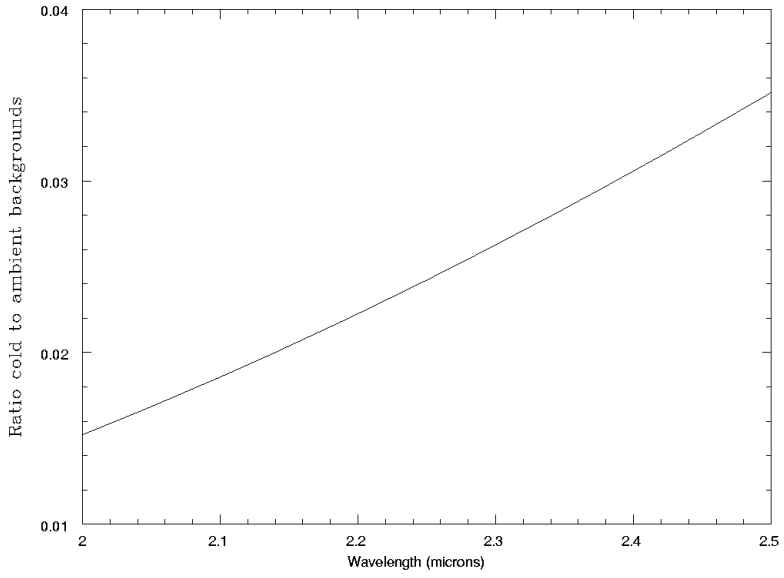

Figure 2 : Relative thermal backgrounds -40°C to +10°C in the K band

For Ag, we have in the wavelength range of interest:

$$1 - \eta_{ins} \sim \varepsilon_{window} \sim 2\% \qquad [10]$$

Finally, [7] writes:

$$N_{warm} + \frac{N_{cold}}{40} \leq \mathcal{F} \times N_{tel} - 1 \qquad [11]$$

With $\mathcal{F} \sim 0.5$ and $N_{tel} = 6$, one gets :

$$N_{warm} + \frac{N_{cold}}{40} \leq 2 \qquad [12]$$

This shows that no more than 2 warm mirrors can be accommodated, while there are no strong limits on the number of cold mirrors. Clearly, any situation with no warm mirrors but plenty of cold mirrors would be preferable so as not to degrade the instrumental background.

It is worth noting that the above calculations and requirements only hold when a cold stop is present in the design at cryogenic temperature (to block any radiation seen from the detector at a large solid angle). This therefore also assumes that the pupil is optically perfectly transferred from telescope to cold stop.

As a last element of the discussion, let us consider the effects of a warm optics in relative terms (relative to a fully cryogenic optics) and not in absolute terms as done above: the impact of having 2 warm mirrors instead of 2 cold or cryogenic mirrors, all other things being the same is simply given by a factor $\sqrt{8/6} = 1.15$, i.e. 15% S/N degradation. This is deemed acceptable.

In conclusion, the lower level specifications on the 'warm' optical parts of the instrument are:

Specification on warm optics:

The instrument shall have a cumulated reflectance of the warm optics of 94% or above, assuming 98% reflectance of the 6 telescope mirrors (note that the ICD specifies 96%). This 6% loss in warm optics reflectance has to be balanced between:

- the entrance window of the cryostat and / or of the cold chamber
- possible warm steering mirrors
- pupil mis-alignment (on cold stop), including optical aberrations and stability

9. ABBREVIATED TERMS

Abbreviations used in this document are provided below.

Abbreviation	Meaning
ADC	Atmospheric Dispersion Compensator
AO	Adaptive Optics
BSM	Beam Steering Mirror
DM	Deformable Mirror
ELT	Extremely Large Telescope
ESO	European Southern Observatory
FALCON	Fibre spectrograph with Adaptive optics on Large Fields to Correct at Optical and Near-infrared
FEA	Finite Element Analysis
FOV	Field of View
FWHM	Full Width at Half Maximum
GLAO	Ground Layer Adaptive Optics
GS	Guide Star
HST	Hubble Space Telescope
ICD	Interface Control Document
IFU	Integral Field Unit
JRA	Joint Research Activity
LGS	Laser Guide Star
LN2	Liquid Nitrogen
mas	Milli-arcsec
MCAO	Multi-Conjugate Adaptive Optics
MLI	Multi Layer Insulation
MOMFIS	Multi-Object, Multi-Field IR Spectrograph
MOAO	Multi-Object Adaptive Optics
MOS	Multi-Object Spectrograph
N/A	Not Applicable
NGS	Natural Guide Star
OWL	Overwhelmingly Large Telescope
PSF	Point Spread Function
PTV	Peak To Valley
QE	Quantum Efficiency
TBC	To Be Confirmed
TBD	To Be Determined
TMT	Thirty Meter Telescope
VPH	Volume Phase Holographic
WFE	WaveFront Error
WFS	WaveFront Sensor

OWL Instrument Concept Study

MOMFIS

Multi-Object, Multi-Field IR Spectrograph

IV. TECHNICAL REPORT

LAM.PJT.MOMF.RAP.050708_01

Prepared by :	Signature
Eric Prieto (project manager), Pascal Jagourel, Pascal Vola, Michel Marteaud, Pierre-Eric Blanc & Jean-Gabriel Cuby Date : 15/09/2005	
Approved by :	Signature
J.-G. Cuby Date : 15/09/2005	

Centre National de la Recherche Scientifique - Laboratoire Astrophysique de Marseille - UMR 6110 BP 8 – 13376 Marseille Cedex 12, Tel. : 33 +4.91.05.59.00 - Fax : 33 .+4.91.05.59.47

Change Records

Date	Issue	Revision	Modification	Pages
08 July 2005	1	0	First release	All
15 Sep. 2005	2	0	Final report	All

Distribution List

Institut	Name	Issue/Révision									
		1.0	2.0								
LAM	J.G. Cuby	X	X								
LAM	J.P. Kneib	X	X								
LAM	E. Prieto	X	X								
LAM	N. Manzone	X	X								
LAM	P.E. Blanc	X	X								
LAM	D. Burgarella	X	X								
LAM	O. Le Fèvre	X	X								
GEPI	F. Hammer	X	X								
GEPI	P. Jagourel	X	X								
GEPI	P. Vola	X	X								
GEPI	M. Marteaud	X	X								
GEPI	M. Puech	X	X								
LESIA	Y. Clénet	X	X								
LESIA	D. Rouan	X	X								
CRAL	R. Bacon	X	X								
CRAL	E. Pécontal	X	X								
CRAL	M. Tallon	X	X								
ONERA	G. Rousset	X	X								
ONERA	T. Fusco	X	X								
ESO	M. Casali	X	X								

Table of content

List of Figures

List of Tables

1. INTRODUCTION

A highlight science case for the European ELT (see the OPTICON ELT science case page) is: First light - The First Galaxies and the Ionization State of the Early Universe. It aims at peering into the Dark Ages when the Universe was being re-ionized by the UV flux emitted by the first sources of light. Recent observations of the high redshift Universe suggest that stars and galaxies started to form and to assemble early at redshifts well above 7. Understanding this key epoch of the Universe is of paramount importance and requires the following exquisite instrument capabilities on an ELT. This science case and its specifications are described in detail in [RD1].

- Multi-IFU observing mode
- 5' x 5' field of view minimum, larger fields desirable
- Number of IFU targets: 40 or higher for a 5' x 5' field of view
- Image quality at 30% ensquared energy: 50 mas or better at selected areas in the field (direction of the IFU targets)
- Spatial sampling: 10-30 mas
- Spectral resolution: 5000-8000

This document describes an instrument concept for OWL that would meet these requirements.

2. SCOPE

The scope of the MOMFIS study was to perform a conceptual study for OWL allowing to meet the scientific requirements for which the instrument is designed. As a first attempt at designing an OWL-instrument, the results of the study shall be regarded as preliminary and aimed at identifying possible implementation, development and interface compliance issues. The emphasis was put on performing a global opto-mechanical design allowing in turn to provide feedback to the telescope designers. Integration, maintenance, reliability and operational considerations have been taken into account in the design.

We essentially adopted the safest options in our design, in particular by resorting to proven technologies rather than speculative ones. In that respect, several budgets in our design are to be regarded as 'worst case' scenarios (e.g. mass, cost, etc.) if new development and technologies ultimately allow to simplify the design.

3. REFERENCES

3.1 Applicable Documents

[AD 01]	OWL-SOW-ESO-00000-0152	1.0	03 Dec. 2004	Statement of work for a conceptual study of an IRMOS for OWL
[AD 02]	OWL-ICD-ESO-00000-0139	1.0	5 Oct. 2004	Interface Control Document
[AD 03]	OWL-CSR-ESO-00000-0147	1.0	24 Sep. 2004	Framework of OWL instrument concept design studies

3.2 Reference Documents

[RD 01]	LAM.SCT.MOMF.SPS.050117_01	1.1	Jan. 17, 2004	MOMFIS. Scientific Specification (Science Case)
[RD 02]	Hammer et al., SPIE 5382, 2003, p. 220.		2003	FALCON: a concept to extend adaptive optics corrections to cosmological fields
[RD 03]	Memo ESO / S. D'odorico		06 June 2005	Draft Adapter Rotator concept
[RD 04]	Memo ESO / L. Louarn		June 2005	OWL AO Analysis report (draft)
[RD 05]	OWL-TRE-ESO-00000-xxxx	Draft	10 May 2005	Sky Coverage for OWL Adaptive Optics: GLAO and MCAO cases
[RD 06]	LAM.PJT.MOMF.RAP.050915_01	1.0	15 Sept. 2005	MOMFIS: executive summary
[RD 07]	LAM.OPT.MOMF.SPT.050128_01	2.0	15 Sept. 2005	MOMFIS: sub-system technical specifications

4. INSTRUMENT SPECIFICATIONS

Table 1 summarises the high level requirement specifications. See [RD07] for more detailed specifications of the system and sub-systems.

Table 1 – High level Instrument Specifications

Item	Requirement	Goal
Field Of View	2'x2'	5'x5'
Number of IFU	40	100
Spatial sampling	30mas & 10mas	
N pixel per IFU	30x30 & 60x60	40x40 (90x90 @10mas)
Image quality	30% encircled energy in 50 mas	50%
Spectral resolution	4000 / 8000	
Spectral coverage	Y or J or H or K in one shot	One octave in one shot
Throughput (excluding the telescope)	30%	40%
Packing	90% of IFUs in 1'	Contiguous FOV
Minimal object separation	5"	

5. SUMMARY

Table 2 summarises some of the MOMFIS characteristics. This table is not exhaustive and is provided as a quick reference guide. See [RD 06] for an executive summary.

Table 2 - Summary of the main MOMFIS characteristics

Item	Performance
Field Of View	Ø 5'
Number of IFUs	30
Individual IFU FOV	0.8" x 0.8"
Number of pixels per IFU	40 x 40
Spatial sampling (pixel)	20 mas
Pixel scale in telescope focal plane	58 µm (F/6)
Pixel scale in slicer plane	2000 µm (F/206)
Pixel scale in slit plane	75 µm (F/7.5)
Pixel scale at the detector	18 µm (F/1.8)
AO Mode	MOAO
N Deformable mirrors	30
N WFS	10
N actuators (per DM)	> 10000
Spectral resolution	4000
Spectral coverage	Y / J / H / K in one shot
Throughput	30%
N cryostats	10
Weight	20-25 tons
Volume	36 cubic meters

6. INSTRUMENT CONCEPT

6.1 Getting started : KMOS2 and TMT/TiPi

The starting point for the study was the KMOS2 instrument concept, proposed for the VLT 2nd generation instrumentation. This concept was relying on beam steering mirrors which provide numerous instrument capabilities and flexibility. LAM is contributing to one TMT study for an IR-MOS instrument led by Caltech University, TiPi, which principle is inspired from the VLT/KMOS2 design, however with significant differences. TiPi is based on a mirror array assembled in the telescope focal plane. These 25" wide mirrors are tilting in both directions to send the incoming beam to a selected steering mirror. Each tile mirror can address all steering mirrors. The steering mirrors can be oriented to acquire the beams from their corresponding tile mirrors and re-direct them to the spectrographs. Focus compensation is achieved both by the steering mirror and by the tile mirror. Figure 1 illustrates this principle.

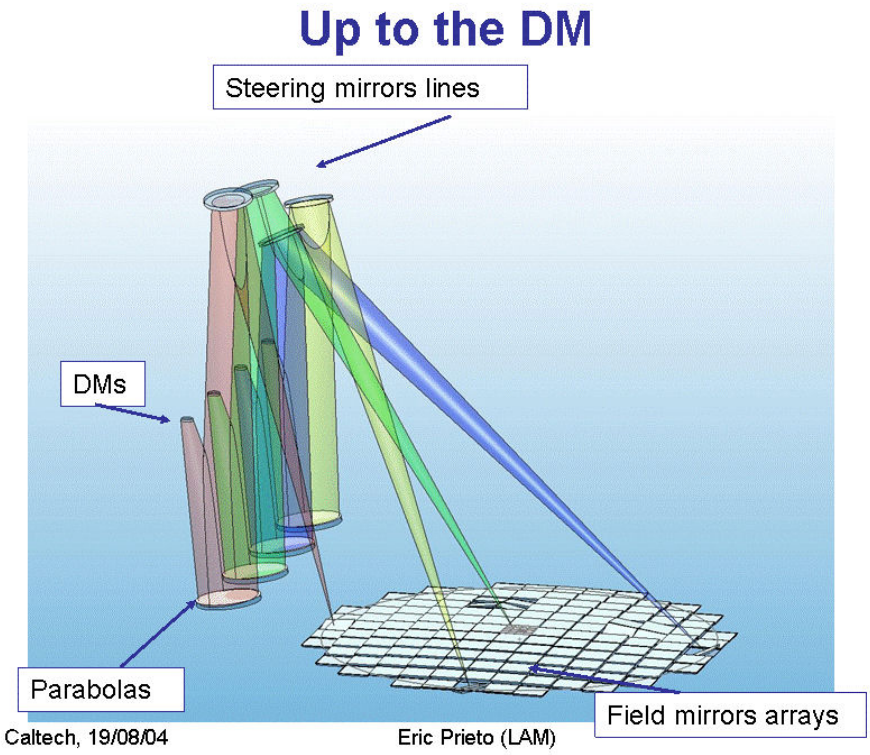

Figure 1 – TMT/Tipi: principle of target acquisition

As the tile mirrors are exactly in the focal plane the target selection can acquire up to four objects as close at 2''. In addition, a unique 6"x6" contiguous field mode is available, using a dedicated faceted mirror located at the center of the FOV. Each facet is coupled to a specific steering mirror. The instrument up to the DM is placed in a cold environment (-40°C), after which the instrument is cryogenically cooled.

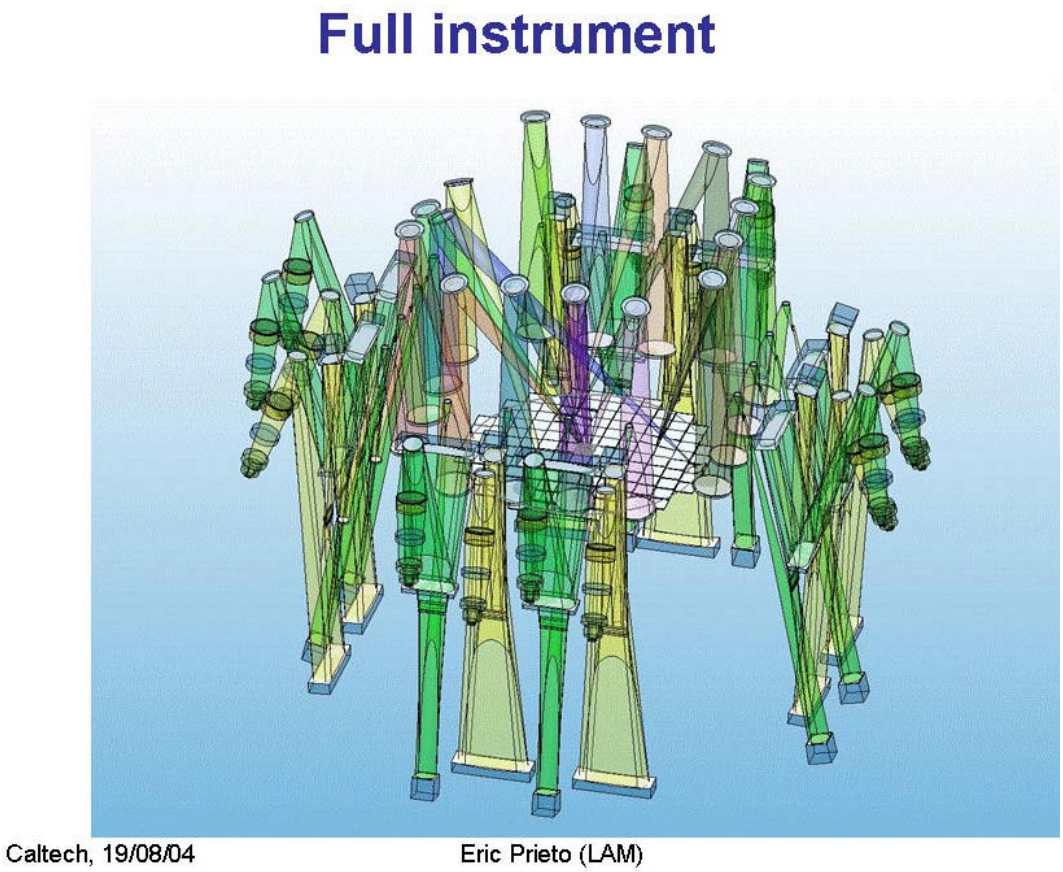

Figure 2 – TMT/Tipi: view of the full instrument

The tile mirrors array and the 16 spectrograph channels are clearly visible
Figure 2 shows an overall view of the optical scheme of the instrument. It is worth mentioning the size of the instrument: ~ 2/3 the size of VIMOS at the VLT.

Table 3 summarizes the main characteristics of TiPi.

Table 3 – TMT/TiPi: main specifications

Item	Value
FOV	5'x5'
Individual FOV	1.5" x 1.5"
Spatial sampling	50 mas
Number of object	16
Spectral resolution	3000-5000
Band of observation	(I) J-H-K
Observational modes	- 16 objects (FOV: 1.5"x1.5") - One contiguous 6"x6" FOV
Minimal separation between objects	2"
Adaptive optics system	MOAO
Volume	1.2 x 1.5 x 1.5 m

The experience with TiPi was used to get started designing MOMFIS. However, a major difference prevented from using exactly the same principle: the fast OWL F/6 input beam which requires the pick-off mirrors to collimate the beams - unlike the TiPi flat mirrors - to keep the beam footprint reasonable in size at the location of the beam steering mirror. This is achieved by spherical pick-off mirrors. The requirement specification for more objects than the 16 TiPI channels was another important difference.

6.2 Other high level design considerations

6.2.1 Adapter / Rotator

Very early in the design phase it was realized that the adapter/rotator provided by the telescope as part of the focal environment ([AD02] and [RD03]) was not suited to our needs, essentially for weight limit reasons (2 tons). For this reason this adapter/rotator was removed (upon agreement from ESO), and replaced by a larger one part of the instrument. This has a number of consequences which are described in section 10.

6.2.2 Thermal stabilisation

We chose to design a thermally stabilized instrument, requiring a thermal enclosure and an entrance window. In spite of the added design and manufacturing complexity, we believe that this will ultimately allow to simplify the instrument operation: stable operating points, no turbulence and added wavefront errors between analysis and correction points inside instrument (several meters of optical path difference), easier calibration (metrology and instrument calibration), etc. Requirement for a thermally stabilized environment would need further investigations and trade off analyses at a later stage of the instrument study.

6.2.3 Number of warm mirrors

As per the analysis presented in [RD 07], the number of warm mirrors that can be tolerated in the instrument without significant degradation of the S/N in the K band (the only band which is thermal background limited) is 2. This is considered in the baseline design which foresees only 2 mirrors (pickoff and beam steering) before the cryostat entrance window. Some flexibility could be gained by having more warm mirrors (and less cryogenic parts) at the expense of the K band performance.

6.3 MOMFIS Operational Concept

Figure 3 shows the target acquisition functional diagram. The science channels are represented in blue and consist of:

- A target selection system: it directs a science beam from the telescope focal plane to the deformable mirror
- A Deformable mirror: it corrects the atmospheric wavefront in the direction of the target

- An Integral Field Spectrograph (FOV in range 0.6 – 1.0", sampling 20-30 mas, spectral resolution 4000-8000).

The reference sources (assumed here to be natural (NGS) but concept can be applied to laser Guide Stars (LGS) equally well) are represented in blue. The NGS beams are directed from the telescope focal plane up to the WFS with a selection system partly similar to the science target selection system. These NGS can be acquired over the full instrument FOV. The current design foresees 10 WFS but this number can be somehow adjusted.

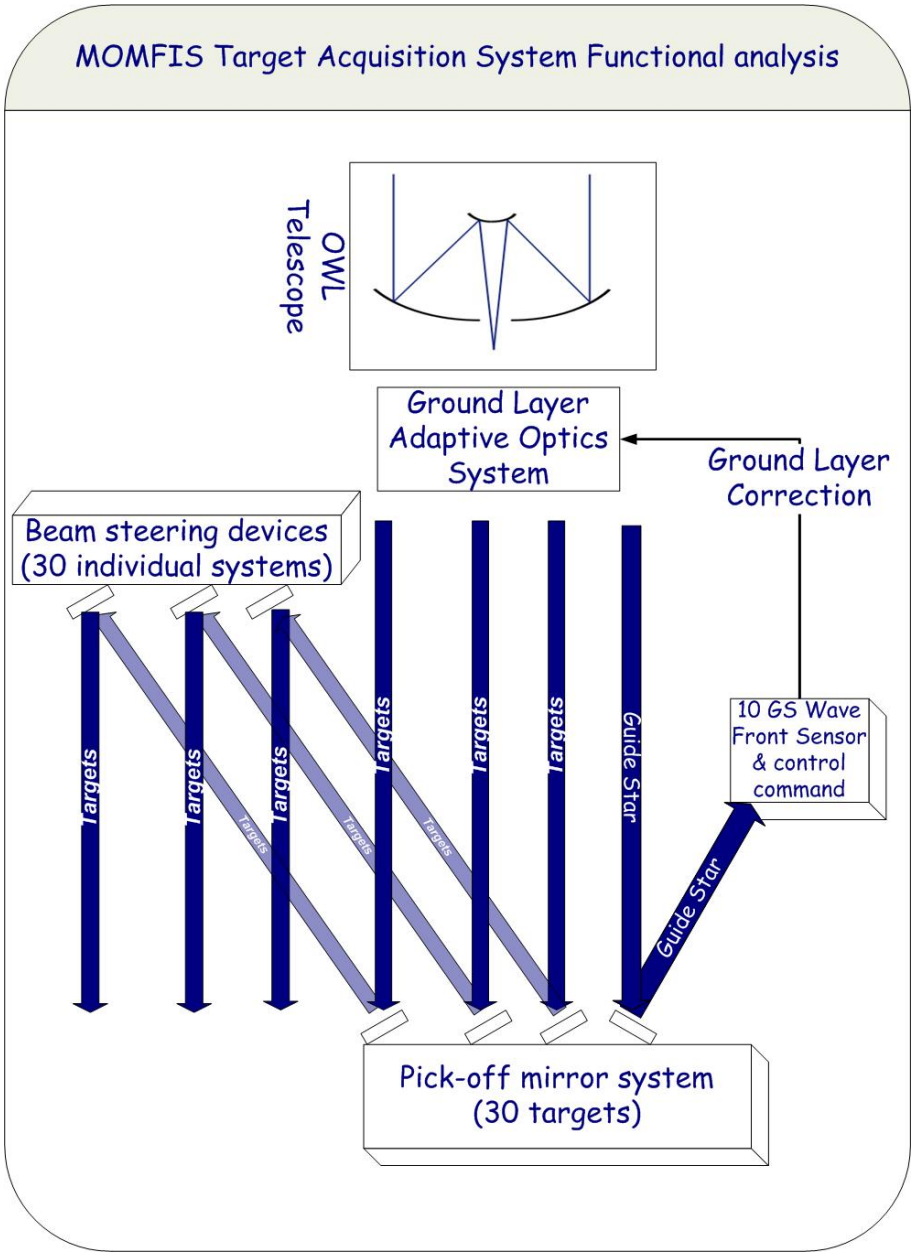

Figure 3 – Target Acquisition Concept

Figure 4 describes the high level instrument operational sequence. The focal plane configuration (pick-off mirrors) is derived from the input catalogs of targets and reference stars.

The detailed configuration of the pick-off mirrors and of their associated beam steering mirror is taken care of by the instrument software. The robot can configure a plate while another one is in observation. While a plate is being positioned the beam steering mirrors, DMs, spectrograph, ADC, etc. are configured. The science exposure can then start.

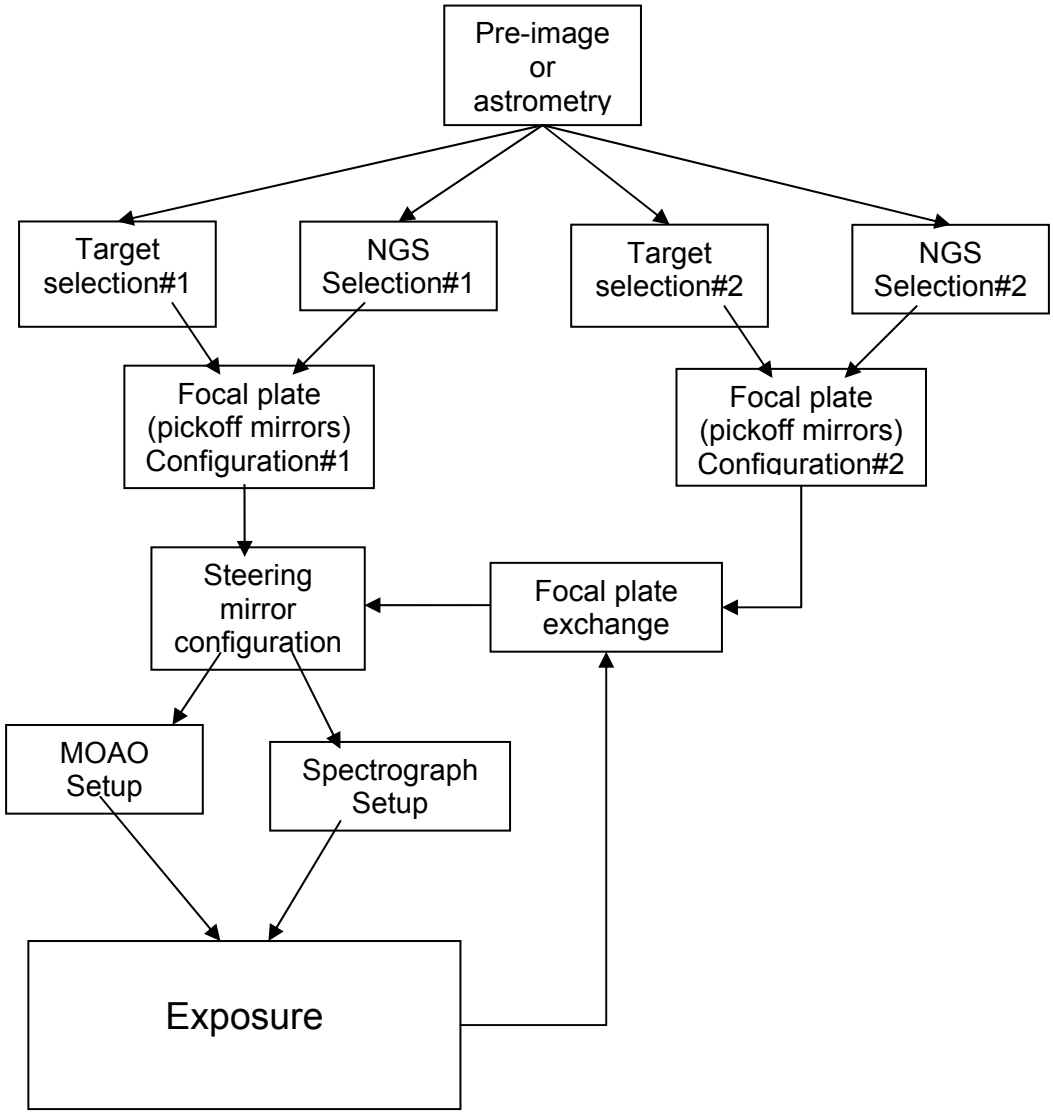

Figure 4 – High level operational sequence

Figure 5 shows the global optical implementation of the system. An important feature of MOMFIS is that it uses the same selection system (pickoff mirrors) to direct the light to the science and WFS channels, providing full configuration flexibility. NGS can be as close as 5" from a target over the full 5' FOV. Up to 10 or more reference sources can be selected. The WFS can be of any type, Shark-Hartmann, Pyramid, Curvature, etc.

Atmospheric dispersion is corrected before the DM. After image correction with the DM the target beams are directed to individual image slicer stacks. The slicer outputs are pseudo slits that form the entrance of the spectrographs. There is one spectrograph per target. Most of the main subsystems are grouped by 3 in terms of opto-mechanical implementation: beam steering mirrors, spectrographs, etc.

The 30 spectrographs cover one spectroscopic band (YJHK) in one shot. All spectrographs observe the same band simultaneously (TBC).

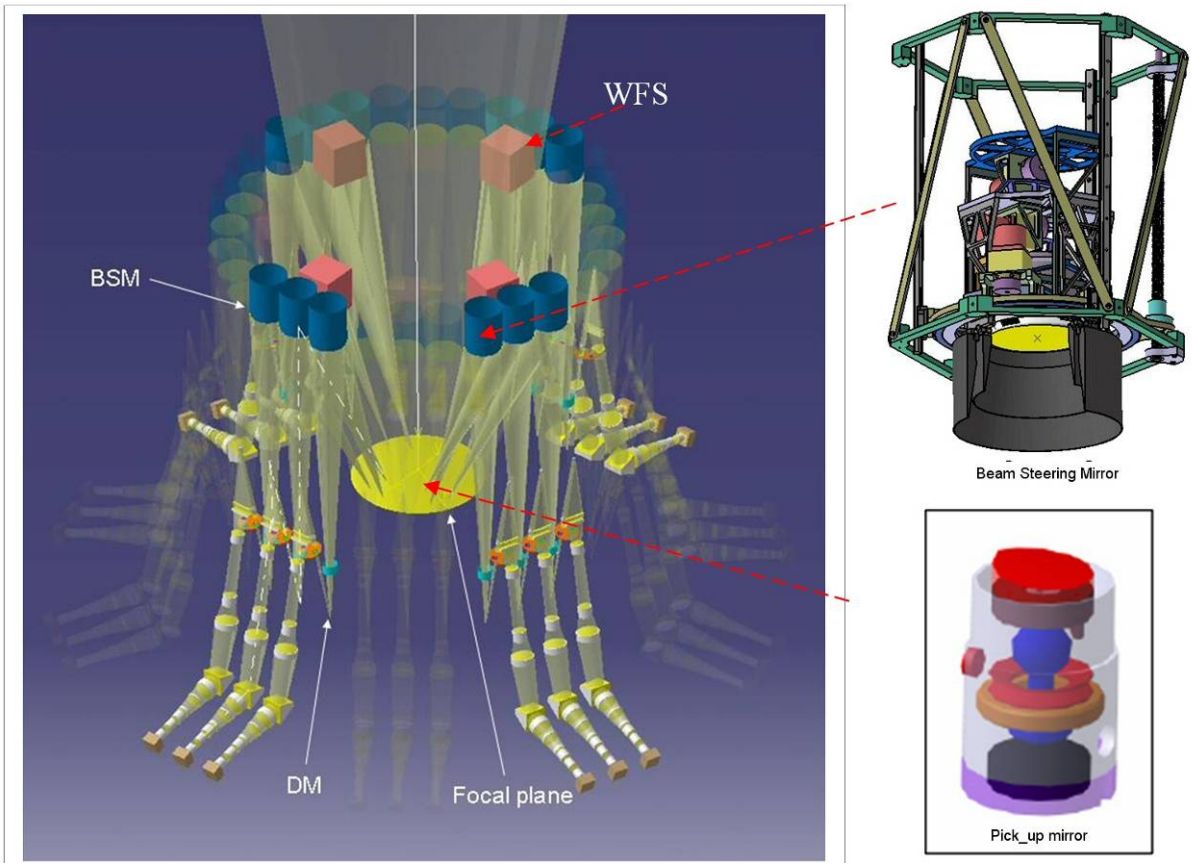

Figure 5 – MOMFIS optical design

In the focal plane pick-off mirrors are positioned with a robot, directing the target beams to the steering mirrors and the reference star beams to the WFS. The 'science' steering mirrors direct in turn the beams to the DM and IFU units.

6.4 Adaptive Optics Concept

6.4.1 Performance considerations

One of the scientific requirements is to have an ensquared energy higher than 30% in a 50 mas resolution element. The GLAO correction [AD2 and RD4], while providing significant image quality enhancement, does not allow to reach this requirement by a large factor.

Table 1 summarises the high level requirement specifications. See [RD07] for more detailed specifications of the system and sub-systems.

Table 1 shows the expected performance of the GLAO correction extracted from [AD2] under the following assumptions:

- 16- 17 mag NGS (6 NGS within a 6' diameter constellation)
- 5916 actuators DM (1 actuator every 1.1 meter)
- R0 = 20 cm @ 0.5 µm (0.5" seeing)

These assumptions are realistic, but maybe for the seeing which may be optimistic, or, say, may reach this value only over limited periods of time.

Table 4 – GLAO ensquared energy in a 50 mas pixel [From AD02])

Wavelength	Ensquared Energy in 50 mas
0.85 µm (I)	≈ 3%
1.22 µm (J)	≈ 5%
1.65 µm (H)	≈ 10%
2.2 µm (K)	≈ 18%

The GLAO performance clearly does not allow to meet the required specification. Correcting the full 5' fov is not possible, and not needed as only specific directions in the line of sight of the science targets need to be corrected. This concept, referred to as MOAO and derived from [RD2] (the Falcon concept), requires that in addition to the GLAO correction provided by the telescope a deformable mirror be used in each IFU optical train to further correct in the direction of each science target. This is achieved by sensing the wavefront over the instrument field of view in as many places as possible and by estimating in open loop the required correction in the directions of the science targets.

See Figure 6 for an illustration of the MOAO concept. Variations on this principle can be considered, e.g. with the wavefront sensors operating in pseudo-closed loop when additional DMs are included in the WFS channels.

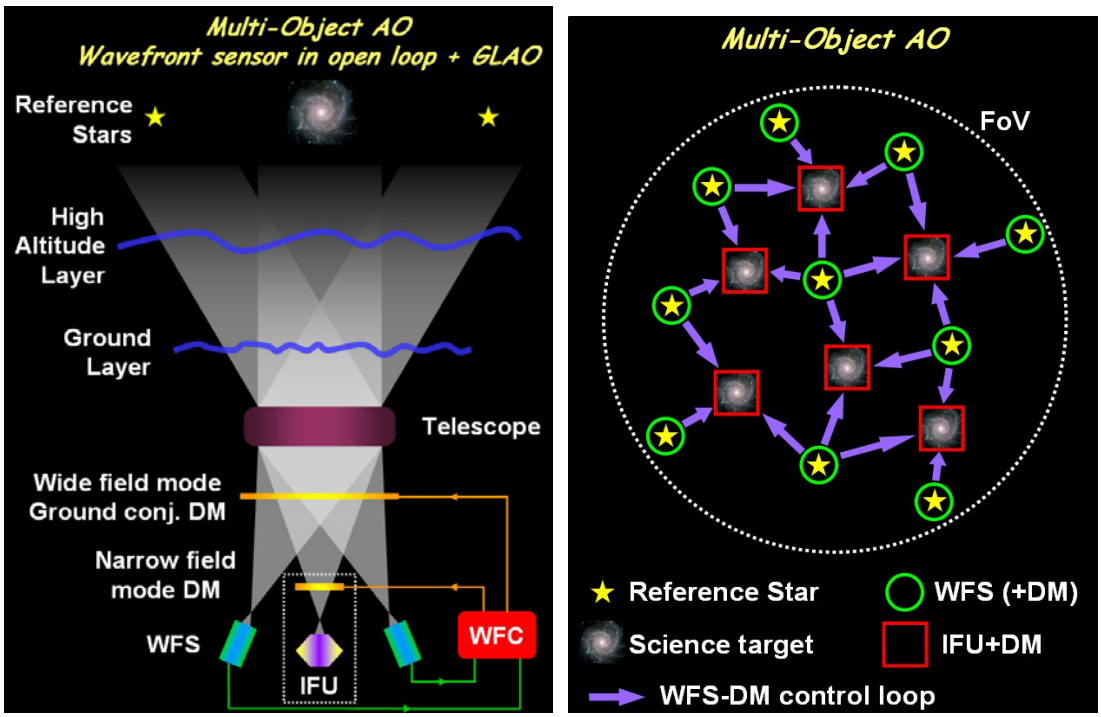

Figure 6 – Concept of Multi-object Adaptive Optics or Distributed Adaptive Optics

MOAO is combined with GLAO, and with wavefront sensors operate in open loop (courtesy ESO / AO department).

Preliminary simulations performed by ESO [RD04] show that while the performance can be reached under good seeing conditions and a reasonable number of actuators / WFS sampling elements (100 x 100), this is only so when using bright guide stars. The situation rapidly deteriorates when the magnitude of the guide stars increases (see Table 5 for an overview of the MOAO simulation performance). This leads in turn to having a low sky coverage, which is a severe issue as such a low sky coverage might prevent from observing specific fields, in particular, for what MOMFIS is concerned, 'public' fields for which multi-wavelength data is available. Table 6 indicates the number of natural guide stars versus magnitude and Galactic latitude ('Besançon' model) for an illustration of the issue, and Figure 7 shows the sky coverage computed by ESO in the GLAO and MCAO situations. Both indicate that the sky coverage, for magnitudes 16 or so, is likely to be extremely low.

Table 5 – MOAO ensquared energy in a 50 mas pixel (from [RD04])

Wavelength	GS magnitudes / Seeing	Number of actuators	Constellation radius	Ensquared energy in 50 mas (%)
K / H / J	10 / 0.5"	100 x 100	2'	50 / 30 / 15
K / H / J	10 / 0.5"	200 x 100	2'	55 / 35 / 20
K / H / J	10 / 1.0"	100 x 100	2'	20 / 05 / 02
K / H / J	15 / 0.5"	100 x 100	2'	30 / 15 / 10
K / H / J	15 / 1.0"	100 x 100	2'	10 / 05 / 01
K / H / J	16 / 0.5"	100 x 100	2'	15 / 06 / 03
K / H / J	16 / 1.0"	100 x 100	2'	05 / 01 / 01

Table 6 – Star density versus magnitude and Galactic latitudes, R band, 5' x 5' fov

Galactic Latitude	30°	60°	90°
Magnitude < 16	8	3	2
Magnitude < 17	14	5	3
Magnitude < 18	22	7	4

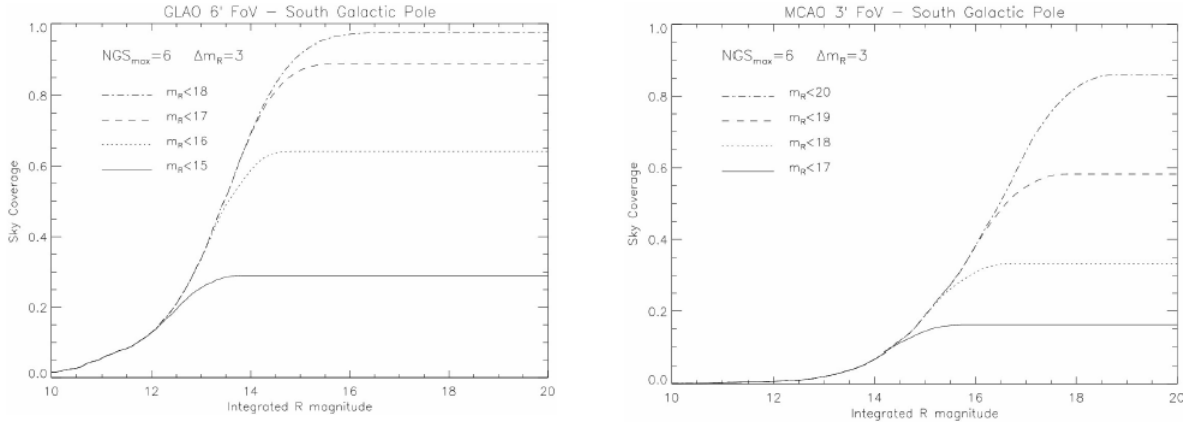

Figure 7 – Sky coverage at South Galactic Pole

The figure shows the sky coverage versus the integrated R magnitude of a constellation of 6 stars, with fainter star of magnitude mR. Left, GLAO case in a 6' FOV ; Right, MCAO case in a 3' case. The MOAO case is probably an intermediate case remaining to be investigated [from RD05, ESO]

Sky coverage with natural guide stars is an intrinsic issue to be dealt with as a whole at the telescope project level, and further simulations are required. Advanced tomography and wavefront analysis techniques may lead to improved performance, e.g. by using several faint guide stars available in the field, etc.

Laser Guide Stars seem an obvious way to overcome the issue of sky coverage. However, using LGS on an ELT is all but straightforward. The performance of LGS is obviously not part of the MOMFIS study and this is deferred to studies carried out elsewhere, e.g. in the ELT Design Study.

For the sake of the present study, we have assumed the MOAO concept as valid, either with NGS or with LGS, and MOMFIS therefore fully uses MOAO. If the MOAO system approach is still in its infancy and deserves extensive further studies, it is however possible for the sake of this study to specify the adaptive optics requirements, e.g. in terms of DM and WFS. We show in Figure 8 the ensquared energy versus pixel scale that can be reached on-axis for 2 different numbers of actuators and for various values of the outer scale of the turbulence. These simulations show the low sensitivity of the ensquared energy with the size of the pixel in the 30 to 100 mas range when the outer scale if realistically assumed to be in the 25-50 meter range. This can be explained by the large ratio of pixel size to diffraction FWHM. With moderate outer scales the instantaneous PSFs stay within the pixel size in a pretty large pixel range.

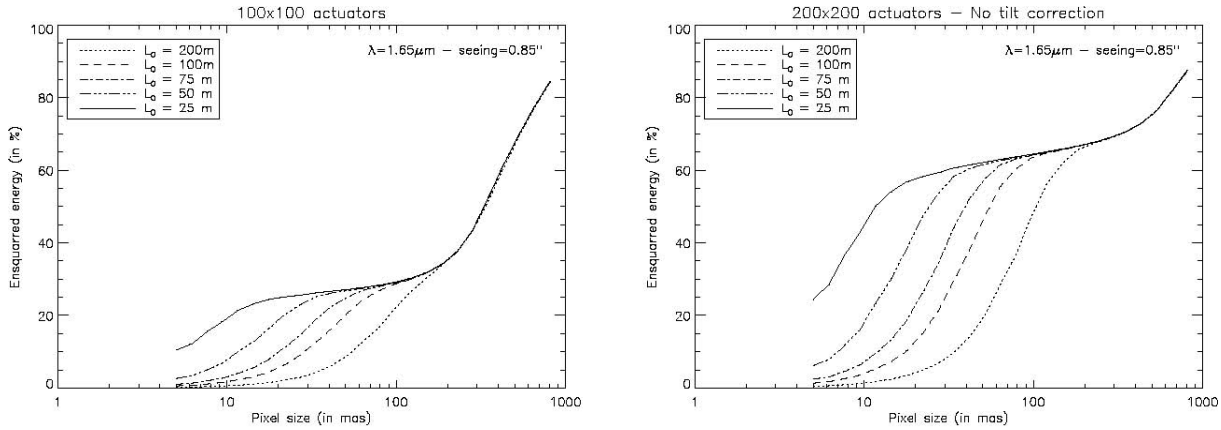

Figure 8 – Ensquared energy versus pixel size

The simulation is for the H band and 0.85" seeing, on-axis wavefront sensing. 100 x 100 actuators (left) and 200 x 200 actuators (right). Various outer scales of the turbulence are considered. [Simulations courtesy T. Fusco, ONERA]

These simulations also show that even in the favourable on-axis wavefront sensing case, the 30% ensquared energy in 50 mas pixels specification is hardly met in H with a 100x100 sampling, a situation that deteriorates even further at shorter wavelengths. An important conclusion is that a 200x200 sampling appears to be necessary if the ultimate science requirements are to be met. Obviously, these requirements can somehow be relaxed, at the expense of increased integration times and / or decreased S/N, and / or loss of spatial information on the targets.

6.4.2 Development risks

MOAO clearly represents a high risk development item: i) its concept has not yet been demonstrated on any system, ii) it requires tough specifications at component level (DMs, WFS, computing power, etc.), iii) it requires a complex system approach, including real time wavefront reconstruction algorithms, open loop operation, etc. Note that MOMFIS could be used without MOAO (see section 7.1) either as a fallback solution and / or in a first phase.

6.4.3 Development plan and roadmap

At least 3 component issues seem to be critical and to require major developments :

- Micro Deformable Mirrors with 100 x 100 (goal: 200 x 200) actuators that can be operated over a large temperature range (goal: at cryogenic temperature). These R&D developments are being carried out e.g. through the OPTICON or ELT Design Study FP6 programmes
- Laser Guide Stars. A multiple LGS system appears as an ideal solution for MOMFIS. Some studies are being carried out within the ELT Design Study. LGS operation shall be aggressively studied at telescope system level.
- Wavefront sensors able to perform a 200x200 sampling in open loop.

At a system level, the following development plan is foreseen:

- Extensive performance simulations and system analyzes, including wavefront control reconstruction algorithms and real-time control
- Breadboard and lab tests. Prototyping and laboratory demonstration are key requirements for the development of a MOAO system.
- Demonstration on sky. When the system has been tested in the lab, it should then be tested on sky, presumably on a 8 m telescope. The comparison of the sky and lab measurements in the 8m configuration will allow validating the simulations and lab tests, hence raising confidence in the 100m simulations and lab tests.

6.5 Optical Concept

6.5.1 Specifications

Table 7 summarizes the high level specification of the optical design.

Table 7 – High level specification for the general optical design

Item	Requirement
Field Of View	2'x2' / 5'x5'
Spatial sampling	30mas & 10mas
N pixel per IFU	30x30 & 60x60
Spectral resolution	4000 / 8000
Spectral coverage	Y or J or H or K in one shot
Throughput (excluding the telescope)	30%

6.5.2 Interfaces

The interface specifications for the optical lay-out are [AD2]:

- F/6 beam
- 100m pupil entrance
- Volume (5mx5mx12m)
- Entrance pupil on M6
- Telescope focal plane is a conic convex surface with a curvature radius of ~2.5m and a conic constant of k=-1.474.

6.5.3 Description

A 50mm focal length pickoff mirror is positioned 50mm behind the telescope focal plane and oriented to send the incoming sky beam to the steering mirror (BSM). The BSM travels along the Z axis and rotates around 3 axes to re-image the pupil onto the DM. The astigmatism generated by the off-axis reflections are corrected by the spherical deformation in two perpendicular directions of the beam steering mirror. An atmospheric dispersion compensator is placed before the DM. The cold stop can be either the DM (in case it can be cryogenically operated), or separate optics shall be used to form a pupil image onto a cold stop (as shown here). Finally, two re-imaging mirrors re-image the FOV onto the slicer mirror stack (see Figure 9).

The spectrograph entrance is the output spherical pseudo slit of the slicer unit. A pupil relay group of lenses makes the beam telecentric, the collimator images the pupil on the Volume Phase Holographic grating, and a 6 lens camera delivers the F/1.8 Beam on the detector (see Figure 10).

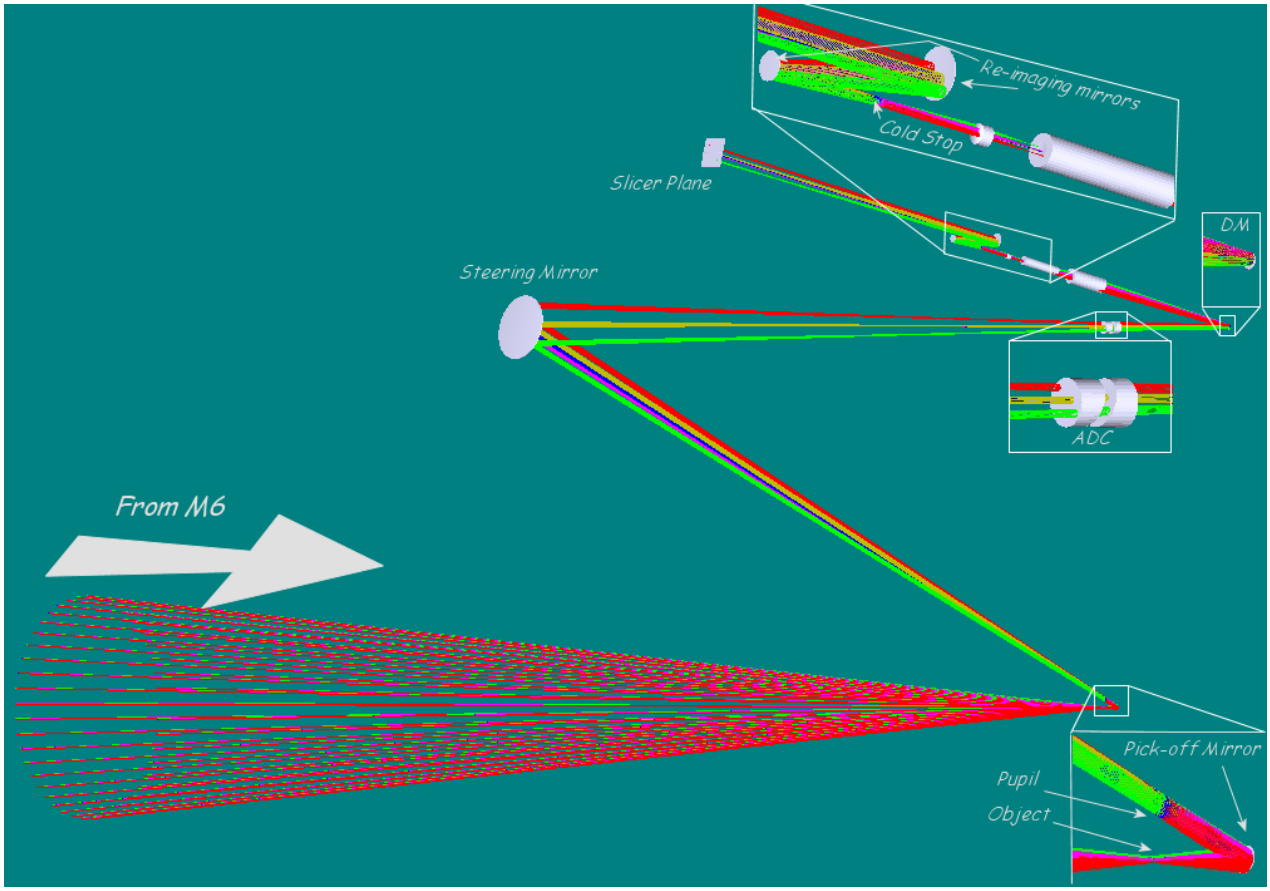

Figure 9 – Optical layout from the entrance plane to the image slicer plane

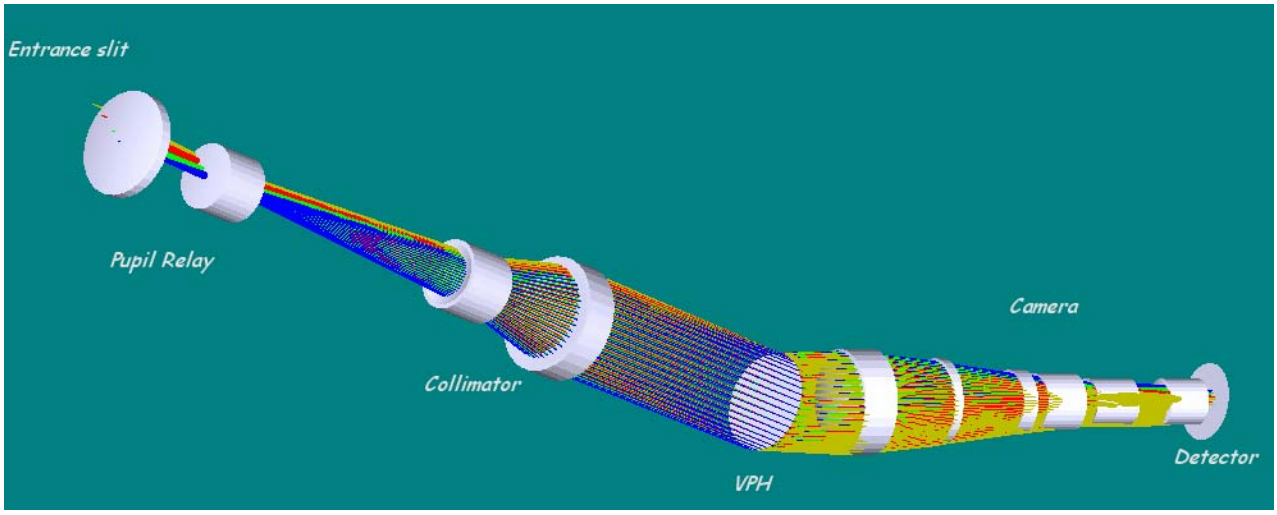

Figure 10 – Spectrograph layout.

6.5.4 Performance and Compliance

The current F/1.8 design uses LIF, BaF2, CaF2 and SF6 lenses. The classical IRG2 glass was not used as it does not seem to be available any longer. Later optimization to achieve lower speeds could be possible, depending on tradeoffs to be performed with the number of channels and the available mass and volume. The current design provides 20 mas sampling.

Table 8 – Summary of the optical characteristics

Item	Performance
Field Of View	5' x 5'
Spatial sampling	20 mas
N pixel per IFU	40 x 40
Individual FOV	0.8" x 0.8"
Spectral resolution	4000
Spectral coverage	Y or J or H or K in one shot
Throughput (excluding the telescope)	30% TBC

6.5.5 Development Risks

The design includes several as yet unproven items:

- Active steering mirror
- Cryogenic micro deformable mirror
- Cryogenic VPH grating

The optical components are more or less classical. A large part of the spectrograph uses aspheric optics but the departure from sphericity is well below the micron. The instrument is largely based on image slicer techniques. If these techniques are not fully mature for mass production as required for MOMFIS, nevertheless some instruments such as KMOS or MUSE will definitively pave the road for such a manufacturing approach.

6.5.6 Development plan & roadmap

Three sub-systems will definitively require specific roadmaps to achieve the required maturity when MOMFIS manufacturing starts:

1. Target acquisition system: this system needs a very accurate and stable positioning of the steering and pick-off mirrors for all telescope positions. This point has to be demonstrated. The JRA5 of OPTICON-FP6 is addressing this point.
2. Slicer unit: lots of efforts are made in Europe for the manufacturing of image slicers. MUSE, KMOS plus the JRA5 are tackling this point and we can consider that by the time of the development of MOMFIS few uncertainties on the manufacturing and performance will remain.

3. VPH Grating: VPH in cryogenic environments are being tested

6.6 Main Structure

This section describes the design of the main structure and gives an estimate of its mass. Compared to our previous work, the positioner is now attached to the structure. There was not enough time to perform a new FEA including the change of the positioner. However the results that were previously obtained with the previous design shall not be significantly changed, and be more than enough for the sake of this report and of the MOMFIS conceptual study

The following drawings are annexed to this section:

- 462-04-02A Main Assembly
- 462-04-11A Main Structure
- 462-04-12A Rotating Flange
- 462-04-13A Higher Ring
- 462-04-14A Spectrograph Support Platform
- 462-04-15A Cryostat interface

6.6.1 Function

The primary function of the structure is to support and ensure the stability of the spectrographs and of the positioner. The mechanical sub-systems supported by the main structure are:

- The thermal enclosure and the entrance window
- The focal plate supporting the pick-off mirrors
- The BSM assemblies
- The WFS
- The 30 spectrographs assembled in 10 cryostats
- The positioner, itself consisting of the robot, the focal plate exchange mechanism and the support structure

6.6.2 Specifications

The design of the main structure is constrained by the following interface and requirement specifications:

1) Volume. The structure shall fit and rotate within the allocated space in the focal station ([AD02]).
2) Mass. The global mass of the overall instrument should not exceed 17000 kg [AD2].
3) Optical stability: the requirement specification is that none of the focal plate, steering mirror and cryostat should tilt by more than 10 µrad during an exposure (typically 15 minutes). In the same time their translations (along the 3 directions) must not exceed 100 µm. This requirement must be understood for a 60° variation in telescope altitude

6.6.3 Interfaces

The main structure interfaces with the telescope focal station. We have based our design on the data given in [AD2]. Since then the focal station design has been updated [RD03]. Adaptation to these 2 versions of the focal station is discussed in a subsequent section.

6.6.4 Description

The concept of the structure is driven by two main items: the geometry and the materials.

6.6.4.1 Geometry

The design of the structure is the result of the following three considerations:

Adaptor/rotator diameter. As mentioned above the ICD adapter / rotator is not suited to MOMFIS: too low weight limit, space above rotator not available, etc. After ESO's approval, we took this rotator off and replaced it by a larger one, 4.5 m in diameter. A large bearing is more adapted to the available space: most part of the volume, including the inner part of the bearing, is left free for the instrument. Second, it makes possible some balance of the masses on both sides of the bearing plane allowing to limit the flexures of the structure and the loads on the bearing itself. This is extensively used in our design where space is used above the focal plane and outside its outer diameter. With this kind of adaptor/rotator the global structure becomes simpler and accessibility and stability are improved. Bearings of the required sizes are commercially available. The final design of the bearing would require further detailed study.

Number of cryostats. The instrument includes 30 identical spectrographs. One single cryostat hosting all the spectrographs is clearly not a good solution: increased complexity, maintenance, exceedingly large cryogenic volume, etc… We have also rejected the solution consisting in having one cryostat per spectrograph: this leads to loosing space at the interface between the cryostats (all cryostats must be fixed independently on a common structure). Our proposal (10 cryostats, 3 spectrographs per cryostat) is regarded as a good compromise allowing to optimize space constraints and integration and maintainability considerations.

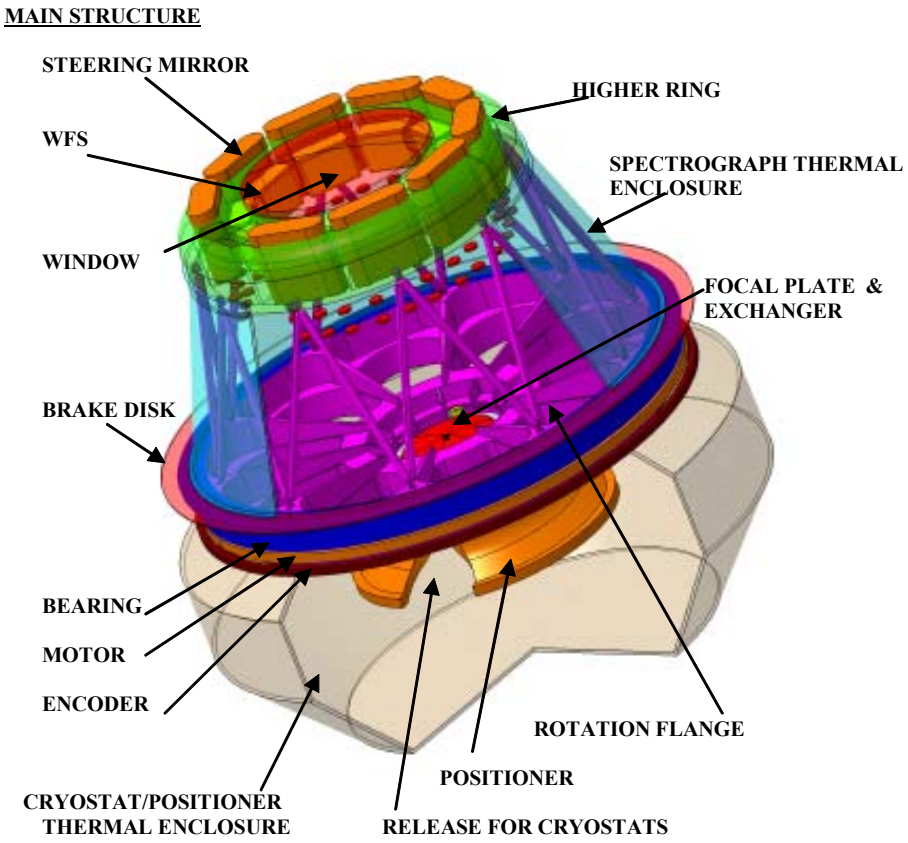

Figure 11 – The main structure concept (1)

The figure shows the main rotator with focal plane plate and cryostat support structure and the steering mirror and WFS support structure.

BSMs support. Considering that the BSMs are far away from the rest of the spectrograph optics, and conversely that they are close to the entrance window, choice was made to separate their support from the spectrographs structure and instead to use a separate structure for the WFS, the BSMs and the entrance window.

The previous considerations led to the design shown Figure 11 and Figure 12. See also the annexed drawings for more details about the different parts of this structure. The thermal insulation is dealt with in section 6.18.

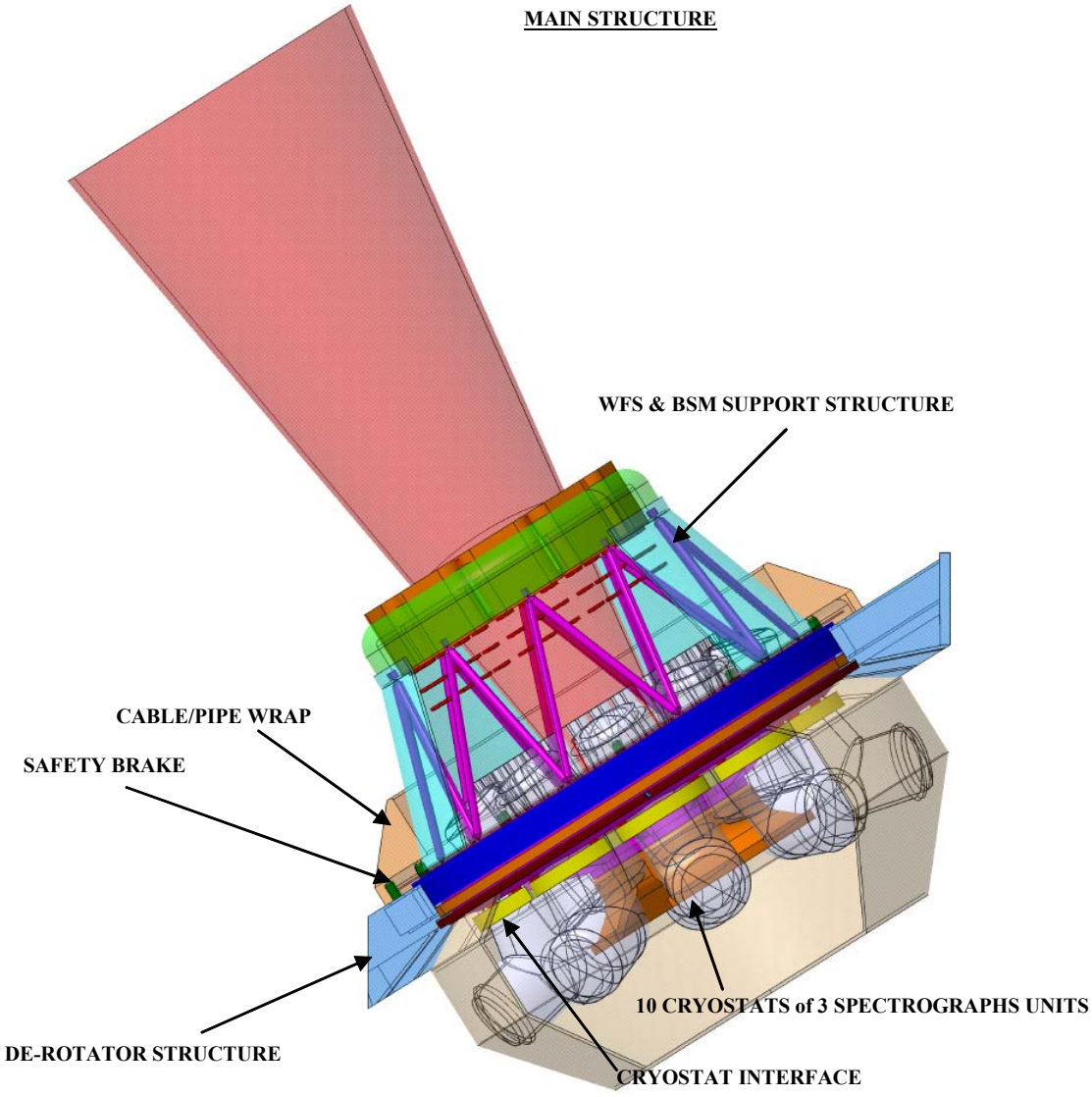

Figure 12 – The main structure concept (2)

6.6.4.2 Materials

The required stability of the structure (flexures and thermal) compared to its size is a quite severe requirement. If we add the quite tight mass budget allowed for the instrument it seems clear that some trade-offs on the structure materials must be reached. We provide in Table 9 some mechanical characteristics of various materials. In addition to "classical" material such as steel or aluminium we list a ceramic (SiC) and a composite based on carbon fibres. The two last materials present a significant advantage compared to the two others in both stiffness to mass ratio and thermal expansion.

Table 9 – Materials characteristics

	Specific mass kg/m^3	Elasticity modulus GPa	Thermal expansion coef. K^{-1}
Steel	7800	210	12
Aluminum alloy	2700	74	23
Silicon carbide	3100	410	4
Composite carbon fibers HM (60%) + epoxy resin. Bidirectional.	1600	117	< 1
Composite carbon fibers HM (60%) + epoxy resin. Mono directional	1600	234	< 1

The choice of silicon carbide does not appear to be a realistic solution at the moment mainly because of its price. Conversely the carbon/epoxy can be manufactured at a reasonable cost and can (with a specific design considering the directions of the fibres) meet the performance of the ceramic. We chose this material for some parts of the baseline structure.

The cryostat envelopes are assumed to be in stainless steel. We suppose also that all the components of the adaptor rotator are built in steel as is its supporting platform. All the rest of the structure i.e. the rotating flange, the focal plate, the triangulated beams, and the higher support ring are built in composite carbon/epoxy. Figure 13 shows the distribution of materials on the instrument. All the composite plates are supposed to be bidirectional. Conversely, the triangulated beams (tubes diameter 80 thickness 6 mm) are built in mono directional composite.

Further studies will be required for the design and feasibility of composite structures and of interfaces between different materials (steel/composite in this case).

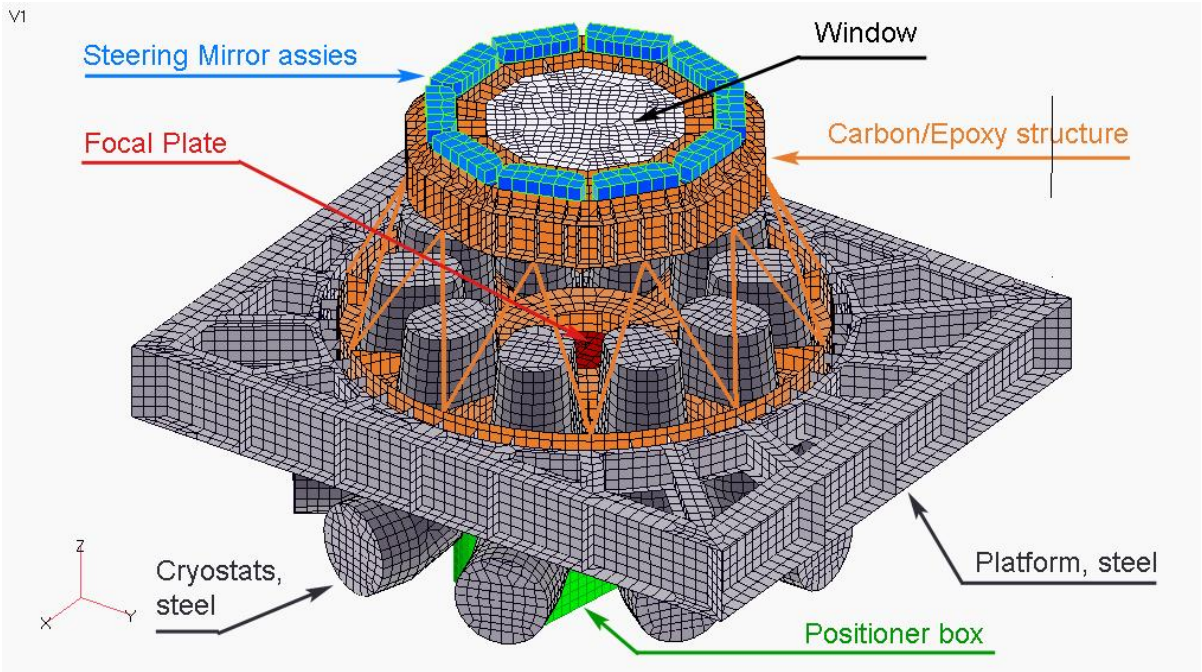

Figure 13 – Main structure: material distribution

6.6.5 Performance and Compliance

A FEA has been carried out using Nastran. The model includes an assumption for the design of the structure: this is a steel structure built of welded I-shaped and U-shaped beams. In the model its external dimensions are 6.191m long, 5.3 m wide and 700 mm thick. The structure is simply calculated in three load cases where 1 g is successively applied along X-axis, Y-axis and -Z-axis. The fixation nodes are located on the outer edges of this platform.

Different sub-system structures such as the one supporting the steering mirrors and the WFS or the positioner remain to be defined. For the moment they are only simulated as simple boxes whose dimensions and centers of gravity have the values given by the design. Their masses, estimated separately, are introduced as "non structural masses" in the model.

The enclosure is not present in the model. Indeed, its mass is quite small: 300 kg. In addition it is mainly supported on the inner ring of the rotator bearing: its impact on the instrument stability is quite limited.

6.6.5.1 Mass budget

The global mass of the Nastran model as shown on Figure 13 is 32000 kg, excluding some items such as cable twist and enclosure. See section 8.1 for the detailed mass budget and discussion therein. The mass of the rotating carbon/epoxy structure is 3500 kg. We have computed that the use of this composite material instead of steel or aluminium allows to save about the same mass, i.e. 3.5 tons, for a similar performance.

6.6.5.2 Stability

The structure is simply calculated in three load cases where 1 g is successively applied along X-axis, Y-axis and -Z-axis. Then we give in these three cases the maximum displacements and rotation induced on four sub-assemblies: the focal plate, the steering mirror assembly, the cryostats and the positioner. The table below summarizes the results.

Then we give in these three cases the maximum displacements and rotation induced on three sub-assemblies: the focal plate, the steering mirror assembly and the cryostats. Table 10 below summarizes the results.

Table 10 – Flexures

	Focal plate		STM/WFS/Window		Spectrographs		Positioner	
	Max motion (µm)	Max tilt (µrad)	Max motion (µm)	Max tilt (µrad)	Max motion (µm)	Max tilt (µrad)	Max motion (µm)	Max tilt (µrad)
1g / X	50	70	75	30	100	50	200	80
1g / Y	30	45	65	30	80	40	180	100
1g / Z	135	20	50	20	130	70	155	10

Of course these results remain very coarse (the design of the structure for example leaves a large margin for optimization) but they show that it should be possible to limit, for any 60° telescope motion in altitude, all optical displacements within 100 µm. This value is compliant with our goal (see section 6.6.2). On the opposite, the specification of 10 µrad stability in rotation is not met. Values around 50 µrad or more is the order of magnitude of what is possible to obtain with this kind of structure. The motions exceeding the requirements will need to be controlled with internal metrology.

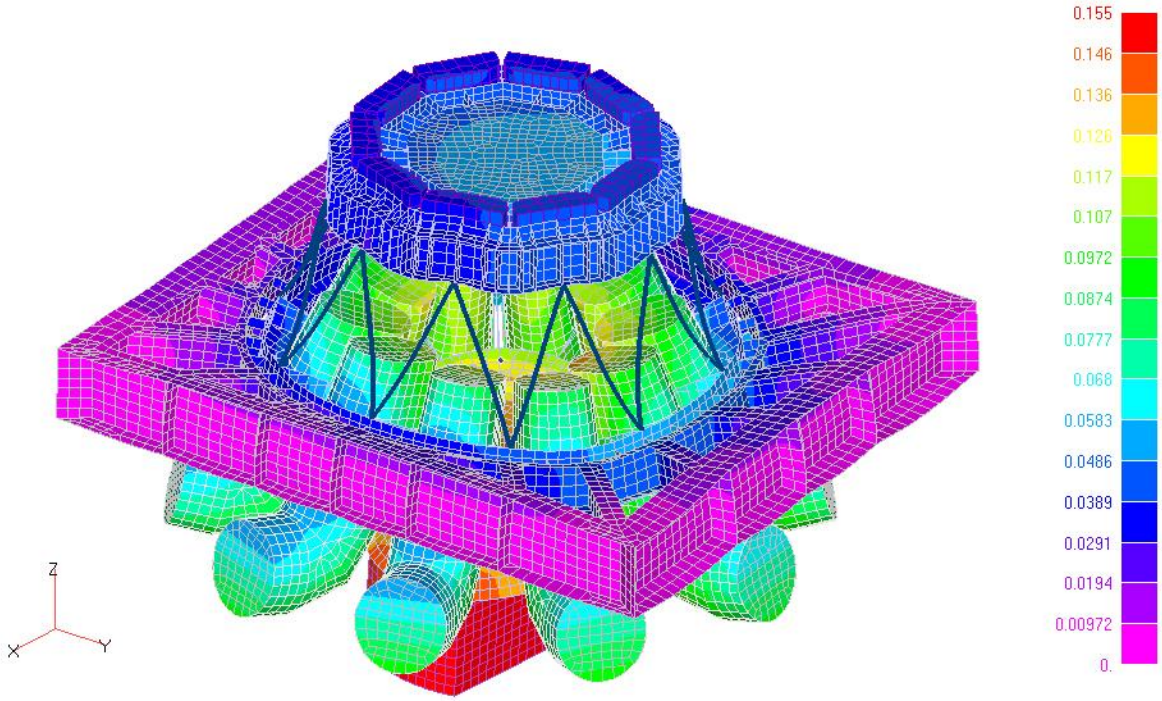

Figure 14 – Deformed structure when 1 g is applied along the Z-axis

6.6.5.3 Adaptation to focal station

The ability to implement the instrument in the given volume of the focal station appears to be a critical issue for the design. We based our design on the data given in [AD2]. [RD3] gives a quite different design for this station: the global volume is larger, the height is significantly increased. This allows the implementation of other equipment (such as the electronic cabinets) inside the focal station. In the two cases unfortunately we have the same difficulty to implement the main structure in the volume because its position is imposed by the location of the telescope focus. Figure 15 outlines the differences between the two versions of the focal station and shows why the implementation of MOMFIS is difficult.
On the left is shown the implementation of the instrument in the old volume: the higher ring of the structure is out of the authorized space by about 445 mm. On the right is shown the instrument positioned in the new focal station, *after* moving the focal plane by 1876 mm. It is otherwise impossible to implement the instrument without this (admittedly major) modification of the focal environment.

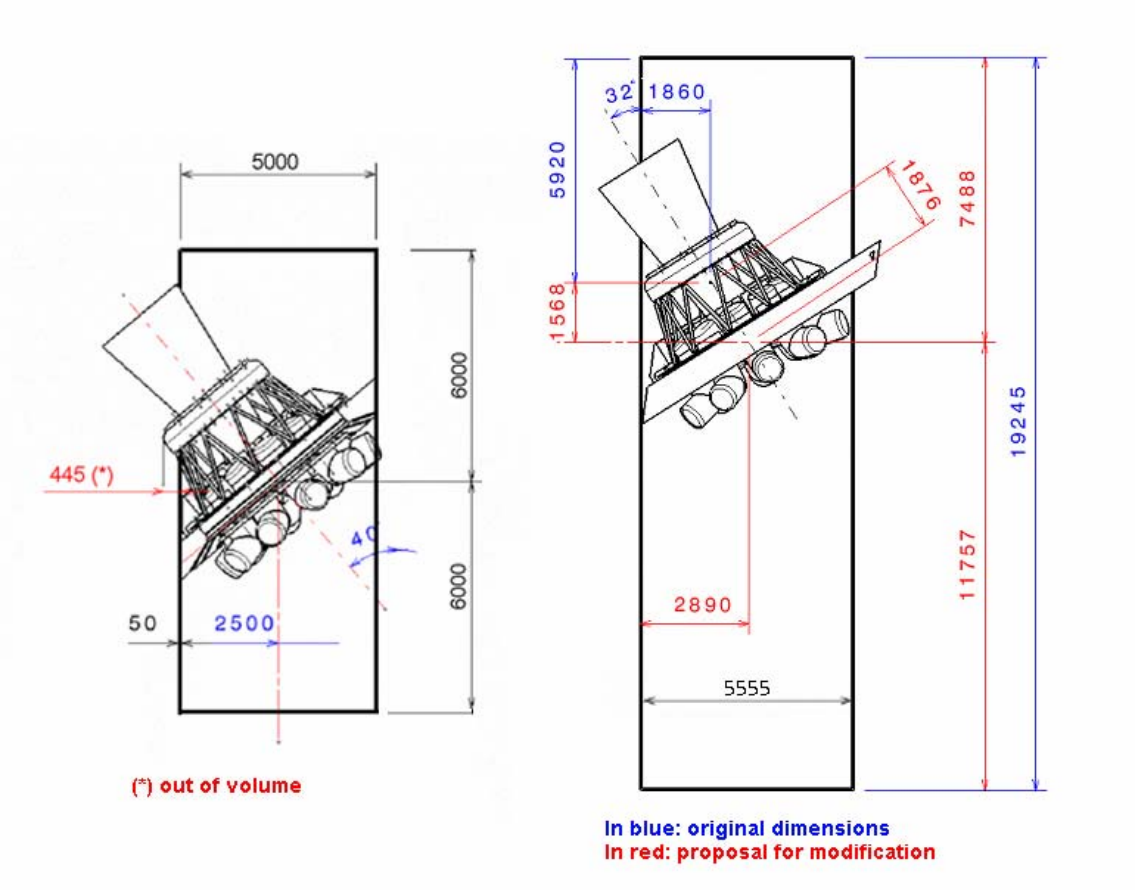

Figure 15 – Instrument implementation in the focal station.

Left: old volume. Right: new volume after translation of the focal plane.

6.6.6 Reliability & Maintainability

Nothing special regarding the structure in that section. One can refer however to the positioner maintenance and extraction concept presented in section 6.7.4.4.

6.6.7 Integration

In that design, some dummy 4.5 m adaptor/rotator shall be available for instrument integration. Obviously this adaptor shall be supported by some turntable allowing the simulation of telescope rotations.

6.6.8 Development Risks

There is no major risk in the development of the structure in itself. Its development is however highly constrained by the high level specifications such as the number of arms versus the allowed volume and mass or the stability requirements.

6.6.9 Development plan & roadmap

The development plan shall consider:

- Definition of higher level specs: volume, mass and stability,
- Feasibility study of a 4.5 meter adaptor/rotator,
- Definition of an appropriate structure for this adaptor (link to telescope),
- Feasibility study of carbon/epoxy structures and interfaces

6.6.10 Cost and FTE

The design of this structure (including specificities of composite definition and calculation) is estimated around 1.5 FTE. The manufacturing cost of a carbon/epoxy structure is about 250 € per kilogram. The mass of the structure is about 3000 kg: 0.9 M€.

The design of the thermal enclosure will need specific analysis: mechanical FEA for optimization of the weight of the beam structure and thermal analysis for the estimation of the instrument thermal stability. The manufacturing should not be too complex. Including the cost of structural material, of insulator (MLI) and of all the small hardware the cost should not exceed 30 k€.

6.7 Positioner Assembly

The positioner concept of MOMFIS heavily relies on two instruments that have been developed at Anglo Australian Observatory: 2dF and Oz-Poz. We adopted in this conceptual study to resort to a proven concept and proven technologies. These instruments being in operation, they demonstrate most part of the feasibility of our proposal. We will limit our description to the adaptation of these principles to the MOMFIS needs: global implementation and access for maintenance, specificity of the pickoff mirrors that are bigger than the2dF and Oz-Poz buttons and which also need to be rotated and adjusted before positioning. Alternative more advanced concepts such as the starbugs also developed at the AAO could obviously be considered at later stages when feasibility is demonstrated and maturity reached.

The following drawings are annexed to this section:

- 462-03-01a_3 Positioner Assembly
- 462-02-01d_2 Baseline of Bug
- 462-03-02a_3 Focal Plate Subassembly
- 462-03-02c_3 Robot Positioner Assembly
- 462-03-02e_3 Robot Head & Bug Adjustment
- 462-03-02g_3 Maintenance Platform

6.7.1 Function

The positioner for MOMFIS allows the positioning of ~ 40 pickoff mirrors (hereafter referenced to as ‘bugs’), including 30 mirrors for the science beams and 10 others for the reference sources (WFS) on a focal plate 876 mm in diameter. Each bug is maintained on the plate by a magnet. The bug includes a spherical mirror and folds the beam towards a steering mirror. The

folding angle of this mirror varies as a function of X&Y position on the focal plate. An orientation function (not present in Oz-Poz) is then necessary.

The robot picks up the bugs from a parking, pre-rotates them according to their target position in the focal plane and the position of their associated beam steering mirrors, then positions them to the configuration focal plate. After the plates are swapped, the robot unloads the previously used focal plate and parks the bugs prior to a new configuration. Note that the bugs need to be rotated around two axes (X, Z). One of the rotation (RZ) is included in the robot head, the other (RX) can be performed either in the robot head or with a dedicated system to appear at the edge of the robot rail close to the bugs parking.

In addition, the system (as it is the case in AAO instruments) must allow the setup of a second focal plate when the first one is in observation. A rotating tumbler exchanges the two focal plates from an "observation" position to a "configuration" position. During an exposure, the "observation" focal plate and the "configuration" focal plate remain attached to this tumbler.

6.7.2 Specifications

▪ Temperature	0 °C to 10 °C - TBC
▪ Focal plate radius (conic-convex)	2200mm - TBC
▪ Field diameter on focal plate	876mm - TBC
▪ Bug positioning accuracy	10μm
▪ RZ Bug Rotation:	range 360°, accuracy TBD
▪ RX Bug Inclination:	range ±10°, accuracy TBD
▪ Stability between 2 bugs	1μm during one 30 min (TBD) exposure
▪ Minimal distance between 2 bugs	< 15 mm

6.7.3 Interfaces

The main mechanical interfaces with the positioner are the following:

- Robot versus main instrument structure
- Focal plate tumbler versus instrument structure,
- Positioner assembly versus maintenance platform. Definition of extraction tools.

6.7.4 Description

Figure 16 below shows one possibility to implement a 2dF type positioner on MOMFIS. The positioning system on the area of the focal surface is of Rθ type (Oz-Poz type) unlike 2dF which relies on a X&Y table.

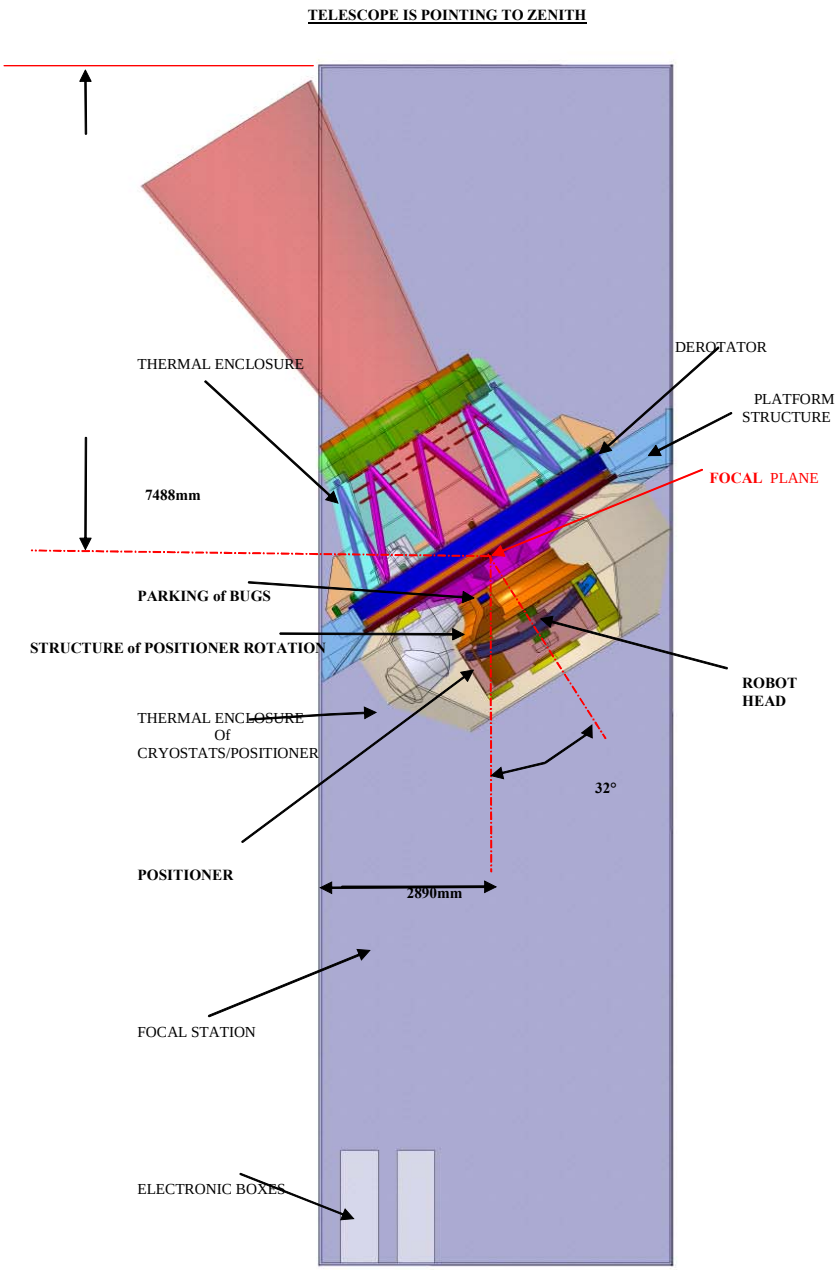

Figure 16 – View of positioner in instrument and focal station

The following subassemblies are described below: the bug, the focal plate tumbler, the robot positioner, the extraction structure and finally the bug adjustment specificities.

6.7.4.1 The bug

The MOMFIS bug is quite different from the buttons that are used in Oz-Poz. Its diameter is bigger, it must include an orientation of the folding mirror it holds toward its corresponding steering mirror, and finally it doesn't have to carry the fibres as with FLAMES. Some specific studies, trade-offs and possibly prototyping will be necessary for defining this critical

component. However we present here a baseline that allows the description of the functions and gives an overview of what this bug shall be.

The bug spherical mirror is fixed on a RX handle that includes a spherical guiding system and a 16 mm long lever arm (see Figure 17). At the end of this arm, two flat surfaces make a guiding in Y direction. In addition these two surfaces are pressed by a spring system TBD that creates friction forces that insure the stability of the mirror after positioning. The rotation RX of the bug is performed by an external finger that actuates the handle end in the Y direction.

The bug includes also two sensors plots fixed at angle 60° on its body. These sensors are necessary for the orientation along RZ of the position of RX axis.

Finally the system is held on its supporting surface by a magnet. Figure 18 shows the main specifications of the system.

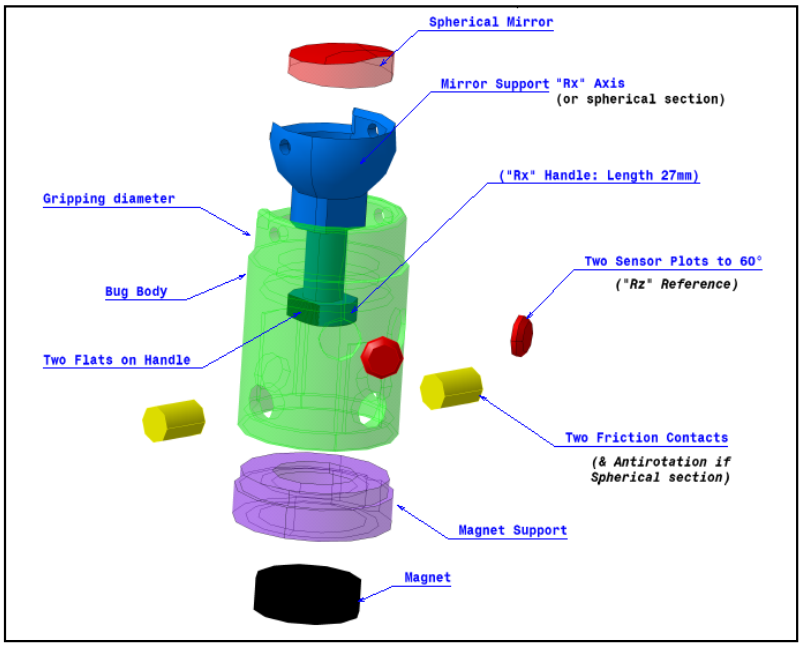

Figure 17 – Components of the bug

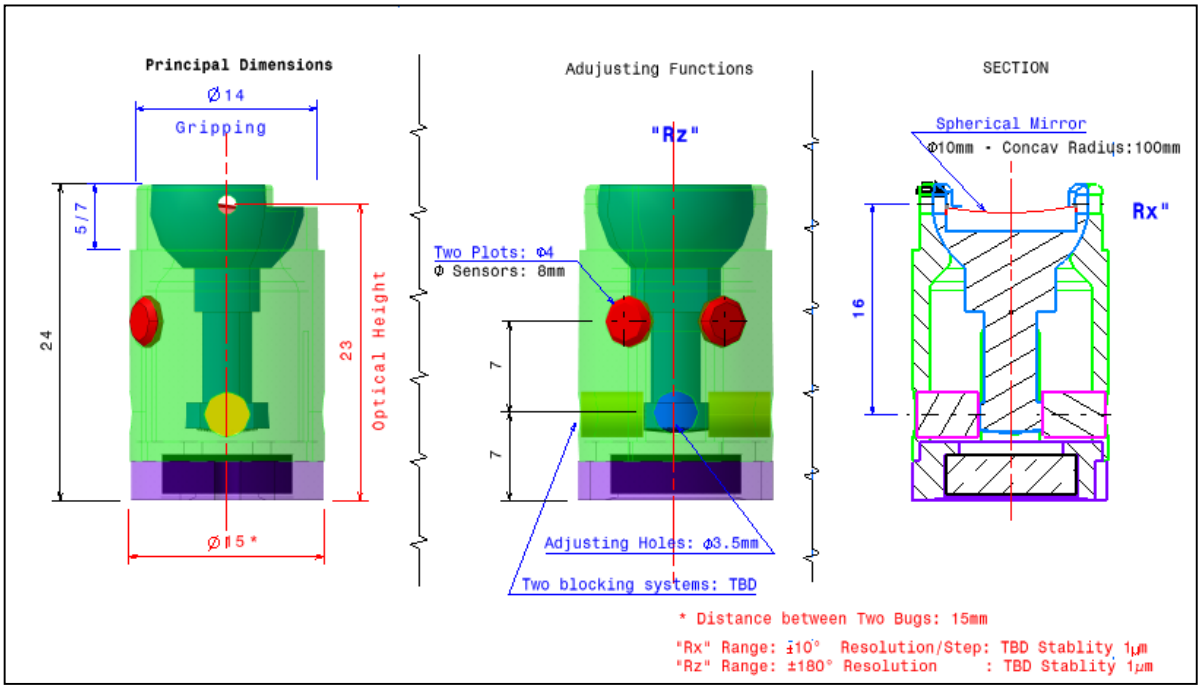

Figure 18 – Bug main specifications

The actuator for the orientation of the bug is the positioner itself and its robot head, see section 6.7.4.5 for a description of the adjustment principle.

6.7.4.2 The focal plate – Exchanger – Parking subassembly

The two focal plates are fixed on both sides of a rotating tumbler (see Figure 19) inspired from the 2dF concept.

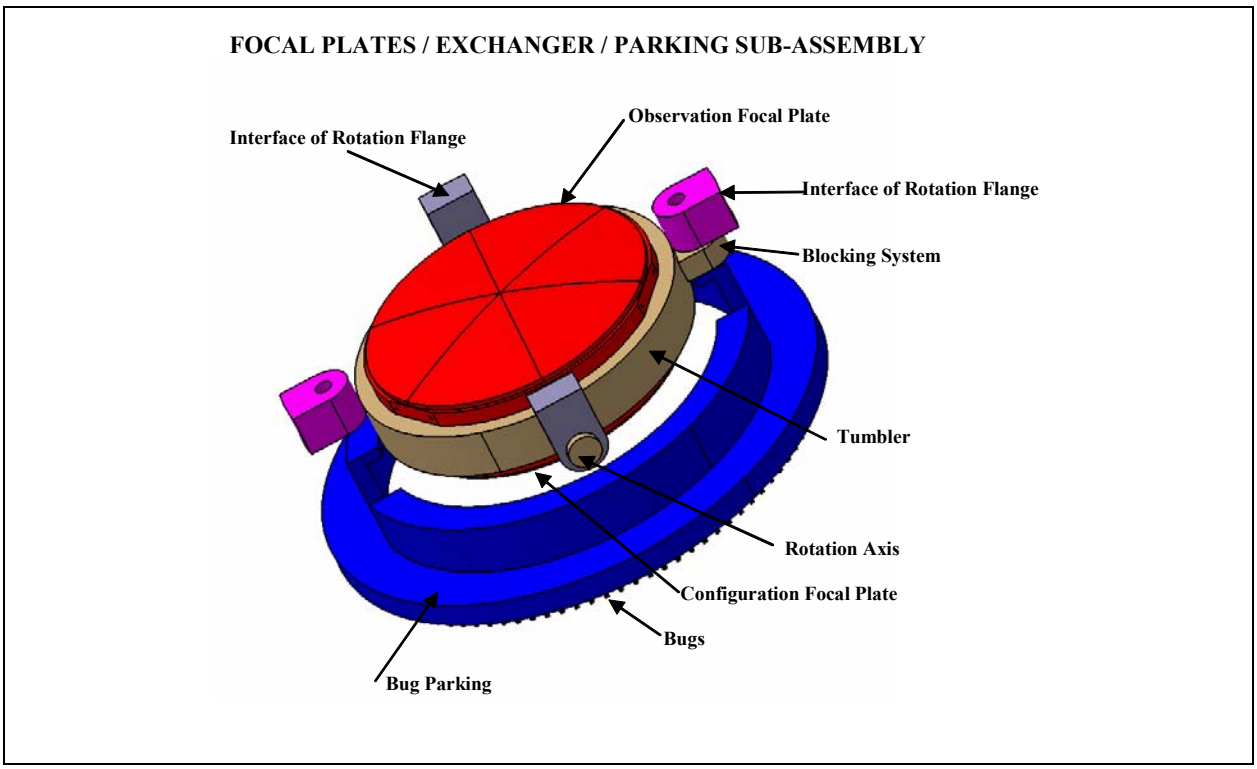

Figure 19 – The focal plate / Exchanger / Parking assembly

In order to fulfill the required stability of 1μm from bug to bug, the focal plate will be built in some composite of carbon/epoxy type which thermal expansion is limited. The magnetism of the plate is then insured with the inclusion of iron TBD in the composite. The accuracy of the focal surface is mainly linked to the rotation accuracies required for the bug (TBD). The possible disturbances during exposures induced by the operation of the robot on the other focal plate shall be analyzed accurately. Some mechanical decoupling of the two plates could be necessary and in that case, a focal plate locating/gripping system shall be implemented on the two sides. In any case, an index and a locking of the tumbler must be implemented in its two positions. Figure 19 shows the two focal plates mounted on their rotating tumbler.

6.7.4.3 The positioning robot

The positioning robot is at the core of the system. We describe hereafter the implementation of its main functions and components.

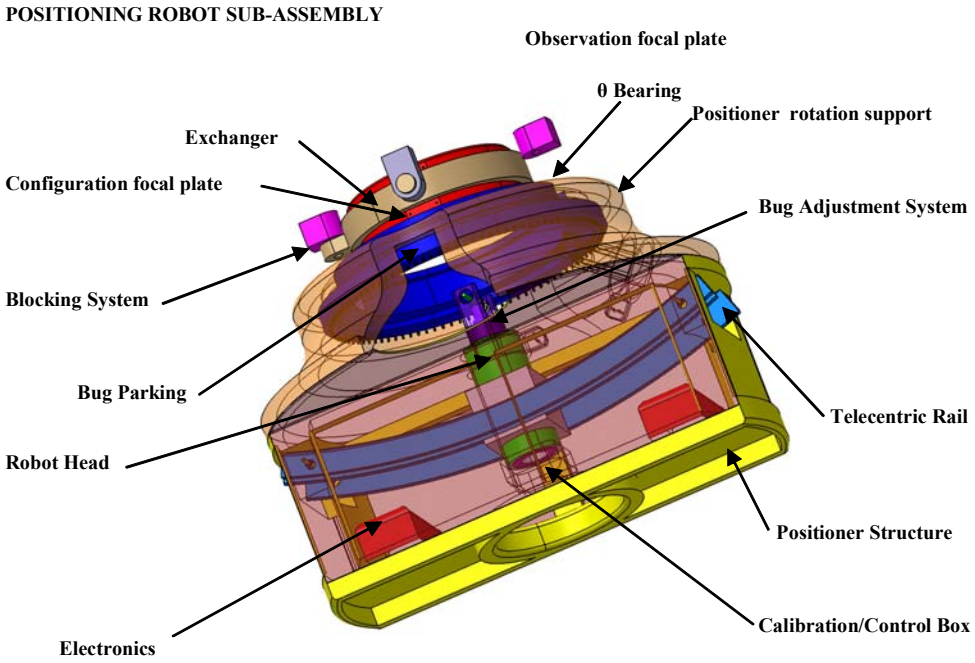

Figure 20 – The positioning robot sub-system

The robot head. This subassembly includes 3 motorized functions: an air pressure gripper, one translation TZ and one rotation RZ.

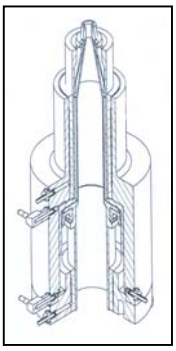

Figure 21 – The Oz-Poz gripper

As a starting baseline we adopted the principle of the Oz-Poz gripper. The only adaptation is to match the gripping diameter to the MOMFIS bugs. Currently, this diameter is 14 mm. In the Oz-Poz design, the gripping is ensured by air pressure. Since the robot rotates with the telescope, the reliability of the air pressure system is a specific issue that needs to be addressed during the development phase. The rotation RZ is needed for the orientation of the bugs. The bug is actually rotating around two axes RX&RZ. The first rotation is implemented in the bug itself. The second is included in the robot head. The functional amplitude of RZ is +/- 180 degrees. This rotation will require some special attention for the transport of the cables and pressurized air pipes.

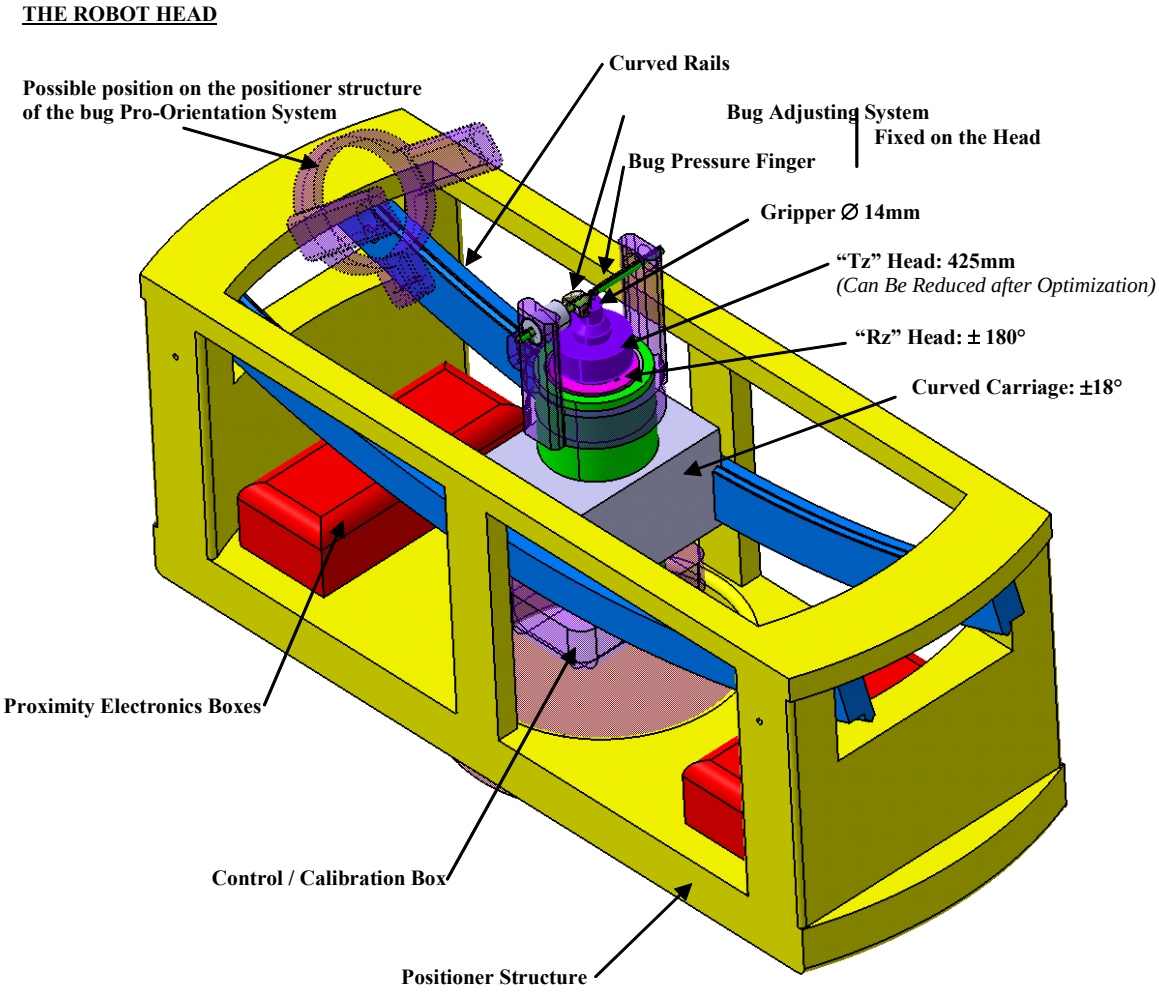

Figure 22 – The robot head on its curved R-rail

The translation TZ is needed to pick up (or to drop) the bug from (or to) its given position. In fact this translation has four main positions. Measured from the centre of the spherical focal surface we obtain:

- Radius on TZ reference: R 2640 mm
- Radius on RX Adjustment position: R 2620 mm
- Radius on parking location: R 2545 mm
- Radius on focal plate: R 2215 mm

The total stroke of this translation is then approximately 425 mm. This stroke is probably a bit long. It could probably be reduced by an optimization of the location of the parking and an increase of the tumbler height (distance between the two focal plates). Figure 22 shows the robot head mounted on its R-rail. Note the envelope implementation of a calibration/control box TBD behind the head.

The R&θ carriage. As on Oz-Poz this carriage allows the positioning in X&Y on the focal plate. The R-rails are curved, concentric to the focal plate surface. The θ rotation, implemented via a 1.4m diameter bearing rotates the full robot assembly. This bearing is located at the level of the interface flange of the positioner assembly (see Figure 20).

This principle, already implemented on Oz-Poz, should satisfy the MOMFIS requirements. However several difficulties shall be analyzed, 1st: the effects of the variation of the gravity vector, 2nd: the probable disturbances induced on the instrument side by the robot accelerations, 3rd: the possible disturbances on observing focal plate induced by the pickup or the release of magnetic bugs.

6.7.4.4 The maintenance platform and extraction carriage

The mounting/dismounting of the positioner assembly will obviously need a specific tool (as for most of the other sub-systems, e.g. the cryostats). We suggest at the moment to implement a maintenance platform below the instrument. This platform includes rails allowing the translation of some extraction carriage. This last carriage could allow the transfer towards the telescope lift (TBC). Figure 23 shows a sketch of the maintenance platform allowing the installation of the positioner and of one cryostat.

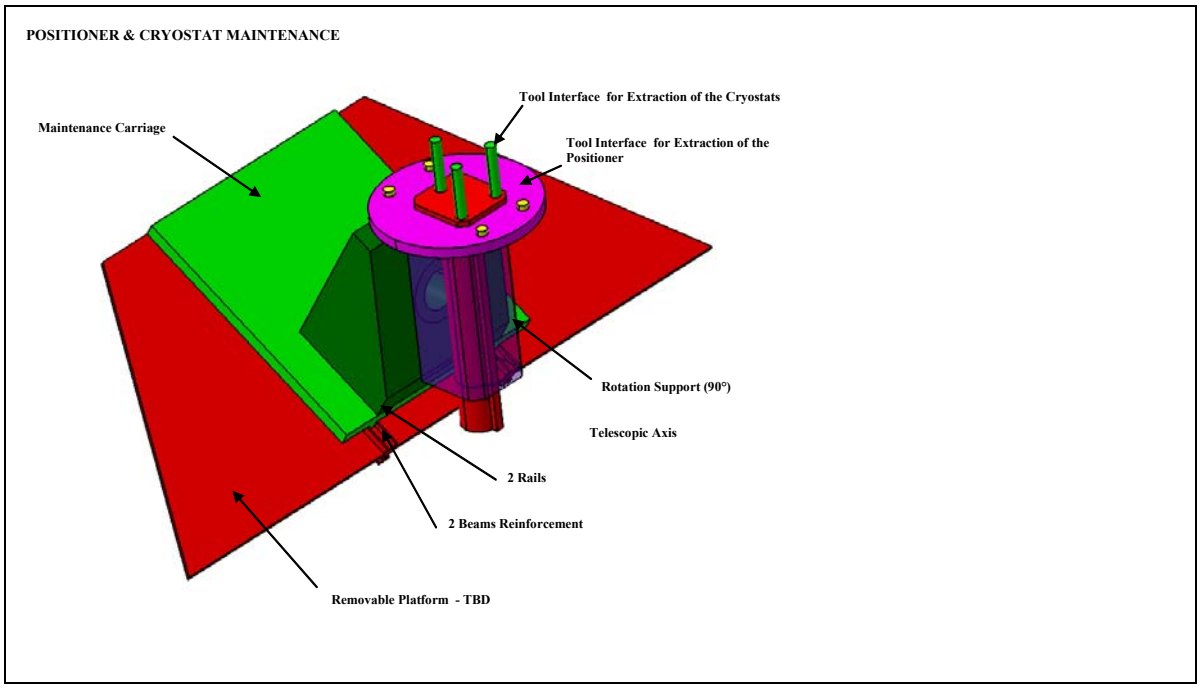

Figure 23 - The positioner assembly on its platform and the extraction carriage

The following Figure 24 shows the implementation of the maintenance platform in the focal station.

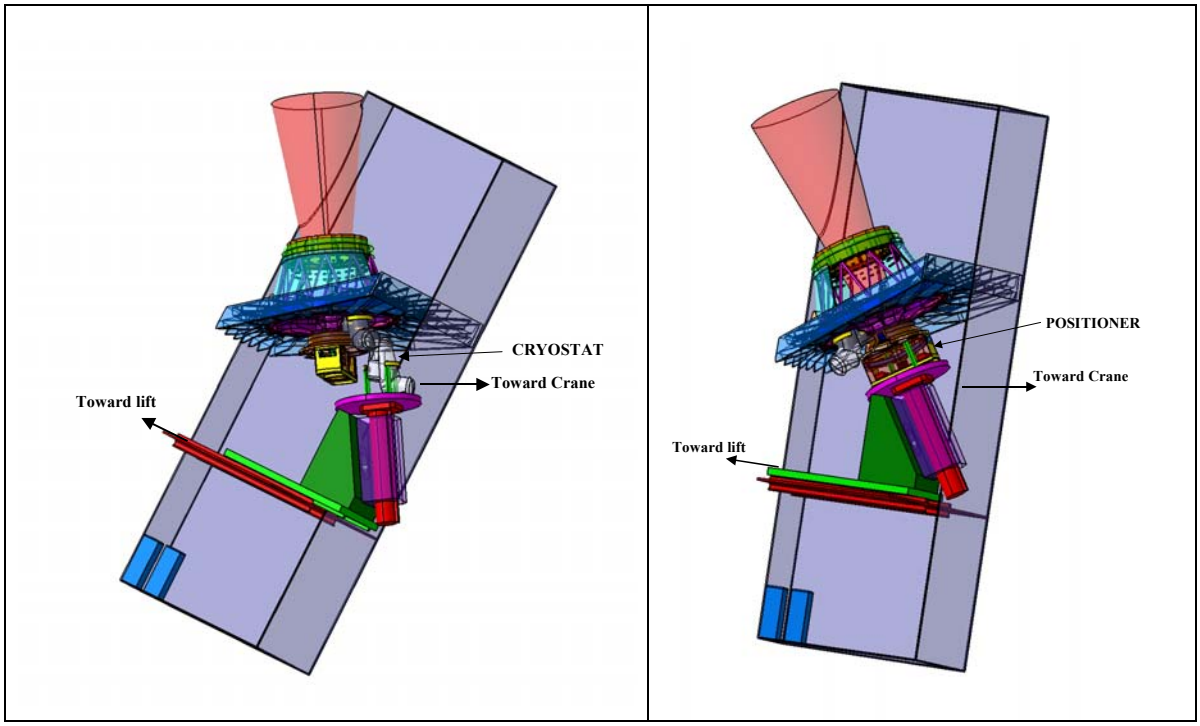

Figure 24 – Extraction of a cryostat (left) or extraction of the positioner (right)

We assume this kind of platform could be required by other instruments of the telescope. Several questions remain to be answered:

1) Can this platform be a fixed part of the "generic" focal station or shall it be specific to every instrument ?

2) For mass limit considerations should it be removed during operation? If yes, only one platform could be necessary to serve all instruments.

6.7.4.5 The bug adjustment

We have described the bug assembly in section 6.7.4.1. This bug includes a RX rotation system that allows the folding of the optical beam toward its corresponding steering mirror. Two options are possible for the bug orientation:

1°- The orientation system is included in the robot head
2°- It is reported on the periphery of the focal plate, in the parking area

The first option is functionally preferable because it allows some possible correction during the X&Y configuration but it obviously implies a more complex robot head design. For the moment we have adopted this approach. This orientation needs two rotations RZ and RX. The first is an orientation of the bug that sets the RX axis in the required position. The second (RX) is an internal rotation of the spherical mirror. It defines the orientation of this mirror as required by the

relative positions of the bug on focal plate and its associated steering mirror. The sketch of Figure 25 shows the sequence for this adjustment:

The actuator of RZ rotation is the robot head. The RZ zero is defined by two magnetic or capacitive sensors placed on the adjustment system (see Figure 17 & Figure 18) 'looking at' two sensors fixed on the bug.

The RX rotation is actuated via a finger (in green on the figures that exerts pressure on the mirror arm. This finger is either fixed on the robot head or on the adjustment system.

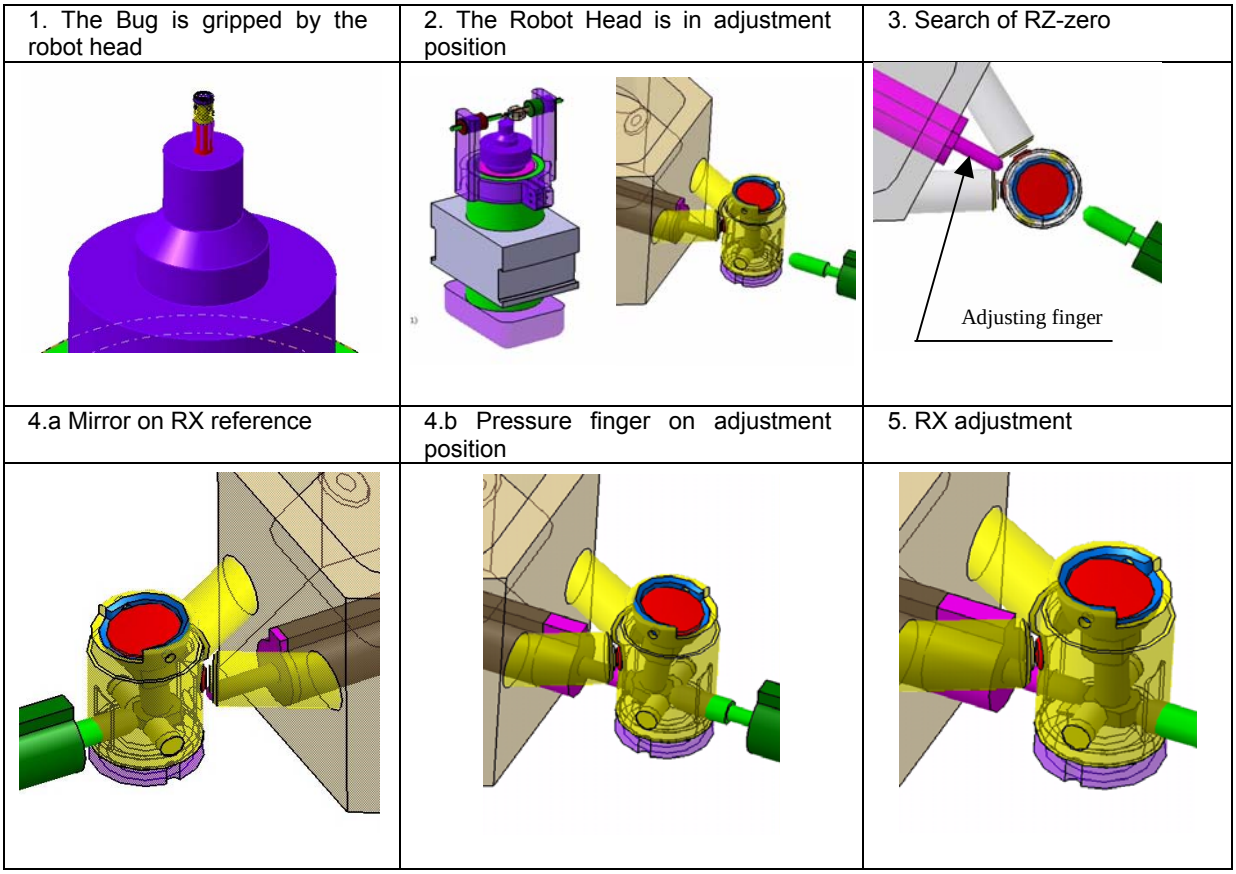

Figure 25 – Sequence of operation for bug orientation

6.7.5 Performance and compliance

The experiences of Oz-Poz and 2dF show that it is possible to obtain the required positioning accuracies in a short configuration time with this positioner principle. The main difference with Oz-Poz consists in the fact that the positioner will rotate around the altitude axis of telescope during operation. This will need additional studies such as for example the stiffness of the mechanisms or the power of the motors, but none of these points appear to be a major critical issue at this stage.

6.7.6 Reliability & Maintainability

The reliability of this complex mechanism will require particular attention during the conception phase. The experience of Oz-Poz will help. It is clear also that the availability of the system will highly depend on the accessibility to the focal station and on the maintenance facilities that will be available. Please refer to section 6.7.4.4 where we suggest the implementation into the focal station of some maintenance platform.

6.7.7 Integration

The integration phase for this assembly is obviously an important issue. It seems realistic at this stage to plan different and specific integration and test tools for each positioner sub-system: robot head, rotating tumbler, R&θ carriage, bug orientation mechanism. The whole system should be integrated on a dummy platform allowing the simulation of telescope motions. Finally, this assembly should be interfaced with the spectrograph assembly mainly to check the compatibility of the two assemblies: relative flexures, micro vibrations, disturbances induced by the robot, etc.

6.7.8 Development Risks

None of the technologies are unknown in the concepts presented here. The main development risk concerns the complexity of the global system (fifteen motorized functions, most of them being interdependent). A system functional analysis of the system (including software) would be required at the beginning of the study.

6.7.9 Development plan & roadmap

The following actions should be taken at the beginning of the development:

- Definition of higher level specs: volume and allowed mass,
- Definition of some maintenance concept and tools for the positioner,
- Development of an advanced prototype for the bug and the robot head,

6.7.10 Cost and FTE

The development studies of this system (including the software and some probable preliminary prototyping) will need approximately 40 FTE. The manufacturing cost should be around 2 M€.

6.8 Beam steering mirror (BSM) Concept

6.8.1 Function

The function of the beam steering mirror is to redirect the light emerging from the pickoff mirrors to the (fixed) DMs and optical trains (see Figure 5).

6.8.2 Specifications

- Mirror shape
  - Mirror diameter: ϕ 200 mm

- Curvature radius R1: 4000 mm +/- 200 mm
  R2: 4000 mm +/- 200 mm
- The radii shall be adjusted separately.

- Mirror motions
  - θx +/- 10° per step of 10" stability 0.1"
  - θy +/- 10° per step of 10" stability 0.1"
  - θz +/- 12° per step of 1'
  - Tz +/- 200 mm accuracy 5/100
  - The stability of the position must be guaranteed for one hour.
  - The mechanism is used at room temperature (20° +/- 0.5°).

6.8.3 Interfaces

- Mechanical interface: The BSM are grouped on sub-structures including 3 units. These sub-structures are assembled in the upper part of the instrument (see Figure 11).
- Thermal interface: No requirement.
- Electrical interface: actuation of the mirror shape, Z motion (perpendicular to the optical surface) and control
- Optical interface

6.8.4 Description

The beam steering mirrors are implemented in 10 groups of 3. The mirror shape is performed with piezo-actuators controlled via the piezo electric current and displacement probes glued on the piezo amplification rings (see Figure 26).

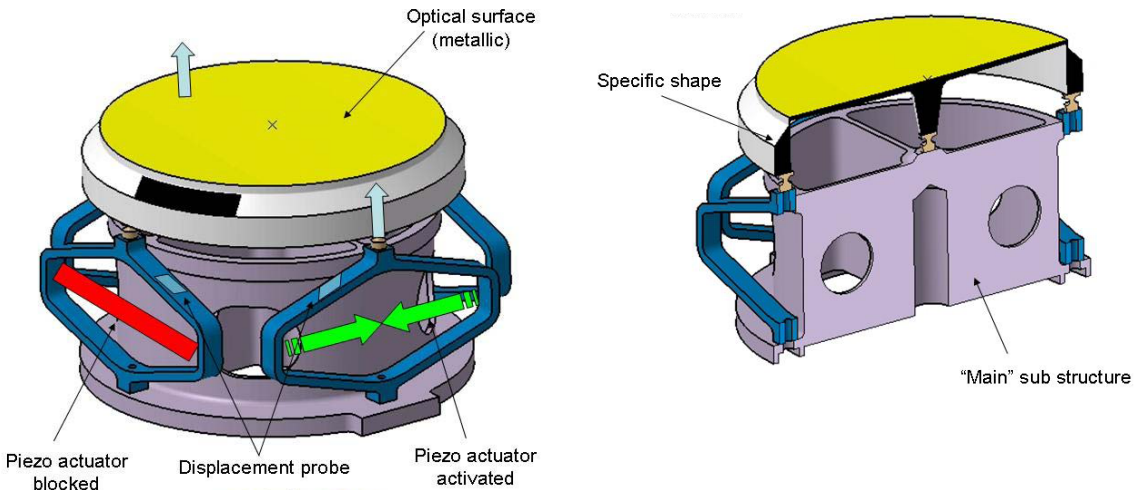

Figure 26 – Control of the BSM shape with piezo-actuator devices.

The mirror orientation requires rotations around the x, y and z axes and the position in z requires a translation stage. This is performed with 4 identical regular stepper motors (see Figure 27).

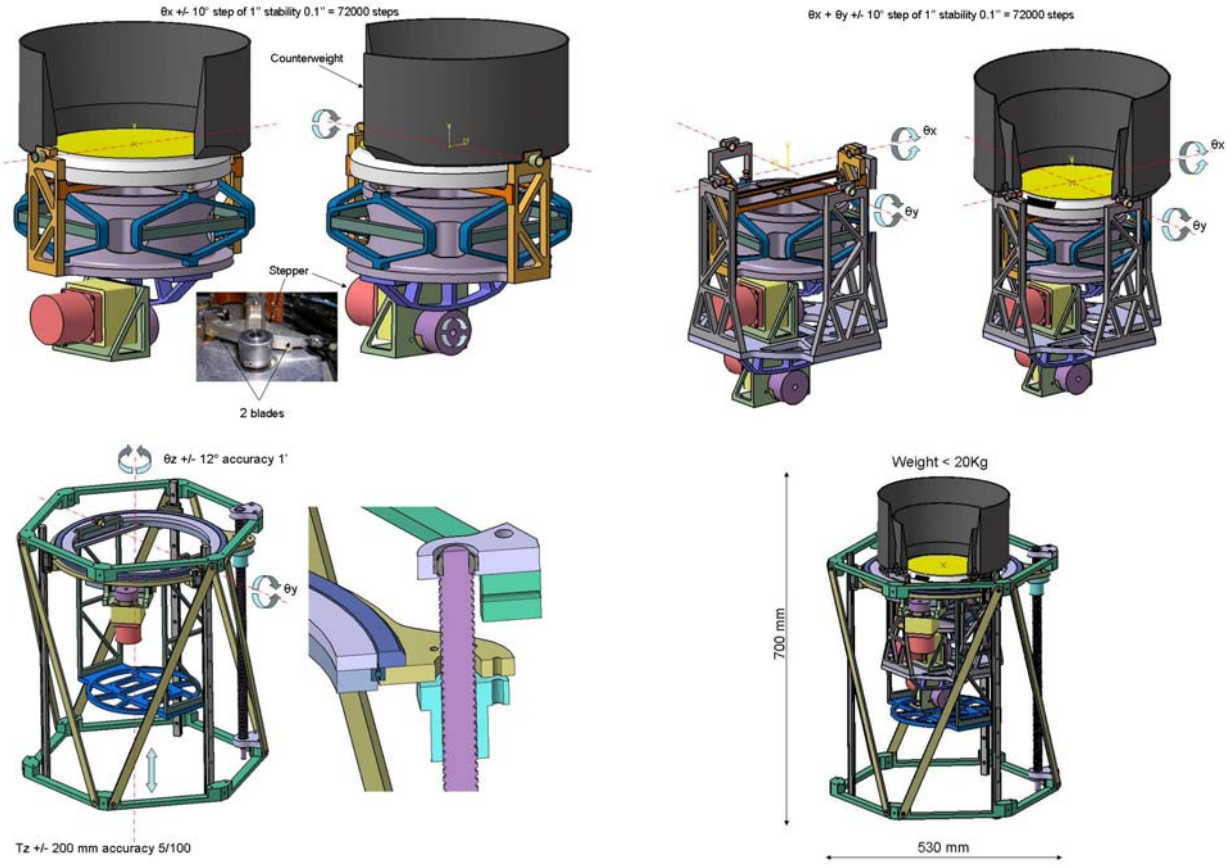

Figure 27 – BSM rotation and translation motions

An alternative solution is being explored for the BSM motions using an hexapod (see Figure 28). While such systems are readily available, it remains to be seen if and how the requirement on the translation range could be met.

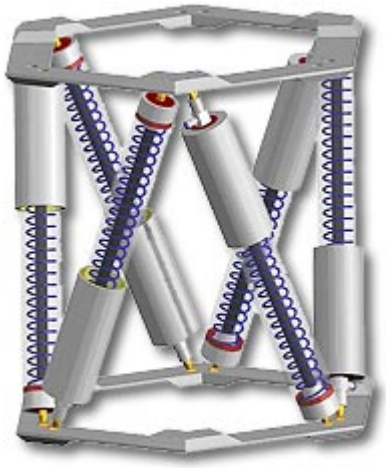

Figure 28 – Hexapod mechanism

6.8.5 Performance and Compliance

We have developed a modeling tool which combines optical and mechanical models, and allowing to design and optimize the geometry of the system and of the attachment points to reach the desired toroidal shape for the mirror. A FEM analysis is performed from which the Zernike polynomials are derived and compared to the optical requirements (see Figure 29). This process is performed iteratively until the adequate design is found. An illustration of the model is shown Figure 30.

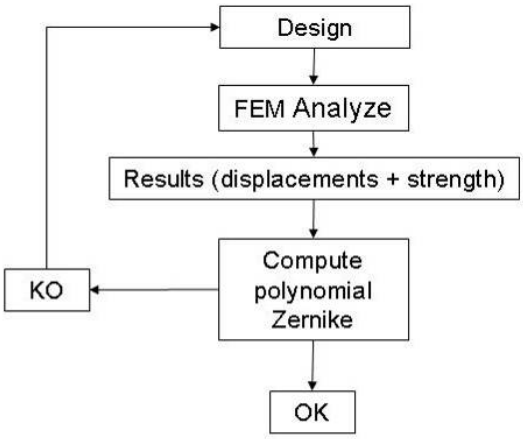

Figure 29 – Model for the BSM geometry

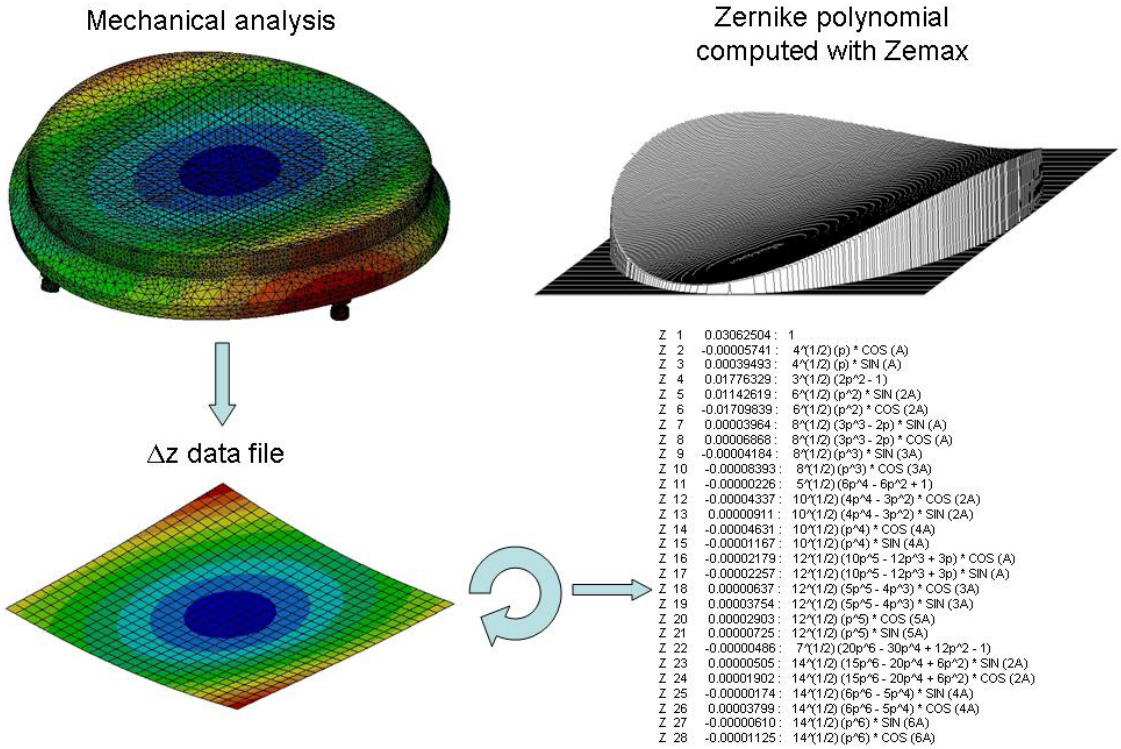

Figure 30 – Example of BSM model

6.8.6 Reliability & Maintainability

All the components of the system rely on existing technologies in use elsewhere. The grouping of the BSM in series of 3 shall allow to simplify the maintainability, and will reduce the impact of technical failures.

6.8.7 Integration

The 3-BSM units will be integrated on the upper sub structure by using a dedicated tool and after integration of the cryostats.

6.8.8 Development Risks

The compactness of the sub-system is currently an issue that shall be studied in further details. The hexapod alternative may offer better characteristics in that respect. Early prototyping of BSM systems shall allow to minimize the development risks.

6.8.9 Development plan & roadmap

Prototyping will be performed as part of the OPTICON JRA5 on Smart Focal Planes. Shall the hexapod system be used, specific developments might be necessary to accommodate the large translation range required.

6.8.10 Cost and FTE

Finalizing the design will require 1 FTE. The control command will require another FTE. The manufacturing cost for one unit is estimated at 80 k€.

6.9 Cryostat Concept

6.9.1 Function

The cryostat must keep the detector at cryogenic temperature (77K). The optical train can tolerate temperature variations inside the cryostat.

6.9.2 Specifications

The cryostat must be compatible with:

- the allowed volume
- detector temperature requirement
- detector temperature stability
- the mass budget
- the mechanical stability (flexures and vibrations)

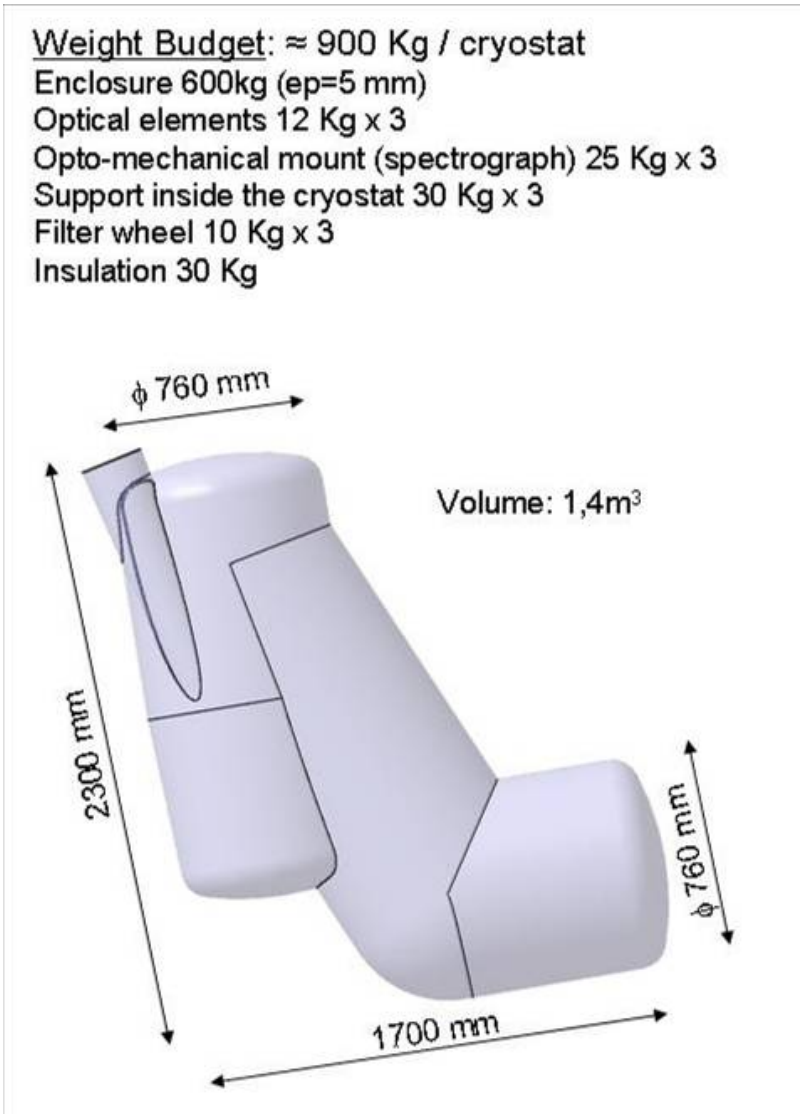

Figure 31 – Cryostat characteristics

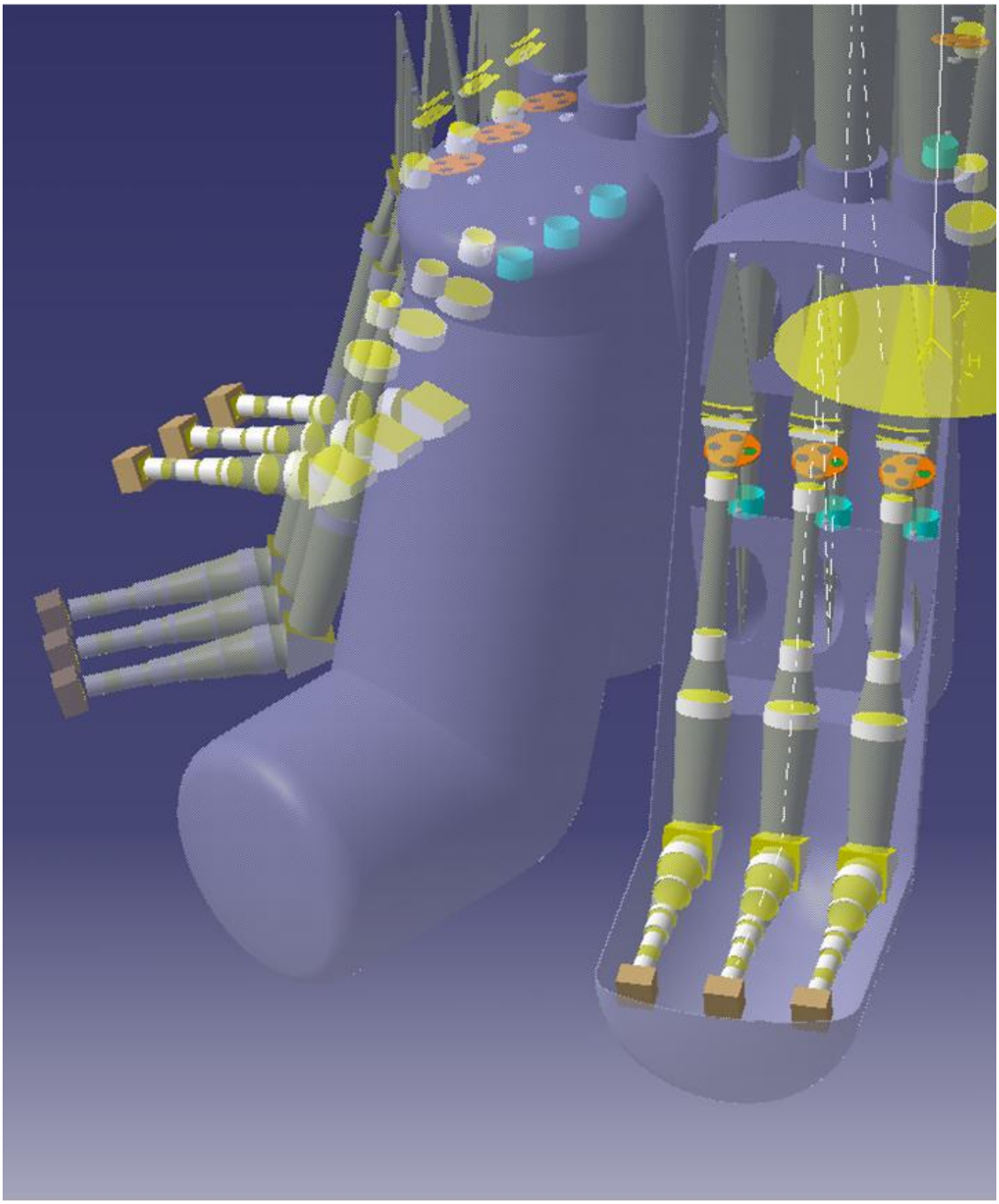

Figure 32 – Cryostat view in instrument

6.9.3 Interfaces

- Mechanical interface: the cryostat is implemented on the main structure of the instrument with a 3 points kinetic mount to avoid stress on the cryostat enclosure and on the support structure.
- Electrical interface: detector, cryogenic motors, heaters, sensors, etc.
- Thermal interface: cryogenic pipes in case of LN2 cooling or electric power in case of cryo-coolers
- Optical interface

6.9.4 Description

The cryostat is designed to integrate 3 spectrographs. It includes most of the MOMFIS optics and includes in particular the DMs, leaving only 2 warm mirrors: the pick-off and the beam steering mirrors.

A preliminary thermal analysis indicates that the required cooling power per cryostat is 360 W for an operating temperature of 77 K. 2 to 3 cryo-coolers would be needed per cryostat. LN2 cooling would require 190 litres/day and per cryostat.

6.9.5 Performance and Compliance

Although of large size, the cryostats are well within the size and volume of cryostats existing on other projects, and rely on proven and reliable technology.

6.9.6 Reliability & Maintainability

A possibility for maintenance is to have an extra cryostat as a spare and replace the cryostats on a rotating basis to perform preventive maintenance activities. This could also help resolving corrective maintenance activities in case of technical failures.

6.9.7 Integration

Dedicated tools and test equipment will need to be developed for the integration of the cryostats, otherwise well within the capabilities of well-equipped laboratories.

6.9.8 Development Risks

The cryostat assembly uses standard technology so the risk is minimum. A detailed thermal study is required to define, together with the telescope project office, the best cooling system.

6.9.9 Development plan & roadmap

The following aspects shall be studied:

- Thermal study for the LN2 and cryo-cooler solutions allowing to meet the detector and optics temperature requirements, including gradients and stability
- LN2 availability at the telescope
- Vibrations

- Electric power consumption
- Development and operational cost
- Maintainability
- Mechanical implementation
- Integration

6.9.10 Cost and FTE

Enclosure (1/3 study + 2/3 manufacturing): 40k€
Thermal shield (LN2 case) (1/3 study + 2/3 manufacturing): 5 k€
Cryo-coolers: 50 k€ per unit
Accessories (windows, taps, connectors, etc …):20 k€
Vacuum pump : 25 k€

6.10 Deformable mirror

The study of the DM in terms of technological developments is beyond the scope of the MOMFIS study, and is widely covered elsewhere in the OPTICON and ELT Design Study FP6 activities. For the sake of this report we list in Table 11 the ideal specifications of the deformable mirrors that are required for MOMFIS as specified.

Table 11 – DM MOMFIS requirements

N°	Parameter	Value	Comments
1	Number of actuators	200x200 (30000 useful actuators on a circular pupil)	Regular square array assumed.
2	Actuator Spacing	≈1mm typical	Smaller spacing is an advantage for the overall DM size and mass. Nevertheless, we have to be aware that the corresponding local slope is in the arcminute range with a 1mm spacing.
3	Clear Aperture Size (or diameter)	≈200mm typical	if difference in x and y: overall slightly elliptical shape
4	Maximum Mechanical Stroke (PV)	≈6 μm (i.e. optical stroke is 12 μm)	Assumptions: 1" seeing is assumed 25 meter external scale 65% is corrected via GLAO (i.e. 35% is corrected using the present DM)
5	Interactuator Mechanical Stroke (PV)	> 1.0 μm	Assumptions: 1" seeing is assumed Infinite external scale
6	Actuator Influence Function	First neighbour coupling coefficient of at least 20%. To be sufficiently smooth to fit the	

		Kolmogorov density spectrum of $k^{-11/3}$.	
7	Overall DM WFE (High order WFE, Hysteresis, DM reproducibility, DM stability…)	≈ 100 nm rms	Overall WFE should be less than 200nm RMS arbitrarily shared into 4 contributions, one of them being the DM WFE.
8	Surface Roughness	< 30 Å rms	TBC (scattering problems)
9	Scratch/Dig Ratio	TBD	
10	Temporal Frequency Response	TBD	Typically first eigenfrequency should be larger than 500 Hz
11	Coatings	>99% above 1.0μm	To Be Confirmed
12	Temperature of operation	77 K as per current design. Shall this prove impossible, the DM would have to be moved outside the cryostat and then operate in the 0 – 15°C range	
13	Thermal specifications	When the DM actuators are operated, its optical surface temperature shall not deviate from ambient temperature by more than 0.1°C (TBC)	At the lowest temperature of operation

6.11 Relay Optics and Cold Stop

6.11.1 Function

The relay optics creates a pupil image onto the cold stop and modifies the scale plate onto the image slicer. This optics is not creating anamorphic magnification. It will be much simpler if the DM can be cryogenic, hence allowing using it as cold stop.

6.11.2 Specifications and interfaces

The input interface is the image of the pupil on the DM. The size of the pupil at this level is 9mm. The entrance FOV is about 2.5°. The output interface is an image plane on the slicer unit. The plate scale at this level has to be 10mas/mm. The F-ratio at the level of the slicer is F/206.

6.11.3 Description

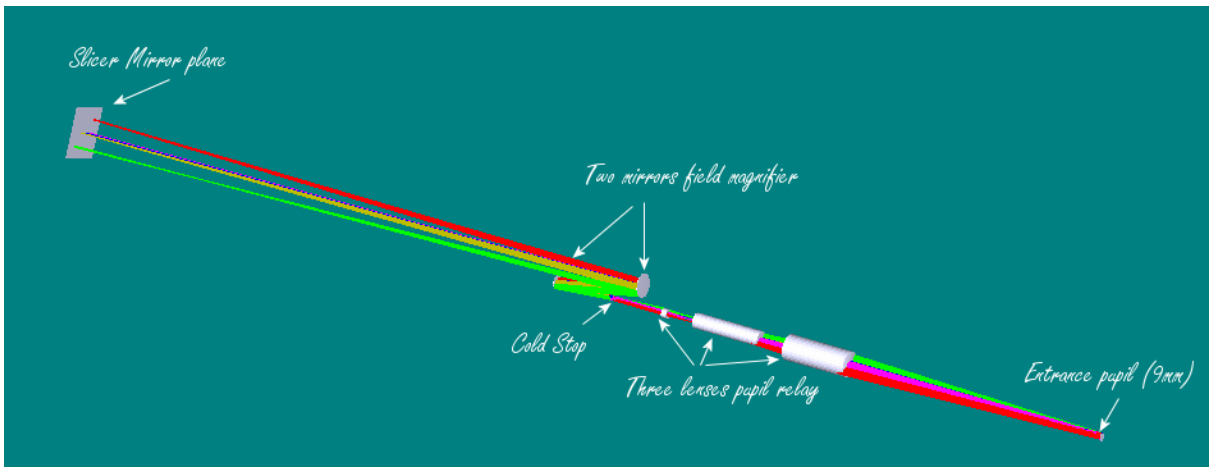

Figure 33 – Layout of the Relay optics system

Figure 33 shows the relay optics concept. As mentioned earlier, this is the worst case solution if the cold stop cannot be on the DM. If cold stop can be on the DM, the relay optics would consist in a simple two mirror system.

6.11.4 Performance and Compliance

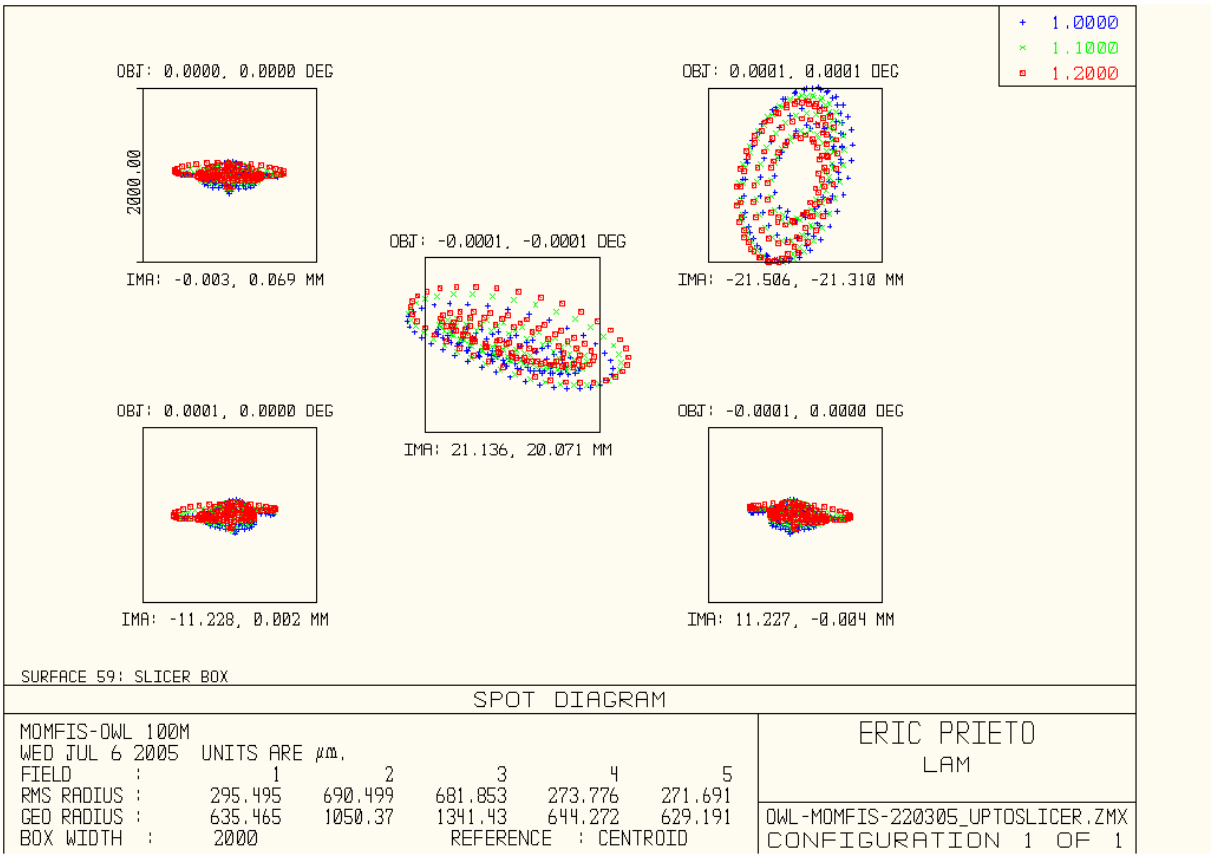

Figure 34 – Spot diagram at the level of the slicer plane in the J band

Figure 34 shows the spot diagram of the system from the sky down to the slicer plane at the zenith. The spot diagram is nearly within one pixel (square box). Figure 35 shows that for all points in the FOV the encircled energy is better that 80% (20 mas is 2mm at this level).

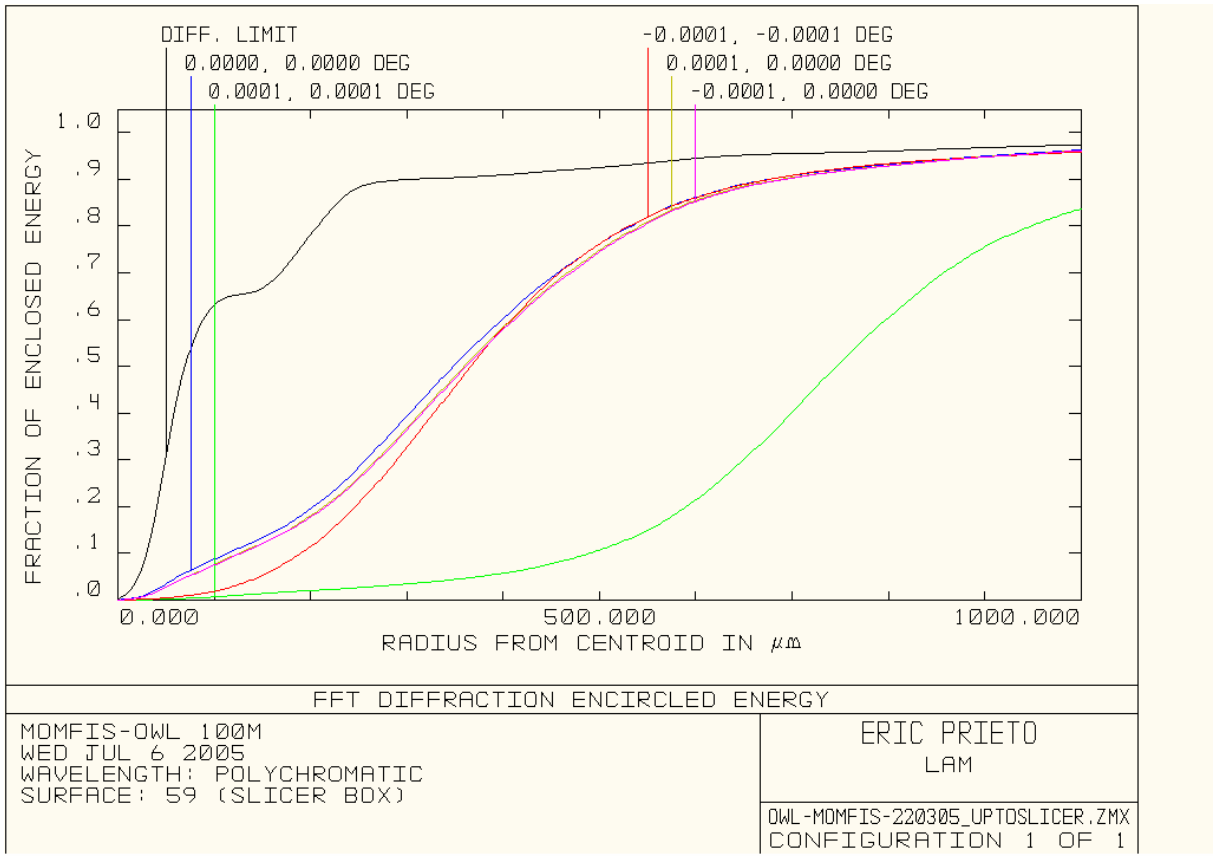

Figure 35 – Encircled energy at the level of the slicer plane.

6.11.5 Reliability & Maintainability

No particular concerns are foreseen here

6.11.6 Integration

The optical interfaces are clear and simple so the integration of this system shall be easy and the tests and characterisation of this sub-system would be conducted separately from the rest of the instrument.

6.11.7 Development Risks

No risky items here. 30 identical units to manufacture.

6.11.8 Cost and FTE

The estimated cost and FTE to develop and deliver this unit is:

- .3 FTE for the optical design
- .3 FTE for the opto-mechanical design
- .3 FTE + .1M€ for the integration plan definition, support equipment design and provisioning
- 2 FTE for the integration and characterisation of the 30 spectrographs
- .2 M€ for the delivering of the 30 spectrograph optics
- .1M€ for the mechanical part

So the overall development effort will be: 2.9FTE and .4M€

6.12 Atmospheric Dispersion Compensator

6.12.1 Function

The ADC function is to compensate for the atmospheric dispersion. It is inserted before the DM.

6.12.2 Specifications

The system has to correct the atmospheric dispersion from 0^0 to 60^0 zenithal distance, in one of the spectral bands at a time. The amplitude of the atmospheric dispersion to correct is illustrated on **Erreur ! Source du renvoi introuvable.**. The site is assumed to be Paranal, consistent with [AD02].

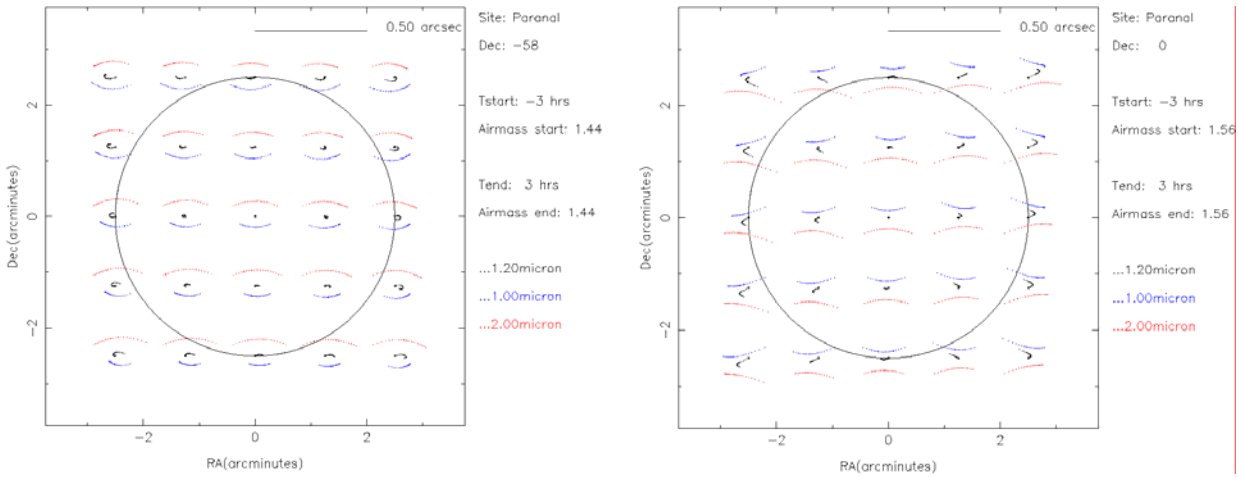

Figure 36 – Simulation of atmospheric effects

Paranal conditions are assumed (latitude and air conditions). Field of view is 5' in diameter. Left: Southern field (-58o), Right: Northern field (0o)

6.12.3 Interfaces

The beam size at the level of the ADC is about 40 mm. It has to be operated at 77K. The operating wavelength are Y,J,H,K.

6.12.4 Description

This system is composed by 2 set of 2 prisms, each set rotating along the Z axis in order to compensate the dispersion. The prisms are made in ZnSe and Cleartran.

6.12.5 Performance and Compliance

The current ADC design, although not yet fully optimized, allows to compensate atmospheric dispersion within 2 'pixels'. Figure 37 shows the ADC spot diagrams.

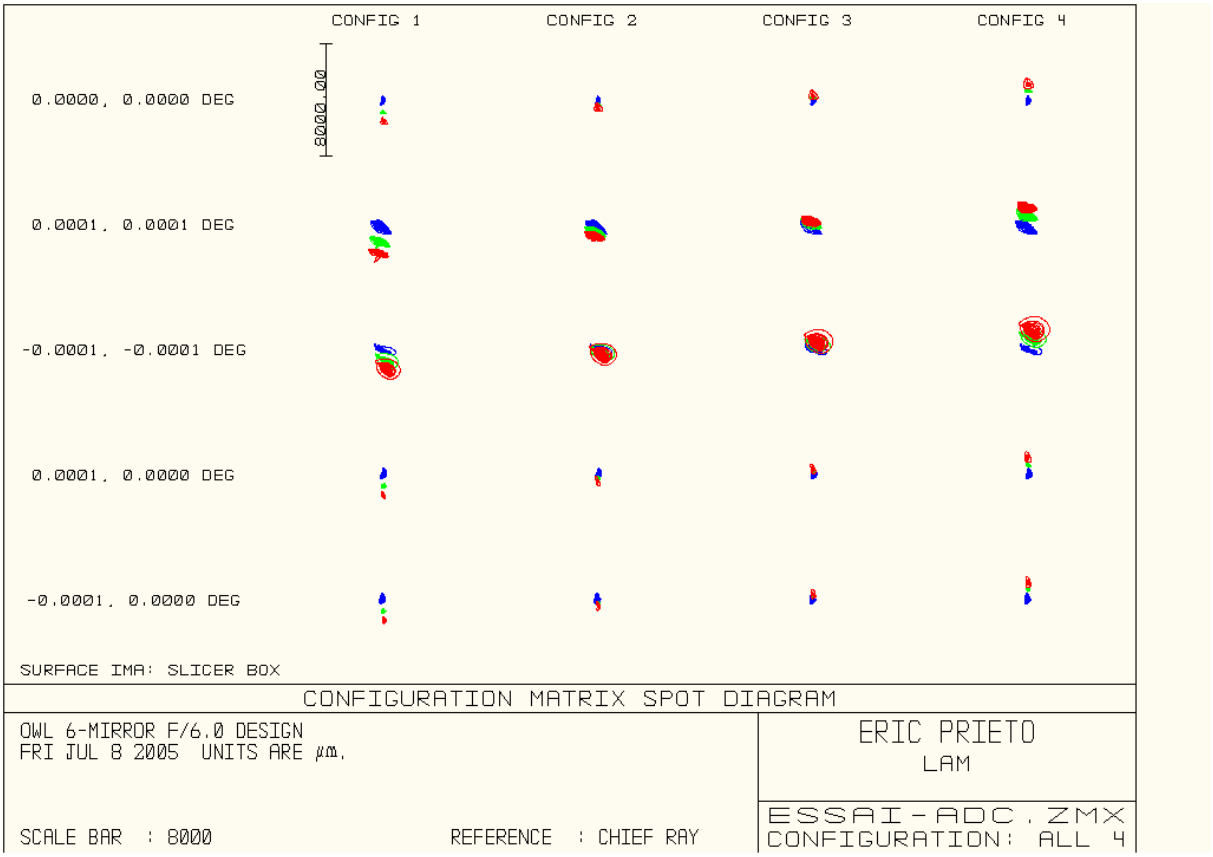

Figure 37 – ADC performance

Spot diagrams at 50°, 30°,10°;0° of zenithal distance ('config' 1 to 'config' 4) in the slicer plane(pixel size: 2000µm)

6.12.6 Reliability & Maintainability

In our baseline design, the ADC is cryogenic. Reliability of the ADC is therefore of utmost importance and special care should be given to the design, however cryogenic functions are

widely used and with KMOS ESO will have gained extensive experience in highly duplicated cryogenic functions. The ADC could also possibly left out of the cryostat.

6.12.7 Integration

This sub-system would be integrated and tested separately from the rest of the instrument.

6.12.8 Development Risks

No risky items here. 30 identical units to manufacture.

6.12.9 Cost and FTE

Hardware may not be the main cost item for this sub-system which will otherwise require extensive manpower for testing and calibration campaigns in cryogenic operation.

- .2M€ of optical parts
- .3M€ of mechanical parts
- 0.4 FTE of opto-mechanical design
- .5M€ of life test campaign
- 1 FTE for life test preparation and execution

In total: 1M€ and 1.4 FTE

6.13 Filter wheel

6.13.1 Function

This component will select the right spectral band among Y,J,H,K

6.13.2 Specifications

The wheel needs 5 positions to select one of the four filters with provision for a closed position. The diameter shall be 40 mm. The temperature of operation is 77 K. The central wavelength and width is TBD but somewhat classical. The stability of the rotation is not critical.

6.13.3 Interfaces

Cryogenic function.

6.13.4 Description

This component has not been designed in detail as this is a fairly standard filter wheel with few positions.

6.13.5 Cost and FTE

- 1M€ of optical parts
- .3M€ of mechanical parts
- 0.4 FTE of opto-mechanical design
- .5M€ of life test campaign
- 1 FTE for life test preparation and execution

The total is: 1.8M€ and 1.4 FTE

6.14 Slicer Unit

6.14.1 Function

The slicer unit separates the FOV in 40 sub-slits and re-images them along a 140mm long entrance slit of the spectrograph.

6.14.2 Specifications and interfaces

The field of view at the level of the slicer is 80mmx80mm. The pixel scale at this level (slice width) is 2mm for 20 mas. The magnification factor is 26. The surface figuring shall be 50nm PTV (for image quality and tolerance of pupil and slit position on different surfaces) with a roughness less than to 2 nm (for throughput and scattered light).

6.14.3 Description

Figure 38 shows a schematics of the image slicer, which consists in:

- 40 slices 2mm wide and 80mm long
- 40 pupil mirrors with 3.5mm pitch
- 40 slit mirrors with the same pitch

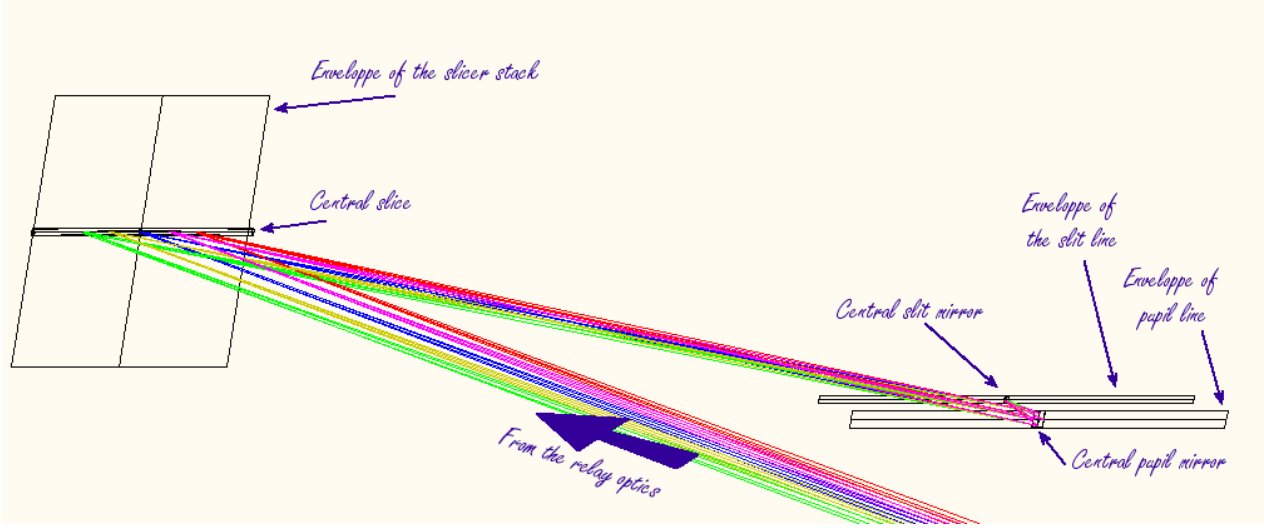

Figure 38 – Image slicer schematics

The distance between the slicer stack and the pupil mirror line is 400mm while the distance between the pupil and slit mirrors is 15mm assuming the magnification factor 26.

6.14.4 Performance and Compliance

Figure 39 shows the spot diagram for the image slicer sub-system. The pixel scale in the slit plane is 75µm.

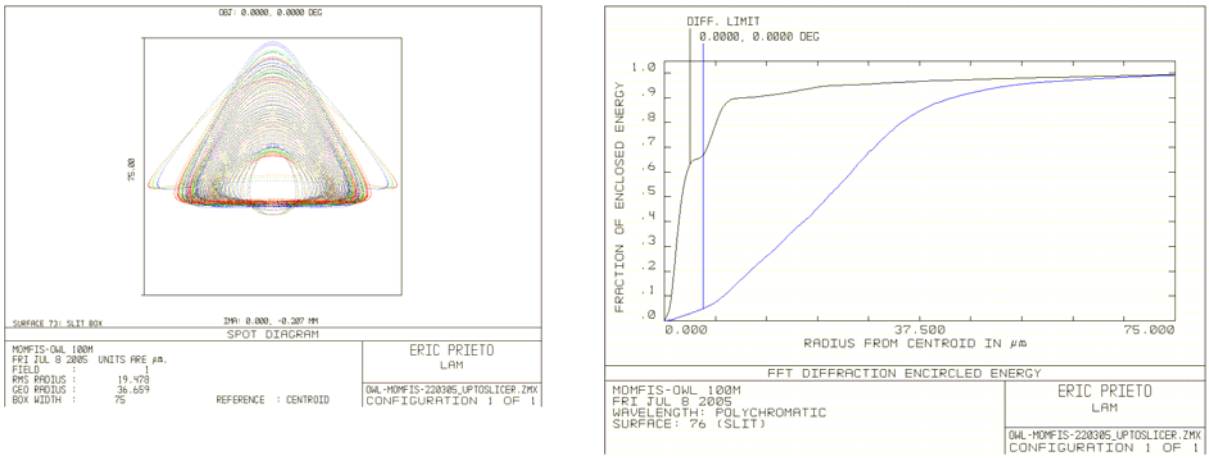

Figure 39 – Image slicer spot diagram

6.14.5 Reliability & Maintainability

This is a passive component, reliability is not an issue.

6.14.6 Integration

Tests, characterisation and integration can be performed separately from the rest of the instrument.

6.14.7 Development Risks

Technology for glass image slicers such as this one is mature and there is no development risk, but cost may be an issue. Monolithic metallic slicers may provide lower development and manufacturing costs but technology is not yet quite meeting the requirements.

6.14.8 Development plan & roadmap

The development of similar systems is currently under way for many systems across Europe. MUSE and KMOS will pave the road for the development and manufacturing of ‘mass’ systems.

In addition, the JRA5 of the OPTICON programme is also addressing the mass production of such systems. The situation shall be clear within a couple of years as to which technology provides the best performance and cost, hence providing a clear roadmap for the development of the MOMFIS slicers.

6.14.9 Cost and FTE

Under the assumption that the monolithic approach will prevail by the time MOMFIS is launched, we estimate the development cost as follows:

- .5 FTE of optical design
- .5 FTE of mechanical design
- 1M€ for the provisioning of the optical components
- .5M€ for the provisioning of the mechanical components
- .3M€ plus 1.5FTE for integration, tests and characterisation

The total is 1.8M€ plus 2.5 FTE.

6.15 Spectrograph

6.15.1 Function

The spectrographs provide one full band (YJHK) spectrum in one shot for each slicer slit. The spectral resolution is 4000.

6.15.2 Specifications

The entrance slit is a 140mm long slit on a 350mm sphere. The entrance pupil is 7m in front of the spectrograph. The speed of the beam on the detector is F/1.8, refocus between bands is allowed. The pupil size (grating / grism) is 150 mm in diameter. The detector can be tilted if tilt is constant for all spectroscopic bands. The image quality has to provide 80% ensquared energy within one pixel.

6.15.3 Interfaces

6.15.4 Description

See Figure 10 for a schematics of the spectrograph, see also section 6.5.

6.15.5 Performance and Compliance

Figure 40 and Figure 41 show the spectrograph performance (spot diagram and encircled energy) in the best case. These results are nearly compliant with the specifications. The full spectrograph optimization at all wavelengths goes beyond the scope of this study. For the sake

of this report it is enough to say that the spectrograph can be designed based on classical technologies and that there are no development risks associated with this sub-system.

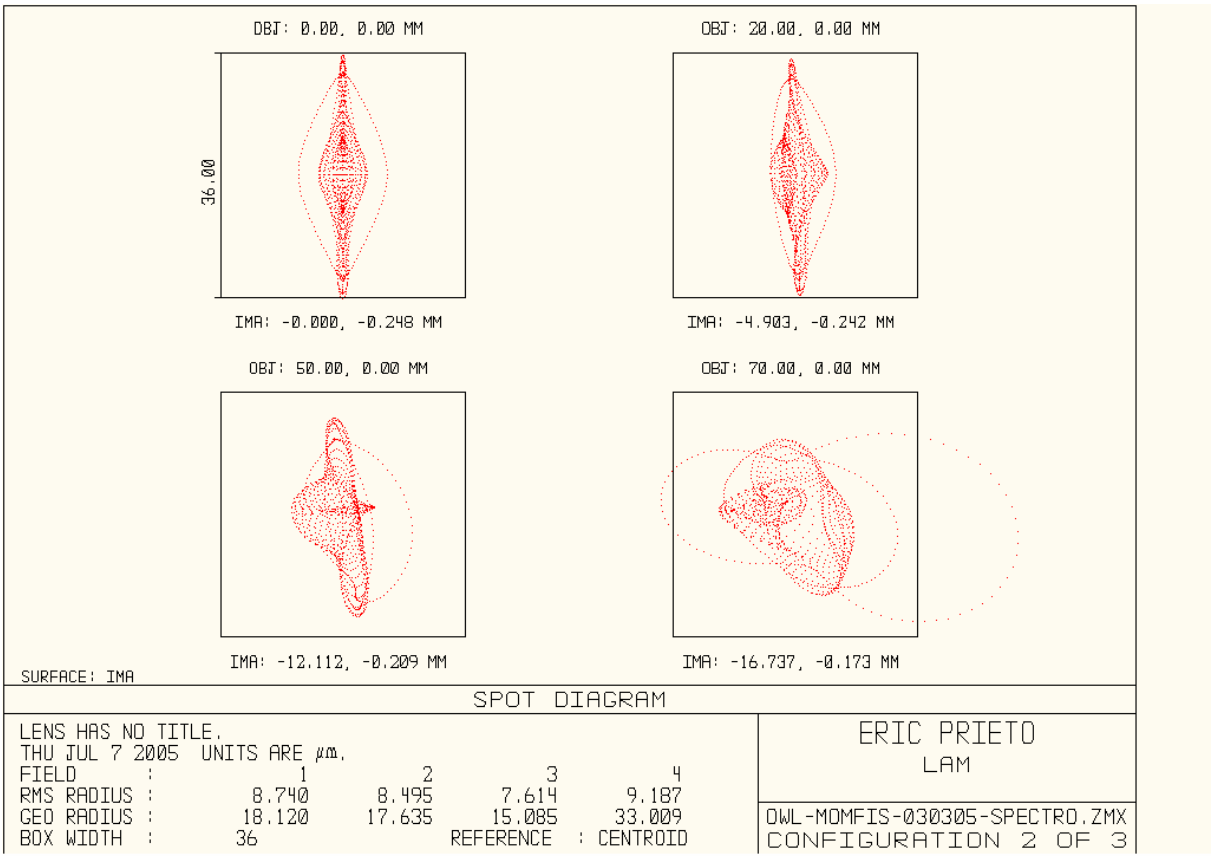

Figure 40 – Spot diagram of the spectrograph in the best case (@1.6µm)

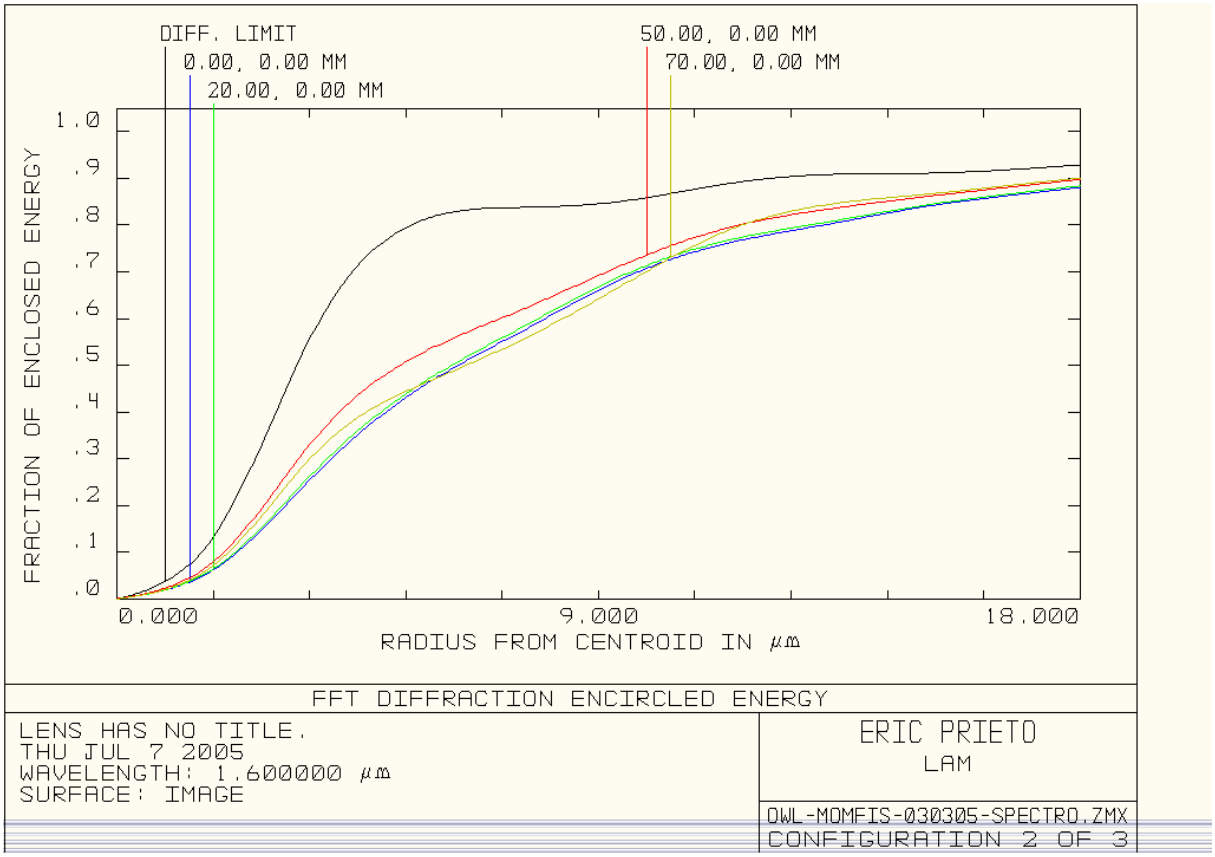

Figure 41 – Encircled energy in the best case (@1.6µm)

6.15.6 Reliability & Maintainability

The reliability issues are with the cryogenic spectrograph mechanisms, in this case the focusing mechanism (other functions are dealt with separately).

6.15.7 Integration

The spectrographs can be tested and characerized independently of the rest of the instrument, they have nice and simple interfaces. Clearly, a major task will be the testing and characterisation of 30 identical spectrographs.

6.15.8 Development Risks

None, the spectrograph relies on classical optics and technologies.

6.15.9 Development plan & roadmap

6.15.10 Cost and FTE

The estimated cost and FTE to develop and deliver the spectrographs is:

- .5 FTE for the optical design of the spectrograph
- 1 FTE for the opto-mechanical design
- 1.5 FTE + .3M€ for the integration plan definition, support equipment design and provisioning
- 5 FTE for the integration and characterisation of the 30 spectrographs
- .5M€ for the mechanical part

So the overall development effort is estimated at: 8FTE and 2.3M€

6.16 Grating

The grating / grism sub-system has not been studied in detail. It is anticipated that the technology of VPH gratings or equivalent systems will be mature and evolved enough that they can be readily manufactured for MOMFIS. The main specifications are: 150 mm pupil diameter, cryogenic operation. The gratings will operate in order 2 at K, 3 at H, 4 at J, etc.

6.17 Wavefront Sensor

A detailed study of the WFS is beyond the scope of the MOMFIS study as it is tightly related to the definition and operation of the telescope and instrument Adaptive Optics for which several open issues remain. Also, the study of the WFS in terms of technological developments is widely covered elsewhere in the OPTICON and ELT Design Study FP6 activities. For the sake of this report we list hereafter the main ideal specifications of the WFS that are required for MOMFIS as specified.

- Zero noise CCD
- High dynamics (resulting in a large sampling at each measurement point : i.e. high number of pixels per subaperture)
- High linearity over the dynamic range
- 200x200 sampling (i.e. typically 1000x1000 pixels detectors)
- Pseudo open loop control
- Compactness
- Overall sensing WFE : 100nm rms To Be Confirmed

The overall WFE should be about 200nm RMS arbitrarily distributed into 4 contributions, the WFS being one of them (as well as cone and elongation effects).

6.18 Thermal Enclosure and thermal budget

6.18.1 Design considerations

We made the choice of a thermally controlled instrument. Considering the length of the optical path along the optical beam and the number of functions to operate in the instrument, we considered that a thermally controlled instrument was a safe choice. Not only will that remove any turbulence inside the instrument, and wavefront errors between the WFS and the entrance

of the cryostat, but that will also ensure that all components of the instruments are always used at the same temperature, which makes it easier to understand, calibrate, maintain and troubleshoot the instrument.

The baseline instrument is stabilized at the median site temperature (10°C as per the ICD, obviously subject to change depending on site), or colder (to reduce thermal background). Note that in Option#2 (see section 7.2) the instrument temperature is -40°C (TBC). The global geometry of the thermal enclosure is the same in the two cases.

The surface of the enclosure is reduced to its minimum to reduce its mass and the heat loads. It includes a 2m diameter window at the entrance of the instrument, and 2 insulating shells that cover the two parts of the instrument below and above the rotator plane. The enclosure rotates with the instrument. There is no need for a rotating joint. The only conducting links from inside the enclosure to outside are the balls of the rotator bearing.

Different types of material for the enclosure could be chosen depending on the exact temperature. In the 'fridge' case (-40°C), the enclosure will consist in some sandwich material with plastic foam inside. In the baseline case (10°C), a simpler, lighter structure covered by MLI will do it.

6.18.2 Mass

In the baseline case, assuming MLI and 6 kg/m^2, the mass of the enclosure is 300 kg.

In the case of option#2 the mass of the walls should be around 40 kg/m^2 leading to a mass of the enclosure of 2000 kg.

6.18.3 Thermal requirements

In the two cases, a value of 0.2 W/m^2/K is taken for the specific conductance of the walls. With a total surface of 50 m^2 we get a conductance of 10 W/K. The heat leaks at bearing level are mostly due to the convection (10 W/ m^2/K) on the surface of the inner ring of bearing plus the conductance of the balls. A value of 50 W/K seems quite conservative. The leaks at window level remains limited: small conductivity of glass and two convective surfaces. The conductance of the window should not exceed 10 W/K. In total, the global conductance of the enclosure shall not exceed 70 W/K.

Knowing that the mass included in the enclosure is about m = 18000 kg with a mean specific heat of Cp = 800 J/kg/K the thermal time constant of the system becomes τ = m*Cp/k = 18000*800/70 = 206 ks = 57 hours.

In addition we can estimate the power exchange and the electrical power required for the thermal control of the instrument. We consider that the range of external environmental temperature is [0 - 15°C].

Case 10°C (baseline). The max power that must be extracted from the enclosure is k*ΔT= 70*(15-10) = 0.35 kW. Assuming a typical efficiency for a fridge of about 1/3, this corresponds to a required electrical power of 1 kW. Conversely, when external temperature is low, the max power that must be brought to instrument is k*ΔT= 70*(10-0) = 0.7 kW.

Case -40°C. The max power that must be extracted from the enclosure is k*ΔT= 70*(15+40) = 3.85 kW, corresponding to a required electrical power of ~ 11 kW.

This is summarized in Table 12.

Table 12 – Thermal budget

Options	Mean power exchange (kW)	Peak thermal power exchange (kW)	Electrical power (kW)
Baseline: Temperature controlled at 10°C	0	0.72	1 (fridge), 0.7 (heater)
Fridge: temperature controlled at -40°C	3.5	3.85	11.5

6.19 Calibration Unit

6.19.1 Specifications

The main purpose of this unit is to provide a flat field and wavelength calibration capability to each channel. The specifications for flat fielding are summarized Table 13, the specifications for arcs are summarized Table 14.

Table 13 – Flat fielding specifications

Item	Value
Spectral range	0.7 to 2.5 µm
Spectral flatness in one band No high frequency variation	10%
FOV	1”
Homogeneity over the FOV	0.5%
Stability over time	5%
Exposure time for SNR=100	< 1mn

Table 14 – Wavelength calibration specifications

Item	Value
Spectral range	0.7 to 2.5 µm
Number of lines along the spectral range	100
FOV	1”
Homogeneity over the FOV	10%
Stability over time	5%
Exposure time for SNR=100	< 1mn

6.19.2 Interfaces

The system has to provide an F/6 beam.

6.19.3 Description

Our proposal is to fully use the flexibility offered by the pick-off and beam steering mirrors system. Figure 42 shows the configuration of the steering mirrors and bugs when the system is observing scientific targets. The principle is to tilt the steering mirrors and align them to send the beam coming from a small integrated sphere located near the focal plate (Figure 43). This principle allows to use the flexibility and the speed offered by the steering mirrors, allowing e.g. to calibrate at night if required.

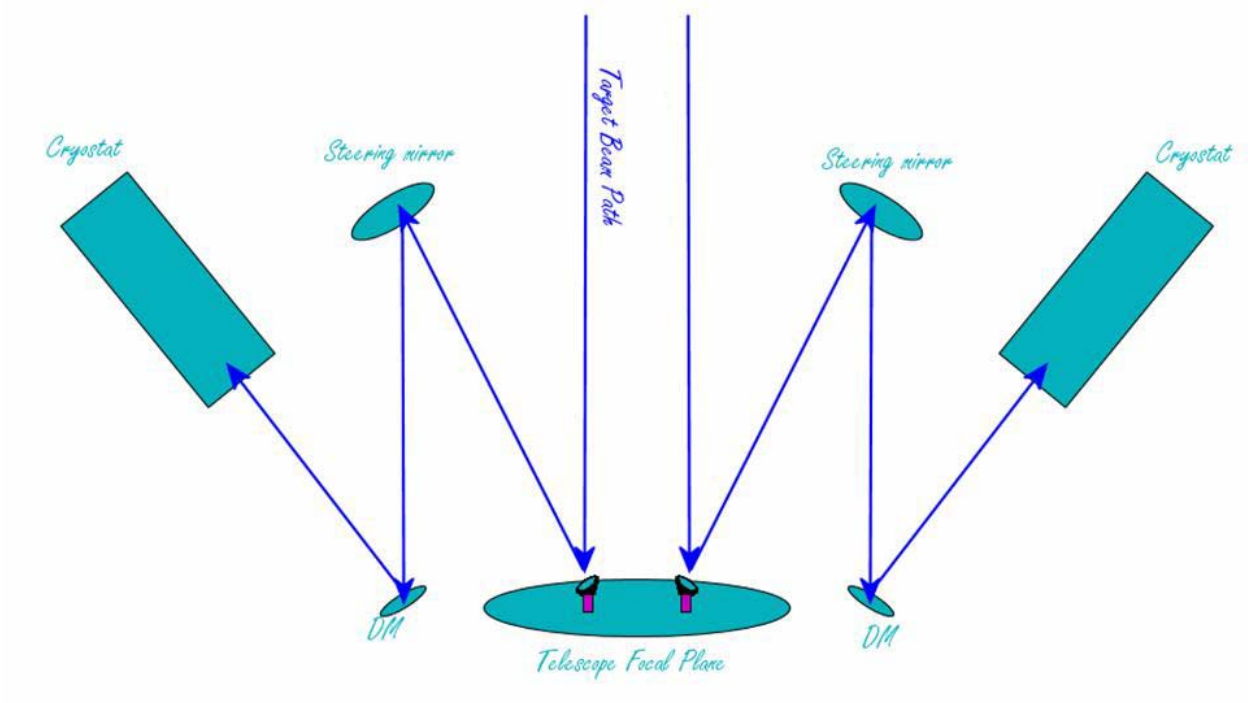

Figure 42 – instrument in target observing mode

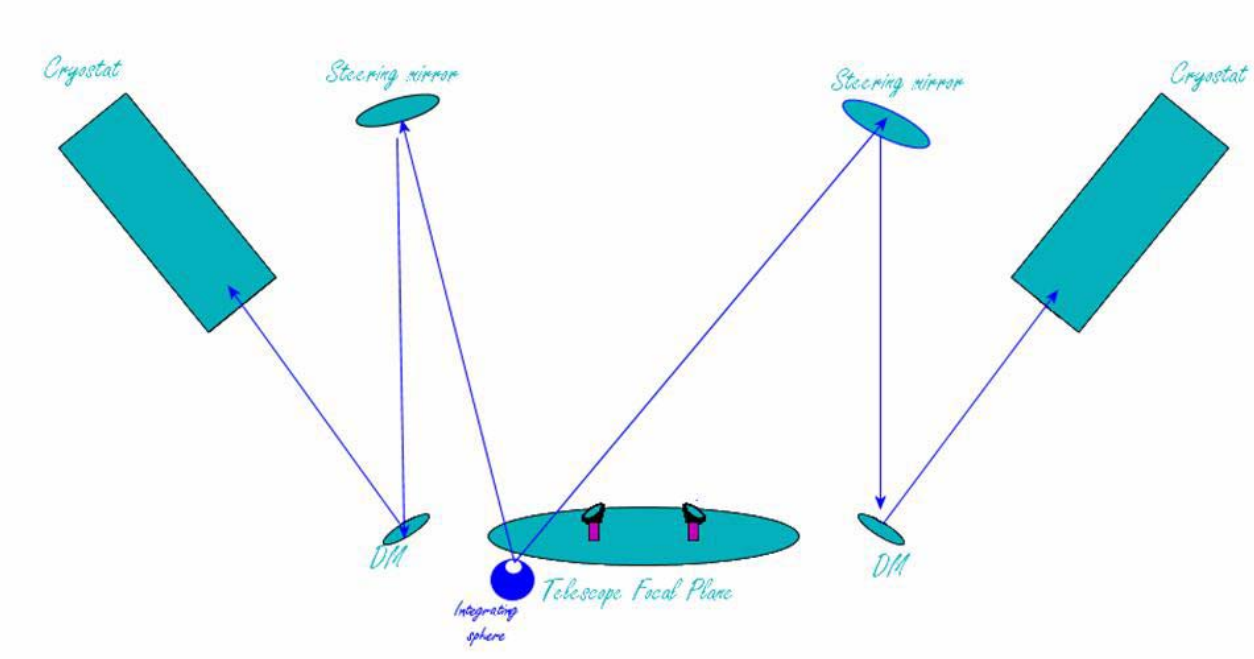

Figure 43 – Calibration Unit concept

6.19.4 Performance and Compliance

This configuration is the simplest one to provide the full pupil illumination. The incoming F/6 beam on the bug will need a very large screen to mimic the pupil while after the pick-off mirror the pupil is only 10mm large. An integrated sphere with an output port a bit larger than 10mm will be enough to mimic the pupil.

6.19.5 Development Risks

No risks are identified

6.19.6 Development plan & roadmap

Early tests should be pursued at the beginning of the instrument development to insure the homogeneity and the integration times.

6.20 Internal metrology

The optical path within the instrument is several meters long. Because the pick-off mirrors shall work at angles that do not introduce too strong aberrations, the BSMs shall be at least 2 meters above the focal plane. The sole optical path length between the pick off mirror and the DM is therefore of ~ 4 meters.

On the other hand, the requirement on spatial resolution (high encircled energy within 50 mas and spatial sampling of 20 mas) leads to tough positioning requirements on the pick-off mirrors and BSM: about one arcsec in position angle, and one micron in position. High stability is also

required. These specifications cannot be met with the structure as designed (or with any other structure that can possibly fit in volume and weight) because of the flexures induced by gravity changing direction with respect to the instrument (see section 6.6.5.2 and Table 10). Therefore, internal metrology is required to measure and control the positions inside the instrument, as it bends with gravity loads. Whether the behavior under flexures will be stable enough to be handled with look-up tables, or closed loop control will be required is TBD. Since internal metrology is anyway required for integration, test, calibration, and maintenance purposes, it is likely that it will also be used for closed loop control.

In addition, the instrument features two deformable surfaces (per channel): the BSM and the DM. At this stage, both the BSM and the DM are undergoing R&D phases and / or prototyping developments, and it is unclear whether they will require wavefront control in operation. However, as above, wavefront control will be required for integration, test, calibration and maintenance.

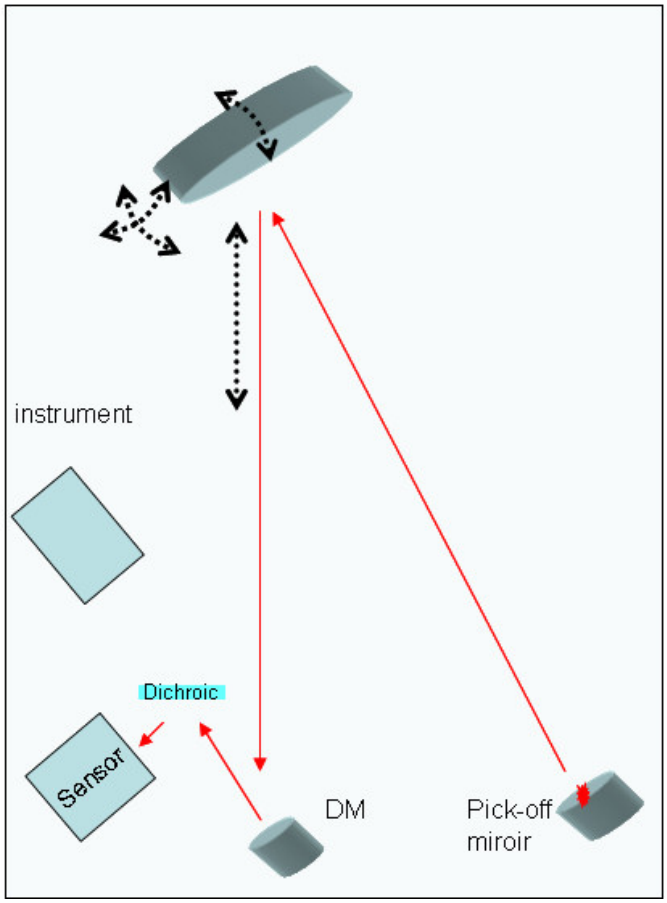

Figure 44 – Principle of the metrology

LAM, within the framework of the OPTICON JRA on smart focal planes, is investigating metrology solutions for an instrument like MOMFIS. A first prototype could be tested in 2006. The principle is to mimic a target in the pick-off mirror environment (diode or laser beam) with a wavefront sensor after the DM (see Figure 44). Such a system shall allow to measure:

- BSM Pointing error
- Focus error
- Astigmatism correction error
- Optionally the DM curvature

6.21 Detectors

2k x 2k HAWAII RG arrays are the default detectors foreseen for MOMFIS. They provide the required performance, quantum efficiency, readout noise, etc. Note that MOMFIS observations are background limited on the continuum between the OH lines after a few minutes of time, hence no strong or specific requirements on readout noise. Detector stability (QE, bias, flat field, etc.) is an important requirement to avoid systematic effects that would limit the performance of long cumulated integrations (tens of hours).

Note that 1k x 1k arrays can be contemplated to reduce cost (see section 7.4).

6.22 Data Rate

The baseline instrument foresees 30 2k x 2k IR arrays. This corresponds to half a GByte per exposure. The range of integration time will be [600-1800] seconds, leading to less than 100 science frames per night. The number of spectroscopic setups is limited (4), which shall limit the number of calibration frames taken during daytime. No night time calibrations are foreseen. In total, the number of frames per day shall be in the range [100-200]. This corresponds to 50-100 GBytes per day.

7. OPTIONS

7.1 Option#1: No MOAO. Fallback solution and / or first phase implementation

In a first implementation phase, MOMFIS could be deployed without the deformable mirrors which can be replaced by flat mirrors, or low order deformable mirrors. Wavefront sensors would still be required for telescope control. Exquisite image quality could still be obtained in the central field of view (1 to 2 arcmin multi-conjugated adaptive optics field), gently degrading towards the outer edge of the OWL field of view (ground layer correction only). More than just a 1st light option, this option is actually also a fallback option in case MOAO developments fail or prove to be more difficult than expected to implement

7.2 Option#2: No K band

This option consists in reducing the size of the cryostats and the number of parts in cryogenic environment. To overcome – at least in part – the effects of the increased thermal background, the whole instrument environment is cooled down to a temperature of -40^{o}C, and only part of the spectrograph (from grating / grism) is kept at cryogenic temperatures. The instrument enclosure is changed (‘fridge’) from the baseline to accommodate this lower temperature. The K

band performance is affected in this configuration, while the H band performance is fully preserved.

This option (fridge + reduced cryogenics) belongs to the class of 'warm IR instruments' which offers interesting alternatives to the whole cryogenic approach, however with limited K band performance. This option is worth presenting as it brings a number of simplifications in the instrument, such as reduced cryogenics, reduced weight, etc. However, it requires a colder instrument environment, of the order of -40°C.

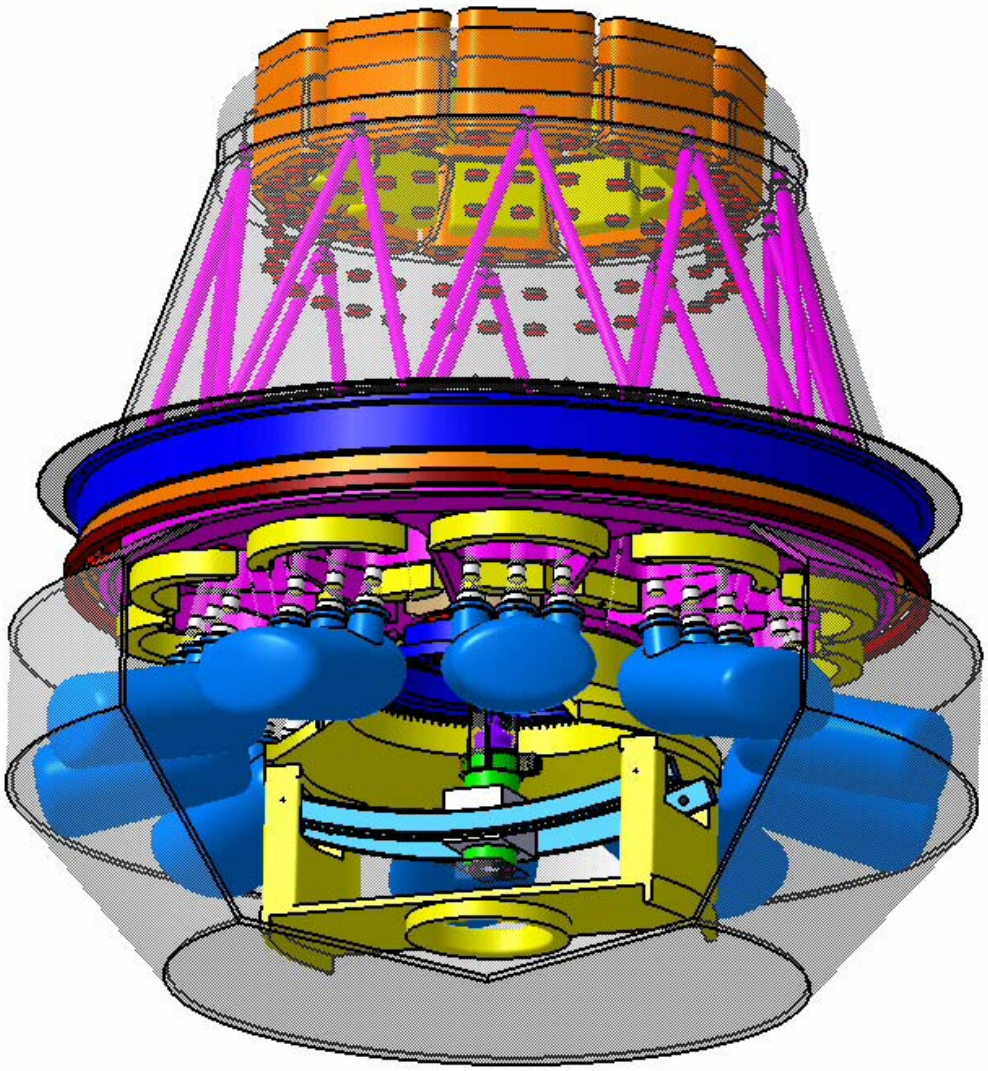

Figure 45 – Option #2: fridge environment and smaller cryostats.

Table 15 presents the pros and cons of option#2 compared to the baseline option.

Table 15 – Option#2 versus baseline: pros and cons

Advantages of Option #2 vs baseline	Disadvantages of Option #2 vs baseline
● Smaller and simpler cryostats ● DM operating at -40°c instead of 77 K ● Lower cost & development risks	● Colder instrument environment: increased maintenance complexity ● The K band becomes unavailable (TBC)

A detailed trade-off analysis including technical and scientific aspects would need to be performed in phase A to further assess the relative merit of this option compared to the baseline.

7.3 Option#3: 2 objects per spectrograph

This option consists in reducing the individual field of view of each IFU by a factor 2 in area, allowing to fit 2 objects within one spectrograph. This option reduces by a factor 2 the number of spectrographs and detectors. This however increases the complexity of feeding one spectrograph with two slicers and two steering mirrors. Further studies would be required for assessing the exact opto-mechanical implementation of the whole system. It is anticipated that one cryostat could be fed by 4 targets (and associated BSM), leading to ~ 7 cryostats in total and 28 channels.

7.4 Option#4: 1 k x 1k detectors

This option is considered as a potential cost saving item. As for option#3, it consists in reducing the individual field of view of each IFU down to 0.6” x 0.6” (30 x 30 slices). This option would be combined with spectral dithering as it samples the slit width with one pixel.

This option comes with additional simplification of the slicer and spectrograph optics, and therefore of cost. The number of cryostats remains the same.

7.5 Option#5: positioner a la Oz-Poz

In this option, the positioner assembly is essentially a duplication of Oz-Poz, the positioner of FLAMES. This type of positioner was part of our initial baseline. Considering that our initial baseline significantly exceeded the weight limit, we changed the positioner concept. We present the original positioner solution as an option for consistency with our previous work. It could still be considered as an option in case of a Nasmyth platform and / or in case of a fiber-feed, both situations which would reduce the weight constraint. Note also that in case of successful starbug developments (i.e., motorized pick-off mirrors) this option would be definitely dropped.

The main differences compared to the baseline are the following:

1°- the assembly is supported by a specific platform,
2°- the two focal plates (in observation and in configuration) exchange mechanism is separated from the main instrument structure and is supported by a platform attached to the focal station.

Figure 46 below shows the implementation of this assembly in the Focal Station. The orientation of the platform assumes that the telescope is pointed to the zenith for access and maintenance.

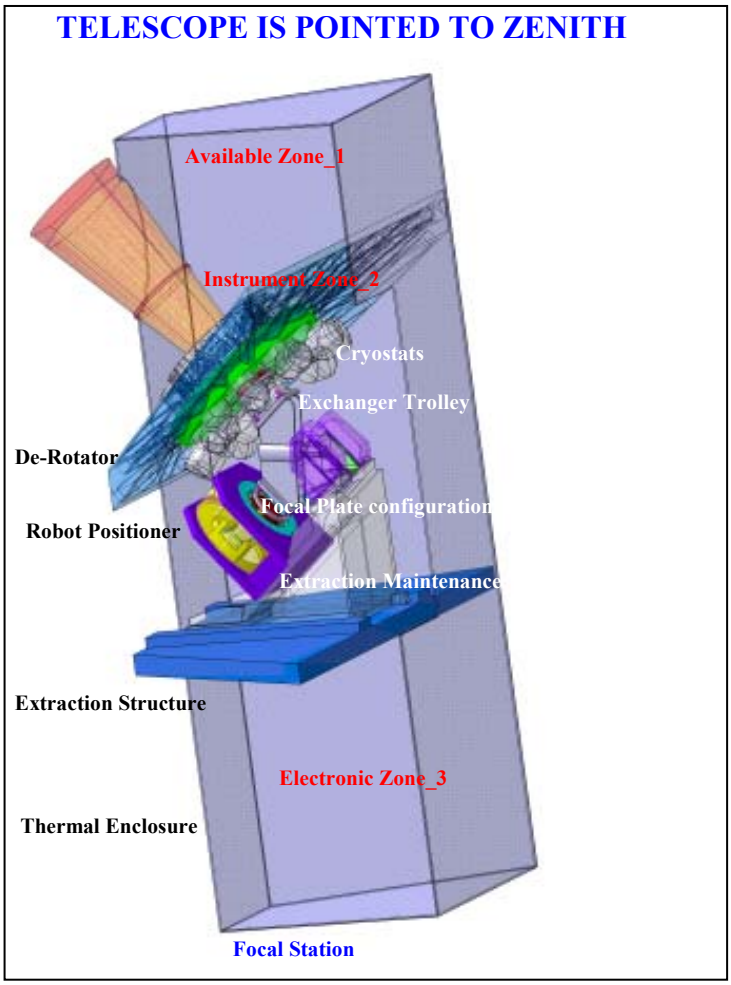

Figure 46 – Implementation of positioner in option #5

The plate exchange operation steps are:

1°- Rotation RZ of rotator to align positioning pins on the spectrograph side
2°- Idem on the positioner side
3°- Translation TZ of exchanger for gripping the "observation" focal plate
4°- Idem on positioner side for "configuration" focal plate
5°- Rotation (180°) of the exchanger
6°- The four first points in inverse order

The whole positioner assembly is located on a platform (Figure 47) that is linked to the telescope structure. This platform, guided on two rails, also serves for maintenance purposes.

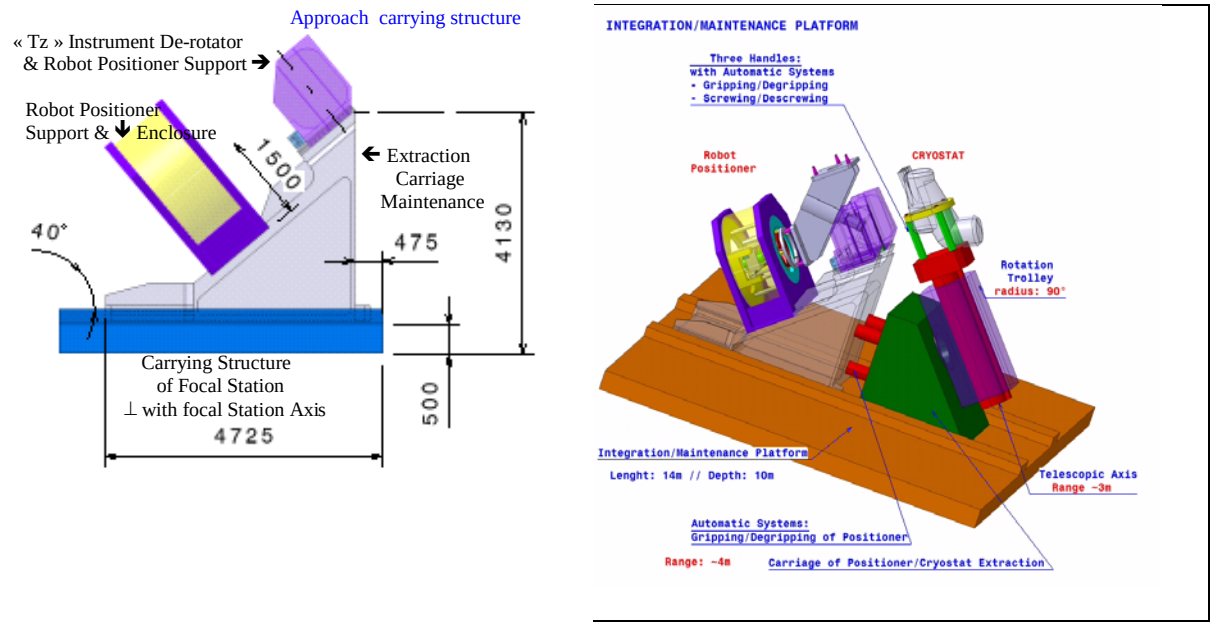

Figure 47 – The positioner assembly on its platform and the extraction carriage

In that option the enclosure must include the overall volume of spectrograph assembly plus the positioner and its platform. In addition this enclosure can't turn with the instrument as it is the case in the baseline. In this option, the implementation of some lightweight insulation of MLI type is possible. This option could not accept operation at -40°C as it would require ~ 120 kW of cooling power.

Table 16 summarizes the pros and cons of this option versus the baseline.

Table 16 – Option#5 versus baseline: pros and cons

Advantages of Option #5 vs baseline	Disadvantages of Option #5 vs baseline
● Easier access for limited maintenance operations ● Positioner completely decoupled from observing plate ● Smaller mass on rotator ● Less development risks	● Mass considerably increased: between 15 and 20 extra tons due to the need for a specific platform ● Higher cost: manufacturing of platform and MAIT of exchanger trolley. ● bigger and heavier enclosure. Can't be thermally controlled.

8. BUDGET ANALYSIS

8.1 Mass

Table 17 details the mass breakdown of the baseline.

Note in the the following budget that our baseline option does not foresee the use of starbugs, as we deliberately chose to resort to proven systems and technologies only. However, the prospect for a successful development of starbugs is bright, which would allow to drop the positioner and therefore to reduce the weight further. Also note that we have considered thermal insulation which comes with the entrance window. Removing this requirement would also reduce weight by more than 1 ton (essentially the entrance window).

Option#2 would allow to reduce the mass by 1.5 ton. Option#3 and #4 would lead to mass reductions significantly higher, not fully quantified, but presumably in the range 3-5 tons.

We have assumed arbitrarily some value for the mass of the adapter / rotator provided by ESO and of platforms presumably (although not described in the ICD [AD02]) foreseen by ESO in the focal station (and we have added our own platform).

In total, the exact mass budget will depend on a number of things, including the exact design of the OWL focal station, the selected option for the instrument, further simplification of the instrument and / or of its specifications (e.g. the number of channels), etc. If the mass of the instrument can possibly exceed the mass limit, this is at this point difficult to quantify firmly. There is a likelihood that the focal station may have to accept bulkier equipment; however there is no immediate cause for alarm.

Table 17 – Mass (kg) breakdown

	nb	Baseline
Spectrographs (rotating item)		
Focal Plate	1	100
Steering mirror assys	30	750
Cryostats & fixations	10	10400
Carbon/epoxy structure	1	3500
Entrance Window	1	1000
Positioner		
Exchanger		150
Robot structure		500
Robot		1000
Insulating enclosure (MLI)	1	300
Electronics		
Control cabinets	2	600
Cable twist	1	2000
TOTAL Instrument		**20300**
Telescope adaptation		
Spectrograph platform (steel)	1	11000
Positioner Platform (steel)	1	
Adaptor/Rotator		5500

TOTAL		**36800**
Removal of the OWL adapter / rotator and anciliary mechanical structures(*)		- [10000-15000]
Grand TOTAL baseline		**22,000-27,000**
Grand TOTAL options		**20,000-25,000**
Grand TOTAL w/o positioner, options		**15,000-25,000**

(*) Estimate, information was not received from ESO

8.2 Throughput

We have estimated the throughput of the instrument with the following hypothesis:

- 8 mirrors gold coated (w/o protection) and 2nm roughness (pessimistic)
- 15 lenses (1.2% losses at each interface)
- VPH grating efficiency 70% (averaged over one band)
- Filter efficiency 90% (average over one band)
- Detector QE: 90%

Figure 48 shows the expected throughput using these hypotheses. The performance of this instrument should be higher than 30% excluding telescope.

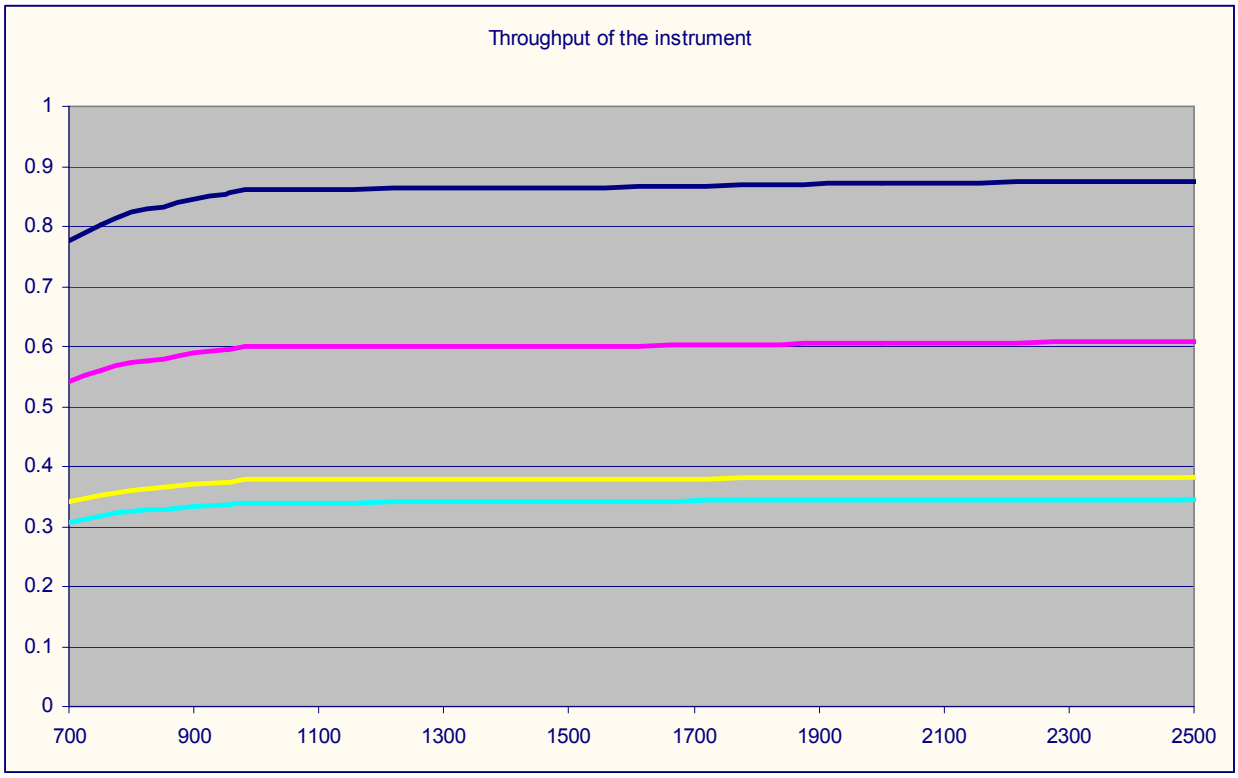

Figure 48 – Intrument throughput

Dark blue - 8 mirrors; pink - plus 15 lenses; Yellow - plus VPH and filter; cyan - plus detector

9. INTEGRATION AND MAINTENANCE

The modularity of the instrument is key to the integration. Each cryostat containing three spectrographs will be integrated, validated and characterized individually before the integration in MOMFIS. This integration will validate the sub-system performance using one common reference system. This modularity also allows provision for one or two spare module(s) that can be used in case of technical failures or for preventive maintenance by exchanging one module for the spare on a rotating basis.

Overall, the instrument is highly redundant and technical failures should have a low impact on the instrument capabilities (1/30th to 1/10th).

The positioning robot has to be independent enough to be tested and validated apart from the overall instrument. Its integration shall be possible during the final integration inside the telescope as a complete sub-module. An extraction and maintenance tool concept is described in section 6.7.4.4.

10. FEEDBACK TO OWL AND NON COMPLIANCE ITEMS

We list herafter non-compliance and / or more general interface issues with the ICD [AD02 and RD03] raised by the MOMFIS baseline design.

Table 18 – Non compliance items

Id	Non Compliance	Comment
1	**Adapter / Rotator**. We have removed the adapter rotator foreseen in the ICD and replaced it with a larger one	Was agreed with ESO. Leads to another non compliance related to the WFS probes (item#2) and available technical field of view (item#3).
2	**WFS probes**. As a result of #1 we have also removed the WFS probes provided in the ICD	Major. We offer alternative but different options for the WFS as part of the instrument that should then become part of the telescope control system. This generates differences between foci.
3	**Technical field of view**. As a result of #1 we have removed the technical fov for adaptive and active optics probes	Major. We offer the full central 5' fov, but the available FOV for WFS probes is reduced by a factor 2 in area.
4	**Focal Plane position**. We are compliant with [AD02] but not with [RD03].	Severe. If interface is as per [RD03] the focal plane is too high in the allocated volume, and severely limits the available space.
5	**Weight**. We exceed the 17 tons limit. The exact amount of overweight is unclear as it depends on the (unknown) weight of the OWL adapter / rotator that is removed and on the availability or not of access platforms in the station.	Major. Simple extrapolation of 8-10 m instrument weights leads to think that OWL instruments may – at least for some of them – be quite heavy. It is unclear if the focal station includes (mandatory) access and / or maintenance platforms and whether these have to be included or not in the weight limit. Also, can the weight limit be exceeded during integration (i.e. during long periods of time) e.g. for removable integration platforms and / or scaffoldings ?
6	**Instrument handling**. It is unclear whether the largest MOMFIS pieces (rotator 4.5 m) can be lifted in the focal station, and how then can be installed.	Severe. Can the core lift [RD3] be used ? How can big pieces be moved from the lifts to the focal station ? What is foreseen for instrument integration in focal station ? Are there (removable) platforms ? Is there a crane ? Etc. Also, how will (up to) 6 different instruments share the same focal station with the same access facilities ? Considering the location of the station, telescope has to remain vertical when any work takes place on the focal station. Severe conflicts between telescope and instrument activities can be anticipated.
7	**Power**. TBD. Compliance to be further	

	investigated when components (e.g. DMs) are better defined.	
8	**Vibrations**. The level of vibrations tolerated at instrument level is not specified but may be an issue if cryo-coolers are used for the cooling of the cryostats	N/A if LN2 is used for cooling
9	**LN2**. Availability of LN2 is not specified but would require direct delivery at instrument level	N/A if cryo-coolers are used for cooling

Beyond these specific interface non-compliance issues, designing MOMFIS led us to formulate a number of general comments on OWL as it stands and to ESO as the organization leading the efforts towards the realization of the European ELT.

- **Telescope diameter**. This can be the subject of much debate largely exceeding the scope of the MOMFIS study. Enough to say here that a large diameter would be largely beneficial to the MOMFIS science case, however a 100 m diameter raises serious concerns on the adaptive optics requirements which are critical to the MOMFIS performance, whether MOMFIS relies on the telescope GLAO/MCAO or on its own embarked MOAO. A degraded adaptive optics on a 100 m diameter could rapidly prove less useful scientifically than a full fledged adaptive optics on a smaller telescope of say 50-60 m.
- **Number of telescope mirrors**. As far as MOMFIS is concerned, the impact of the number of telescope surfaces is mostly in the K band (thermal background limited). Considering that alternative ELT designs may well require extra (warm) mirrors for adaptive optics beyond the bare minimum of 3 mirrors, it is unclear at this stage if the 6-mirror design of OWL really affects the performance compared to other telescope designs.
- **F/6 beam**. This is certainly one of the most severe constraints for a MOMFIS-like instrument. It limits the back focal distance that can be used for the opto-mechanical implementation. It prevents from using simpler and more elegant solutions for the beam steering and pickoff mirrors (see section 6.1). Admittedly, this fast beam is somehow the result of the large aperture. Should some scaling down of the later take place, it would be highly desirable to increase the f/ratio.
- **Focal station vs gravity**. The fact that the focal station is not stable with gravity (unlike a Nasmyth platform) is another severe constraint. Although non gravity stable instruments have been successfully used for ages on most telescopes, including 8 m telescopes (VLT, Gemini, etc.), it is a fact that gravity stable platforms bring dramatic advantages to designing instruments in terms of mechanical design, control, maintenance, and integration. As far as MOMFIS is concerned, a Nasmyth platform would allow to nicely simplifying the design (e.g. relaxing the requirements for internal metrology) and therefore the cost. Even better would be the possibility to fold vertically the optical beam as this would allow keeping the whole instrument stable with respect to gravity.
- **Adaptive Optics**. As mentioned above adaptive optics is central to the performance of OWL instruments, in particular MOMFIS. Clearly, adaptive optics developments need to be fully considered at Observatory level, whether they are part of the telescope or of the instrument. For what MOMFIS is concerned (MOAO), we strongly encourage that ESO

continues to foster AO developments in close collaboration with the community, at component and system levels.

- **Sky coverage**. Sky coverage is as important for any ELT project as adaptive optics or telescope diameter. Low sky coverage does not seem to be an option for many ELT science cases (but for extra-solar planets). Limited sky coverage may prevent from carrying out some of the programs already identified in the ELT science case, but may also prevent from carrying out some of the as yet unknown programs that will be in fashion in 15 years from now. In other words, as a future discovery facility, an ELT shall certainly have a strong specification on sky coverage. Also, multi-wavelength observations are a must of today's astronomy, and requires for a telescope to observe fields where other data from other facilities exist. A telescope with limited sky coverage would have either to impose – if at all possible - those fields that will be observed by other worldwide facilities, or would run the risk of not being able to observe such fields. We therefore strongly encourage that using laser guide stars (as of today the only known solution to increase sky coverage) be aggressively raised as an essential component of OWL as an integrated system and as an Observatory.
- **Standardization**. Like for the VLT, standardization will be key to the success of an ELT and of its instrumentation. Preliminary definition of the standards shall start as soon as possible. This applies in particular, but not only, to electronics. We for instance assumed for MOMFIS a weight reduction of the electronics standing by the instrument by a factor of 10 compared to the VLT.
- **Preparing the community**. ELT instruments will require resources and facilities in the community that may well exceed the resources that were devoted to the development of the whole VLT / VLTI project. Preparing as soon as possible the community to work in a coordinated and collaborative way towards the realization of the European ELT instruments will later help their development. The European Framework Programs such as OPTICON or the ELT Design Study are already extremely successful in that respect and shall be continued and further strengthened.
- **Extending instrument studies**. We firmly believe that the OWL instrument studies, in spite of their short duration, have been extremely beneficial to ESO and to the community in making substantial progress on the project and in raising interest for it. Work will continue as part of the OPTICON and ELT Design Study, however with only partial emphasis on the instrumentation and with (as yet) no telescope interface. Because instrumentation is central to the scientific motivation of the project and of the community, we recommend that instrument studies be continued and further detailed. In particular, the MOMFIS case clearly shows that decision making between the various options and / or alternative designs will require delicate trade-off analyses. Such analyses shall be carried out with care and time, from scientific, technical and managerial standpoints, on the basis of relatively detailed designs and R&D achievements.

11. DEVELOPMENT RISKS, KEY R&D AREAS, PROTOTYPING

We briefly list hereafter the main items that we have identified in terms of development risks, key R&D areas, and prototyping.

Development risks:

- ✓ Adaptive Optics: components (DMs) and more generally MOAO at system level. This development risk is to be pondered with our option (see section 7.1) which contemplates MOMFIS operation without MOAO or with limited AO correction, at least for some time during the instrument lifetime (phased implementation).

Key R&D areas

- ✓ Adaptive Optics. The R&D activities in Adaptive Optics are described elsewhere in the OWL blue book.
- ✓ Starbugs. The concept of motorized elements that could move autonomously in the focal plane are actively studied by the Instrumentation Group of the Anglo-Australian Observatory, and are part of the OPTICON JRA on smart focal planes. The deployment of starbugs that could carry the pick-off mirrors and handle their orientation and positioning would allow to significantly simplify the instrument design (and operation) by removing the positioner and the need for exchangeable focal plane plates.
- ✓ metrology
- ✓ BSM

12. COST ESTIMATE

Table 19 is a very preliminary attempt at costing the development of MOMFIS. Hardware and FTE costs are included, under the assumption that the instrument development would more or less follow the scheme used for VLT instruments, that is: development in institutes (with or without ESO participation) managing the project and carrying out most of the studies.

Differences from values indicated in the text may occur, in particular for the FTEs which were sometimes only accounted for the design phases.

Figure 49 presents the cost breakdown in pie charts.

Table 19 – Cost Estimate

Item	Cost (M€)	FTEs	Comments
Management			
PI		10	10 years of development
Project Manager		10	
Project Controller		10	
Quality insurance		10	
Contract Officer		5	
Total Management	**0**	**45**	
System engineering			
Optical System		5	
Mechanical System		5	
Thermal System		5	
Instrument integration	2	12	2 persons during 3 years plus 1 person during 6 years. Does not include integration hall development costs

Instrument scientist		10	
AO System		10	
Control electronic		5	
Software		5	
Total System	**2**	**57**	
Sub-system			
Main structure	.9	3	
Rotator	1	2	To Be Confirmed
Positioner	2	20	
Beam Steering Mirror	2.4	10	
Deformable Mirror	2-4		TBD – range of 'acceptable' costs. Higher costs might require to choose option#1, or to delay implementation of the baseline.
Relay optics and cold stop	0.4	3	
ADC	1	2	
Filter wheel	1.8	2	
Slicer unit	1 – 1.8	4	1M€ is for the 1k x 1k detector option, 1.8M€ is for the 2k x 2k option
Spectrograph	1.5 - 2.3	8	1.5 M€ is for the 1k x 1k detector option, 2.3M€ is for the 2k x 2k option
Grating / Grism	1.5	2	To Be Confirmed
Detector Unit	1.5 - 6	5	TBD – 1.5M€ case is for 1k x 1k configuration, 6M€ is for 2k x 2k detectors
Cryostat	.8 - 1.9	5	Small cryostat case and large one
Wave-Front Sensor	1.5	5	Only the MOAO WFS
AO Controller	1	10	To be Confirmed
Maintenance tools	1	3	To be Confirmed
Software	.5	18	3 people during 6 years (TBC)
Control Electronic	2	12	TBD – Depends on new electronics standards
Total sub-system	**24 – 33**	**79**	
Total	26 – 35	114	
Overheads (15%)	4 – 5		
Grand Total	**30 – 40**	**215**	

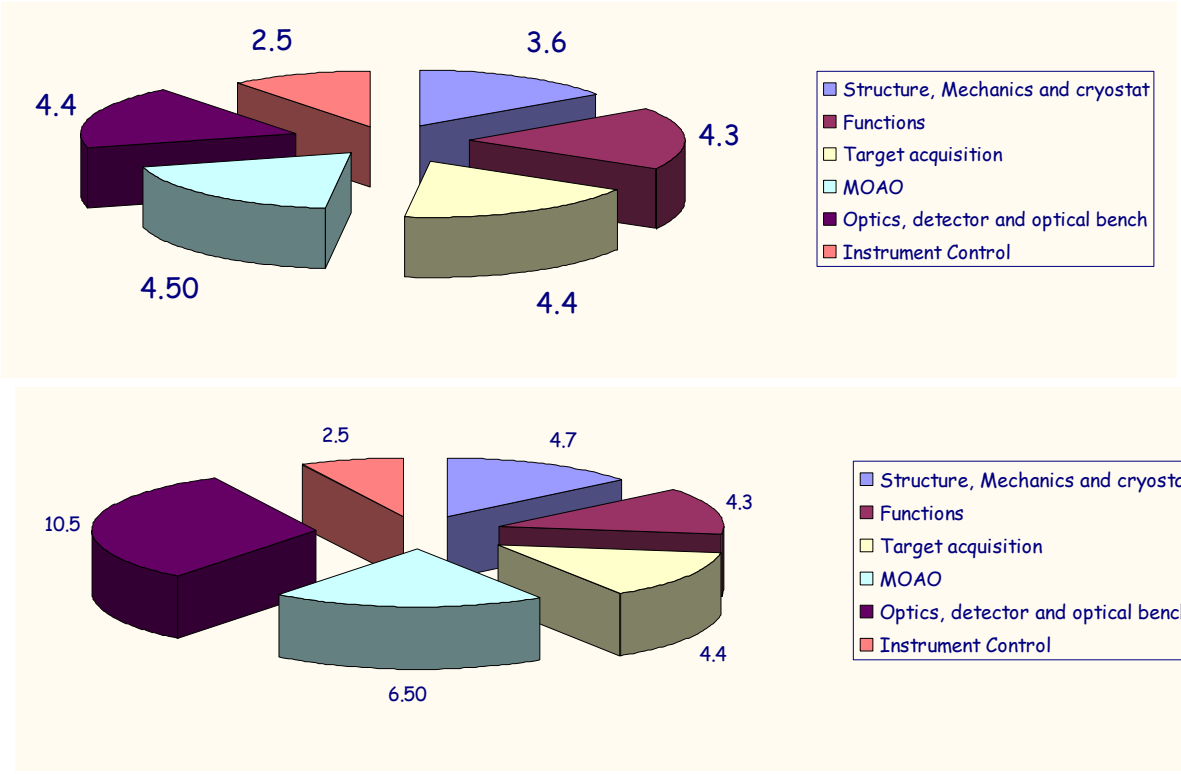

Figure 49 – Cost breakdown for two extreme combination of options.

Up: 1K x 1K detector, small cryostat and 'low cost' DMs price (Total cost: 29.5 M€)
Down: 2k x 2k detectors, large cryostat and 'high cost' DMs (Total cost: 40.1 M€)

13. DEVELOPMENT SCHEDULE

Figure 50 shows a development schedule assuming the MOMFIS baseline. It foresees continuing R&D and Phase A activities until 2011 followed by accelerated Preliminary and Final design phases. This scheme allows taking advantage of new developments on sub-systems as late as possible. This schedule is also made compatible with the tentative OWL schedule. Should there be any opportunity for an accelerated telescope schedule, the MOMFIS schedule could also be accelerated by e.g. reducing the R&D and phase A activities and freezing earlier the technical solutions finally adopted for the design.

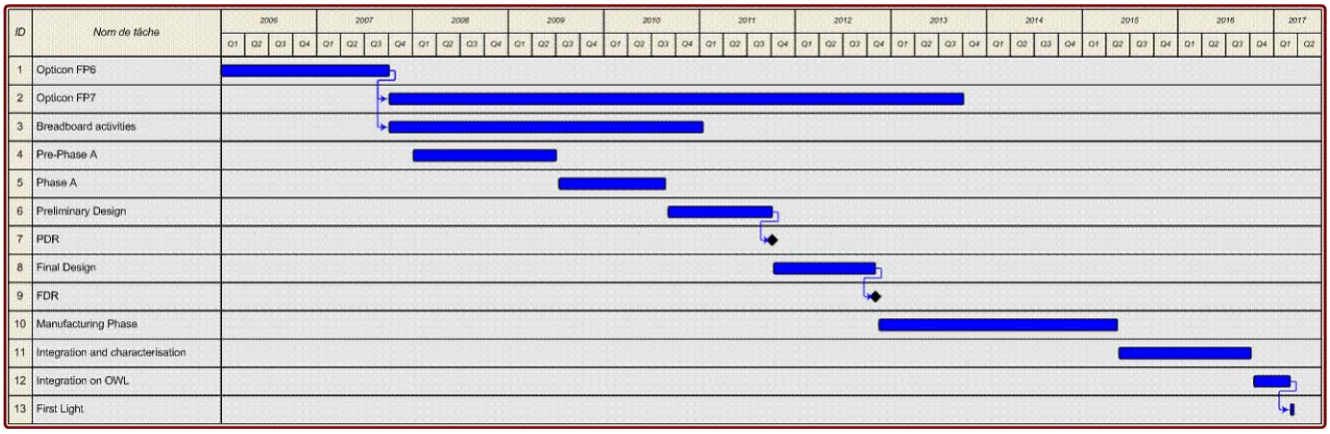

Figure 50 – MOMFIS Development schedule

14. ABBREVIATED TERMS

Abbreviations used in this document are provided below.

Abbreviation	Meaning
ADC	Atmospheric Dispersion Compensator
AO	Adaptive Optics
BSM	Beam Steering Mirror
DM	Deformable Mirror
ELT	Extremely Large Telescope
ESO	European Southern Observatory
FALCON	Fibre spectrograph with Adaptive optics on Large Fields to Correct at Optical and Near-infrared
FEA	Finite Element Analysis
FOV	Field of View
FWHM	Full Width at Half Maximum
GLAO	Ground Layer Adaptive Optics
GS	Guide Star
HST	Hubble Space Telescope
ICD	Interface Control Document
IFU	Integral Field Unit
JRA	Joint Research Activity
LGS	Laser Guide Star
LN2	Liquid Nitrogen
mas	Milli-arcsec
MCAO	Multi-Conjugate Adaptive Optics
MLI	Multi Layer Insulation
MOMFIS	Multi-Object, Multi-Field IR Spectrograph
MOAO	Multi-Object Adaptive Optics
MOS	Multi-Object Spectrograph
N/A	Not Applicable
NGS	Natural Guide Star
OWL	Overwhelmingly Large Telescope
PSF	Point Spread Function

PTV	Peak To Valley
QE	Quantum Efficiency
TBC	To Be Confirmed
TBD	To Be Determined
TMT	Thirty Meter Telescope
VPH	Volume Phase Holographic
WFE	WaveFront Error
WFS	WaveFront Sensor

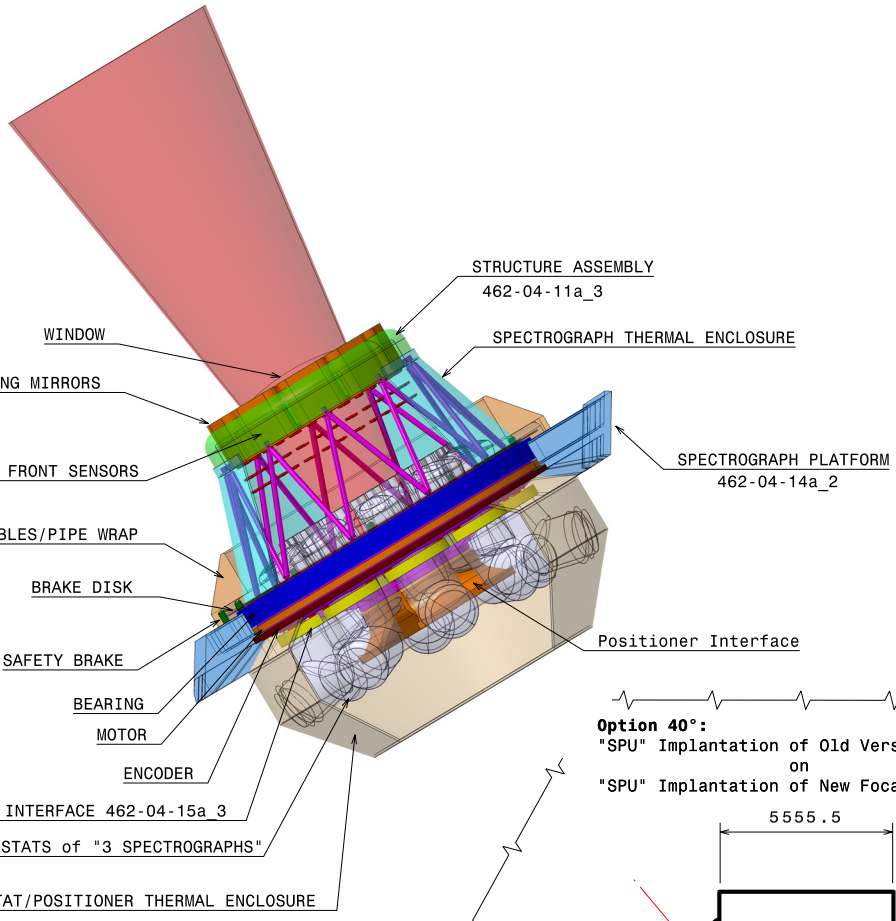

Option 40°:
"SPU" Implantation of Old Version Station
on
"SPU" Implantation of New Focal Station

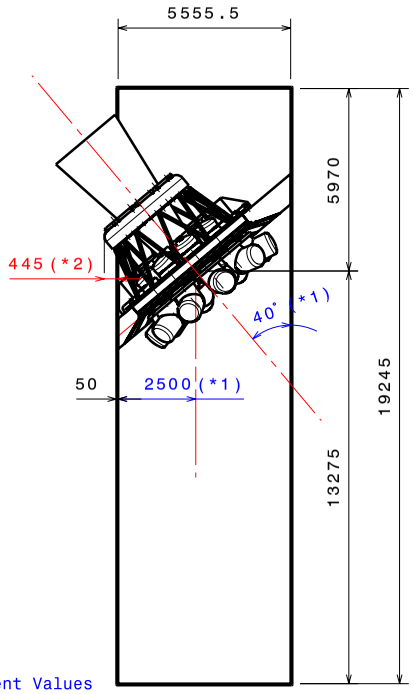

Option 32°:
"SPU" Adaptation at the New Focal Station

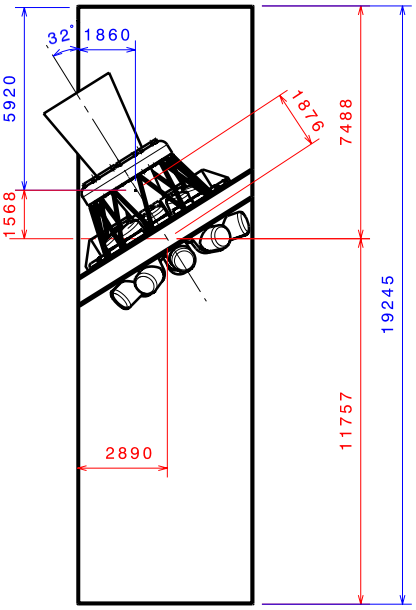

(*1) Precedent Values
(*2) Dimension out the Volume

Red Line: Modification dimensions
Blue Line: Origin dimensions

Observatoire de PARIS-MEUDON GEPI : P.I. : BE_PROJET 5 place Jules Janssen 92195 MEUDON			
Roughness *(Def. Ra 6.3)*	CAO-System Catia-V5_R13	Phone 01.45.07.76.53	Naming : SPECTROGRAPH ASSEMBLY
Therm. Treatments *(Def. None)*	Name MARTEAUD	DATE 05-09-2005	Surfacing Treat. *(Def. None)* ** / Number : 1
Edges *(Def. 0.25 to 45°)*	Project ESO-OWL	Instrument MOMFIS	Drawing Name ODP-SPU-DWG-462-04-02A / 3
Temperature Reference *(Def. 20° C)*	Material **	Global Tolerance *(JS13-js13)*	Format A3V / Scale : *** / Mass ...g

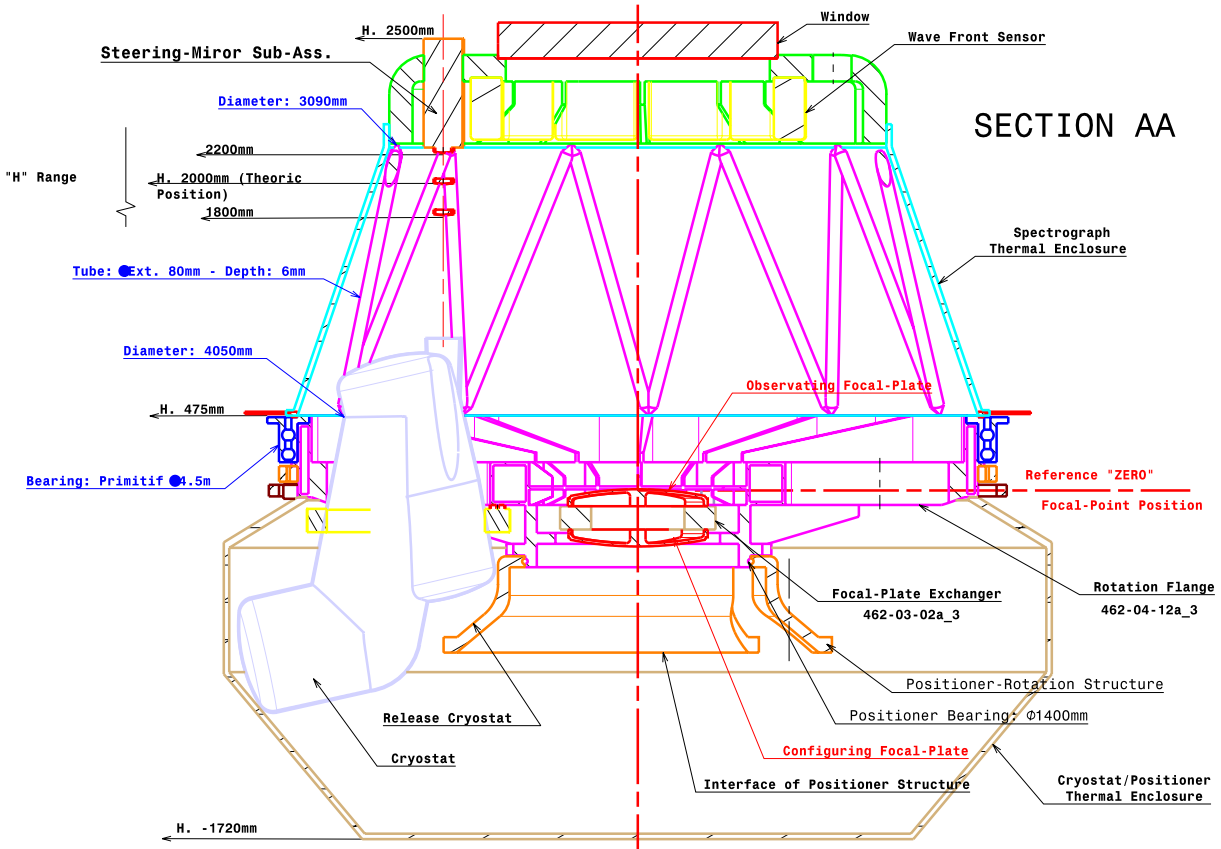

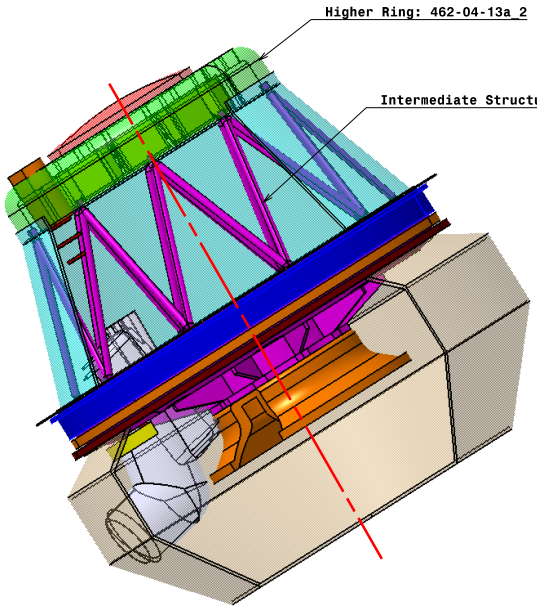

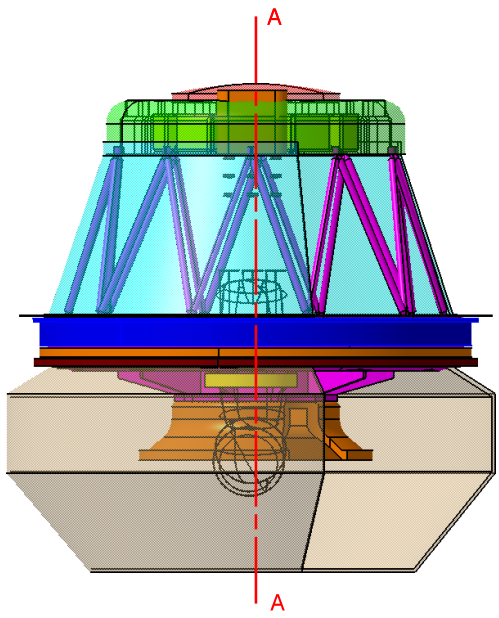

Observatoire de PARIS-MEUDON GEPI : P.I. : BE_PROJET 5 place Jules Janssen 92195 MEUDON			
Roughness *(Def. Ra 6.3)*	CAO-System Catia-V5_R13	Phone 01.45.07.76.53	Naming : Structure Assembly
Therm. Treatments *(Def. None)*	Name MARTEAUD	DATE 06-09-2005	Surfacing Treat. *(Def. None)* ** / Number : 1
Edges *(Def. 0.25 to 45°)*	Project ESO-OWL	Instrument MOMFIS	Drawing Name ODP-SPU-DWG-462-04-11A / 3
Temperature Reference *(Def. 20° C)*	Material **	Global Tolerance *(JS13-js13)*	Format A3V / Scale : *** / Mass ...g

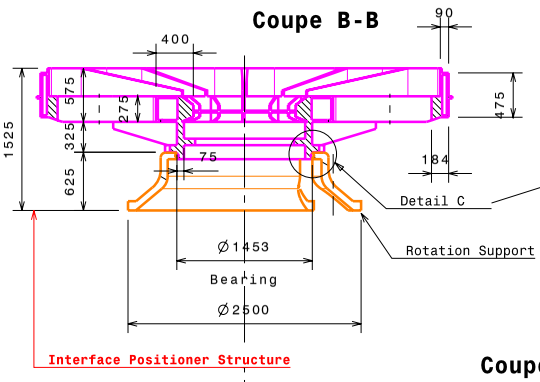

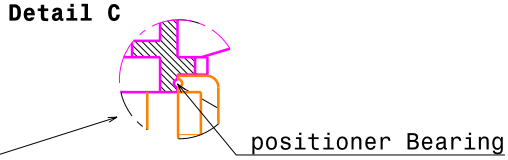

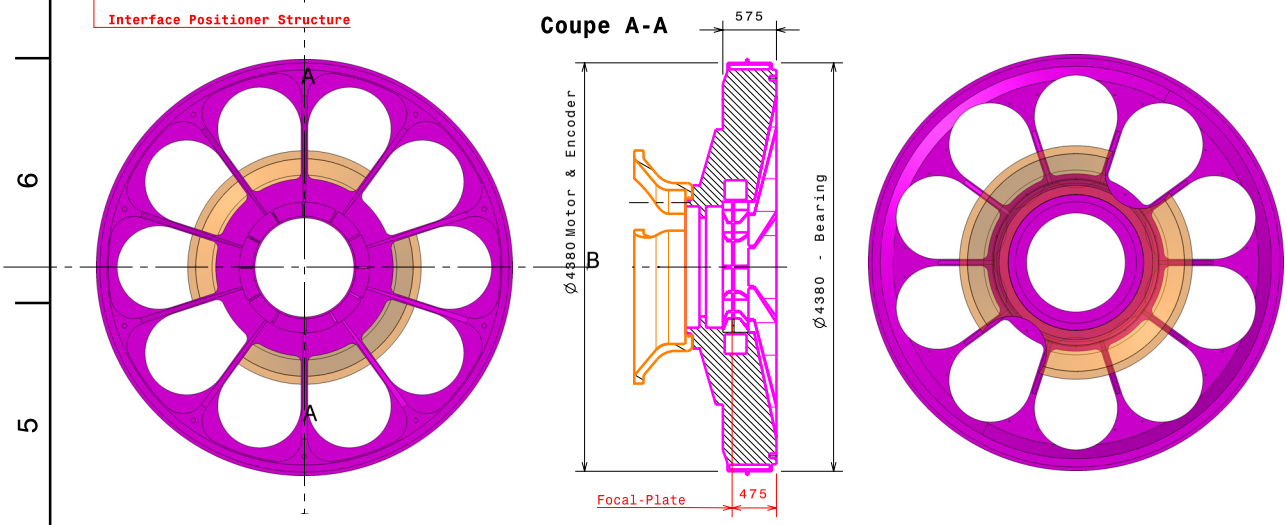

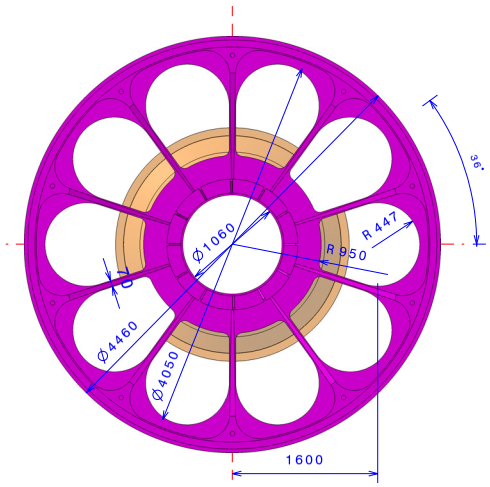

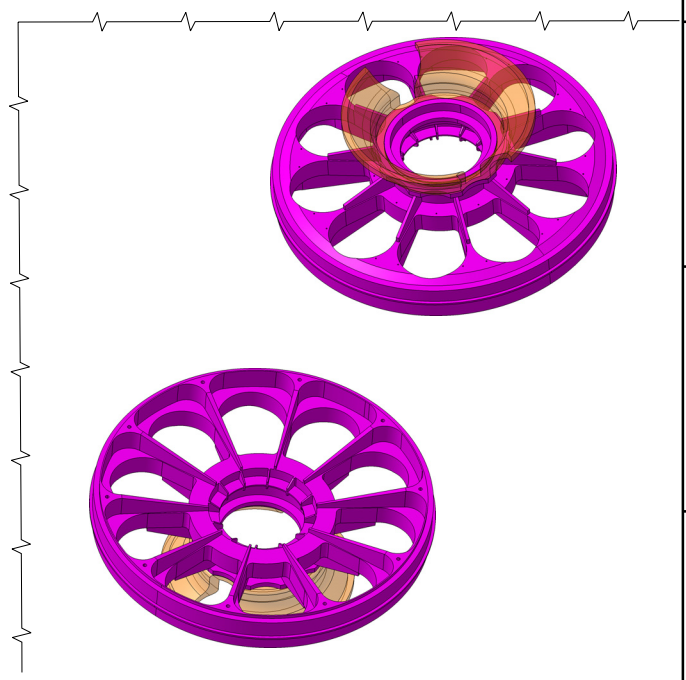

Observatoire de PARIS-MEUDON GEPI : P.I. : BE_PROJET 5 place Jules Janssen 92195 MEUDON			
Roughness *(Def. Ra 6.3)*	CAO-System Catia-V5_R13	Phone 01.45.07.76.53	Naming : Rotation Flange
Therm. Treatments *(Def. None)*	Name MARTEAUD	DATE 06-09-2005	Surfacing Treat. *(Def. None)* ** / Number : 1
Edges *(Def. 0.25 to 45°)*	Project ESO-OWL	Instrument MOMFIS	Drawing Name ODP-SPU-DWG-462-04-12A / 3
Temperature Reference *(Def. 20° C)*	Material **	Global Tolerance *(JS13-js13)*	Format A3V / Scale : *** / Mass ...g

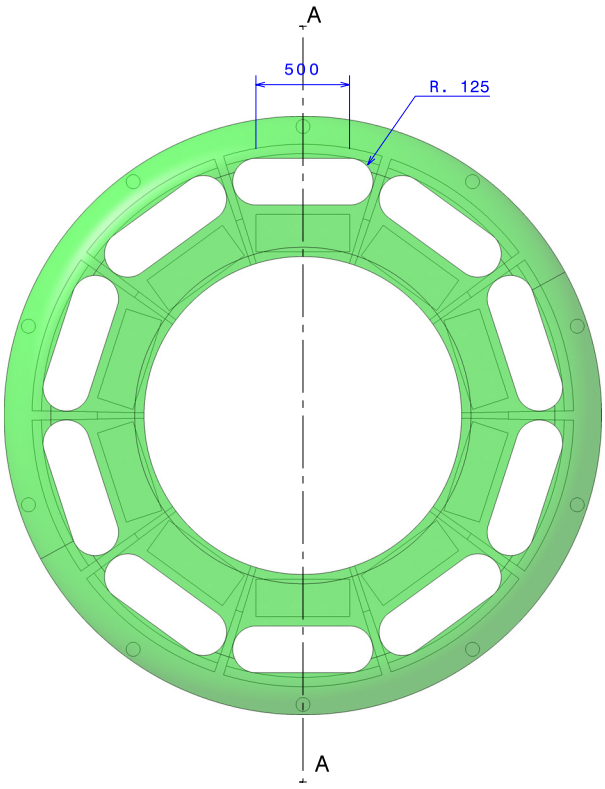

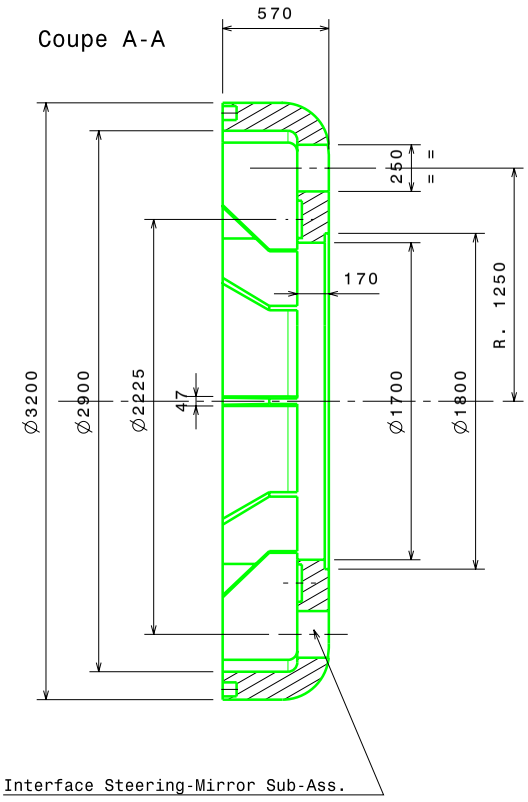

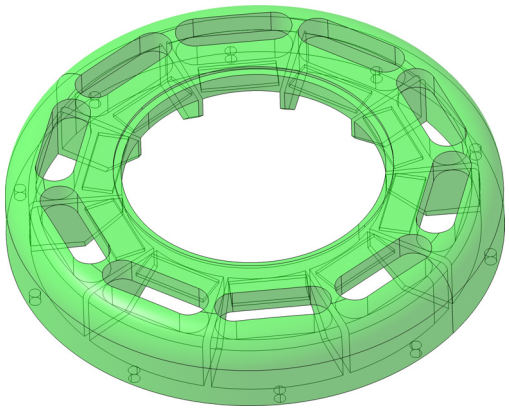

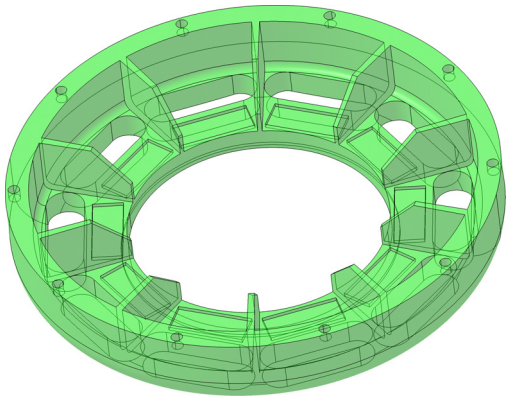

Observatoire de PARIS-MEUDON GEPI : P.I. : BE_PROJET 5 place Jules Janssen 92195 MEUDON			
Roughness *(Def. Ra 6.3)*	CAO-System Catia-V5_R13	Phone 01.45.07.76.53	**Naming :** Higher Ring
Therm. Treatments *(Def. None)*	Name MARTEAUD	DATE 06-09-2005	Surfacing Treat. *(Def. None)* ** — **Number :** 1
Edges *(Def. 0.25 to 45°)*	Project ESO-OWL	**Instrument** MOMFIS	**Drawing Name** ODP-SPU-DWG-462-04-13A — 2
Temperature Reference *(Def. 20° C)*	Material **	Global Tolerance *(JS13-js13)*	Format A3V — Scale : *** — Mass ...g

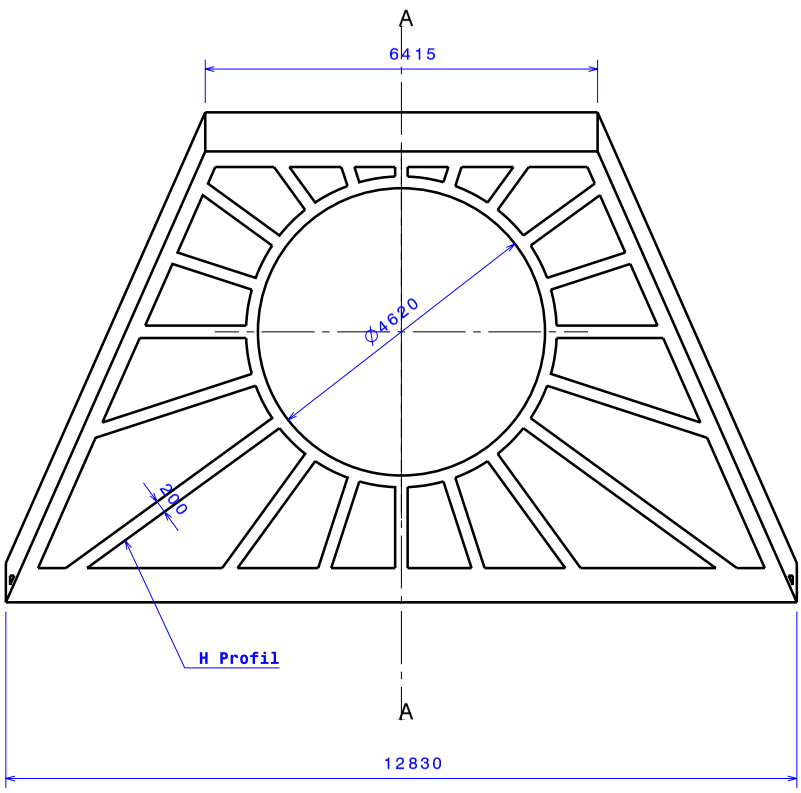

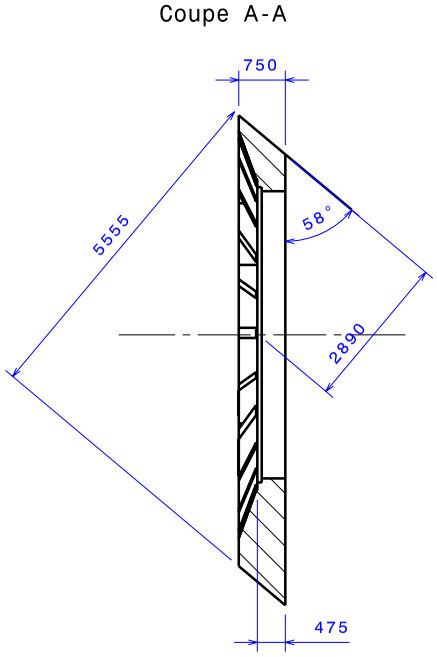

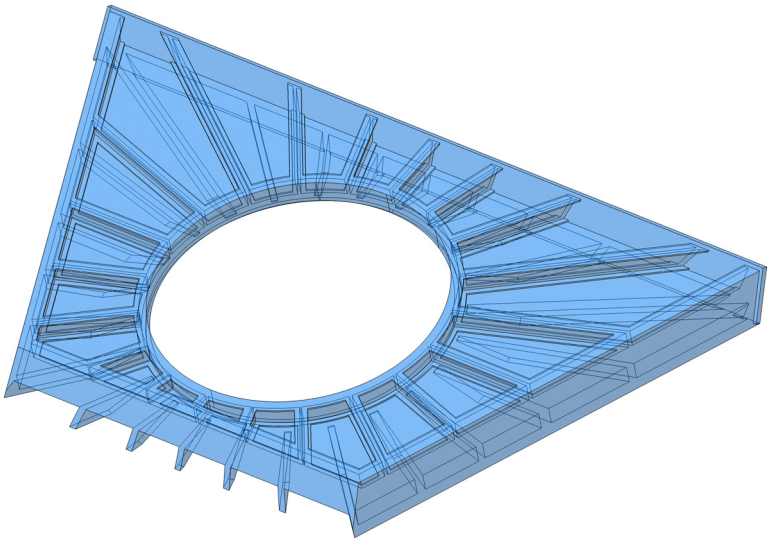

Observatoire de PARIS-MEUDON GEPI : P.I. : BE_PROJET 5 place Jules Janssen 92195 MEUDON			
Roughness *(Def. Ra 6.3)*	CAO-System Catia-V5_R13	Phone 01.45.07.76.53	**Naming :** Spectrograph Platform
Therm. Treatments *(Def. None)*	Name MARTEAUD	DATE 06-09-2005	Surfacing Treat. *(Def. None)* ** / **Number :** 1
Edges *(Def. 0.25 to 45°)*	Project ESO-OWL	**Instrument** MOMFIS	**Drawing Name** ODP-SPU-DWG-462-04-14A / 2
Temperature Reference *(Def. 20° C)*	Material **	Global Tolerance *(JS13-js13)*	Format A3V / Scale : *** / Mass ...g

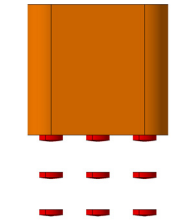

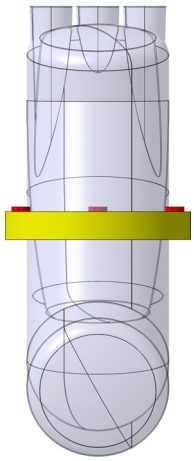

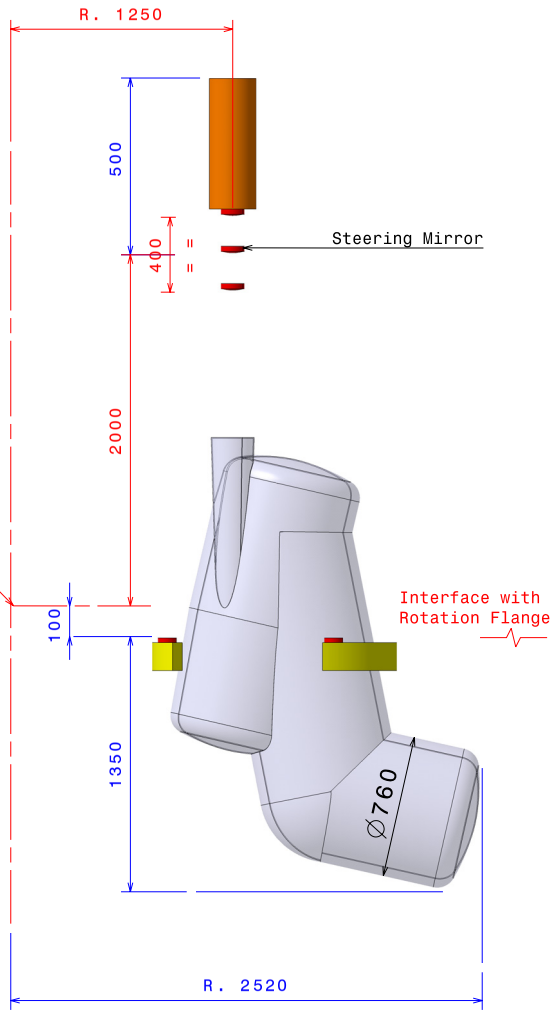

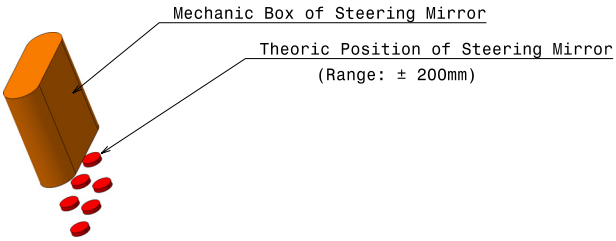

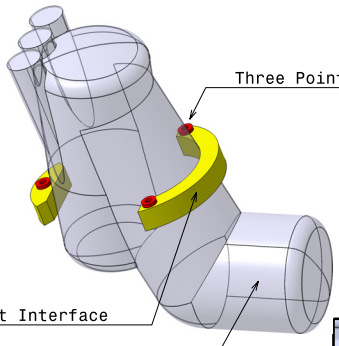

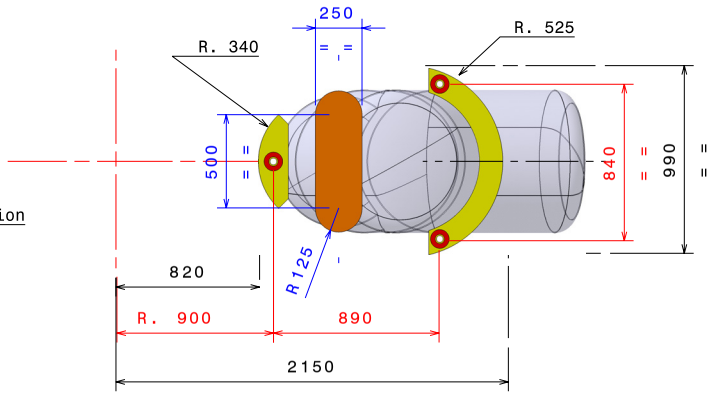

Observatoire de PARIS-MEUDON GEPI : P.I. : BE_PROJET 5 place Jules Janssen 92195 MEUDON			
Roughness *(Def. Ra 6.3)*	CAO-System Catia-V5_R13	Phone 01.45.07.76.53	**Naming :** Crysotat Interface
Therm. Treatments *(Def. None)*	Name MARTEAUD	DATE 06-09-2005	Surfacing Treat. *(Def. None)* ** / **Number :** 1
Edges *(Def. 0.25 to 45°)*	Project ESO-OWL	**Instrument** MOMFIS	**Drawing Name** ODP-SPU-DWG-462-04-15A / 3
Temperature Reference *(Def. 20° C)*	Material **	Global Tolerance *(JS13-js13)*	Format A3V / Scale : *** / Mass ...g

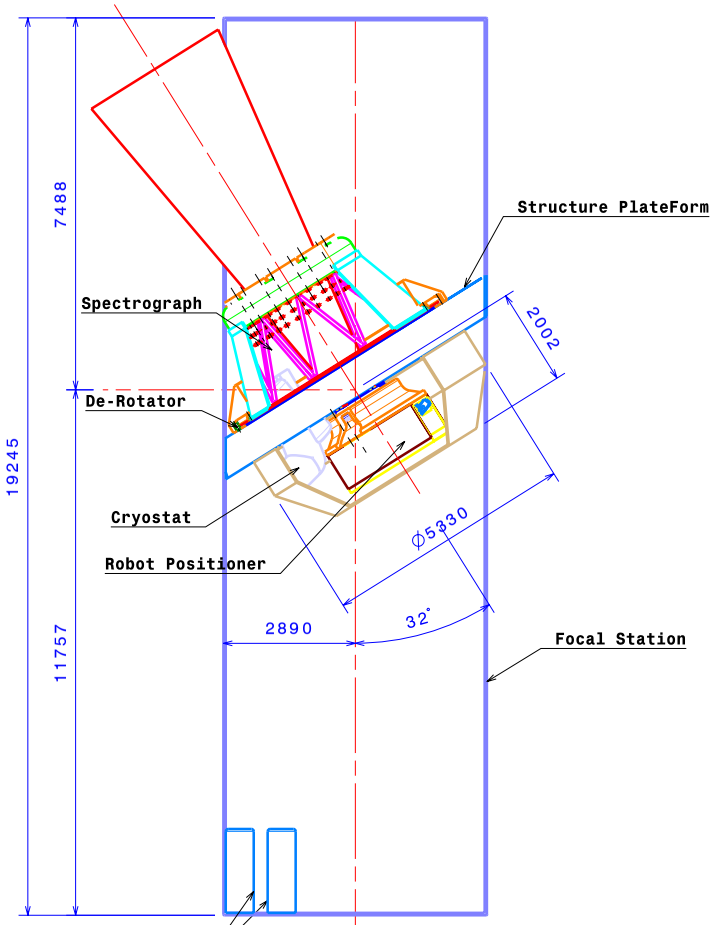

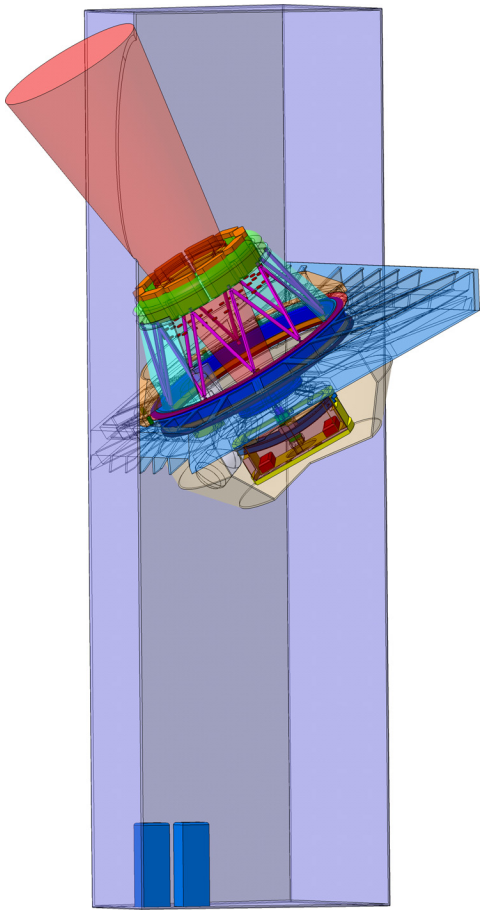

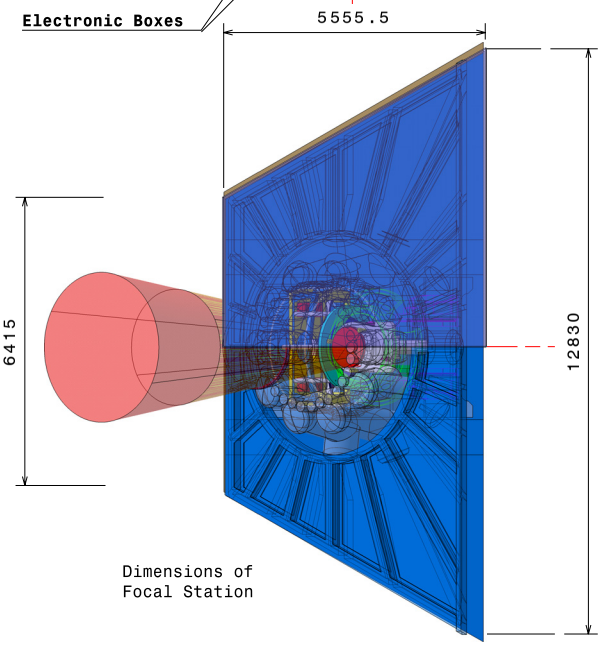

Dimensions of
Focal Station

Roughness (Def. Ra 6.3)	CAO-System Catia-V5_R13	Phone 01.45.07.76.53	Naming : Positioner Assembly
Therm. Treatments (Def. None)	Name MARTEAUD	DATE 07-09-2005	Surfacing Treat. (Def. None) ** / Number : 1
Edges (Def. 0.25 to 45°)	Project ESO-OWL	Instrument MOMFIS	Drawing Name ODP-POS-DWG-462-03-01A / 3
Temperature Reference (Def. 20° C)	Material **	Global Tolerance (JS13-js13)	Format A3V / Scale : *** / Mass ...g

Observatoire de PARIS-MEUDON
GEPI : P.I. : BE_PROJET
5 place Jules Janssen
92195 MEUDON

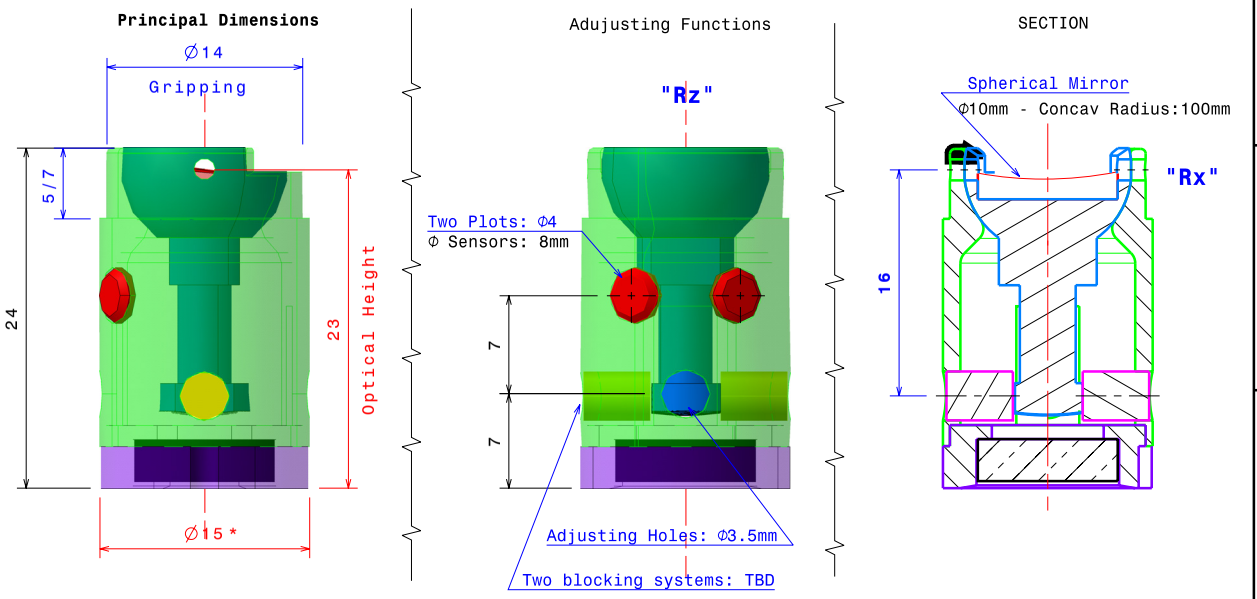

* Distance between Two Bugs: 15mm

"Rx" Range: ±10° Resolution/Step: TBD Stablity 1µm
"Rz" Range: ±180° Resolution : TBD Stablity 1µm

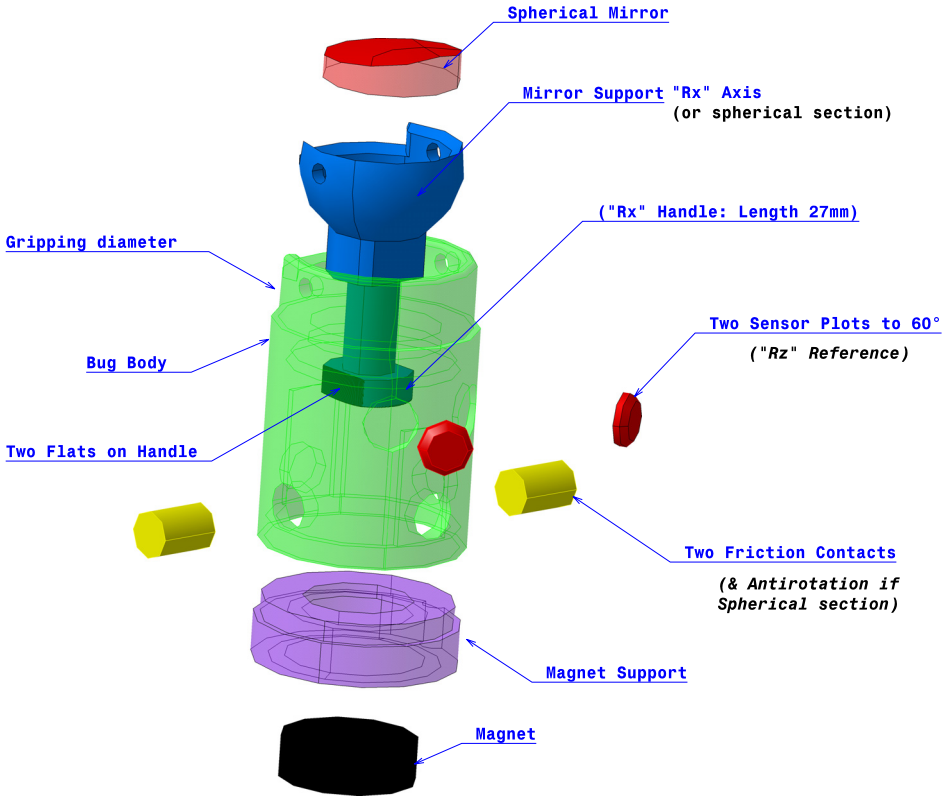

Observatoire de PARIS-MEUDON GEPI : P.I. : BE_PROJET 5 place Jules Janssen 92195 MEUDON			
Roughness *(Def. Ra 6.3)*	CAO-System Catia-V5_R13	Phone 01.45.07.76.53	Naming : Base Line of Bug
Therm. Treatments *(Def. None)*	Name MARTEAUD	DATE 06-09-2005	Surfacing Treat.*(Def. None)* ** / Number : 1
Edges *(Def. 0.25 to 45°)*	Project ESO-OWL	Instrument MOMFIS	Drawing Name ODP-BUGS-DWG-462-02-01D / 2
Temperature Reference *(Def. 20° C)*	Material **	Global Tolerance *(JS13-js13)*	Format A3V / Scale : ** / Mass 25/30g

SECTION AA

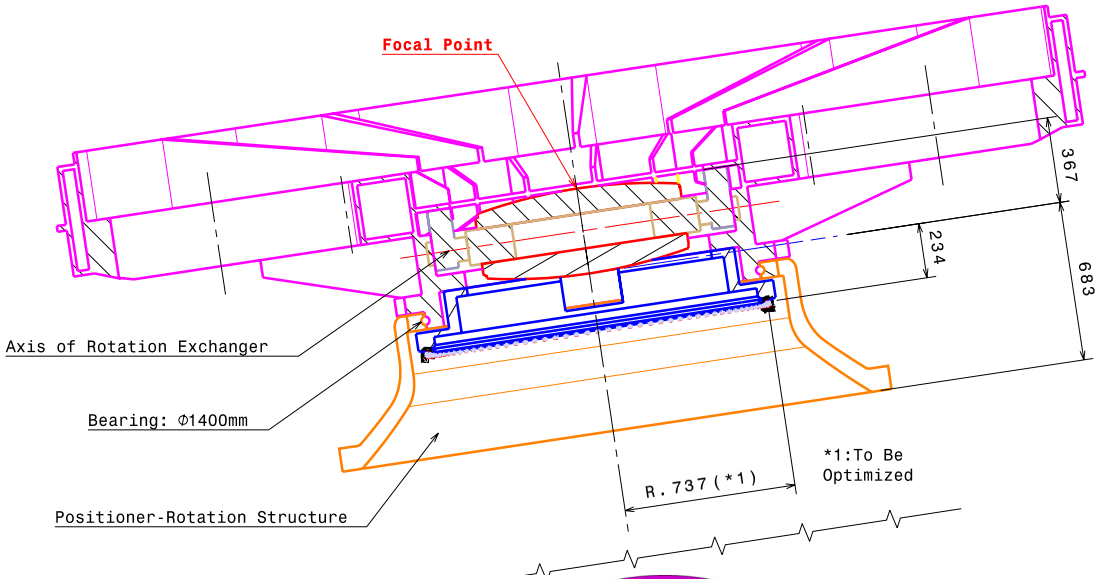

SPECTROGRAPH SIDE

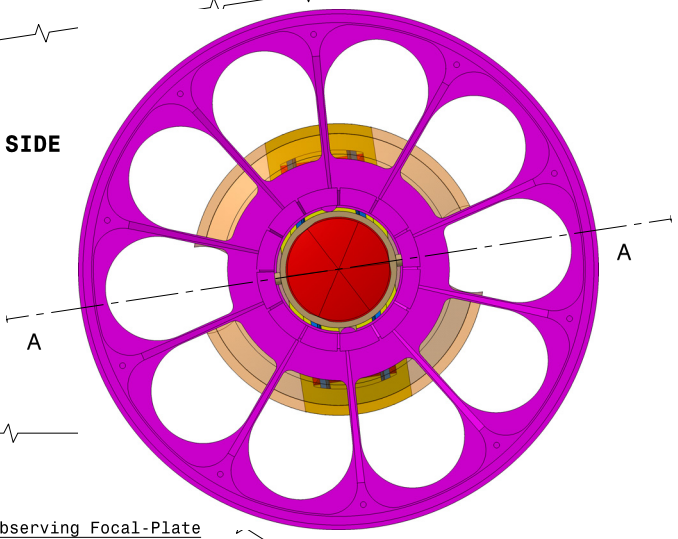

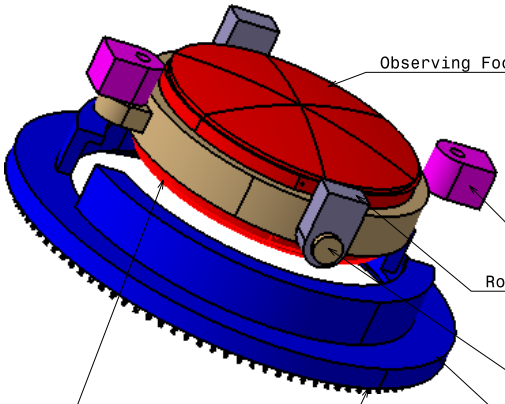

l'Observatoire de Paris — Galaxies Etoiles Physique et Instrumentation — GEPI			Observatoire de PARIS-MEUDON GEPI : P.I. : BE_PROJET 5 place Jules Janssen 92195 MEUDON
Roughness *(Def. Ra 6.3)*	CAO-System Catia-V5_R13	Phone 01.45.07.76.53	**Naming :** Focal-Plate/Exchanger/Parking Sub-Ass.
Therm. Treatments *(Def. None)*	Name MARTEAUD	DATE 06-09-2005	Surfacing Treat.*(Def. None)* ** — **Number :** 1
Edges *(Def. 0.25 to 45°)*	Project ESO-OWL	**Instrument** MOMFIS	**Drawing Name** ODP-POS-DWG-462-03-02A — 3
Temperature Reference *(Def. 20° C)*	Material **	Global Tolerance *(JS13-js13)*	Format A3V — Scale : *** — Mass ...g

SECTION AA

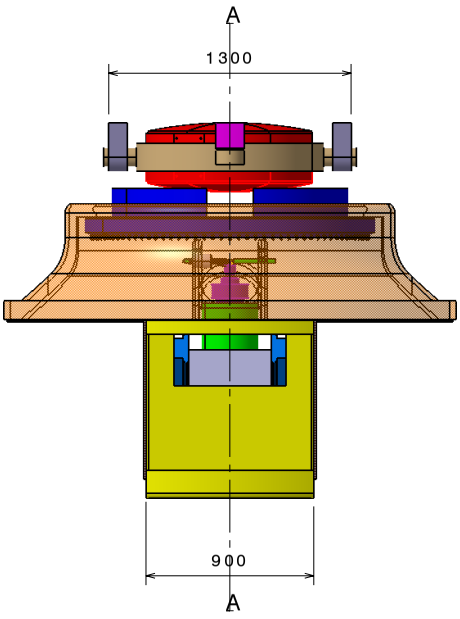

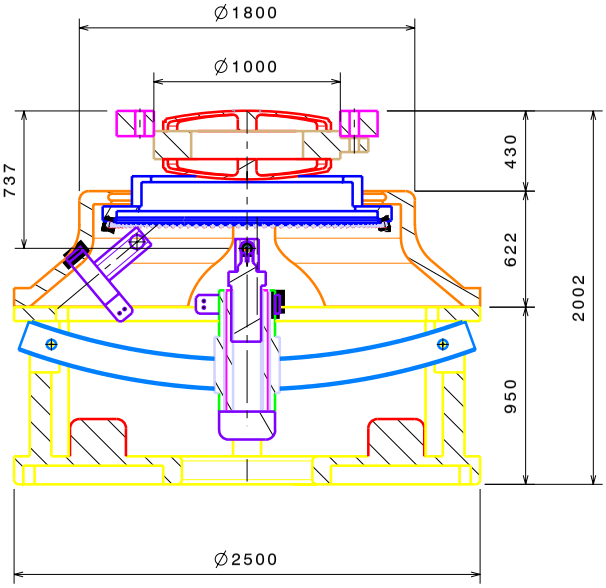

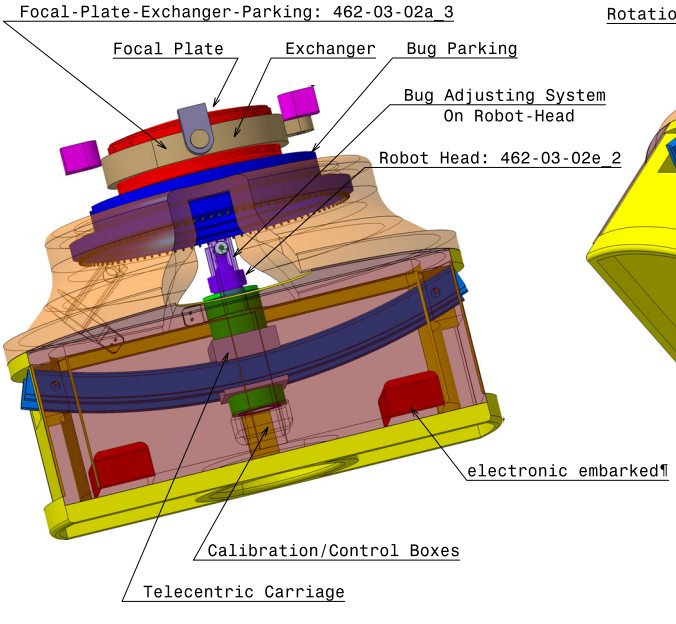

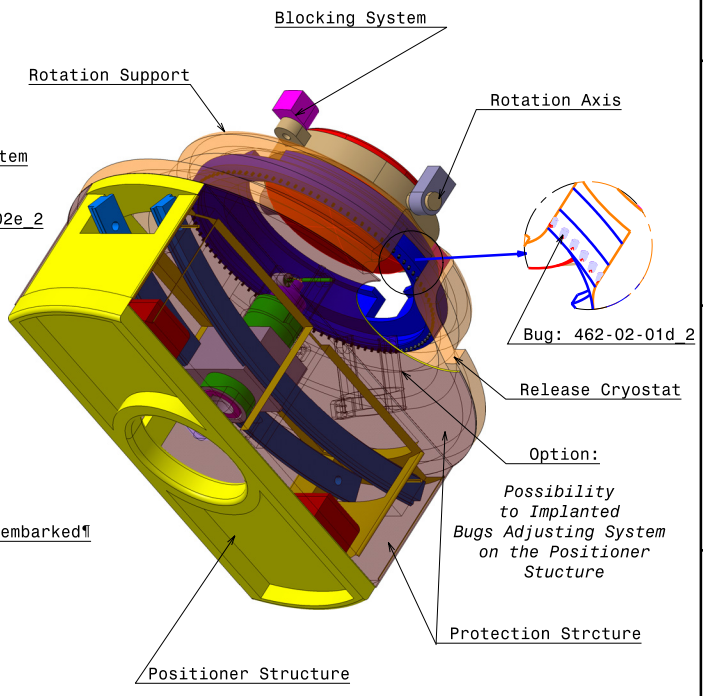

Observatoire de PARIS-MEUDON GEPI : P.I. : BE_PROJET 5 place Jules Janssen 92195 MEUDON			
Roughness *(Def. Ra 6.3)*	CAO-System Catia-V5_R13	Phone 01.45.07.76.53	**Naming :** ROBOT-POSITIONER ASSEMBLY
Therm. Treatments *(Def. None)*	Name MARTEAUD	DATE 06-09-2005	Surfacing Treat.*(Def. None)* ** / **Number :** 1
Edges *(Def. 0.25 to 45°)*	Project ESO-OWL	**Instrument** MOMFIS	**Drawing Name** ODP-POS-DWG-462-03-02C / 3
Temperature Reference *(Def. 20° C)*	Material **	Global Tolerance *(JS13-js13)*	Format A3V / Scale : *** / Mass ...g

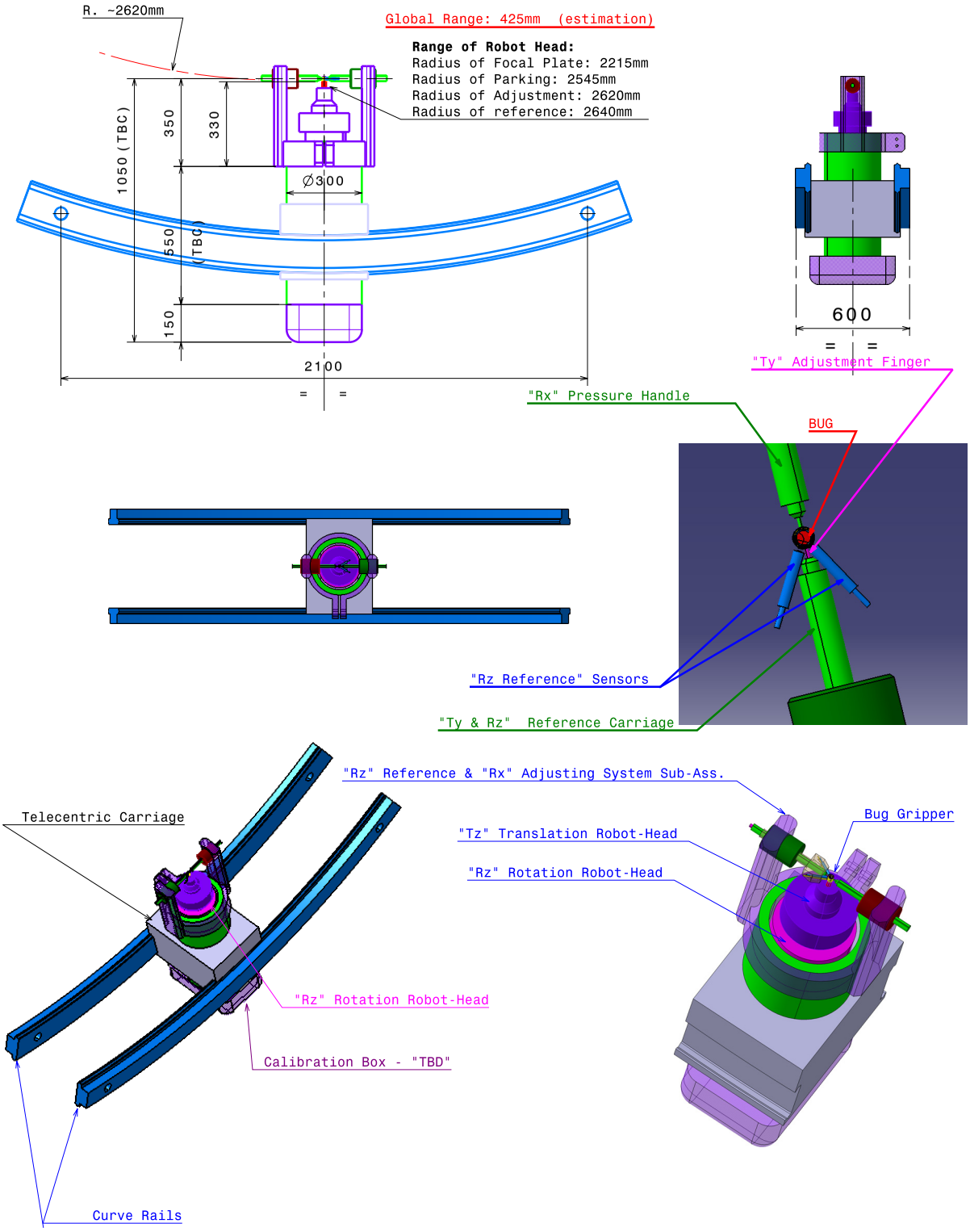

Observatoire de PARIS-MEUDON GEPI : P.I. : BE_PROJET 5 place Jules Janssen 92195 MEUDON			
Roughness *(Def. Ra 6.3)*	CAO-System Catia-V5_R13	Phone 01.45.07.76.53	**Naming :** Robot-Head & Bug-Adjustment
Therm. Treatments *(Def. None)*	Name MARTEAUD	DATE 06-09-2005	Surfacing Treat. *(Def. None)* ** / **Number :** 1
Edges *(Def. 0.25 to 45°)*	Project ESO-OWL	**Instrument** MOMFIS	**Drawing Name** ODP-POS-DWG-462-03-02E / 3
Temperature Reference *(Def. 20° C)*	Material **	Global Tolerance *(JS13-js13)*	Format A3V / Scale : *** / Mass ...g

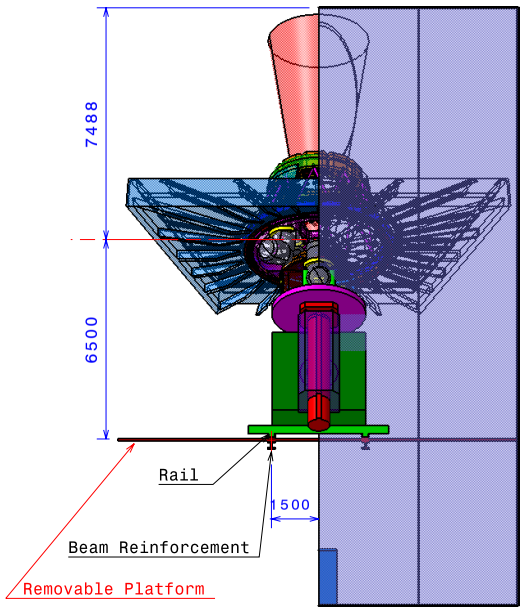

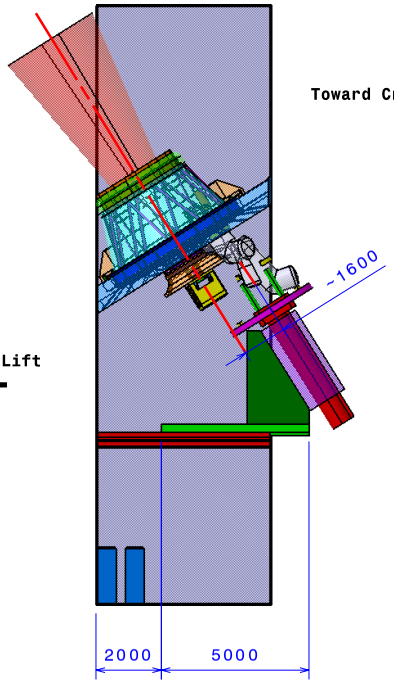

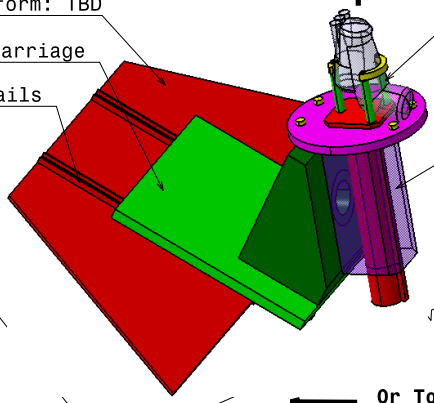

POSITIONER MAINTENANCE

Toward Crane

Or Toward Lift

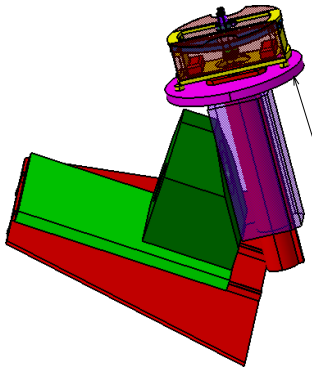

CRYOSTAT MAINTENANCE

Or Toward Lift

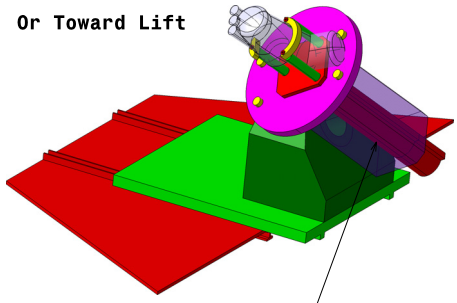

Observatoire de PARIS-MEUDON GEPI : P.I. : BE_PROJET 5 place Jules Janssen 92195 MEUDON			
Roughness *(Def. Ra 6.3)*	CAO-System Catia-V5_R13	Phone 01.45.07.76.53	**Naming :** Maintenance Platform
Therm. Treatments *(Def. None)*	Name MARTEAUD	DATE 09-09-2005	Surfacing Treat. *(Def. None)* ** / **Number :** 1
Edges *(Def. 0.25 to 45°)*	Project ESO-OWL	**Instrument** MOMFIS	**Drawing Name** ODP-POS-DWG-462-03-02G / 3
Temperature Reference *(Def. 20° C)*	Material **	Global Tolerance *(JS13-js13)*	Format A3V / Scale : *** / Mass ...g